



Trinity College Dublin

Coláiste na Tríonóide, Baile Átha Cliath

The University of Dublin

Investigating the Impact of the Non-Structural Proteins of Respiratory Syncytial Virus on the Type I Interferon Response

Claudia M Efstathiou

B.Sc. Biochemistry, M.Sc. Immunology and Immunotherapy

A Thesis submitted to
Trinity College Dublin for the degree
of Doctor of Philosophy

Supervised by Dr. Nigel John Stevenson

Viral Immunology Group

School of Biochemistry and Immunology

2023

Declaration of Authorship

I declare that this thesis has not been submitted as an exercise for a degree at this or any other university and it is entirely my own work.

I agree to deposit this thesis in the University's open access institutional repository or allow the Library to do so on my behalf, subject to Irish Copyright Legislation and Trinity College Library conditions of use and acknowledgement.

I consent to the examiner retaining a copy of the thesis beyond the examining period, should they so wish (EU GDPR May 2018).

Claudia Efstathiou

Acknowledgements

This thesis would not be possible without the help and guidance of my supervisor Dr. Nigel Stevenson, though the ups and downs of this project I have appreciated the time you've spent working with me and I'd like to thank you for giving the opportunity to work on this project. Special thanks to past and present members of the Stevenson lab; Richard, Daniah, Siobhán, Orla, Aziz, Lowela and Juber. I'd particularly like to thank Yamei Zhang - your help has been invaluable and I'm going to really miss working with you!

I'm extremely grateful for the technical help of Gavin McManus and Barry Moran for support with the confocal microscope and flow cytometry data. Having their expertise on hand when setting up those experiments made a huge difference. I would like to thank Mag Needham who has been the best CL3 lab manager I could ask for and has been a great help sorting all things technical and keeping us running through Covid.

This project would not have been possible without our funders, the National Children's Hospital at Tallaght, thank you for supporting this work. I would also like to thank the individuals that helped coordinate paediatric sample collection; Dr. Nadeem Galysed, Dr. Laura Whitla, Dr. Caitriona Ní Chathasaigh and Dr. Stanley Koe, as well as the patients and their families for donating samples to the project.

I've been lucky to share a lab and office with some amazing people - both the Dunne and McLoughlin labs have been great to work alongside. I've made some fantastic friends in my time in Dublin, special mention to Hannah, Sinead and Eva who have been there throughout this project and have always minded me. I'd like to thank Emillio for his help troubleshooting literally everything and Clíodhna and Lianne for the many cups of tea and emergency biscuits. Many thanks to Andy for all the chats over pints and introducing me to many podcasts. The support from my lab mates has been invaluable, from technical advice to emotional support, our little office has been a place of sanctuary

though the last four years. I cannot imagine doing this PhD without you.

I would like to thank my family, my mum has always believed in me and encouraged my interest in science from a young age - and you were right maths A level was a good idea! My dad has been fantastic at listening to me talk about my work and offering advice on how to improve things. I think he's as surprised as I am how closely I've ended up following his footsteps.

Finally, I'd like to recognise my fiance Ed who has always been there for me and at this point could probably run a western blot just from hearing me talk about them so much. I'm lucky to have you in my life and can't wait to build our lives together.

Abstract

Respiratory syncytial virus is the leading cause of bronchiolitis in infants, causing 33.2 million hospital admissions and over 118,000 deaths each year. The primary site of RSV infection are the epithelial cells of the respiratory tract. On infection RSV evades the immune response through several mechanisms, including subversion of responses to the anti-viral cytokine IFN α by interacting with the JAK-STAT pathway. IFN α is a potent antiviral cytokine that quickly causes an up-regulation in over 500 IFN stimulated genes to make the cell less permissive to infection and viral growth. The action of RSV prevents the up-regulation of ISGs, including MxA, ISG15, USP18 and PKR, which prevents infected cells from mounting a robust anti-viral response. Our research focuses on the immune evasive role of RSV's two non-structural proteins, NS1 and NS2, and the mechanism by which they limit JAK-STAT signalling.

We expressed NS1 and NS2 in human alveolar epithelial cells (A549) and bronchial epithelial cells (BEAS 2b) and analysed their effect upon the JAK-STAT pathway. We discovered that expressing NS1 in A549 and BEAS 2b cells lead to a significant reduction in ISGs, while NS2 had no significant effect. There was no matched reduction in pSTAT1 or pSTAT2 in either cell line. However, BEAS 2b had increased STAT1 and STAT2 phosphorylation with NS1 expression. By studying the subcellular localization of STAT1 we have shown that expression of NS1 reduced STAT1 trafficking to the nucleus, and altered STAT2 localization, providing a new mechanism by which RSV NS1 prevents efficient JAK-STAT signalling. While the primary site of RSV infection is epithelial cells of the upper respiratory track, there is some evidence that immune cells can be infected by RSV. To examine the extent of the permissiveness of circulating immune cells, adult PBMCs were incubated with RSV and the resulting infection measured. We found that around 2% of lymphocytes became infected and that there was a reduction in IFN α sensitivity after RSV infection. This reduction in responsiveness to IFN α may result in delayed viral clearance and altered phenotypic differentiation.

Taken together, this work has shown that RSV NS proteins have key immune evasion roles that are used to overcome the IFN α response by reducing the signalling through the JAK-STAT pathway. The ability of RSV NS proteins to limit the activity of IFN α identifies the NS proteins as targets for therapeutic treatments for RSV. Our work gives a better understanding of how RSV NS proteins acts to subvert the immune response in the most clinically relevant cell types.

Publications

Efstathiou C., Zhang M., Gaylesayed N., Stevenson N.J. RSV NS proteins use multiple mechanism to limit JAK-STAT signaling depending on cell type. *Manuscript in preparation*.

Wubben R., **Efstathiou C.**, Stevenson N.J. The interplay between the immune system and viruses. *Hormones, Regulator and Viruses* vol 117. 2021; p1-15. doi: 10.1016/bs.vh.2021.06.011

Efstathiou C., Abidi SH., Harker J., Stevenson N.J. Revisiting respiratory syncytial virus's interaction with host immunity, towards novel therapeutics. *Cell Mol Life Sci.* 2020;77(24):5045-5058. doi:10.1007/s00018-020-03557-0

Abbreviations

ANOVA	Analysis of Variance
APC	Antigen Presenting Cell
BSA	Bovine Serum Albumin
CCR	Chemokine (C-C motif) Receptor
CoV	Corona Virus
CPE	Cytopathic Effect
DAMP	Danger Associated Molecular Pattern
DAPI	4',6-diamindion-2-phenylindole
DC	Dendritic Cell
DMEM	Dulbecco's Modified Eagle's Media
DMSO	Dimethyl sulfoide
DNA	Deoxyriboncleic Acid
DTT	Dithiothreitol
EGF	Epidermal Growth Factors
eIF2 α	Eukaryotic initiation factor factor 2 α subunit
ELISA	Enzyme-linked Immunosorbent Assay
EV	Empty Vector
FBS	Foetal Bovine Serum

FSC	Forward Scatter
GA	Gestational age
GAS	Gamma Activation Site
GAF	Gamma Activation Factor
GFP	Green Fluorescence Protein
h	Hour
HCV	Hepatitis C Virus
HIPV	Human Parainfluenza Virus
IAV	Influenza A Virus
IFN	Interferon
IFNAR	IFN α Receptor
IFNGR	IFN γ Receptor
IFNLR	IFN λ Receptor
IL	Interlukin
ILC	Innate Lymphoid Cells
IRK	Interferon Regulatory Factor
ISG	Interferon-Stimulated Gene
ISG15	Interferon Sensitive Gene 15

ISGF3	ISG factor 3
ISRE	IFN Sensitive Response Element
JAK	Janus Kinase
LN	Liquid Nitrogen
mDC	Myeloid Dendritic Cell
MFI	Mean Fluorescence Intensity
MHC	Major Histocompatibility Complex
min	Minute
MOI	Multiplicity of Infection
mRNA	Messenger RNA
MxA	Myxovirus Resistance A
NK cell	Natural Killer Cell
NPC	Nuclear Pore Complex
NVRL	National Viral Reference library
OAS	2'5'-oligoadenylate sythetase
P/S	Penicillin and Streptomycin
PAMP	Pattern Associated Molecular Pattern
PBMC	Peripheral Blood Mononuclear Cell
PBS	Phosphate Buffered Saline

PD-L1	Programmed Death-Ligand 1
pDC	Plasmacytoid Dendritic Cell
PFA	Paraformaldehyde
PKR	Protein Kinase R
PMSF	Phenylmethylsulfonyl Fluoride
PRR	Pattern Recognition Receptor
PMT	Post Translational Modifications
PVDF	Polyvinylidene difluoride
RIG-I	Retinoic-acid-inducible Gene 1
RMPI	Roswell Park Memorial Institute
RNA	Ribonucleic acid
RPS15	Ribosomal protein 15
RSV	Respiratory Syncytial Virus
RSV-A2-GFP	RSV A2 strain expressing GFP
RSV- Δ NS-GFP	RSV A2 NS deletion mutant expressing GFP
RT	Room Temperature
RT-qPCR	Real Time Quantitative PCR
SD	Standard Deviation

SEM	Standard Error of the mean
SOCS	Suppressor of Cytokine Singalling
SSC	Side Scatter
STAT	Signal Transducer and Activator of Transcription
TCR	T Cell Receptor
Th Cell	T-Helper Cell
TIR	Toll/Interleukin 1 Receptor
TLR	Toll-Like Receptor
Treg	Regulatory T cell
TYK	Tyrosine Kinase
USP18	Ubiquitin Specific Peptidase 18
VZV	Varicella zoster virus

Contents

Declaration of Authorship	i
Acknowledgements	ii
Abstract	iv
Publications	vi
Abbreviations	vii
1 Introduction	1
1.1 Identification of Respiratory Syncytial Virus	2
1.2 Virology of RSV	4
1.2.1 Viral Structure	4
1.2.2 Pathology	5
1.2.3 Risk Factors for Severe Disease	7
1.2.4 Clinical Treatment of RSV	8
1.3 Immune Clearance of Viruses	11
1.3.1 Pathogen Detection	11
1.3.2 Interferons	12
1.3.3 Nuclear Translocation of STATs	17
1.3.4 IFN Regulation	17
1.3.5 Key ISGs	24
1.3.6 Immune Evasion of RSV and Related Viruses	26
1.3.7 Immune Evasion by RSV Structural Proteins	26
1.3.8 The Immune Evasion by RSV Non-Structural Proteins	29
1.4 Role of Immune Cells in RSV	32
1.4.1 Neutrophils	32

1.4.2	Natural Killer Cells	33
1.4.3	Antigen Presenting Cells	33
1.4.4	Lymphocytes	34
1.5	Research Question	35
1.5.1	Specific Aims	35
2	Materials and Methods	36
2.1	Materials	37
2.1.1	Cell lines	37
2.1.2	Viruses and Constructs	37
2.1.3	Western Blotting Materials	37
2.1.4	Quantative RT-PCR materials	39
2.1.5	Antibodies for Flow Cytometry	39
2.1.6	Cell Culture Reagents	40
2.2	Methods	41
2.2.1	Bioinformatics	41
2.2.2	Plasmid Transformation	41
2.2.3	Plasmid Purification	42
2.2.4	Culture of Cell Lines	42
2.2.5	Viral Propagation	42
2.2.6	Cell Transfection	44
2.2.7	Treatment of Cells	45
2.2.8	Treatment of Cells with Conditioned Media	45
2.2.9	RNA extraction using TRIreagent	45
2.2.10	Reverse Transcription	45
2.2.11	Quantitate Real-Time Polymerase Chain Reaction (RT-qPCR)	46
2.2.12	Western Blotting	47
2.2.13	Confocal Microscopy	48
2.2.14	Quantative Analysis of Confocal Microscopy	49
2.2.15	Patient Criteria	51
2.2.16	Peripheral Blood Mononuclear Cell purification from whole blood	51
2.2.17	Treatment of PBMCs and Staining for Flow Cytometry Analysis	51
2.2.18	Ethical Approval	54
2.2.19	Statistical Analysis	54
3	RSV NS1 and NS2 Reduced Interferon Sensitive Gene Expression in	

both A549 and BEAS 2b Epithelial Cell Lines	60
3.1 Introduction	61
3.2 Specific Aims	64
3.3 Results	65
3.3.1 RSV-NS1 and RSV-NS2 are highly conserved and contain puta- tive E3 ligase domains	65
3.3.2 Expression of NS1 and NS2 in Epithelial Cells	70
3.3.3 The Effect of RSV NS1 and NS2 upon ISG Expression	73
3.3.4 Effect of RSV NS proteins upon SOCS expression in epithelial cell lines	80
3.3.5 The Change in SOCS Levels is Not Linked to Altered Cytokine Response	87
3.3.6 RSV infection alters ISG or SOCS expression dependent on cell line	91
3.4 Discussion	97
4 RSV NS1 enhances STAT activation in BEAS 2b bronchial epithelial cells but not A549 alveolar epithelial cells	101
4.1 Introduction	102
4.2 Specific Aims	103
4.3 Results	104
4.3.1 Expression of NS1 proteins enhance STAT activation, but has no effect on total STAT protein levels in A549 cells	104
4.3.2 Expression of RSV NS proteins increases STAT1 and STAT2 ac- tivation and reduces total STAT2 levels in BEAS 2b cells	112
4.3.3 Transfection with pCI-neo empty vector increases basal ISG levels and renders cells insensitive to IFN α and IFN λ treatment	118
4.3.4 NS1 Expression Limits Nuclear Translocation of STAT1 and Al- ters the Cellular Localization of STAT2	122
4.3.5 STAT1 is reduced with RSV-A2-GFP infection	128
4.4 Discussion	130
5 RSV infection of Peripheral Blood Mononuclear Cells	134
5.1 Introduction	135
5.2 Specific Aims	136
5.3 Results	137
5.3.1 Viability of Frozen Paediatric PBMCs	137

5.3.2	Infection of Adult PBMCs with RSV-A2-GFP	144
5.4	Discussion	157
6	General Discussion and Future Work	160
6.1	General Discussion	161
6.1.1	Introduction	161
6.1.2	NS proteins as E3 ligases	161
6.1.3	Implications of cell line on the function of the RSV NS proteins .	162
6.1.4	RSV NS1 disrupts nuclear translocation of STAT1 and STAT2 . .	163
6.1.5	Implications of RSV infection of immune cells	164
6.1.6	The impact of the COVID-19 pandemic on RSV infections	165
6.1.7	Conclusions	165
6.2	Future Work	168
7	References	169
	A1 Supplementary Figures	207

List of Figures

1.1	RSV positivity annually in Ireland 2019-2022	3
1.2	The Structure of RSV and its genome	5
1.3	IFN Signalling	14
1.4	SOCS Proteins and their Domains	20
1.5	Ubiquitination Mechanism	22
1.6	Schematic of the Th1/Th2 bias in RSV infection	28
2.1	Confocal Quantification Strategy using IMARIS	50
2.2	Gating of CD3+ cells	53
3.1	Sequence alignment of the circulating hRSV-NS1 and hRSV-NS2 protein sequences, with the RSV-A2/long strain sequence.	67
3.2	Sequence alignment of the RSV-NS1 and RSV-NS2 constructs used in our study	68
3.3	Sequence alignment of the circulating hRSV-NS1 and hRSV-NS2 protein sequences, with the bRSV-NS1 and bRSV-NS2	69
3.4	Expression levels of RSV-NS1 and NS2 after transfection of A549 cells .	71
3.5	Expression levels of RSV-NS1 and NS2 after transfection of BEAS-2b cells	72
3.6	The effect of RSV NS1 and NS2 on ISG expression in A549 epithelial cells.	75
3.7	The effect of RSV NS1 and NS2 on ISG expression in BEAS-2b epithelial cells.	76
3.8	Summary of the effect of RSV NS proteins on MxA, PKR, USP18 and ISG15 mRNA	77
3.9	Expression of NS1 reduced MxA protein expression in A549 epithelial cells.	78
3.10	Expression of NS1 reduced USP18, while expression of NS1 and NS2 reduced MxA in BEAS 2b epithelial cells.	79

3.11	Expression of RSV NS proteins alters CIS, SOCS1 and SOCS3 in A549 cells.	82
3.12	Effect of RSV NS protein expression upon SOCS5 and SOCS7 in A549 cells.	83
3.13	Expression of RSV NS proteins reduces SOCS1 in BEAS 2b cells.	84
3.14	Effect of RSV NS proteins expression upon SOCS4, SOCS5 & SOCS7 in BEAS 2b epithelial cells.	85
3.15	Summary of the effect of RSV NS proteins on SOCS expression.	86
3.16	Expression of NS proteins has no impact on IL-6 expression.	88
3.17	Expression of NS proteins has no impact on IFN- λ expression.	89
3.18	Conditioned media from NS1 and NS2 expressing A549 cells does not induce SOCS1 or CIS.	90
3.19	Infection of A549 cells with RSV-A2-GFP.	92
3.20	Infection of BEAS 2b cells with RSV-A2-GFP.	93
3.21	Percentage of GFP expressing cells after infection in RSV-A2-GFP or RSV- Δ NS-GFP.	94
3.22	Infection with RSV-A2-GFP causes an increase in ISG mRNA expression.	95
3.23	Infection with RSV-A2-GFP causes an increase in SOCS mRNA expression.	96
4.1	Expression of RSV NS proteins has no impact on STAT1 phosphorylation in A549 epithelial cells.	106
4.2	Expression of NS proteins has no impact on STAT1 levels in A549 epithelial cells.	107
4.3	Expression of NS proteins has no significant impact on the rate of STAT2 phosphorylation in A549 epithelial cells.	108
4.4	Expression of NS proteins has no impact on STAT2 levels in A549 epithelial cells	109
4.5	NS1 increases STAT1 phosphorylation in A549 epithelial cells	110
4.6	NS transfections have no effect on pSTAT2 or STAT2 levels in A549 epithelial cells.	111
4.7	RSV NS1 increases STAT1 phosphorylation in BEAS-2b epithelial cells.	114
4.8	RSV NS1 increases STAT2 phosphorylation and both NS1 and NS2 decrease STAT2 in BEAS 2b epithelial cells.	115
4.9	STAT2 reduced by RSV NS1 expression at 24h in BEAS 2b epithelial cell	116
4.10	The degradation of STAT2 by RSV NS1 is not reduced by MG132.	117

4.11 IFN α and IFN λ stimulation increases ISG expression in A549 epithelial cells.	119
4.12 Transfection of pCI-neo vector renders A549 cells insensitive to IFN α and IFN λ stimulation	120
4.13 Transfection with Empty Vector pCI-neo increases basal MxA mRNA expression and reduces cells sensitivity to IFN α	121
4.14 Quantification of STAT1 nuclear translocation in BEAS 2b cells by confocal microscopy.	123
4.15 Expression of NS1 limits nuclear translocation of STAT1 in BEAS 2b cells.	124
4.16 Quantification of STAT2 nuclear translocation in BEAS 2b cells by confocal microscopy.	125
4.17 Nuclear translocation of STAT2 is not significantly impacted by IFN α treatment or NS1 expression in BEAS 2b cells.	126
4.18 Expression of NS1 causes STAT2 to localise adjacent to the nucleus.	127
4.19 RSV-A2-GFP infection reduces STAT1.	129
5.1 Flow chart of paediatric samples	139
5.2 Viability of Paediatric PBMCs	141
5.3 Relative abundance of T cells in adults compared to paediatric PBMCs	142
5.4 STAT activation in Paediatric PBMCs.	143
5.5 Confirmation of in vitro RSV infection of primary human immune cells	146
5.6 Gating strategy for adult RSV infected PBMCs	147
5.7 RSV infection in PBMCs	148
5.8 RSV infection in CD3 ⁺ T Cells	149
5.9 RSV infection in CD11c ⁺ and CD56 ⁺ Cells	150
5.10 RSV infection reduces pSTAT1 and pSTAT3 response to IFN α stimulus	151
5.11 RSV infection reduces T cell pSTAT1 response to IFN α stimulus	152
5.12 RSV infection has no impact on CD14 and CD56 cell pSTAT1 response to IFN α stimulus	153
5.13 RSV infection has no significant impact on T cell pSTAT3 response to IFN α stimulus.	154
5.14 RSV infection has no significant impact on CD11c, CD14 and CD56 cell pSTAT3 response to IFN α stimulus	155
5.15 Impact of RSV infection on total STAT1 levels in PBMCs	156

6.1 Comparison of the NS proteins on the JAK-STAT pathway in A549 and BEAS 2b epithelial cells	167
A1.1 RSV infection increases total STAT1 in BEAS 2b cells	207
A1.2 Incubation of BEAS 2b cells with RSV- Δ NS-GFP does not result in substantial infection	208

List of Tables

1.1	Functions of SOCS in Cytokine Regulation	21
1.2	Summary of the Immune Evasion roles of RSV proteins	31
2.1	Western Blotting Antibodies	38
2.2	Western Blotting Materials	39
2.3	Reagents for RT-qPCR	39
2.4	Fluorochrome Conjugated Antibodies for Flow Cytometry	55
2.5	Cell Culture Reagents	56
2.6	Cytokines	56
2.7	Primer Sequences	57
2.8	Phosphatase and Protease Inhibitor Concentration	58
2.9	Resolving Gels	58
2.10	Stacking Gels	58
2.11	Immunohistochemistry Antibodies & Stains	59
2.12	Flow Cytometry Panels	59
5.1	Summary of viral screens from infants in this study with RSV bronchiolitis	140

1 Introduction

1.1 Identification of Respiratory Syncytial Virus

Respiratory syncytial virus (RSV) is an enveloped, negative sense RNA virus within the Pneumoviridae family. It is the leading cause of bronchiolitis in children under 5 years old, globally causing 33.1 million cases of bronchiolitis and around 118,000 associated deaths annually and the leading cause of viral pneumonia (Nair et al., 2010, Shi et al., 2017). RSV was first isolated from laboratory chimpanzees in 1955, but was soon found to be a common human infection (Chanock et al., 1957). In particular, young children and infants are at risk of significant RSV infection, whereas in older children and adults it commonly only results in a mild disease. Severe RSV disease in infancy has been linked with the development of asthma in childhood, with changes in cytokine production and immune cell activation linked with increased asthma risk (Henderson et al., 2005, Fauroux et al., 2017, Scheltema et al., 2018, Korsten et al., 2019). The elderly make up the second major risk group for RSV, with 3-10% of elderly adults at risk of severe infection, depending on the presence of comorbidities (Falsey, 2007, Lee et al., 2013).

RSV spreads readily through direct contact and is widespread in the population; the epicentres of RSV outbreaks are often day care centres and residential care facilities, where those at high-risk come in close contact for prolonged periods. The virus follows a seasonal infection pattern in temperate climates, within Europe the season typically extends from October to January. As the virus thrives in cool temperatures (6.3°C), high humidity, cold, wet winters seeing higher RSV related illness than warm winters (Price et al., 2019). This seasonality is likely also driven by people spending more time indoors during the winter, where crowded areas and low ventilation increase viral spread. It should be noted that during the COVID-19 pandemic the RSV seasons have been markedly different, both in Ireland and globally, with exceptionally low levels of RSV infection in 2020/2021, and a much earlier peak in infection in 2021/2022 as seen in Fig. 1.1. This was likely due to the reduction in social contacts, school closures and reduced household mixing, as well as increased hand hygiene and the use of masks (Agha and Avner, 2021, Williams et al., 2021).

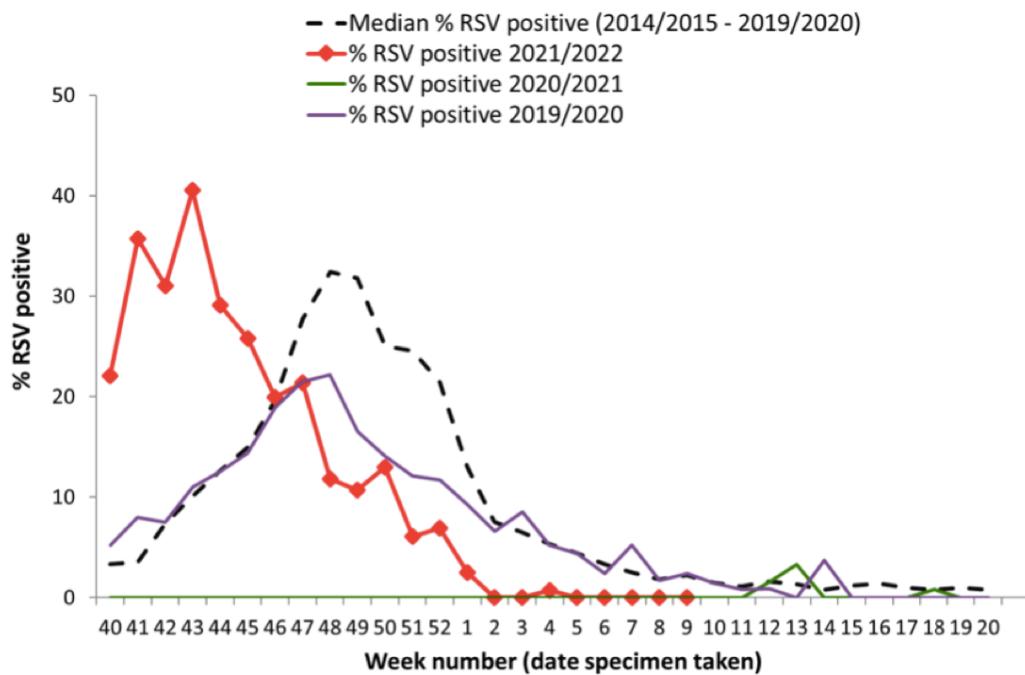


Figure 1.1: RSV positivity annually in Ireland 2019-2022

Data from the Influenza Surveillance Report Weekly Report - Week 9. NVRL non-sentinel RSV positivity by week for 2021/2022, 2020/2021 and 2019/2020 compared to median % RSV positivity (2014-2020) Source: NVRL, 2022

Despite this major global health burden, there remains no curative therapeutics nor vaccines for RSV, with the only licenced treatment being a preventative monoclonal antibody, Synagis (Medimmune, 1999). Unfortunately, Synagis is of limited benefit, as it requires monthly intramuscular injections for the duration of the RSV season. Synagis treatment is costly (€3,400-€5,600 each season) and has questionable efficacy, meaning its use is limited only to high-risk infants and therefore debates over its cost effectiveness continue (Teale et al., 2009, Borse et al., 2014, Shahabi et al., 2018, ElHassan et al., 2006, Mac et al., 2019). Recently a new prophylactic monoclonal antibody treatment, Nirsevimab, has been developed by AstraZeneca and Sanofi Pasteur (Griffin et al., 2020). Nirsevimab targets the pre-fusion form of the RSV F protein and is effective against both A and B strains of the virus; it has shown effective reduction in RSV infections and hospitalizations with a single dose per season (Hammit et al., 2022). There are multiple vaccines for RSV under development, but vaccine-enhanced disease caused by the initial formalin inactivated vaccine stunted RSV vaccine research for several decades (Kim et

al., 1969, Openshaw et al., 2001, Bergeron and Tripp, 2021). As a result, children admitted to hospital with RSV related bronchiolitis receive fluids, humidified oxygen via a nebuliser and suction to keep the airways clear; but no curative anti-viral treatment exists (AAP, 2006, Ralston et al., 2014). It is hoped that improving our understanding of RSV and its immune evasion strategies will lead to the development of new therapeutics and improve outcomes for patients.

1.2 Virology of RSV

1.2.1 Viral Structure

RSV is a 15.2kb negative sense RNA virus, with 10 genes that produce 11 proteins (Fig. 1.2). The viral envelope has three transmembrane proteins: the fusion glycoprotein (F), attachment glycoprotein (G) and the small hydrophobic protein (SH). The other structural proteins are the nucleoprotein (N), large RNA polymerase (L), phosphoprotein (P), matrix protein (M) and transcription factors (M2-1 & M2-2). In addition, RSV produces two non-structural (NS) proteins, NS1 and NS2.

There are two major antigenic strains of RSV, RSV-A and RSV-B, which have distinct epitopes in the F and G proteins, as well as molecular differences in M2, SH and P proteins (Mufson et al., 1985, Johnson et al., 1987a). The G protein shows the most variability within its ectodomain which is variable between RSV-A and RSV-B strains, but a 13 amino acid region in the centre which is well conserved (Johnson et al., 1987b). Both strains co-circulate among populations with alternating dominance (Broberg et al., 2018), with high levels of RSV-A being associated with increased morbidity (Melero and Moore, 2013, Tabatabai et al., 2014, Tan et al., 2013).

Most RSV-infected patients recover after only a mild illness, but it is important to note that a study focused on children under the age of 2 years in the UK reported a small percentage (6.9%) developed acute respiratory infection (ARI) and required hospital admission, 2.7% needed intensive care and 1.5% required a ventilator (Deshpande and Northern, 2003). As the RSV estimated to cause 33.1 million cases of respiratory infection each year, this small percentage of severe cases scales to 3.2 million hospital admissions and a huge number of patients affected globally. Infants and the elderly are particularly at risk of developing severe RSV infection and the burden is highest in low and middle-income countries (Shi et al., 2017).

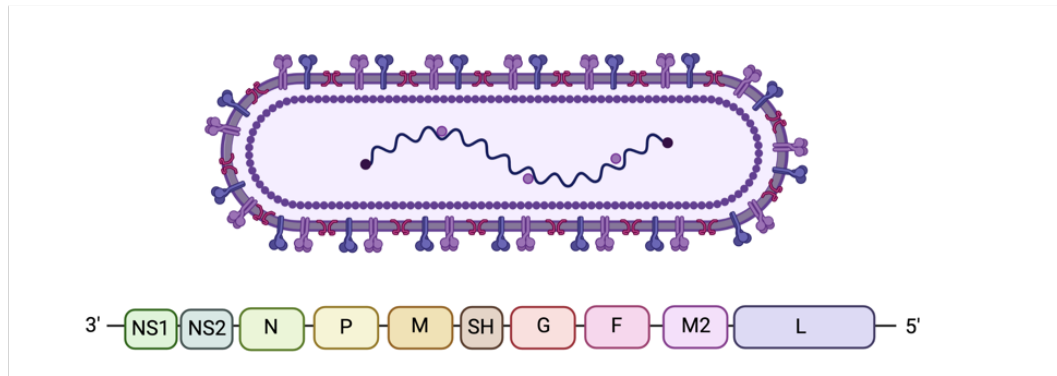


Figure 1.2: The Structure of RSV and its genome

RSV is a 15.2kb negative sense RNA virus, with 10 genes that produce 11 proteins. The viral envelope has three transmembrane proteins: the fusion glycoprotein (F), attachment glycoprotein (G) and the small hydrophobic protein (SH). The other structural proteins are the nucleoprotein (N), large RNA polymerase (L), phosphoprotein (P), matrix protein (M) and transcription factors (M2-1 & M2-2). In addition, RSV produces two non-structural (NS) proteins, NS1 and NS2.

There are two major antigenic strains of RSV, RSV-A and RSV-B, which have distinct epitopes in the F and G proteins, as well as molecular differences in M2, SH and P proteins (Mufson et al., 1985, Johnson et al., 1987a). The G protein shows the most variability within its ectodomain which is variable between RSV-A and RSV-B strains, bar a 13 amino acid region in the centre which is well conserved (Johnson et al., 1987b). Both strains co-circulate among populations with alternating dominance (Broberg et al., 2018), with high levels of RSV-A being associated with increased morbidity (Melero and Moore, 2013, Tabatabai et al., 2014, Tan et al., 2013).

1.2.2 Pathology

RSV is spread by droplet, contact and aerosol transmission and its primary infection site is the respiratory tract epithelium (Kulkarni et al., 2016). Infection can rapidly proceed to the lungs, causing serious disease; with the sloughing of dead cells enabling the virus to spread further into the respiratory airways (Griffiths et al., 2017). Evidence also suggests severe RSV infection in early life increases the likelihood of asthma development (Henderson et al., 2005, Sigurs et al., 2010, Fauroux et al., 2017, Zhang et al., 2022a). Though this phenomenon could also be linked to a genetic predisposition, meaning further, longer-term studies are still needed to fully elucidate this theory (Wu and Hartert,

2011). With a lack of vaccines and effective preventative therapeutics, the spread of RSV infection is limited to basic good hygiene and hand washing; however, the close proximity of individuals at day care centres and schools make these locations the epicentre of RSV outbreaks (Kulkarni et al., 2016, Rodriguez-Fernandez et al., 2017, England, 2016).

The epithelium of the respiratory tract is the primary site of RSV infection. There are multiple receptors on the cell surface that RSV may use to bind, including CX3CR1 (Johnson et al., 2015), ICAM1 (Behera et al., 2001) TLR4 (Marchant et al., 2010), heparan sulphate proteoglycans (HSPGs) (Donalisio et al., 2012) and nucleolin (Tayyari et al., 2011). RSV infects epithelial cells of the respiratory tract (Ioannidis et al., 2012) and the main risk factor for severe RSV infection is age; infants and the elderly are the most at risk, with comorbidities (congenital heart disease, lung disease, diabetes, immunodeficiency and prematurity in the case of infants) adding to the risk (Nair et al., 2010, Griffiths et al., 2017). In healthy adults, with a functional immune response there are multiple degenerate pathways to ensure that the pathogen cannot outrun the immune response; the developing immune system of an infant does not have as many degenerative pathways as an adult, relying heavily on their innate immune response and maternal antibodies to protect against infection (Strunk et al., 2011). In addition to an antibody response efficient clearance of a virus requires a strong Th1 response in order to activate IFN- γ producing cytotoxic T cells (Muraro et al., 2017, Farrar et al., 2002).

Multiple studies have shown that infants with RSV infection have a skewed response, producing a Th2 cytokine profile (Becker, 2006, Lee et al., 2012, Barnes et al., 2022). RSV infection in young infants increases expression of Thymic Stromal Lymphopoietin (TLSP) which has been shown to be vital for immunopathology in mouse models, and has been linked to later asthma development (Malinczak et al., 2019, Lee et al., 2012). TLSP alters T cell differentiation through dendritic cells (DCs), with TLSP primed DCs causing CD4+ T cells to express Th2 characteristic cytokines (Soumelis et al., 2002) (Ziegler et al., 2013). TLSP is also able to induce type two innate lymphoid cells (ILC2) which play a significant role in allergy (Malinczak et al., 2019, McKenzie, 2014).

ILC are innate immune cells which regulate other immune cells and support the immune response by producing cytokines. ILCs are most abundant at mucosal membranes where they interact with commensal microbes and pathogens to regulate the immune response. There are several types of ILCs described based on the cytokines they produce; ILC1,

ILC2 and ILC3. ILC1 activity overlaps with NK cells, though they are less cytolytic. ILC1 express IFN- γ in response to IL-12, IL-15 and IL-18 which act on macrophages and DC causing them to increase their expression of MHC and adhesion molecules (Panda & Colonna 2019). ILC2 secrete type-2 cytokines in response to TSLP, IL-25 and IL-33 (Saravia et al., 2015, Besnard et al., 2011). ILC3 are dominant in the respiratory tract and respond to IL-23 and IL1b, producing IL-22 and IL-17. Of particular interest in RSV, IL-22 acts on epithelial cells in induce secretion of antimicrobial peptides and increase mucus production in goblet cells, the excessive production of mucus can contribute to blocked airways in severe RSV infection. The ability of RSV to increase levels of TSLP and IL-33 and thus promote a Th2 response, may be responsible for negatively influencing the overall antiviral response and the development of post RSV wheeze.

In infants, decreased IFN- γ and CCL5 expression with enhanced IL-17 expression in nasal mucosa samples correlated to more severe disease (Thwaites et al., 2018). IFN- γ is released by mucosal epithelial cells and immune cells to stimulate the expression of antiviral ISGs (Muraro et al., 2017). CCL5 is a chemoattractant which recruits T cell, monocytes and eosinophils to the area to clear infection (Culley et al., 2006). IL-17 causes the mobilization of neutrophils to the area, with high levels of neutrophil infiltration associated with more significant RSV infection in adults (Habibi et al., 2020). The protective effect of reduced CCL5 and IFN- γ indicates that some of the damage caused during RSV infection is caused by the excessive immune cell recruitment and activity. In adults, IL-4, IL-6, IL-13, IL-33 and IL-10 are all elevated in the nasal mucosal swabs of patients with symptomatic RSV, similar cytokine enhancement is seen in plasma samples with IL-6, IL-10, IL-12, IL-13 and IL-15 all increased in RSV cases compared to healthy controls (Barnes et al., 2022).

1.2.3 Risk Factors for Severe Disease

Prematurity, defined as a birth before 37 weeks gestational age (GA), is a significant risk factor in developing severe RSV (Nair et al., 2010). The lungs of the foetus reach a critical developmental point at around 38 weeks GA, before this point the surface area of the alveolar sacs is very much smaller than in the lungs of a fully developed foetus (Smith et al., 2010). In combination with this, the bronchial lumens are not sufficiently developed, being narrower and therefore more likely to be blocked by mucus produced in response to infection, leading to reduced air flow, poor gas exchange in the alveoli and low blood oxygen levels (Smith et al., 2010). The primary cause of RSV pathogenicity is inflammation of the bronchioles, caused by the release of cytokines including IFNs,

and the over-production of mucus that can block the bronchioles restricting airflow (Griffiths et al., 2017). Interestingly, the sex of the infant is also linked to postnatal lung development, with female infants tending to have smaller lungs, with fewer bronchioles, which mature faster than males (Gern et al., 2006). These sex-related differences are particularly important in the case of RSV as the risk of severe infection is greater in males than females (Chu et al., 2017).

As mentioned, as well as children, the burden of RSV illness is also significant in the elderly population, with 3-10% of adults contracting an RSV lower respiratory tract infection (LRTI) in the USA each year (Falsey, 2007, Lee et al., 2013). The mean age of adults admitted to hospital with RSV LRTI is 75 years, with the average length of stay being 13 days (Lee et al., 2013). The rate of elderly infections are increased if they live in a residential facility or have frequent contact with children (Falsey, 2007). Elderly patients often have additional comorbidities, which enhance their risk of developing severe RSV infection. In addition to this, the elderly have a reduced immune output; immune function diminishes with age through a process known as immunosenescence, leading to decreased cytokine production and dysregulated immune cell migration (Fulop et al., 2017). Immunosenescence is a general term for a spectrum of effects; it varies between individuals and the level of immune function loss is reliant on health and activity of the individual. In general it refers to a decrease in overall T cell numbers, a shift to a Th2 type cytokine profile, an increase in natural killer (NK) cell numbers (but a decrease in their function), defects in macrophage activity and increased IL-6 production (Ginaldi et al., 2001, Aiello et al., 2019). This impaired immune response allows pathogens to easily infect tissues and cells, leading to enhanced pathogenesis. Adults admitted to hospital with RSV LRTI and a combination of these factors have a >10% mortality rate. Furthermore, these factors often lead to extended hospital stays, which in turn, increase the likelihood of contracting hospital-acquired infections, such as Methicillin-resistant *Staphylococcus aureus* (MRSA), which can be fatal for older patients (van Hal et al., 2012).

1.2.4 Clinical Treatment of RSV

Struggles in Vaccine Design and Vaccine Enhanced Disease

RSV vaccine research began soon after the virus was first isolated in 1956, but has proven challenging. The 1966 trial of a formalin-inactivated RSV vaccine (FI-RSV), caused antibody enhanced RSV disease (ERD) and sensitised children to the virus, leading to

severe disease in the immunised cohort. Ultimately this resulted in hospitalisations and the death of two children (Kim et al., 1969, Openshaw et al., 2001, Acosta et al., 2015). This failure of the FI-RSV vaccine instilled caution over new RSV vaccines. However, research continued, focusing instead on the immune evasion and modulatory mechanisms of RSV; generating significant developments in our understanding of the virus.

More recently an RSV vaccine has been revisited by several groups, with subunit and attenuated vaccines thought to be viable options. Subunit vaccines can be used to stimulate a strong antibody response to external epitopes of RSV, particularly the F protein (Anderson et al., 2013). Several attenuated strains have been produced which lack the NS1 and 2, SH, or M2 proteins, highlighting the important role of these proteins in pathogenicity and viral replication (Karron et al., 1997, McFarland et al., 2018, Teng et al., 2000, Whitehead et al., 1999). To date none of these have reached target end points.

Part of the challenge of an RSV vaccine lies in its target groups: the two main risk groups for severe RSV have different requirements from a vaccine. Young infants (>6 months of age) have an immature response with limited IFN and TLR signalling (Delgado et al., 2009). This impacts the cytokine milieu, often leading to a T helper (Th)2 cell response over a Th1 response; this limits efficient viral clearance and can cause immunopathology. The second risk group are those over 70 years of age. The elderly often have reduced vaccine responses, making the highly immunogenic subunit a good option. For protection of infants maternal RSV vaccines have been investigated, with vaccines designed to be given to mothers in their third trimester (Beugeling et al., 2019). These should increase the levels of RSV antibodies available for passive transfer to the infant, offering protection from birth. This is a potentially attractive option as RSV is most severe in children under six months; indeed modelling has shown a maternal RSV vaccine could have a significant impact on hospitalisations (Hogan et al., 2017). There have been multiple maternal vaccine candidates, though none have successfully completed clinical trials (Novavax, 2018, Madhi et al., 2020), however a vaccine candidate developed by Pfizer, RSVpreF, has shown promising results in phase 1 and 2 study and has been granted breakthrough therapy designation by the US food and drug administration (Walsh et al., 2022).

RSV presents a challenging pathogen to control. Several high-risk patient groups would particularly benefit from an effective RSV treatment. Indeed, RSV can be fatal for neonates and immunocompromised individuals, for whom any vaccines offer little protection. It is RSV's multiple "anti-immune" effects, that cloud our current understanding.

Therefore, increased knowledge of RSV's cellular and molecular interactions and subversive mechanisms are fundamental in facilitating future drug and vaccine design.

Development of anti-RSV Drugs

Children who arrive in hospital with RSV related bronchiolitis currently have limited treatment options. In the first instance they are given humidified air and bronchodilators; while bronchodilators are not a recommended treatment for RSV, this allows for a differential diagnosis of an asthma attack (Gadomski and Brower, 2010, Ralston et al., 2014). Ribavirin is the only anti-viral drug on the market for use against RSV, though it is currently not recommended by the American Association of Paediatrics, and guidelines vary between regions (Eiland, 2009, AAP, 2006, HSPC, 2019, Ralston et al., 2014, Schmidt and Varga, 2017). First developed in 1972, Ribavirin is a guanosine analogue, which limits replication of several RNA and DNA viruses. While originally licenced for treatment of RSV, its most significant use has been in the management of Hepatitis C Virus (HCV) (Te et al., 2007). In HCV treatment, Ribavirin is used to good effect in conjunction with other drugs, including the anti-viral cytokine, IFN α (Te et al., 2007, Gonzalez et al., 2012, Thomas et al., 2012). While not widely prescribed, Ribavirin can be used in severe RSV cases (Eiland, 2009, HSPC, 2019).

Early on in the treatment of RSV intravenous immunoglobulins (RSV-IGIV) were given to patients. This was manufactured from neutralizing antibodies from donors, and helped to drive the antibody dependent immune response. However, RSV-IGIV had limited effectiveness and high cost (Groothuis et al., 1993, Rodriguez et al., 1997). A prophylactic preventative anti-RSV antibody, Palivizumab, has been available since 1998. Produced by MedImmune, this monoclonal antibody is administered through monthly intramuscular injections during the RSV season and is 50 times more potent than the RSV-IGIV (Medimmune, 1999). Accurately measuring the effectiveness of Palivizumab has proved difficult, as it is given prophylactically. Evidence suggests that Palivizumab significantly reduces RSV-related hospitalisations (Anderson et al., 2017, Morris et al., 2009, Wegzyn et al., 2014). However, it has been shown to be cost effective in only a small population (Shahabi et al., 2018, Mac et al., 2019, ElHassan et al., 2006) and has no impact on subsequent wheezing (Scheltema et al., 2018). Additionally, as Palivizumab is a monoclonal antibody if the target epitope of the virus changes it will no longer be effective; to date three strains have been identified that are resistant to Palivizumab (Hashimoto and Hosoya, 2017, Pandya et al., 2019). Updated guidelines from the American Academy of Paediatrics stated that Palivizumab "has limited effect on RSV hospitalizations on a

population basis, no measurable effect on mortality, and a minimal effect on subsequent wheezing” (AAP, 2014). Palivizumab’s expensive cost (between €3,400-€5,600 over the season) generally constrains its use to only high risk children, including infants born prematurely, those with congenital heart disease (CHD) or chronic lung disease (CLD) (Welliver et al., 2010, Nuijten et al., 2009, Whelan et al., 2016a). A randomized trial has shown that Palivizumab should not be used as treatment; administering Palivizumab to infants with RSV bronchiolitis had no impact on outcomes (Alansari et al., 2019). Palivizumab’s effectiveness and cost are major limiting factors in its use against RSV; therefore, global research aims must remain focussed on development of an effective treatment and preventative vaccine.

The high cost and monthly injections required for palivizumab have made it difficult to roll out its use beyond the most vulnerable infants. However, the development of the Nirsevimab, which completed clinical trials in March 2022, could make prophylactic treatment more accessible (Hammitt et al., 2022). Nirsevimab is a stabilized monoclonal antibody that provides protection from both RSV infection and associated hospitalisations and can be given as a single dose prior to the start of the RSV season. Produced by AstraZeneca and Sanofi Pasteur, Nirsevimab binds the pre-fusion form of the RSV F proteins in both RSV-A and RSV-B strains (Hammitt et al., 2022). Nirsevimab recently received approval from the European Medicines Agency (EMA), the cost of treatment has not yet been announced, but it could greatly limit the burden of RSV infection (AstraZeneca, 2022).

1.3 Immune Clearance of Viruses

1.3.1 Pathogen Detection

The immune response to pathogens is highly organised and tightly controlled. Broadly, it can be split into two branches: the innate and adaptive response. The innate response is semi-specific, responding quickly to pathogen associated molecular patterns (PAMPs) and damage associated molecular patterns (DAMPs) (Janeway and Medzhitov, 2002). Included in the innate response are neutrophils and NK cells, with antigen presenting cells (APCs), such as macrophages and dendritic cells (DCs), acting to span the innate and adaptive response by activating lymphocytes (Chaplin, 2010). The initial fast response of innate immunity gives time for the adaptive response to form, with lymphocytes undergoing clonal selection for the specific pathogen, producing antigen-specific T cells and B cells (Chaplin, 2010). T cells migrate to the site of infection and differentiate

into several subsets determined by the cytokine milieu. Once mature, B cells produce antigen specific antibodies creating immune memory (Chaplin, 2010).

Viral dsRNA detection

The Toll-like receptors (TLRs) are a family of 10 pathogen recognition receptors (PRRs) which drive the innate response to various types of infection (Kumar et al., 2011). Viral infections are detected through endosomal TLR3 and TLR7, which detect double stranded (ds)RNA and single stranded (ss)RNA respectively. Once a PAMP is bound by its TLR, the TLR undergoes a conformational change allowing signal transduction proteins such as MyD88 to bind. This begins a signalling cascade ending in the activation of the transcription factor NF- κ B and expression of NF- κ B responsive genes (Kawai and Akira, 2010). The MyD88 pathway is used by all TLRs (except TLR3) and is responsible for the production of key inflammatory cytokines, including TNF and IL-1. Alongside the MyD88 pathway, there is also a MyD88 independent pathway which instead uses TIR domain-containing adaptor inducing IFN- β (TRIF) (Kawasaki and Kawai, 2014). The TRIF-dependent pathway is utilised by TLR3 and TLR4, and results in the activation of the transcription factor Interferon Regulatory Factor (IRF)-3, which upregulates expression of Type I IFNs. In addition to TLR3, dsRNA can also be recognised in the cytoplasm by several dsRNA sensors, Protein Kinase R (PKR), Retinoic acid-inducible gene I (RIG-I) and Melanoma Differentiation-Associated protein 5 (MDA5); these molecules are activated by dsRNA and cause activation of NF- κ B and IRF3 which also promote Type I IFNs transcription (Brisse and Ly, 2019, Lee and Ashkar, 2018).

1.3.2 Interferons

IFNs are a family of cytokines that stimulate a host of antiviral and regulatory genes. Although they share common signalling pathways, variation in expression of receptors alters which cells are able to respond to them (Schneider et al., 2014). Use of different IFN subtypes gives a malleable and nuanced immune response, which can respond to infections without causing excessive damage to host tissues (de Weerd and Nguyen, 2012).

Broadly IFNs are split into three subgroups based on which receptors they signal through; each of these have their own role in shaping the immune response. All IFNs share a conserved α -helical bundle, but have little sequence homology outside this region (de Weerd and Nguyen, 2012). The different classes of IFNs have varying tissue expression;

all cell types are responsive to and can produce IFN-I, though during infection pDCs are the most important source of IFN-I (Hagberg et al., 2011, Arimoto et al., 2018). T cells and NK cells produce IFN-II, while IFN-III has been seen to be produced in the epithelial cells of the intestine and lung (Sommereyans et al., 2008, Mordstein et al., 2008). Each IFN type has its own family of class II alpha helical receptors. The IFN receptors (IFNAR1, IFNAR2, IFNGR1, IFNG2, IFNLR1, IL10R) have differential tissue expression, allowing tissue specific response to IFNs (de Weerd and Nguyen, 2012).

Type I IFN - A Far Reaching Defence

The induction of Type I IFNs is key in the generation of a fast acting, transient, antiviral defence, with over 500 ISGs upregulated in response to IFN stimulation. Type I IFNs can be produced by most cells types and acts in an autocrine and paracrine manner, driving the immune response to a pathogen by acting on immune cells, such as NK cells, while also causing the upregulation of anti-viral genes in the infected cells. Type I IFNs are a family of structurally similar cytokines, IFN- α (of which there are 13 subtypes), and IFN- β , IFN- ϵ , IFN- χ , IFN- ω , IFN- σ , IFN- ξ , and IFN- τ (Gibbert et al., 2013). Each of these is able to bind the IFN alpha receptor (IFNAR) which is composed of two chains, IFNAR1 and IFNAR2. In canonical type I-induced signalling the binding of IFN causes the transphosphorylation and activation of Janus Kinase 1 (JAK1) and Tyrosine Kinase 2 (TYK2), which phosphorylate the IFNAR tails, providing docking sites for Signal Transducers and Activators of Transcription (STAT)1 and STAT2 (Fig. 1.3).

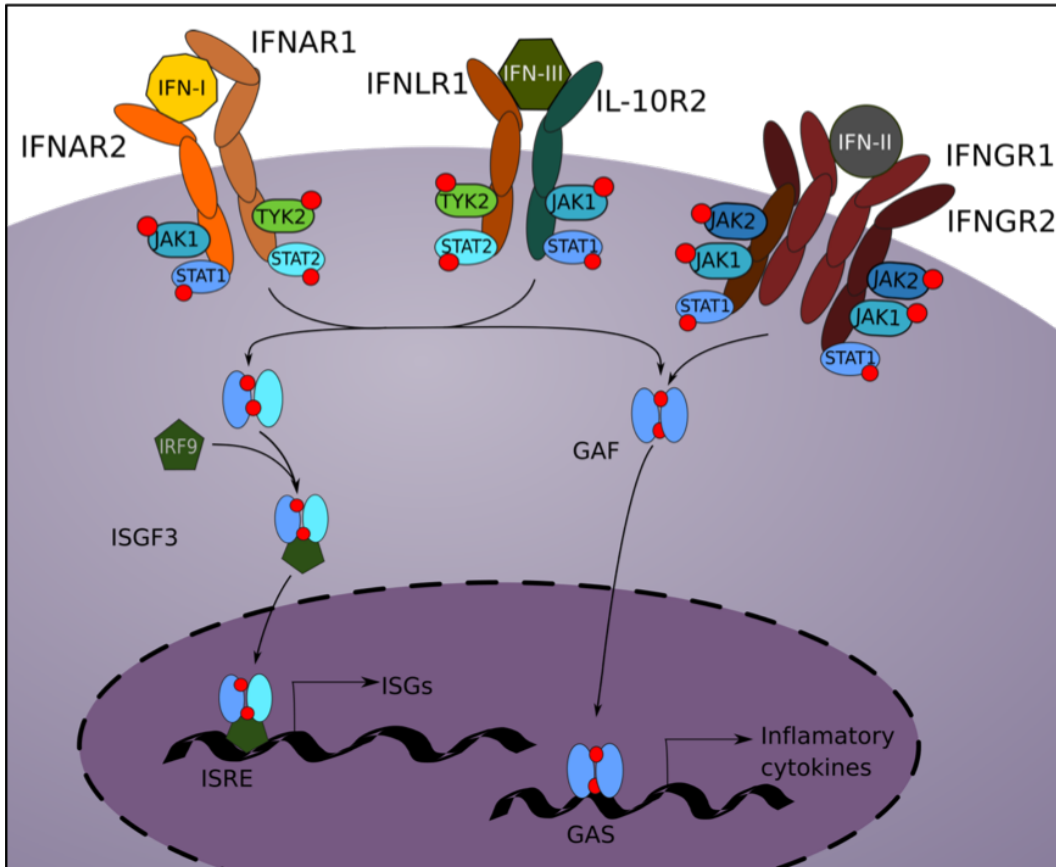


Figure 1.3: IFN Signalling

Binding of the cognate ligand causes a conformational change in the cytoplasmic tail of the receptor. Associated JAKs are activated, further phosphorylating the receptor tails, creating docking sites for STATs. Once bound the STATs are phosphorylated allowing them to form dimers. STAT1:STAT2 heterodimers associate with IRF9 to form the ISGF3 transcription factor, while STAT1 homodimers form the GAF transcription factor. These act on ISRE and GAS promoter regions respectively, causing the expression of over 500 ISGs.

The kinases phosphorylate STAT1 and STAT2 promoting dimerization. Heterodimers of STAT1:STAT2 are most common, which interact with IFN-regulatory factor 9 (IRF9) to form the IFN-stimulated gene factor 3 (ISGF3) transcription factor. ISGF3 then translocates to the nucleus and binds IFN Sensitive Response Element (ISRE) regions within the gene promoters. ISRE is defined as 5'-AGTTTCNNTTTCN-3' where N can be any nucleotide. STAT2 can also interact with IRF9 in the absence of STAT1 to form an ISGF3-like transcription factor, also promoting ISRE containing genes (Ivashkiv and Donlin, 2014). As well as the STAT1:STAT2 heterodimers, STAT1:STAT1 homodimers can also form after IFN-I stimulation. The STAT1 homodimer, known as Gamma activating factor (GAF) acts as a transcription factor for the genes containing a Gamma IFN Activation Site (GAS) promoter, defined as 5-TTCNNGAA-3, to induce pro-inflammatory genes. In this way IFN-I is able to induce the expression of over 500 ISGs, many of which have antiviral functions, including MxA, OAS1-3 and ISG15, which act to inhibit various stages of the viral life cycle (Michalska et al., 2018). IFN-I have been used therapeutically since the mid 1990's, revolutionising the treatment of HCV and multiple sclerosis (Filipi and Jack, 2020, Rong and Perelson, 2010).

Type II IFN - Shaping the Response

Type II IFN contains only one family member, IFN- γ , which signals through the tetrameric IFNGR, formed from two IFNGR1 and two IFNGR2 subunits. IFN-II is a highly pleiotropic protein which acts to direct the adaptive and innate immune cellular response, as well as increasing ISG expression. When IFN-II is bound by its receptor the JAKs associated with the IFNGR, JAK1 and JAK2, transphosphorylate and activate, phosphorylating the IFNGR cytoplasmic tails to provide docking sites for STAT1 (Fig. 1.3). Once bound to the receptor tails STAT1 is phosphorylated by the associated JAKs and forms GAF, which translocate to the nucleus to cause the upregulation of GAS containing genes including SOCS1, PKR and IRF1 as described above (Michalska et al., 2018, Lee and Ashkar, 2018). Importantly, while most cells are able to produce and respond to IFN-I, only a subset of immune cells produce and respond to IFN- γ (Green et al., 2017). As a result, the effect of IFN- γ is focused on shaping the cellular immune response. The primary producers of IFN- γ are NK and T cells, with antigen presenting cells (APCs) the most responsive to IFN- γ stimulation (Lee and Ashkar, 2018, Martin-Fontecha et al., 2004). When IFN- γ acts on APCs, such as monocytes, macrophages and dendritic cells (DCs) it enhances antigen presentation, increases DC maturation and the expression of the co-stimulatory CD80, allowing effective priming of Th1 cells (Goldszmid et al., 2012).

Additionally, IFN- γ stimulation acts to polarise macrophages to a pro-inflammatory M1 type, increasing expression of proinflammatory cytokines such as IL-1b, IL-12 and TNF, providing a Th1 supporting milieu and resulting in a robust antiviral response (Wang et al., 2018, Mills et al., 2000, Wu et al., 2014).

Proper IFN- γ function can also protect against inappropriate immune response through the regulation of IL-33 expression. This is particularly important during respiratory infections, including RSV and influenza A (IAV), as IL-33 increases levels of innate lymphoid cells (ILC)2, which supports a Th2 type response and has been associated with the development of allergic asthma (Duster et al., 2018, Besnard et al., 2011). Investigations using both RSV and IAV in mice have shown that ablation of IFN- γ increases ILC2 activity in the lungs, leading to increased lung pathology (Califano et al., 2018, Stier et al., 2017).

Type III IFN - Protecting the Barriers

The final family of interferons are type III IFNs (IFN-III). This is made up for four members, IFN- λ 1, IFN- λ 2, IFN- λ 3 and IFN- λ 4. These all signal through the IFNLR which is made up of two receptor chains: IFNLR1 and IL10R2. The response of IFN- λ is broadly similar to IFN-I; as with type I IFN, binding of IFN-III to the receptor causes activation of JAK1 and TYK2 and the phosphorylation of STAT1 and STAT2. As with IFN-I, this leads to ISGF3 and GAF formation and the expression of a host of ISGs (Figure. 1.2).

Much like IFN-I, type III IFNs induce an anti-viral state. However, while IFN-I are recognised by almost all nucleated cell types, IFN-III can only be detected by a subset of cells, typically those in the mucosal membranes, as well as macrophages, lymphocytes, pDCs and epithelial cells (Zhou et al., 2018). This response is controlled by restricted expression of IFN-III receptors which allows enhanced response in specific targets without stimulating neighbouring cells, which could lead to inappropriate and damaging immune response. The restricted response to IFN-III may allow it to act only in high risk areas, creating a localised immune response which can clear a pathogen, but is unlikely to cause immunopathology (Wack et al., 2015, Broggi et al., 2020). Most mucosal membranes have been shown to be responsive to IFN-III, with the respiratory tract, gut and genitals all expressing IFNLR. Both type I and III IFNs are produced by and can act on airway epithelial cells, revealing type III IFN's importance in the context of viral respiratory infections (Zhou et al., 2018, Major et al., 2020). Indeed, IFN-III is the predominant

IFN in the nasal epithelium during viral infection (Okabayashi et al., 2011), and has been shown to play an important role in immune responses to both Influenza A virus (IAV) and RSV infection (Kalinowski et al., 2018, Klinkhammer et al., 2018, Hillyer et al., 2017, Hillyer et al., 2018).

1.3.3 Nuclear Translocation of STATs

For the STAT complexes to act as transcription factors they must travel to the nucleus, where they bind exposed GAS or ISRE promoter regions. The complexes are larger than 35kDa and cannot pass through the nuclear membrane, requiring active transport to move through the nuclear pore complex (NPC) (Shen et al., 2021, McBride et al., 2002). To facilitate this Importin- α binds exposed nuclear localization sequences (NLS) and recruits importin- β to the complex. Importin- β interacts with multiple phenylalanine-glycine repeats on the NPC, allowing importin- β and its cargo into the nucleus. The cargo protein is separated from the importins in a GTP-dependent manner; importin- α is removed from the nucleus by cellular apoptosis susceptibility gene product (CAS) and importin- β /RanGTP is recycled to the cytoplasm. This releases the STAT complex, allowing it to bind a promoter regions and induce gene expression. The movement of STAT into the nucleus can happen without phosphorylation, but it is much less efficient than transport of phosphorylated STAT (Majoros et al., 2017). Any disruptions to this process can affect normal trafficking of STATs and related inducible gene expression. Several viruses, including Nipah V virus (Rodriguez et al., 2002), Varicella zoster virus (VZV) (Nagel et al., 2014), Hepatitis B virus (HBV) (Mitra et al., 2019), SARS-CoV (Zhang et al., 2022b) and SARS-CoV-2 (Wang et al., 2021), have been shown to impact nuclear transport. This can be a result of hijacking cellular machinery, or specifically limiting host antiviral response.

1.3.4 IFN Regulation

IFNs are potent anti-viral effector molecules and are tightly regulated. IFN signalling initiates a classical negative-feedback loop, which prevents excessive ISG induction, thereby preventing a cytokine storm and damage. There are multiple negative regulators of IFN signalling, including phosphatases, receptor gene down-regulation, receptor endocytosis, proteolytic degradation of the receptor and suppressor of cytokine signalling (SOCS) proteins (de Weerd and Nguyen, 2012, Ivashkiv and Donlin, 2014). The IFN signalling pathway can also be regulated through post-translational modifications (PTM), such as

dephosphorylation and ubiquitination.

Phosphorylation

The addition of a phosphate group to serine, threonine and tyrosine residues alters how the proteins can interact with downstream signalling effector molecules. Multiple points of the JAK-STAT pathway are regulated by phosphorylation state. Dephosphorylation is performed by phosphatases, which remove activating phosphate groups from signalling molecules (such as the STATs), and thus curtailing downstream signal transduction. The Src homology phosphatases (SHP)1 & 2, negatively regulate IFN-1 signalling. SHP1 achieves this by dephosphorylating JAK1 and STAT1 (David et al., 1995), while SHP2 dephosphorylates JAK1, STAT1, and STAT2 (You et al., 1999). This prevents JAK's kinase activity and prevents the dimerisation of the STAT proteins, limiting the signalling cascade.

Suppressors of Cytokine Signalling

The SOCS proteins are a family of 8 related proteins which act to regulate several signalling pathways, and are the principle regulators of the JAK/STAT pathway. All members of the SOCS family share a conserved SH2 domain, which is able to bind phosphotyrosine residues, and a SOCS-box domain at the carboxyl-terminus and an amino terminal domain which can recruit E3 ligase complexes to ubiquitinate target proteins. In addition to these conserved domains, SOCS1 and SOCS3 also contain a kinase inhibitory region (KIR) domain; this allow these SOCS to engage directly with the JAK substrate binding domain, as a pseudosubstrate, to limit its action (Kershaw et al., 2013, Liao et al., 2018). SOCS3 and CIS also contain a unstructured PEST domain, a region which is rich in proline (P), glutamic acid (E), serine (S) and threonine (T) residues. The PEST domain limits the half-life of the SOCS protein, promoting a faster turnover rate, aiding regulation (Babon et al., 2006).

The SOCS proteins bind phosphorylated tyrosine residues through the SH2 domain on either the IFN receptor or the JAK proteins which inhibits the phosphorylation of STAT proteins, limiting signal transduction. SOCS proteins are able to direct the ubiquitination of proteins through the SOCS-box domain leading to their proteasomal degradation, to reduce the number of kinases available and so limit STAT activation (Schneider et al., 2014). High basal levels of SOCS can limit the cells sensitivity to IFNs, reducing their ability to enter an effective antiviral state (Hong and Carmichael, 2013).

The degree of similarity between SOCS proteins is significant, showing their degenerate function and shared domains (Fig. 1.4). That said, each SOCS has been shown to have distinct roles; for example, SOCS2 is vital in the regulation of growth hormone signalling, with SOCS2 deletion in mice leading to 30-40% growth advantage over wild type pups (Metcalf et al., 2000). Selective deletion of SOCS1 and SOCS3 in mouse models of rheumatoid arthritis predictably cause an increase in inflammation; however, this inflammation is caused by distinct pathologies, with SOCS1 leading to greater monocyte infiltration and SOCS3 leading to greater neutrophil infiltration (Wong et al., 2006, Egan et al., 2003). SOCS1 is also the most potent SOCS, and has been shown to inhibit IFN- $\alpha/\beta/\gamma$, IL-12 and IL-23, IL-4 and IL-13 and IL-2 family cytokines (Liau et al., 2018).

CIS regulates signalling pathways that involved STAT3, STAT5 and STAT6. Mice unable to express CIS have increased airway inflammation and eosinophil enhanced pulmonary disease (Yang et al., 2013). This is due to the crucial role of CIS in effective T cell differentiation, in the absence of CIS naïve T cells cannot regulate the IL-2 signalling though STAT5 and IL-4/IL-13 signalling through STAT6, which results in Th2 polarisation (Yang et al., 2013). The enhanced differentiation of Th2 cells results in an increase in IL-13 production which drives eosinophilia in CIS knockout mice. CIS primary controls the activity of STAT5 which is used by a host of cytokine signalling pathways, listed above. As a result, the activity of CIS is involved in NK cell differentiation (Bernard et al., 2022), DC and macrophage development (Miah et al., 2012). CIS also regulates TCR signalling though the exact mechanism is unknown (Palmer et al., 2015).

While SOCS1-3 and CIS have clear roles in cytokine signalling the remaining family members, SOCS4-7 are more important in the control of receptor tyrosine kinases, regulating growth factors and insulin (Sobah et al., 2021). The deletion of SOCS5 and SOCS6 show no obvious phenotype. Initial studies of SOCS4 show it has an important role in controlling cytokine storm and potentially regulates T cell receptor (TCR) activation (Kedzierski et al., 2014, Ren et al., 2019), though further investigations are needed. The broad spectrum of SOCS effects is still being discovered, but these well conserved proteins are clearly vital in cytokine regulation (Table 1.1). Ultimately, increased levels of SOCS lead to a reduction in IFN signalling by reducing the activity of JAK or targeting signalling molecules for ubiquitination and proteasomal degradation.

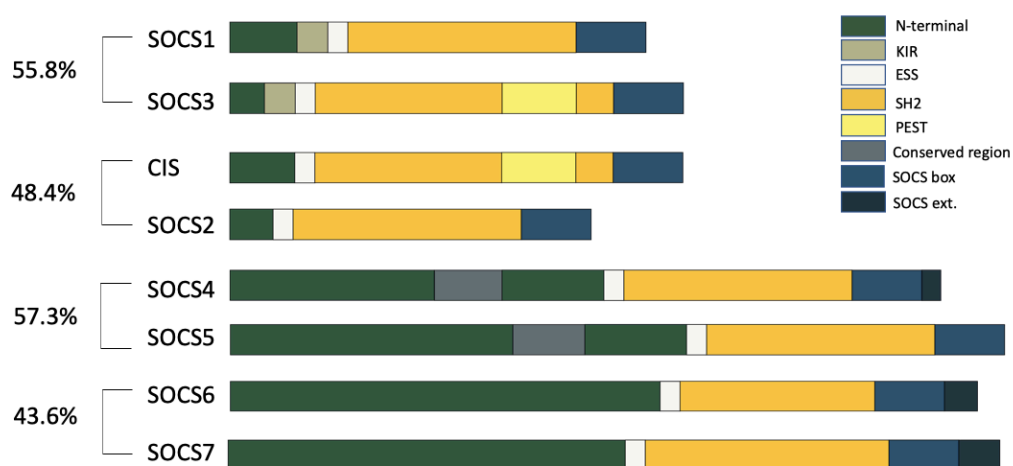


Figure 1.4: SOCS Proteins and their Domains

The SOCS proteins contain multiple conserved domains that determine their function. SOCS1 and SOCS3 have Kinase Inhibitory Region (KIR) domains, SOCS3 and CIS contain PEST domains which reduce stability of these SOCS proteins. SOCS4 and SOCS5 both contain a conserved region, SOCS4, SOCS6 and SOCS7 all contain an extended SOCS domain (SOCS ext) at the C terminal end. All the SOCS proteins contain a conserved N-terminal, Src Homology 2 (SH2), extended SH2 (ESS) and SOCS box domains. The SOCS are shown in pairs based on the similarity of the amino acid sequence. Conserved domains are distinguished by colour as described in the key.

Ubiquitination and Proteasomal Degradation

Ubiquitination of target proteins can either induce functionality or mark proteins for proteasomal degradation, depending on the linkage structure of ubiquitin chains. Ubiquitin (Ub) is an 8kDa protein containing seven lysine (Lys) residues, which are covalently linked to proteins. Ub chains linked by either Lys29 or Lys48 mark the target protein for proteasomal degradation, while ubiquitin chains linked by Lys63 will activate the target protein. The addition of ubiquitin can also affect the cellular localisation of proteins, with monoubiquitination allowing proteins to be identified for trafficking by late endosomal compartment, known as multivesicular bodies (Katzmann et al., 2002). As well as effecting cell localization, the Ub chains are themselves able to interact with other Ub chains and proteins, enhancing protein-protein interaction (Haglund and Dikic, 2005). Ubiquitination is reversible, with deubiquitylating enzymes (DUBs), able to remove Ub molecules to alter the fate of the protein (Liu et al., 2018). Three enzymes catalyse the

Table 1.1: Functions of SOCS in Cytokine Regulation

SOCS	Cytokine Regulated	Reference
SOCS1	IFN I, IFN III, IL-12, IL-2	Liau et al., 2018
SOCS2	Growth hormone, prolactin, G-CSF, IL-6	Morris et al., 2018
SOCS3	IL-6, G-CSF, leptin, IL-12	Babon and Nicola, 2012
SOCS4	Epidermal Growth factor (EGF)	Kedzierski et al., 2014
SOCS5	EGF, IL-6, IL-4	Kedzierski et al., 2017
SOCS6	None, role in Cancer	Lin et al., 2013
SOCS7	IFN I	Noguchi et al., 2013
CIS	IL-2, IL-4, IL-15	Morris et al., 2018

addition of Ub monomers to the target protein as summarised in Fig. 1.5: Ub-activating enzyme (E1), Ub-conjugating enzymes (E2) and Ub-protein ligases (E3). In humans there are only two E1s, which chemically activate Ub in an ATP-dependent manner, binding it to the E1 by a thioester bond (Bulatov and Ciulli, 2015).

E1 provides the ubiquitin-adenylate intermediate which is passed to an E2 enzyme (Pickart, 2001). There are 37 E2 enzymes, though all share a conserved central domain of approximately 150 amino acids that contains the catalytic site. The variable regions of E2 determine which E3 it can interact with, as a result E2 all have distinct roles. The specificity of the ubiquitination comes from the E3 enzyme, of which there are over 600 in humans. The E3 binds the target protein and then covalently links the Ub molecule to the target. Despite their diversity, all known E3s are classed as either homologous with E6-associated protein C-Terminus (HECT) or Really Interesting New Gene (RING) domain E3s, these two families follow different catalytic models and have little conservation (Berndsen and Wolberger, 2014).

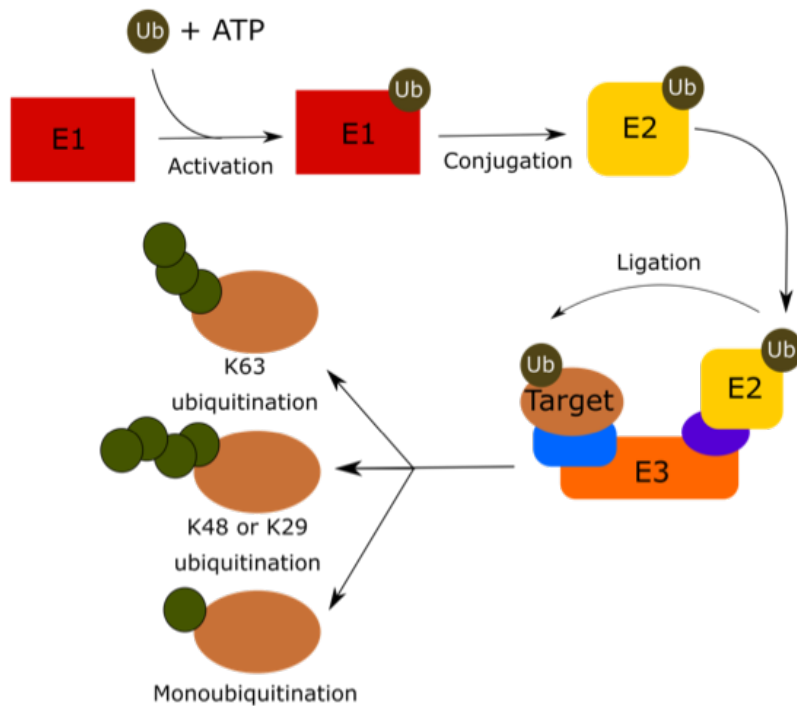


Figure 1.5: Ubiquitination Mechanism

Ubiquitin is added in a stepwise manner through 3 enzymes. Ub is activated by E1 in an ATP dependent reaction. This is then conjugated to one of 37 E2 proteins, which can interact with one of 600 E3 ligases. Here a RING E3 is shown, which can directly add the Ub molecule to the target protein. Ub molecules can be added as monomers (identifying proteins for trafficking), Lysine (K)63 linked Ub chains (activating the target protein) or K48 or K29 linked chains (which lead to proteosomal degradation of the target protein).

The RING E3s are the most abundant in humans, with 200 different types identified (Bulatov and Ciulli, 2015). They are able to transfer the Ub from the E2 directly to the target protein, while the HECT E3s must transfer the Ub to a catalytic cysteine on the E3 before moving it to the target protein (Fig. 1.5). RING E3s are made up of a combination of different subunits, allowing the large diversity needed to selectively ubiquitinate specific proteins. Briefly, RING-E3s are made up of a receptor and adaptor proteins, linked to a cullin scaffold and a RING-box domain. There are multiple proteins which can be recruited into the E3 ligase structure, making it a highly specific structure (Bulatov and Ciulli, 2015).

STAT and U-STAT Signalling

There are seven members of the STAT family STAT1-5a, 5b and STAT-7, all of which have a role in signalling. STAT3 can be phosphorylated by cytokines which receptors interact with TYK2, including IFN-I, IL-6, EPO and EGF. However, it appears to be redundant in IFN signalling, likely due to its transient activation (Tsai et al., 2019). Instead, the role of STAT3 maybe in nuanced regulation of JAK/STAT (Tsai et al., 2019, Wang et al., 2011). Once phosphorylated STAT3 is able to form heterodimers with STAT1, depleting it from the cytoplasm, thus reducing the formation of both GAF and ISGF3 transcription factors (Ho and Ivashkiv, 2006). This function likely limits the risk of a hyper-inflammatory response. Additionally, STAT3 can interact with transcriptional repressors such as Phospholipid Scramblase 2 (PLSCR2) which limits ISGF3 interaction with ISRE promoters, preventing ISG production (Tsai and Lee, 2018). However, viral targeting of STAT3 suggests it may be involved in the antiviral response; both hepatitis C virus (HCV) and mumps reduce levels of STAT3 by proteasomal degradation (Ulane et al., 2003, Stevenson et al., 2013), and STAT3 has been shown to be key in the expression of a subset of ISGs (Mahony et al., 2017). Based on this, it is likely that STAT3 functions as a finely tuned mediator of the IFN response, both able to suppress ISG expression through sequestering STAT1 and blocking ISRE activation, and also enhancing a subset of ISGs during viral infection. STAT4 is expressed in lymphoid tissues and is involved in IFN-I, IL-12 and IL-23 signalling (Nguyen et al., 2002, Philips et al., 2022). STAT5A and STAT5B are highly homologous proteins which are activated by a range of cytokines including IL-2, IL-3, GM-CSF, and IL-5 (Able et al., 2017). The final STAT to be identified was STAT6 which is phosphorylated after IL-4 stimulation. When phosphorylated all STATs bind to specific promoter regions of DNA to stimulate gene expression (Philips et al., 2022).

Further regulation of the JAK/STAT pathway may come from unphosphorylated STATs. In the canonical JAK/STAT pathway STATs are thought of as inert, waiting to be activated so they can form dimers and translocate to the nucleus. In reality STATs may have a more dynamic role; there is evidence for STATs being able to promote ISGs in the absence of IFN stimulation (Wang et al., 2017, Michalska et al., 2018, Nan et al., 2018) and stabilise heterochromatin structure (Yan et al., 2011). When cells are stimulated with low levels of exogenous IFN there is an increase in levels of STAT1, STAT2 and IRF9, among other proteins. Higher levels of JAK/STAT signalling components allow more STATs to be activated (pSTAT), providing a more robust ISG response if those cells are re-stimulated, making them less vulnerable to viral infections. However, it's also been

shown that increasing levels of STAT1, STAT2 and IRF9, independent of IFN stimulation, can increase the expression of a subset of ISGs, and that unphosphorylated STAT1 is able to bind to promoter regions of ISGs (Wang et al., 2017, Cheon and Stark, 2009). In addition to canonical signalling, STAT2 also has a regulatory role (Ho et al., 2016). This is achieved through semi phosphorylated binding where unphosphorylated STAT2 (U-STAT2) binds a pSTAT1 molecule in an antiparallel conformation stopping their interaction with importin α , preventing nuclear import (Ho et al., 2016). Additionally, U-STAT2 can also complex with IRF9 to form U-STAT2:IRF9 which can dimerise and cause ISRE controlled gene expression in the absence of IFN stimulation. In response to IFN stimulation this can readily moves to a classic ISGF3 complex (pSTAT1:pSTAT2:IRF9) (Platanitis et al., 2019).

The phosphorylation of STATs allows them to form stable dimers, but the formation of transient dimers and nuclear localization is possible without phosphorylation. This offers the possibility that unphosphorylated STATs can control ISG expression, in particular basal levels of ISGs.

1.3.5 Key ISGs

Those genes which are upregulated in response to IFNs are collectively known as ISGs. Some of ISGs are involved in regulation of the JAK/STAT pathway; SOCS, STATs and IRFs are all upregulated by IFNs, as described previously. Many ISGs have a direct antiviral function; the antiviral genes target multiple points of the viral life cycle, or are involved in viral detection in an effort to enhance the antiviral response and limit replication. Polymorphisms in a host of ISGs has been linked with poor virus clearance, highlighting the importance of the IFN response (Knapp et al., 2003, Choi et al., 2015). While there are over 500 transcripts defined as ISGs (Schneider et al., 2014), in this thesis we have focused on four well characterised ISG to measure the ISG response. These each function in different ways to limit viral replication.

The Myxovirus resistance genes, MxA and MxB, are small GTPases which prevent viral replication. MxA oligomerises to create ring-like structures around the virus particle (Haller and Kochs, 2011). The interaction of the MxA rings activates their GTPase activity, leading to the degradation of viral structures. Though the full mechanism of MxA has yet to be defined, the oligomerisation is key, with mutations that prevent oligomers ablating MxA activity (Gao et al., 2010). Although a paralog of MxA, MxB does not have the same widespread antiviral function, though it does have a role in

targeting the HIV-1 viral capsid (Kane et al., 2013) and restricts Herpesvirus replication (Cramer et al., 2018). MxB has a cytoplasmic and nuclear form, caused by alternative splicing at the carboxy tail which removes a nuclear localization sequence.

Protein Kinase R (PKR) acts as a non-specific dsRNA sensor. When multiple PKR monomers bind dsRNA the PKR auto-phosphorylates to expose its kinase domains and phosphorylates the translation initiation factor eIF2 α (Gal-Ben-Ari et al., 2018, Lemaire et al., 2008). The phosphorylation of eIF2 α impairs its ability to recycle between successive rounds of translation initiation, leading to a slowdown of translation and eventually resulting in the cessation of cellular and viral protein synthesis (Schulz et al., 2010, Dar et al., 2005). The importance of PKR in viral infection is underscored by a 2003 study, which showed that polymorphisms in PKR correlate with HCV infection outcome (Knapp et al., 2003).

Interferon Stimulated Gene 15 (ISG15) has been known to be upregulated by IFN since early research into IFN and ISGs (Perng and Lenschow, 2018, Korant et al., 1984). Despite its long association with the antiviral response, its function has taken time to elucidate. A member of the ubiquitin family, ISG15 can be conjugated to lysine residues in a number of target proteins including IFIT1, MxA, PKR, RIG-I and IRF3 (Perng and Lenschow, 2018, Zhao et al., 2005, Giannakopoulos et al., 2005). The addition of ISG15 modulates the function or stability of the target protein, for example ISGylation of PKR enhances its ability to phosphorylate eIF2 α stifling protein synthesis (Okumura et al., 2013); while ISGylation of activated IRF3, an important transcription factor, inhibits its degradation (Zhang et al., 2015, Shi et al., 2010). ISGylation can be reversed by Ubiquitin specific protease 18 (USP18), another ISG discussed below (Malakhov et al., 2002, Basters et al., 2017). ISG15 has also been implicated in the disruption the viral budding of viruses from the cell, including HIV-1 and Ebola, with ISG15 exerting its activity by modulating viral proteins (Okumura et al., 2006, Okumura et al., 2008). ISG15 can also be secreted, inducing NK cell proliferation, and act as a chemotactic factor to recruit neutrophils to the site of infection (Werneke et al., 2011, D’Cunha et al., 1996, Owhashi et al., 2003). Overall, the increased expression of ISG15 upon IFN stimulation increases antiviral activity by enhancing the functionality of a range of ISGs, interrupting viral protein function, and recruiting immune cells to the area.

Ubiquitin-specific protease 18 (USP18) is significantly upregulated in response to IFN-I, IFN-III, TNF and LPS. USP18 holds two independent functions to modulate the IFN response; regulating IFN receptor activity and reversing ISGylation. At a receptor

level USP18 negatively regulates IFN signalling by binding to IFNAR2 receptor, competing with JAK1 for binding sites, reducing the activation of JAK1 and down regulating STAT activation (Malakhova et al., 2006, Honke et al., 2016). The specificity of USP18 to IFNAR2 results in specific regulation of the IFN-I signalling (Francois-Newton et al., 2011). Independent from this, USP18 also acts as a protease, reversing ISGylation by cleaving ISG15 from a range of proteins (Basters et al., 2017, Malakhov et al., 2002). The effect of ISGylation often enhances the anti-viral role of other ISGs, USP18 nullifies this effect, attenuating the IFN response. Interestingly, while USP18 reverses ISGylation, USP18 itself is stabilised by ISG15 and this is essential to its function as a IFN regulator (Speer et al., 2016).

1.3.6 Immune Evasion of RSV and Related Viruses

In order to survive in the host, all pathogens must be able to avoid and regulate the immune response. RSV has evolved several techniques to limit or misdirect the immune response of the host (Gonzalez et al., 2008, Lambert et al., 2014). As a result, RSV elicits a limited antibody response in its hosts, allowing repeat infections, even within the same season (Yamaji et al., 2016, Gonzalez et al., 2008). RSV also affects the type of immune response generated, with the virus able to skew the immune response from an anti-viral type 1 response, towards a type 2 response (Fig. 1.6) (Legg et al., 2003, Barnes et al., 2022, Zhu et al., 2010). This misdirection reduces the efficiency of viral clearance, allowing RSV to go unhindered and continue replicating in and infecting other host cells. Of the 11 proteins RSV produces, five have been linked to immunomodulation (Table 1.2).

1.3.7 Immune Evasion by RSV Structural Proteins

RSV F

The primary role of the F protein is fusion between the virion and the cell membrane. The F protein can interact with a number of attachment proteins on the cell surface and once it has bound a membrane protein a conformational change is triggered, forcing the fusion on the membranes and allowing viral entry into the cell. The targeting of the F protein by antibodies should create protective immunity, as seen by the success of Palivizumab and Nirsevimab (Eiland, 2009, Hammitt et al., 2022). However, variable regions within the F protein allow antigenic change between seasons limiting antibody effectiveness (Beeler and van Wyke Coelingh, 1989). In addition, the RSV F can also be

detected by TLR4 leading to IL-6 production and the netosis of neutrophils (Rallabhandi et al., 2012, Kurt-Jones et al., 2000, Funchal et al., 2015).

RSV G

The RSV G exists as both a membrane bound protein and soluble (s)G which lacks a transmembrane domain and is secreted by the virus (Bukreyev et al., 2012). The membrane bound G proteins primary role is the adherence of the virus to the target cell through its CXCR1 domain; deletion of the RSV G protein severely attenuates the virus and limits its infection (Chirkova et al., 2013, Chirkova et al., 2015, Karron et al., 1997). The sG protein can bind the CXCL10 chemokine, impacting immune cell migration (Tripp et al., 2001). The G protein is the most highly variable protein of RSV and is heavily glycosylated, limiting the immune memory response (Rudd et al., 2001, Johnson et al., 1987b). In addition to this, the RSV protein has also been implicated in altering the T cell response to RSV (Tripp et al., 1999, Boyoglu-Barnum et al., 2014).

RSV SH and N

The SH protein acts as an ion channel and limits the response of infected cells to cytokine stimulation and prevents apoptosis in infected cells (Fuentes et al., 2007, Russell et al., 2015, Gan et al., 2012). Though the role of SH is not fully understood SH deletion mutants are severely attenuated and have been put forward as possible vaccination strains (Karron et al., 1997, Jin et al., 2000, Russell et al., 2015). The RSV genome is coated in N protein which complexes as decameric rings (Bakker et al., 2013). The N protein interacts with each other and the negative-sense RNA, creating a flexible left handed helix with the RNA nestled between the grooves (Bakker et al., 2013). The N protein provides protection for the viral RNA, and is also necessary for replications and transcription (Cao et al., 2021). In addition to its structural role the N protein also has a role in immune evasion, limiting the formation of the immunological synapses, thus reducing T cell activation (Cespedes et al., 2014). Furthermore, N has been seen to colocalize with RIG-I and mitochondrial antiviral signalling (MAVS) proteins within viral inclusion bodies, inhibiting IFN expression (Lifland et al., 2012).

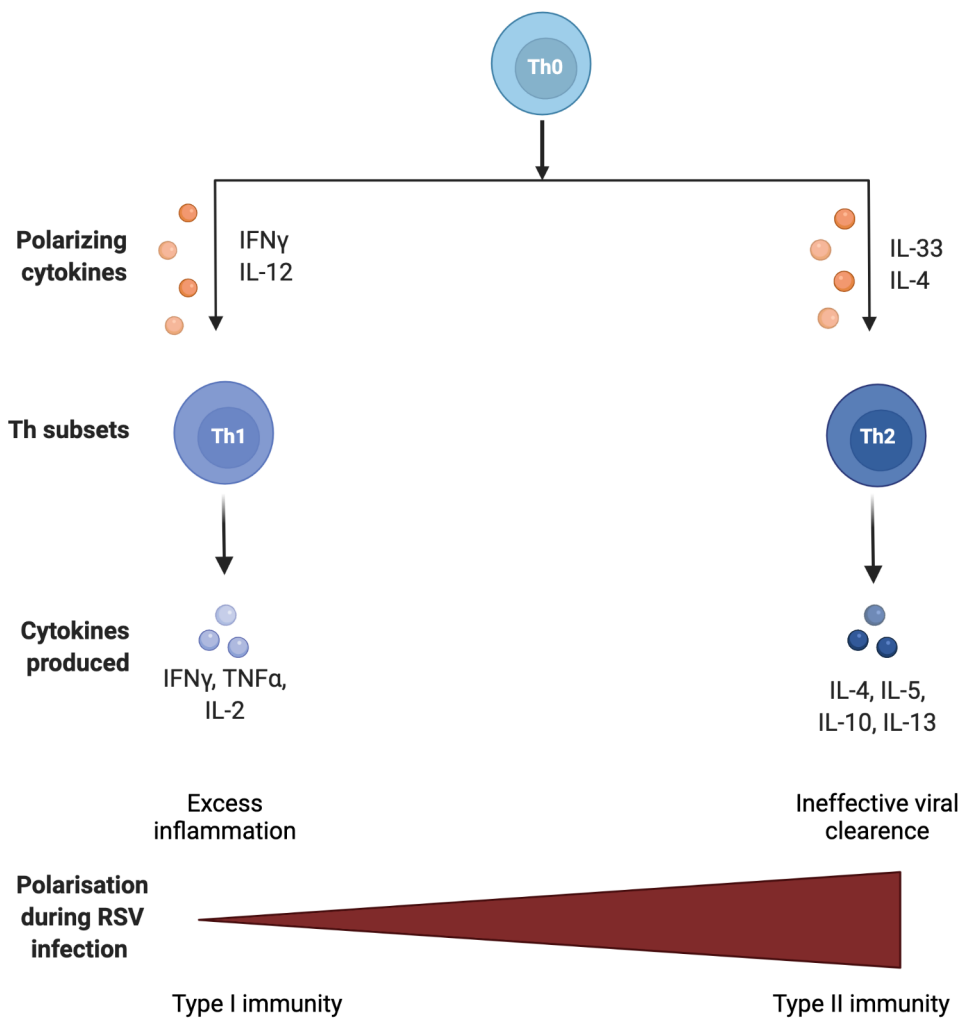


Figure 1.6: Schematic of the Th1/Th2 bias in RSV infection

During RSV infection elevated levels of "type II" cytokines can be measured in the airways. This bias towards a Th2 type response hampers viral clearance and could result in inappropriate immune response, resulting in the development of allergy.

1.3.8 The Immune Evasion by RSV Non-Structural Proteins

NS1 and NS2 of RSV are not essential for viral growth, but have been shown to play a significant role in blocking immune signal transduction. These two proteins show little sequence homology, except for a short region at the C-terminus (Bitko et al., 2007), though are both documented to suppress JAK/STAT signalling (Zhang et al., 2005, Elliott et al., 2007, Lo et al., 2005, Ramaswamy et al., 2006).

RSV NS1

The NS1 protein has been shown to have several immune evasion mechanisms. NS1 acts as a cellular E3 ligase, which enables the selective targeting of STAT2 for ubiquitination and proteasome-mediated degradation (Elliott et al., 2007, Spann et al., 2005). In removing cellular STAT2, RSV acts to limit anti-viral JAK/STAT signalling, thereby attenuating the normal function of Type 1 IFNs, ultimately reducing ISG transcription in 293T cells (Elliott et al., 2007). The presence of NS1 has been seen to modulate the T cell response, reducing the number anti-viral CD8+ T cells and Th17 cells, while also bolstering the activation of Th2 cells, which, when uncontrolled, progresses the physiological symptoms of disease (Munir et al., 2011, Becker, 2006). Typically, the symptoms of RSV (wheezing, fever, coughing and congested or runny nose) are as a result of enhanced mucus production caused by infection and poor oxygen exchange in the lungs. Inappropriate immune activation, in this instance the recruitment of eosinophils, mast cells and Th2 cells, do little to clear the infection and in fact cause greater pathogenicity (Becker, 2006). NS1 also induces SOCS1 and SOCS3, negative regulators of JAK-STAT signalling (Xu et al., 2014, Zheng et al., 2015). NS1 can also impact gene expression of infected cells, reducing microRNA 24 (miR-24) levels to suppress cell cycle arrest (Bakre et al., 2015) and directly interacting with enhancers and promoters in the nucleus to alter gene expression early in infection (Pei et al., 2021).

RSV NS2

NS2 also plays an important role in viral replication. RSV lacking NS2 have been shown to display small plaque morphology *in vitro* and reduced viral growth kinetics in the Hep2 cell line. Using Δ NS1, Δ NS2 and Δ NS1/2 RSV strains, it has been reported that both NS1 and NS2 proteins lowered RSV titres in mice 100-fold (Kotelkin et al., 2006).

In addition to limiting IFN signalling, NS2 also stimulates the phosphoinositide 3-kinase (PI3K) pathway, leading to delayed cell death and enhanced cell survival in A549 cells.

This prevents the action of NK and CD8⁺ T cells to induce apoptosis, allowing the virus to continue replicating in the infected cell (Bitko et al., 2007). RSV NS2 is also able to upregulate the expression of the programmed cell death ligand, PD-L1, allowing infected cells to attenuate CD8 T cell-mediated killing (Telcian et al., 2011), showing the virus uses multiple mechanisms to limit cell death. As well as the direct ubiquitination of STAT2, NS1 and NS2 have been linked to the reduction of several signalling molecules, including RIG-I, IRF3, TRAF3 and IKK ϵ (Ling et al., 2009, Swedan et al., 2009, Ren et al., 2011). NS2 has also been directly linked to the ubiquitination and degradation of STAT2 (Whelan et al., 2016b). This study was carried out in HEK93T cells, which are derived from human embryonic kidney cells. Investigating these effects in respiratory epithelial cells is necessary to confirm these effects during normal RSV infection.

While NS1 and NS2 together severely impair the IFN response in humans, the exact mechanism used to limit IFN signalling is not fully understood.

Table 1.2: Summary of the Immune Evasion roles of RSV proteins

RSV Protein	Primary Function	Immune Evasion Function
F	Fusion Protein	Contains variable regions to limit immune memory response between strains (Beeler and van Wyke Coelingh, 1989).
G	Attachment to cell membrane	Heavily glycosylated, limiting recognition by antibodies (Rudd et al., 2001). Contains variable regions to limit immune memory response between strains (Johnson and Collins, 1988). CXC3R1 binding ability (Chirkova et al., 2013). Soluble 'decoy' form to limit immune cell migration (Bukreyev et al., 2012, Tripp et al., 2001). Promotes a Th2 response (Tripp et al., 1999, Boyoglu-Barnum et al., 2014).
SH	Ion Channel	Reduces TNF α sensitivity (Fuentes et al., 2007). Reduces IL-1 β sensitivity (Russell et al., 2015). Inhibition of apoptosis (Fuentes et al., 2007). Disruption of cell surface membrane (Perez et al., 1997, Rixon et al., 2004).
N	Nucleoprotein	Co-localised with RIG-I & MAVS to attenuate IFN response (Lifland et al., 2012). Impairs immunological synapse formation (Céspedes et al., 2014).
NS1	Immune Evasion	Limits IFN signalling (Jin et al., 2000, Zhang et al., 2005, Elliott et al., 2007, Lo et al., 2005, Spann et al., 2005, Swedan et al., 2009). Targets STAT2 for ubiquitination and degradation (Elliott et al., 2007, Lo et al., 2005, Spann et al., 2005). Co-localised with MAVS to attenuated the IFN response (Boyapalle et al., 2012).
NS2	Immune Evasion	Limits IFN signalling (Jin et al., 2000, Zhang et al., 2005, Kotelkin et al., 2006, Ling et al., 2009, Swedan et al., 2009). Limits CD8+ memory (Kotelkin et al., 2006). Delays cell death (Bitko et al., 2007).

1.4 Role of Immune Cells in RSV

During RSV infection circulating immune cells have an important role in controlling infection. The innate immune cells are recruited to the area by the release of chemokines from infected cells and local immune cells, which first detect the infection in the mucosa. This allows for a semi-specific immune response driven by the stimulation of PRRs. These innate cells begin to target infected cells, inducing cell death to limit viral replication, as well as inducing anti-viral gene expression in the surrounding cells, by producing IFNs and IL-33, which increase ISG expression and mucus production by goblet cells to trap shedding viral particles. Several innate immune cells act as APCs, such as macrophages and DCs, which arrive at the site of infection and become activated by viral PAMPS. The APCs will take-up RSV by phagocytosis, the virus is broken down within the endosome and viral antigens are processed for presentation. The APCs then travel to the lymph nodes where they present the processed RSV antigens via MHC receptors to naïve T and B cells, beginning the development of the adaptive immune response. Once the T and B cells have been activated and undergo clonal selection, they too will travel to the site of infection. The T cells then differentiate into a range of effector cells with specific functions to clear the infection. An effective response from circulating immune cells is key to stopping the spread of a viral infection and providing immune memory to limit reinfections.

1.4.1 Neutrophils

The first immune cells to respond to a viral infection in the respiratory tract are polymorphonuclear leukocytes (PMNs). This includes neutrophils, eosinophils, basophils and mast cells, with neutrophils comprising the up to 80-93% of innate immune cells in infant bronchoalveolar lavage (Everard et al., 1994, McNamara et al., 2003). The influx of neutrophils is likely due to an upregulation of the neutrophil chemokine IL-8, caused by RSV F protein stimulation of TLR4 (Funchal et al., 2015). While neutrophils have an important role in controlling infection, excessive neutrophil activity can damage epithelial cell integrity (Deng et al., 2020) and has been linked to more RSV severe disease (Johnson et al., 2007, Stokes et al., 2013), though other have found an inverse correlation (Kirsebom et al., 2020, Linssen et al., 2022). While the precise role of neutrophils in RSV infection is still being investigated, the timing of neutrophil recruitment is likely to be a factor in their impact, with a fast neutrophil response being protective, but if the infection is left unresolved it may become symptomatic (Tahamtan et al., 2021).

1.4.2 Natural Killer Cells

Natural killer (NK) cells are a cytotoxic innate immune cell able to induce cell death without prior exposure to an antigen (Abel et al., 2018). NK cells are activated by the binding of an antibody to a Fc gamma receptor, which itself is bound to a virally infected cell. This causes antibody dependent cell mediated cytotoxicity (ADCC) with the release of granzymes and perforins, which break down the cell membrane of the infected cell causing it to lyse (Smyth et al., 2005). Infants with RSV infection have lower activation of NK cells, resulting in reduced IFN- γ production, compared to healthy children (van Erp et al., 2020). NK cells can also trigger cell death by binding Fas on the infected cell via the Fas ligand (FasL) (Smyth et al., 2005).

1.4.3 Antigen Presenting Cells

Antigen presenting cells (APCs) are a group of immune cells including macrophages, DCs and B cells which display antigen through major histocompatibility complexes (MHC), providing a link between the innate and adaptive immune response. Specialised local APCs which reside in the respiratory tract, such as alveolar macrophages and plasmacytoid DCs (pDCs), constantly sample their surroundings through macropinocytosis and through PRRs on their surface that recognise pathogenic markers (Musumeci et al., 2019, Murray and Wynn, 2011). When a pathogen, such as RSV, is detected these cells release cytokines and chemokines to attract other immune cells, initiating the immune response. pDCs are the most significant producer of IFN-I and III, which act on immune cells and surrounding epithelial cells, to induce ISG expression making them more resistant to infection (Musumeci et al., 2019). Activated APCs will also migrate to the local lymph nodes where they interact with naïve lymphocytes. A lymphocyte with a cognate receptor to the antigen presented via the MHC will form an immunological synapse with the APC and receive secondary activation signals, triggering its maturation (Smith-Garvin et al., 2009).

The activity of APC is vitally important in both the immediate response to the pathogen and the creating of robust immune memory to limit future infections. RSV infection of DCs is able to block the formation of the immunological synapse and so prevent T cell activation (Gonzalez et al., 2008, Gonzalez et al., 2017), and RSV replication has been shown to upregulate the expression of macrophage migration inhibitory factor (MIF), resulting in altered cytokine production in alveolar macrophages (de Souza et al., 2019).

1.4.4 Lymphocytes

Within the lymph node naïve lymphocytes will interact with APCs by presenting antigen. CD4⁺ cells can interact with the antigen presented through the MHC class II and form a synapse with the APC and be activated by secondary signals, such as CD40. MHC class I interacts with CD8⁺ cells (Smith-Garvin et al., 2009). Activated lymphocytes will undergo clonal selection to produce a highly specific T cell receptor (TCR). Clonally selected CD4⁺ T cells differentiate into mature CD4⁺ T cells (Th0) and migrate to the site of infection to act against the pathogen. During this time the Th0 cells are exposed to cytokines which cause them to polarise to a more specialised Th type (Zhu et al., 2010). There are a spectrum of CD4⁺ T cell subsets, however the Th1 and Th2 cells play a particular role in RSV infection and so will be the focus of this section. The polarisation towards a Th1 or Th2 phenotype depends on which cytokines the Th0 cell is exposed to (Zhu et al., 2010). This has a lasting implication for the clearance of infection; Th1 cells will produce IFN- γ , TNF and IL-2, resulting in the type I immune response driving phagocytosis and viral clearance; while Th2 cells produce IL-4, IL-6, IL10, and IL-33 resulting in type II immunity, better adapted for the removal of large parasites such as helminths this increases mucus production and enhances IgE class switch by B cells (Lloyd and Snelgrove, 2018, Spellberg and Edwards, 2001). During RSV a type II immune response is typically seen (Fig. 1.6), with increased mucus and IL-33 during RSV infection (Nikonova et al., 2021, Wu et al., 2020, Barnes et al., 2022). This changes the cytokine milieu surrounding the infection site, altering both the recruitment of other immune cells and delaying viral clearance. In all infections a balance must be struck between a type I and type II immune response, during RSV infection the enhanced type II response leads to limited T cell mediated viral clearance.

The activity of all cells is ultimately controlled by signalling pathways. Any corruption of these will have a profound effect on the efficiency of the immune response. To date investigations have shown that RSV NS proteins can impact the signalling in cell lines, thereby reducing the JAK-STAT signalling but the exact mechanism of this remains debated, nor is it known whether the same effect can be seen in circulating immune cells.

1.5 Research Question

RSV is known to limit the immune response, both of the infected cell and disrupting immune cell activity. While there are several RSV proteins that have been shown to have an anti-immune effect, the non-structural proteins NS1 and NS2 have been shown to target the JAK-STAT pathway in a number of ways, depending on the cell type. As epithelial cells are the primary target of RSV infection we endeavoured to investigate the mechanism behind the NS inhibition of IFN α in cell lines representative of the upper respiratory track.

In addition to this the impact of RSV on immune cells is understudied; though RSV has been shown to affect immune cell behaviour, the specific effects of RSV have only been investigated in a subset of immune cells. Quantifying if RSV is able to infect immune cells, and if this has any impact on the activity of the JAK-STAT pathway, will also inform on the potential mechanism used by RSV to reduce immune cell activity observed by others.

Ultimately, better understanding of how RSV limits the immune signalling through the JAK-STAT pathway could inform future drug design and improve outcomes for those with severe infections.

1.5.1 Specific Aims

- To measure the impact of RSV NS expression on antiviral ISGs in A549 and BEAS 2b epithelial cell lines.
- Determine the mechanism for NS inhibition of JAK-STAT in a respiratory epithelial cell line.
- Investigate the impact of RSV infection on circulating immune cells.

2 Materials and Methods

2.1 Materials

General laboratory materials purchased from Sigma-Aldrich (USA) unless otherwise specified.

2.1.1 Cell lines

The A549 cell line was a kind gift from Dr. Siobhan Gargan (Trinity College, Dublin). The Hep2, BEAS 2b, and Vero cell lines were a kind gift from Prof. Ultan Power (Queen's University Belfast, UK).

2.1.2 Viruses and Constructs

The RSV-NS1 and RSV-NS2 plasmids were a kind gift from Dr. Monika Bajore (Pasteur Institute, Paris), both ampicillin resistant in the pCI-neo vector. The pCI-neo empty vector was purchased from Promega, USA. GFP expressing RSV-A2 (RSV-A2-GFP) and the NS1 and NS2 deletion mutant (RSV- Δ NS1/2-GFP) were kindly provided by Prof. Mike Teng (University of South Florida, USA).

2.1.3 Western Blotting Materials

All chemicals used for western blotting were purchased from Sigma-Aldrich (USA) unless otherwise specified. Anti-pSTAT1, anti-pSTAT2, anti-STAT1 and anti-STAT2 were purchased from Cell Signalling Technology (USA). Anti- β -actin was purchased from Sigma (USA). Anti-NS1 and anti-NS2 were kindly provided by Prof. Mike Teng (University of South Florida, USA). Secondary rabbit and mouse were purchased from Fisher (USA). Blots for STAT, pSTAT, SOCS5 and SOCS6 were run on a 10% denaturing polyacrylamide gel. Blots for NS1, NS2, SOCS1, SOCS2 and SOCS3 were run on a 16% denaturing polyacrylamide gel. All gels used a 10% polyacrylamide stacking gel. A full list of Western Blotting antibodies and materials can be found in Tables 2.1 and 2.2 respectively.

Table 2.1: Western Blotting Antibodies

Antibody	Secondary	Dilution	Manufacture
pSTAT1	Rabbit	1:1000	Cell Signalling
pSTAT2	Rabbit	1:1000	Cell Signalling
pSTAT3	Rabbit	1:1000	Cell Signalling
STAT1	Rabbit	1:1000	Cell Signalling
STAT2	Mouse	1:1000	Santa Cruz
STAT3	Rabbit	1:1000	Cell Signalling
RSV-NS1	Rabbit	1:4000	Gift
RSV-NS2	Rabbit	1:400	Gift
Mx1	Rabbit	1:1000	Cell Signalling
PKR	Rabbit	1:1000	Cell Signalling
ISG15	Rabbit	1:1000	Cell Signalling
USP18	Rabbit	1:1000	Cell Signalling
β -actin	Mouse	1:2000	Cell Signalling

Table 2.2: Western Blotting Materials

Reagent	Manufacture
Western blotting molecular weight marker	BioRad (USA)
Enhanced Chemiluminescent (ECL)	BioRad (USA)
Polyvinylidene difluoride (PVDF) Membrane	Fisher (USA)

Table 2.3: Reagents for RT-qPCR

Reagent	Manufacture
TriReagent	Sigma-Aldrich (USA)
SYBR Green mastermix	BioRad (USA)
96-well PCR plates	BioRad (USA)
PCR plate seals	BioRad (USA)
SensiFast cDNA synthesis kit	Bioline Reagents (UK)

2.1.4 Quantative RT-PCR materials

Quantative Reverse Transcriptase Polymerase Chain Reaction (RT-qPCR) was carried out using BioRad machine and thermocycler. A full list of materials used can be found in Table 2.3.

2.1.5 Antibodies for Flow Cytometry

To achieve intranuclear staining, Cytofix buffer and Phospho Perm buffer III (Becton Dickinson, USA) were used. Fluorescently labelled antibodies purchased as indicated in table 2.4.

2.1.6 Cell Culture Reagents

Cell culture reagents are detailed in table 2.5.

2.2 Methods

2.2.1 Bioinformatics

To align multiple protein sequences to compare similarities, the Clustal Omega sequence alignment tool was used (<https://www.ebi.ac.uk/Tools/msa/clustalo/>). To identify comparative sequences the NCBI Basic Local Alignment Search Tool (BLAST) was used to screen for comparative sequences in the Nucleotide collection (nr/nt) database. The amino acid sequences screened against Non-redundant protein sequences (nr) using BLASTP, excluding RSV sequences. Sequences for RSV-A (NC_038235.1) and RSV-B (KF893260.1) strains were identified by searching the NCBI database for complete human RSV sequences.

Promoter regions for genes were retrieved from the Eukaryotic Promoter Database (Dreos et al., 2015). In each case the proximal promoter, the 499 nucleotides preceding the transcription start site (TSS), were aligned with the GAS and ISRE promoter regions using ClustalOmega (Madeira et al., 2019). ISRE is defined as 5'-GAAANNGAA-3' where N can be any nucleotide; IRFs are also able to bind ISRE half sites 5'-GAAA-3' (Csumita et al., 2020). The presence of a promoter regions within the proximal promoter does not guarantee this site is accessible to transcription factors, chromatin modelling will influence which sites are exposed; neither does this take account of enhancers or silencers which will affect the transcription of genes. However, it gives an indication of which transcription factors could control expression.

2.2.2 Plasmid Transformation

Transformation involves the introduction of exogenous DNA to cells. The plasmid contains a gene for a viral protein and an antibiotic resistance marker, ensuring only successfully transformed cells grow on plates containing the appropriate antibiotic. Culturing these cells and then purifying the DNA plasmids allows high concentration of plasmid DNA which can then be used to transfect cells, causing them to produce the viral protein. Competent E.coli cells (Clontech, USA) were stored at -80°C prior to use and thawed on ice. 1µl of plasmid DNA was added to 5µl of bacteria and left on ice for 30 minutes (min). The mixture was then heat shocked at 42°C for 45 seconds and then moved to ice for 2 min, this induces the uptake of the plasmid by the bacteria. 1ml of warmed Luria-Bertani (LB) broth was added and the mixture was placed on a shaker at 37°C for 1 hour. 200µl of bacteria was spread on to LB agar plates containing 100µg/ml

ampicillin and moved to a 32°C incubator for 16 hours (h).

2.2.3 Plasmid Purification

To generate high volumes of plasmid DNA a single colony was selected and added to 100ml of autoclaved LB broth containing 50µg/ml ampicillin and placed on a shaker for 16-18h. A stock was taken by adding 750µl overnight bacterial culture to 750µl glycerol and stored at -80°C for future use. The plasmid DNA was then purified using a Qiagen Midi Prep kit following the manufactures instructions. The concentration of the resulting precipitate was calculated using a NanoDrop 2000 (Thermo Fisher, USA) and frozen at -20°C for future use.

2.2.4 Culture of Cell Lines

The alveolar basal epithelial (A549), bronchial epithelial cells (BEAS 2b), laryngeal epithelial type 2 (Hep2), human embryonic kidney (HEK293T) and African Green Monkey kidney (Vero) cell lines were cultured in Dulbecco's Modified Eagles Medium – high glucose (DMEM) containing 10% FBS and 1% P/S. Cells were seeded at a density of 2×10^5 cells per ml and passaged every two to three days as they reached 80% confluence. Briefly, media was removed from the flask and the surface of the cells were washed with 3-5ml PBS to remove residual media. 2-3ml trypsin was then added and the flask returned to the incubator for 5 min to allow the cells to detach. 7-8ml warmed media was then added to the flask to collect the cells, giving a final volume of 10ml. At this point the cells were counted and the cells pelleted at 2420RFC for 5 min. The media was discarded and the pellet of cells resuspended in 10ml of fresh media and seeded in to flasks or plates as needed. To freeze down cells, the cells were counted using a haemocytometer before being pelleted; the cell pellet was then resuspended at 1×10^6 cell/ml in freezing medium (20% FBS, 10% DMSO in DMEM). The cell suspension was aliquoted into cryovials and frozen using a Mr. Frosty cool cell (Nalgene, USA) at -80°C.

2.2.5 Viral Propagation

RSV-A2-GFP

In order to propagate full length RSV-A2-GFP Hep2 cells were infected with stocks. Hep2 cells were cultured as previously described before being seeded into a T175 flask

at 1×10^7 cells per flask in 25ml complete DMEM (10% FBS, 1% P/S) and left in the incubator for 24h to reach 70% confluency. To infect the Hep2 with RSV-A2-GFP, all media was aspirated from the flasks and the cells washed with 10ml warmed PBS. The viral stock was diluted to 0.1pfu/cell in 3ml serum free (SF) media, assuming that the number of cells had doubled over night. RSV-A2-GFP was propagated and collected as detailed below.

RSV- Δ NS1/2-GFP

Propagation of RSV- Δ NS1/2-GFP follows a similar protocol to the RSV-A2-GFP. However, as the removal of the NS proteins attenuates RSV growth in immune competent cells the Vero cell line must be used. Vero cells are maintained as above and seeded into a T175 plate at 1×10^7 cells per flask in 25ml complete DMEM (10% FBS, 1% P/S) and left in the incubator for 24h to reach 70% confluency. To infect the Vero with RSV- Δ NS1/2-GFP, all media was aspirated from the flasks and the cells washed with 10ml warmed PBS. The viral stock was diluted to 0.1pfu/cell in 3ml SF media, assuming that the number of cells had doubled over night. RSV- Δ NS1/2-GFP was propagated and collected as detailed below.

Virus Collection

Alongside the virus growth flask a control flask was also prepared, with 3ml of SF media added. The 3ml of media is dispersed over the cell monolayer and the flasks returned to the incubator for 2h to allow for virus adsorption. After 2h, 22ml of warmed complete media is added to each flask. The flasks are returned to the incubator for 24h. In order to facilitate viral replication the cells are serum reduced by removing 22ml of media from each flask. This is collected and centrifuged at 1500RPM, 4°C for 5min, allowing any cells are free RSV to be collected. The supernatant is discarded and the pellet resuspended in 22ml of warmed SF media, before being transferred back into the flask. Flasks are incubated for a further 24h. Once cytopathic effect (CPE) reached 80% cells were harvested by scrapping the cells from the flask using a rubber cell scraper. The dislodged cells and media is collected into 50ml flacon tubes and sonicated for 2min in an ice bath. The resulting RSV is highly heat liable and must be snap frozen in liquid nitrogen (LN) in order to preserve it. The RSV is aliquoted into cryovials and snap frozen, it is then moved to a LN Dewar and stored in the vapour phase.

Calculating Viral Titre

To calculate the level of virus propagated serial dilutions of the viral stock is made and used to infect permissive cells. Hep2 are used for RSV-A2-GFP, while Vero are used for RSV- Δ NS1/2-GFP. Cells are seeded into 96 well plates with 2×10^4 cells per well in 200 μ l complete DMEM, cells are incubated for 24h until confluent. Media is removed from the cells and gently washed with warmed PBS. Serial dilutions of viral stocks are added to the wells in triplicate, alongside stocks from the control flask. The plate is then returned to the incubator for 2h to allow the virus to adsorb to the cells. The inoculum is then removed from the wells and replaced with 200 μ l complete DMEM. The plate is returned to the incubator for 5 days. The media is discarded and the plate washed with PBS. Cells are fixed by adding 100 μ l of 2% hydrogen peroxide in methanol to each well, taking care not to disturb the cell monolayer. The monolayer is washed with 1% BSA in PBS and stained with biotinylated anti-RSV F diluted in 1% BSA for 1h at room temperature. The plate is washed twice with 1% BSA, followed by 100 μ l of a 1 in 500 dilution of Extravidin Peroxidase (Merck, USA) added to each well for 1h at room temperature. and focus forming units (FFU) are counted. To calculate the multiplicity of infection (MOI): $MOI = FFU / \text{number of cells infected}$.

2.2.6 Cell Transfection

Transfection with viral proteins forces mammalian cells to express a specific viral protein without infecting the cells with the full-length virus. A549 cell line were seeded into 6 or 12 well plates at a density of 2.5×10^5 cells per ml and allowed to grow for 24h, or until they had reached 70% confluency. They were then transfected with 1 μ g DNA per well. Briefly, the plasmid DNA for each construct was diluted to 100ng/ μ l in sterile RNase free H₂O (Sigma, USA). 10 μ l of this was added to 250 μ l warmed SF DMEM in an autoclaved Eppendorf. In a second Eppendorf 2 μ l of Lipofectamine reagent was added to 250 μ l cold SF DMEM and left at room temperature (RT) for 5 min. The lipofectamine mix was then added to the DNA mix, giving a total volume of 500 μ l in each Eppendorf, and left at RT for 20 min. The final transfection mix was added to each well of cells as needed. Cells were treated with the empty vector (EV) control, single transfections of hRSV-NS1, hRSV-NS2 or a double transfection of hRSV-NS1/NS2. Cells were returned to the incubator for 24h.

2.2.7 Treatment of Cells

After seeding and transfection cells were treated as described. The cytokine was diluted to the required concentration in serum free (SF) DMEM. IFN- α was used at 100IU/ml, and IFN- λ was used at 100ng/ml.

2.2.8 Treatment of Cells with Conditioned Media

To generate conditioned media cells were transfected for 24h as described above. The transfection media was then replaced with complete DMEM for a further 24h to collect cell secreted factors. This was used to treat naïve cells for the time indicated.

2.2.9 RNA extraction using TRIreagent

Total RNA was extracted from cells using TRIreagent (Sigma, USA) following manufacture instructions. Briefly, after treatment the media was removed and the cells washed with 500 μ l ice cold PBS. The PBS was discarded and 500 μ l TRIreagent added to the cells and incubated at RT for 5 min. The resulting cell suspension was moved to labelled Eppendorf tubes. 100 μ l chloroform was added to each Eppendorf and shaken vigorously for 15 seconds. They were then left at RT for 5 min to allow two layers to form, and centrifuged for 15 min at 2420RFC at 4°C. The upper aqueous RNA layer was moved to fresh Eppendorf tubes and resuspended in 250 μ l isopropanol by shaking. This was incubated at RT for 10 min and centrifuged for 10 min at 2420RFC at 4°C. The isopropanol was removed and the pellet was resuspended in 500 μ l 75% ethanol. This was centrifuged for 5 min at 970RFC at 4°C. The ethanol was removed as before and the samples left to dry in a biological safety hood for 15 min before being resuspended in 20 μ l RNase free water (Sigma, USA) and incubated at 60°C for 10 min to dissolve the RNA pellet. The concentration and purity of each sample was assessed using a NanoDrop 2000 (Thermo Fisher, USA).

2.2.10 Reverse Transcription

All RNA samples were diluted to 250ng in 18.5 μ l (13.5ng/l) in RNase free water (Sigma). The RNA was converted to cDNA using the SensiFAST cDNA Synthesis kit (Bioline, UK) with 0.25 μ l reverse transcriptase enzyme, 0.25 μ l RNase free water and 1 μ l 5x buffer added to each sample. The mix was then thermocycled with the following settings: 25°C for 10 min (for primer annealing), 42°C for 15 min (for reverse transcription), 85°C

for 5 min (for inactivation of the enzyme) and 4°C hold. Samples were frozen at -20°C for future use.

2.2.11 Quantitate Real-Time Polymerase Chain Reaction (RT-qPCR)

All RT-qPCR reactions were carried out in duplicate. For each sample 1µl cDNA, 4µl SYBR green PCR master mix (BioRad, USA), 4µl RNase free water (Sigma), 0.5µl forward primer and 0.5µl of reverse primer was added to the well, giving a total volume of 10µl. The plate was then placed in the BioRad quantitative PCR system with the following parameters: 95°C for 15 min, 92°C for 30 seconds, 65°C for 1 min, 72°C for 30 seconds. This was repeated 40 times. A list of primers used can be found in Table 2.7.

Data analysis was carried out following the $2^{-\Delta\Delta ct}$ method. The relative expression of each result was calculated based on expression of the constitutively expressed housekeeping gene ribosomal protein 15 (RPS15) or β -actin. To calculate $2^{-\Delta\Delta ct}$, the ct value of the housekeeping gene was subtracted from the gene of interest ct value, giving a Δct for each sample. The Δct value for the control was subtracted from the Δct of each test sample, giving a $\Delta\Delta ct$. This was then inputted into the formula $2^{-\Delta\Delta ct}$ and these values plotted relative to the control.

2.2.12 Western Blotting

Sample Preparation

All samples for western blotting were collected in radioimmunoprecipitation assay (RIPA) buffer, which was supplemented with phosphatase and protease inhibitors immediately prior to use. For 1ml buffer: 10 μ l Phenylmethylsulfonyl fluoride (PMSF), 10 μ l Na₃VO₄, 10 μ l Leupeptin, 1 μ l Dithiothreitol (DTT) was added to 969 μ l RIPA buffer.

To lyse samples, cells were resuspended in 100 μ l supplemented RIPA buffer and left on ice for 30 min, agitating every 10 min. Samples were then centrifuged at 2420RCF for 10 min and the supernatant, containing the proteins of interest, were collected and stored at -20°C. For infected patient samples prepared in the Containment Level (CL)3 lab the samples added to loading buffer containing 200mM/ml DTT and boiled for 10 min before being moved to the main lab and stored at -20°C. Cell line samples were defrosted on ice and added to loading buffer containing 200mM/ml DTT and then boiled for 10 min immediately before use.

Western Blotting and Analysis

Reducing sodium dodecyl sulphate polyacrylamide gel electrophoresis (SDS-PAGE) allows proteins in the sample to be separated out by size down an acrylamide gel. The proteins are then transferred on to a polyvinylidene difluoride (PVDF) membrane and the proteins of interest are probed for using specific antibodies. Secondary antibodies are then used which will bind the primary antibody and visualise as a dark band when treated with ECL. The density of these band is directly related to the concentration of that protein in the initial sample. To ensure that any change in band density is a result of the sample and not a loading error, each blot was probed for β -actin as a loading control.

The BioRad vertical gel kit was used to cast 10% w/v SDS polyacrylamide resolving gel and a 5% w/v SDS poly acrylamide stacking gel. The gels were then placed in the BioRad Mini-PROTEAN Tetra apparatus with running buffer (250mM Trisaminomethane, 1.8M glycine, 1% w/v SDS) and samples loaded into the wells (10 μ l in 10 well combs, 8 μ l in 12 and 15 well combs) alongside 2.5 μ l of the Precision Plus Protein Dual Color standard (BioRad, USA). The apparatus was attached to a power supply set at 80 volts (V) and left for 20 minutes to allow the sample through the stacking gel; the voltage was then set at 110V for 1h 30 min.

The protein from the gel was then transferred to the PVDF membrane. The PVDF was soaked in methanol to activate it and then rinsed in transfer buffer (11.86M Trisaminomethane, 3.99M glycine in 20% methanol). Two pieces of filter paper and sponges were soaked in transfer buffer, the transfer was then set up as follows: sponge, filter paper, PVDF membrane, gel, filter paper, sponge. This sandwich was then clipped into the BioRad transfer apparatus and run at 400amp for 90 min with the tank filled with transfer buffer.

The membranes were blocked with 5% w/v marvel to limit non-specific antibody binding. Membranes were incubated overnight at 4°C with primary antibody diluted as stated in Table 2.1. After at least 16h incubation the membranes were washed 3 times with TBST and probed with the relevant secondary antibody for 1h at RT. The membrane was activated using the Clarity Western ECL blotting substrates kit. The protein bands were viewed using a Gel Doc EZ imager (BioRad, USA). The densitometry for each band was carried out using Bio-Rad Image Lab software (BioRad, USA). The data produced from this software was exported to GraphPad Prism 8 where it was graphed and analysed.

Analysis of phosphorylated STAT and total STAT were performed on separate membranes, no stripping buffers were used.

2.2.13 Confocal Microscopy

Confocal microscopy allows high-resolution images to be made of appropriately stained biological samples. The level of detail enables the study of sub-cellular localization of proteins within individual cells. For immortalized cell lines, cells were seeded onto glass cover slips 24h before use and infected or transfected as required. After appropriate treatment the cells were fixed with 4% paraformaldehyde (PFA) for 20min. Cells were washed with PBS and permabilised with 0.2% Triton X-100 for 30min before blocking in 0.5% BSA for 1 hour at room temperature. The slides were then moved to a humidified chamber and incubated with primary antibodies (table 2.11) overnight at 4°C. The slides were washed and incubated in secondary antibodies for 1 hour in the dark at RT. Slides were washed a final time and mounted on slides using DAPI ProGold Mounting media (ThermoFisher). These were allowed to cure over night and sealed with clear nail varnish before and imaging using a Lecia SP8 scanning confocal microscope.

2.2.14 Quantative Analysis of Confocal Microscopy

Quantitative image analysis was performed using IMARIS (Oxford Instruments). Three images were collected from each sample at different coordinates to ensure reproducibility across each slide. To quantify the level of each protein in the nucleus vs the cytoplasm a “surface” was created over the areas of the image stained with DAPI (the nucleus), and within each of these surfaces the level of STAT1 or STAT2 stain was quantified. An additional channel was then created excluding the areas stained with DAPI (the cytoplasm), a “surface” was created over this and levels of STAT1 or STAT2 quantified. This was done either in cells expressing GFP (denoting NS1 transcription or RSV-GFP infection) or in all cells for controls (Fig. 2.1). Fluorescence intensity is shown in each condition, or relative fluorescence intensity, which shows the relative intensity between the cytoplasm and the nuclear compartments.

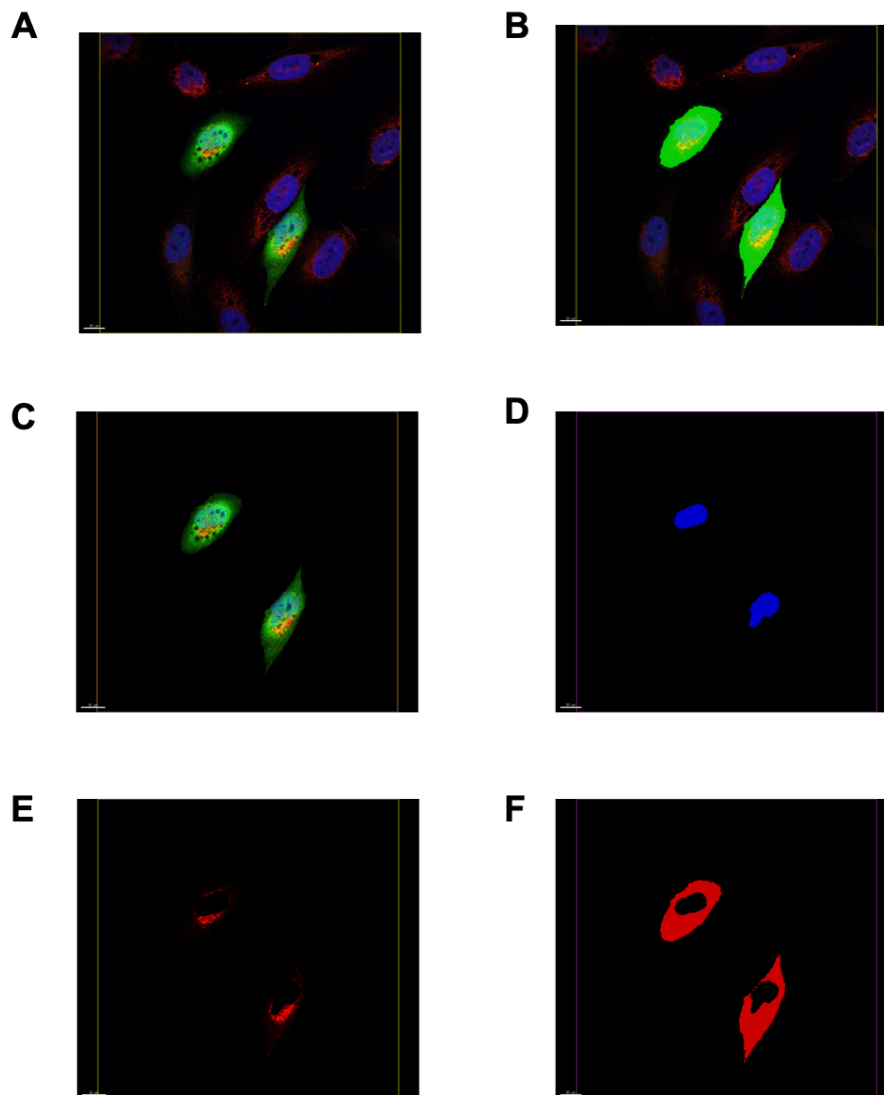


Figure 2.1: Confocal Quantification Strategy using IMARIS

To quantify STAT expression in transfected or infected cells A) the initial image captured by confocal microscopy was loaded onto the IMARIS software. B) A surface was created over the cells fluorescing in the GFP channel, C) allowing only those infected or transfected cells to be analysed. D) A surface was created over the DAPI expressing regions (the nuclei), and levels of STAT expression under this surface was quantified, E) the DAPI surface was then excluded from the image and F) a surface was created over the cytoplasm of each cell to quantify STAT levels in this area alone.

2.2.15 Patient Criteria

As RSV causes most significant pathology to children and infants; this study is designed to monitor the effect of natural RSV infection on the innate immune response of key cell types. Children admitted to Tallaght Hospital Children's Emergency Department with bronchiolitis were invited to take part in the study. After informed consent was granted by parents or guardians, a nasopharyngeal aspirate sample and 2ml blood sample was obtained at the next opportunity. Healthy paediatric blood samples were obtained from children attending the routine phlebotomy clinic in Tallaght Children's Hospital, children with active infection were excluded from the study. Blood samples were collected in lithium heparin tubes and stored at RT for a maximum of 24h before processing.

2.2.16 Peripheral Blood Mononuclear Cell purification from whole blood

Whole blood was collected in lithium heparin tubes. This was diluted 1:1 with warmed PBS and layered on 7ml Ficoll Paque (GE healthcare, USA) in a 15ml falcon tube for paediatric samples. Tubes were centrifuged at 900G for 20 min with the break set to 0 to maintain the density gradient layers. The Peripheral blood mononuclear cell (PBMC) layer was removed using a pasture pipette and moved to 10ml warmed PBS. Tubes were centrifuged at 900G for 10 min with the break at 9 as normal. The supernatant was discarded and the cells resuspended in 10ml warmed PBS, the cells were centrifuged again at 900G for 20 min, the supernatant discarded and the cells resuspended in 10ml RPMI (supplemented with 10% FBS and 1% P/S) and counted. PBMCs were centrifuged at 900G for 10 min and the pellet resuspended in freezing media, 10% DMSO (Sigma, USA) in FBS, to give a concentration of 10^6 cells per ml and frozen at -80C using a Mr. Frosty (Nalgene, USA). After a minimum of 24h the samples were moved to liquid nitrogen storage.

2.2.17 Treatment of PBMCs and Staining for Flow Cytometry Analysis

Frozen PBMCs were removed from liquid nitrogen and added to warmed complete media (RPMI supplemented with 10% FBS and 1% P/S) and centrifuged at 350G for 10 min. The supernatant was discarded and the cells resuspended in complete media, seeded at a density of 10^6 cells per well, and placed in an incubator for at least 12h.

PBMCs were treated with either 1000IU or 0IU IFN α and returned to the incubator for 15 min. The cells were collected into Eppendorf tubes and centrifuges 250G for 5 min. Samples centrifuged at 250G for 5 min, the supernatant discarded and cells resuspended in 50 μ l Brilliant Stain Buffer (BD Bioscience, USA) and extracellular cytokines, these were incubated for 30 min in the dark at RT. 50 μ l BD CytoFix A (BD bioscience, USA) was added to the cells and incubated for a further 15 min. 100 μ l of PBS was then added and the samples and tubes were centrifuged at 250G for 10 min. Supernatants were discarded and the cells resuspended in 200 μ l 5% FBS in PBS and centrifuged as before and the supernatants discarded. Cells were resuspended in 100 μ l Phosflow Perm Buffer III (BD Bioscience, USA) and incubated on ice for 30 min before intracellular antibodies were added. Cells were then centrifuges at 250G for 10 min and resuspended in 150 μ l 5% FBS in PBS. OneComp beads (Thermo Fisher, USA) were used for all compensations, except the Zombie Near IR Live dead stain and the pSTAT2-FITC antibodies for which cells were used. Gating was determined relative to the unstained control, an example is given in Fig. 2.2.

Two staining panels were created as listed in table 2.12 to allow for levels of intracellular STAT and pSTAT to be quantified. Data was analysed using FlowJo (Tree Star, USA).

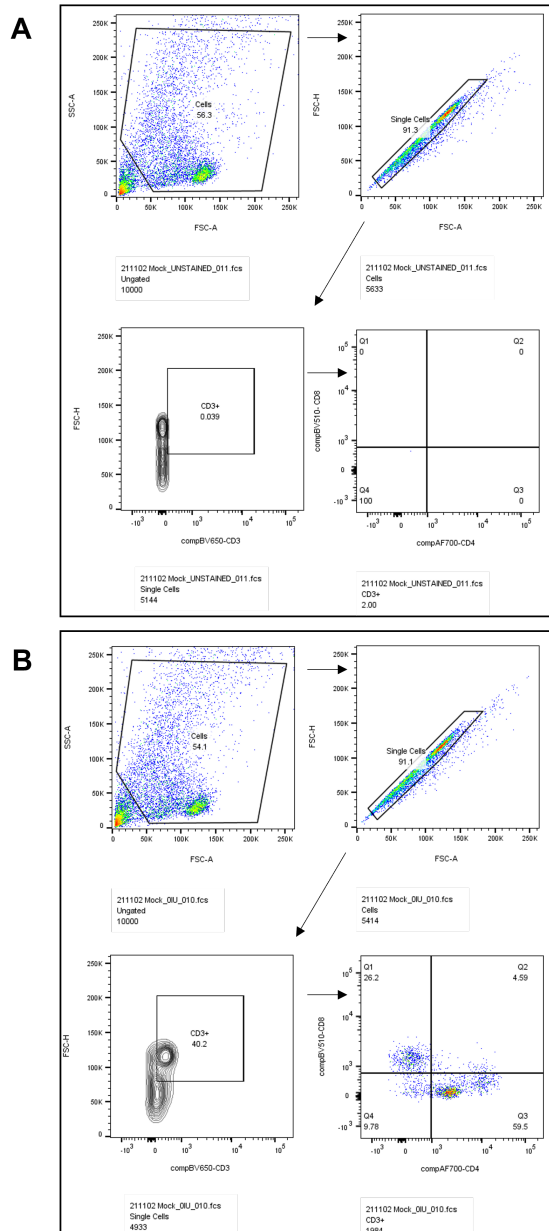


Figure 2.2: Gating of CD3+ cells

Gating of CD3+ cells was determined relative to an unstained control. A) An unstained population of PBMCs has no CD3+ signal while B) PBMCs stained with CD3-BV650 have a positive population present.

2.2.18 Ethical Approval

Ethical approval for this study was granted by the Tallaght University Hospital and St. James Hospital Joint Research Ethics committee under 2019-09 List 33 (6) and 2018-08 List 30 (1) for the collection of paediatric samples. Whole blood sample collected from healthy adults was approved by the TBSI research ethics committee under BI-RW-010921.

2.2.19 Statistical Analysis

Statistical comparisons between groups were performed using GraphPad Prism statistical analysis software (version 9). Data is represented as the mean \pm SD unless otherwise stated. Normal Gaussian distribution determined through the Shapiro-Wilk test. Outliers were identified using ROUT. A p value <0.05 (*) was considered significant, a p value <0.01 (**) was considered highly significant. One-way Analysis of Variance (ANOVA) was used for comparison of more than two independent groups, with Dunnett's multiple comparison post hoc test to compare the means of the treatment groups to the control, or Sidak's multiple comparison post hoc test to compare the means of pre-selected treatment group pairs as applicable. A Student's t-test was used to compare two treatment groups with normally distributed data. Heatmap data was generated through GraphPad Prism, with significance between groups determined by Student's t-test.

Table 2.4: Fluorochrome Conjugated Antibodies for Flow Cytometry

Antibody	Flouorochrome	Volume per 10⁶ cells(μl)	Manufacture
Live/Dead	Zombie Near IR	1	Biologend
CD11c	BV711	2	Becton Dickinson
CD14	AF700	2	Becton Dickinson
CD19	BV605	2	Becton Dickinson
CD3	BV650	2	Becton Dickinson
CD4	AF700	2	Becton Dickinson
CD8	BV510	2	Becton Dickinson
CD56	BV650	2	Becton Dickinson
pSTAT1	AF647	2	Becton Dickinson
pSTAT2	FITC	2	Thermo Fisher Scientific
pSTAT3	BV421	2	Becton Dickinson
STAT1	PE	2	Becton Dickinson
STAT3	PE	2	Biologend

Table 2.5: Cell Culture Reagents

Reagent	Manufacture
Dulbecco's Modified Eagle Media (DMEM)	Sigma-Aldrich (USA)
Roswell Park Memorial Institute Media (RPMI)	BioRad (USA)
Fetal Bovine Serum (FBS)	BioRad (USA)
Penicillin-Streptomycin (P/S)	BioRad (USA)
Trypsin-EDTA	Bioline Reagents (UK)
Dimethyl sulfoxide (DMSO)	Sigma-Aldrich (USA)
Trypan Blue solution	Sigma-Aldrich (USA)
T25 Flasks	Fisher Scientific (USA)
T75 Flask	Fisher Scientific (USA)
T175 Flask	Corning (USA)
6 and 12 well plates	Fisher Scientific (USA)

Table 2.6: Cytokines

Reagent	Manufacture
IFN- α	Sigma-Aldrich (USA)
IFN- λ	BioRad (USA)

Table 2.7: Primer Sequences

Gene	Forward Primer	Reverse Primer	Manufacture
RPS15	CGGACCAAAGCGATCTCTTC	CGCACTGTACAGCTGCATCA	Sigma
PKR	TCTCAGCAGATACATCAGAGT	TCGGAGTTGCCTCTTAAGACTGT	Sigma
MxA	GGTGGTGGTCCCCAGTAATG	ACCACGTCCACAACCTTGTCT	Sigma
ISG15	TCCTGCTGGTGGTGGACAA	TTGTTATTCCTCACCAGGATGCT	Sigma
USP18	TCGTGCCTGGCTCACATAAG	CAACCAGGCCATGAGGGTAG	Sigma
SOCS1	AGCTTATCTGTATCTGGAGC	AAAAATAAAGCCAGAGACCC	Sigma
SOCS3	ATCCTGGTGACATGCTCCTC	CAAATGTTGCTTCCCCCTTA	Simga
SOCS4	GAGATACATCCAGAAAGTGC	CACATAACCGTCTTTTCTGTC	Invitrogen
SOCS5	TACAGCAAGCAGTCAAAGCC	ACAGAGAAGAGGTAGTCCTC	Sigma
SOCS6	TCTCACCATTGCTACCTCCA	GAGTCCCTGATTGAATGCTC	Sigma
SOCS7	CTTCTCGGAAGGGCTCCTTC	AACGCTGGCTACAAAGCTGC	Sigma
CIS	GATCTGCTGTGCATAGCCAA	ACAAAGGGCTCACCAGTTT	Sigma
RSV-NS1	GCAGAACCTCTCTTCGSCAACG	ACGATGTTGTTGTTGGGGCA	Sigma
RSV-NS2	ACATCATCACCCACCGTTTC	AAAGTGGCCTGCCTCTCATC	Simga
RSV-F	GGCAAATAACAATGGAGTTG	AAGAAAGATACTGATCCTG	Sigma

Table 2.8: Phosphatase and Protease Inhibitor Concentration

Reagent	Final Concentration in RIPA
PMSF	1mM
Na ₃ VO ₄	1mM
Leupeptin	5μg/ml
DTT	1mM

Reagent	10%	12%	16%
dH ₂ O	4.8ml	3.5ml	2.3ml
Acrylamide	5ml	6.3ml	7.5ml
TRIS pH8.8	5.6ml	5.6ml	5.6ml
SDS	150μl	150μl	150μl
TEMED	15μl	15μl	15μl
APS	150μl	150μl	150μl

Table 2.9: Resolving Gels

Reagent	Volume
dH ₂ O	4.61ml
Acrylamide	1ml
TRIS pH6.8	750μl
SDS	30μl
TEMED	12μl
APS	60μl

Table 2.10: Stacking Gels

Table 2.11: Immunohistochemistry Antibodies & Stains

Stain	Secondary	Dilution	Manufacture
STAT1	Mouse	1:250	ThermoFisher
STAT2	Mouse	1:50	Santa Cruz
RSV-NS1	Rabbit	1:3000	Gift
Anti-Rabbit - CF568	Goat	1:100	Merck
Anti-Mouse - AF647	Goat	1:1000	Biolegend
Phalloidin Rhodamine	N/A	1:1000	AbCam

Table 2.12: Flow Cytometry Panels

Panel 1	Panel 2
CD3-BV605	CD14-AF700
CD4-AF700	CD56-BV650
CD8-BV510	CD11c-BV711
CD19-BV650	STAT1-PE
STAT1-PE	STAT2-PerCP
STAT2-PerCP	pSTAT1-AF647
pSTAT1-AF647	pSTAT2-FITC
pSTAT2-FITC	pSTAT3-BV421
pSTAT3-BV421	

3 RSV NS1 and NS2 Reduced Interferon Sensitive Gene Expression in both A549 and BEAS 2b Epithelial Cell Lines

3.1 Introduction

The JAK-STAT pathway has been shown to be impacted by RSV, with the NS proteins implicated in attenuating normal signalling; however, the precise mechanism of this in respiratory epithelial cells remains unknown. While the NS proteins have been shown to play a key role in viral replication, with NS deletion mutants of RSV failing to replicate efficiently in IFN competent cells (Jin et al., 2000, Teng et al., 2000, Teng and Collins, 1999, Whitehead et al., 1999, Jin et al., 2003). The role of each NS protein is not fully understood; some studies have shown that NS1 is the key player, able to target STAT2 for ubiquitination and degradation (Elliott et al., 2007, Chatterjee et al., 2017), others have postulated that the reduction in STAT2 is mediated by SOCS1 (Xu et al., 2014), and that NS1 acts against IFN regulatory factor 3 (IRF3), to prevent signalling – a mechanism also seen in bovine RSV (Ren et al., 2011, Bossert et al., 2003). NS2 has also been identified to limit the IFN response (Kotelkin et al., 2006, Ling et al., 2009), and is also postulated to use the host ubiquitination machinery (Whelan et al., 2016, Ramaswamy et al., 2006). Additionally several reports have shown that NS1 and NS2 work cooperatively to limit IFN signalling (Spann et al., 2004, Lo et al., 2005, Zheng et al., 2015, Hastie et al., 2012).

In the context of viral infections, the most significant output of the JAK-STAT pathway is the upregulation of hundreds of antiviral genes. Any impact by RSV to limit normal signal transduction through this pathway will limit the expression of various ISGs, making the cell more permissive to viral growth. Many ISGs have direct antiviral functions (MxA and PKR), while others regulate the pathway to limit over stimulation and damage to the cell (ISG15, USP18 and SOCS). ISGs are defined as any genes which is up-regulated after IFN treatment (Schneider et al., 2014), these genes contain ISRE (3'-TTTCNNTTTC-5') or GAS (3'-TTCNNNGAA-5') elements within their promoter region, which can be bound by ISGF3 (STAT1:STAT2:IRF9) or GAF (STAT1:STAT1), respectively (Ivashkiv and Donlin, 2014). Each gene can also hold other elements within its proximal and distal promoter regions, allowing them to be controlled by a range of transcription factors (Schneider et al., 2014). The most well studied ISGs include MxA, PKR, ISG15 and USP18, which act against various points of the viral life cycle.

The Mx protein was first identified in mice to inhibit virus entry into the cells (Verhelst et al., 2012, Verhelst et al., 2013). MxA is a dynamine-like GTPase that prevents intracellular trafficking of viral particles. At low concentrations MxA proteins form tetramers but when MxA is more abundant the MxA molecules oligomerise to form a large ring

formation (Verhelst et al., 2013). This triggers GTPase activity against the viral nucleocapsid, limiting viral replication (Gao et al., 2010). PKR is a double stranded RNA (dsRNA) sensor; on binding dsRNA PKR forms homodimers and autophosphorylates at multiple serine and threonine sites. Once active, PKR inhibits protein synthesis by phosphorylating the alpha subunit of eukaryotic initiation factor 2 α (eIF2 α) on serine 51, preventing cap-dependent translation preventing the production of viral and cellular proteins (Dey et al., 2005, Okumura et al., 2013).

The 15kDa ubiquitin-like IFN sensitive protein, ISG15, has pleotropic effects. Unlike MxA or PKR, ISG15 does not act directly against viral particles, instead it is added to target proteins in a process known as ISGylation. Similarly to ubiquitination, ISGylation can change the function or fate of the protein it is attached to (Malakhova et al., 2003). Investigation of ISG15 has found a huge range of proteins are targeted; the transcription factor IRF3 is stabilised by ISGylation allowing it to actively signal for longer; while ISGylation of cyclin D1 causes its destabilisation, leading to cell cycle arrest. While many ISGs are directly antiviral, some ISGs work to control the response to IFN and negatively regulate the IFN pathway. The ubiquitin-specific peptidase 18 (USP18) desensitises the cell to IFN signalling by interacting with IFNAR and removing ISG15 conjugates from targets, which is mediated via deISGylation, through its isopeptidase activity (Malakhov et al., 2002).

Alongside USP18, key negative regulators of the JAK-STAT pathway are SOCS1 and SOCS3. The SOCS family contains eight proteins, SOCS1-7 and CIS, which limit cytokine signalling. SOCS1 is primarily associated with the inhibition of JAK-STAT signalling while, the other SOCS control a range of cytokine responses. All SOCS proteins share a conserved homology including a SOCS box domain. The SOCS box enables the recruitment of E3 ligase and engagement with adaptor proteins elongin B and C, and the scaffold protein Cul5. This stabilizes the interaction between the target protein and the ubiquitination machinery leading to its proteasomal degradation. The regulation of SOCS can have a significant impact on the cellular response, with many pathogens known to drive SOCS to limit the immune response, HCV and VZV induce SOCS3 expression (Collins et al., 2014, Choi et al., 2015) and IAV and ZIKA induce both SOCS1 and SOCS3 expression (Pauli et al., 2008, Seong et al., 2020). In addition to causing the ubiquitination of target proteins, SOCS1 and SOCS3 also contain a KIR domain, which allows them to block the catalytic activity of JAKs, limiting the phosphorylation of STATs (Kershaw et al., 2013, Liao et al., 2018).

Previous investigations into the effect of RSV NS proteins found that RSV-NS1 contains a putative SOCS box and targets STAT2 for proteasomal degradation (Elliott et al., 2007). Several viruses have been shown to contain E3 ligase functions, and are able to interact with Cul proteins (Cai and Yang, 2016). Several adenoviruses (adenovirus type 12, 16, 40 and 41) contain BC boxes in E4 open reading frame 6 (E4orf6) and are able to form E3 ligases by interacting with Cul2 (Cheng et al., 2011), these E3 ligases are substrate specific targeting host proteins, such as p53 (Moore et al., 1996). The Human Immunodeficiency Virus (HIV) Vif protein has also been shown to degrade antiviral APOBEC3, STAT1 and STAT3 proteins through its interaction with Cul5 and elongin C (Conticello et al., 2003, Gargan et al., 2018); while in the bovine analogue, BIV, the Vif protein interacts with Cul2 to degrade APOBEC (Zhang et al., 2014). The function of proteins is driven by specific domains held within their structure. Analysing the sequence of amino acids that make up the proteins can provide an insight into their function, this is done using bioinformatic tools to align the sequences of known functional domains, thus identifying if they are present in the protein of interest (Chenna et al., 2003).

The activity of a protein can also be impacted by the cell it is expressed in. Immortalised cell lines are commonly used to investigate the mechanisms of cell signalling and regulation; however, the creation of immortalized cells and antigenic drift over time can cause them to behave differently to primary cells and result in significant variation between cell lines (Hillyer et al., 2018, Villenave et al., 2012). Much of the research on RSV NS proteins have used HEK293 cells as they are well characterised and readily express transfected proteins well. However, HEK293 cells were originally isolated from human embryonic kidney cell (Graham et al., 1977), but are now thought to be a neuronal cell type (Shaw et al., 2002). Consequently HEK 293 cells do not reflect respiratory epithelial cells, most commonly infected by RSV. Data generated in this cell line is informative, but should to be confirmed in more physiologically relevant cell types. The basal epithelial alveolar type II cell line, A549, is also commonly used in RSV studies. These cells were originally collected from a patient with adenocarcinoma in 1972, as they are a respiratory tract cell line they are more representative of a cells infected during RSV infection (Giard et al., 1973). In addition to A549 cells, the bronchial epithelial cell line, BEAS 2b, is widely used in respiratory research. This cell line originated from a healthy patient in 1988 and was transformed using the SV40 large T antigen to produce a stable immortalised cell line (Reddel et al., 1988, Ke et al., 1988). Understanding how the RSV NS proteins behave in different cell lines is important in building a clear understanding

of their effect upon immune signalling and responses.

The value of the NS proteins to RSV is clear: the virus requires them for efficient replication in immune competent cells. Indeed, without the NS proteins the virus can be targeted by the cell's antiviral response and fails to thrive. What is not clear, however, is the molecular processes and mechanistic strategies of RSV NS proteins in epithelial cells through which the NS proteins achieve the attenuation of the IFN pathway. To begin to answer this question, we transfected the NS proteins either singly or together into the A549 alveolar basal epithelial cell line and BEAS 2b bronchial epithelial cell line, before measuring the impact on the IFN- α and JAK-STAT pathway.

3.2 Specific Aims

- Identify if RSV NS proteins contain SOCS box domains
- Investigate the impact of RSV NS expression on antiviral ISGs in A549 & BEAS-2b cell lines
- Determine the effect of RSV NS expression upon SOCS levels in A549 & BEAS-2b cell lines
- Analyse how the effect of RSV-A2 infection upon ISG and SOCS expression varies between A549 & BEAS 2b cells.

3.3 Results

3.3.1 RSV-NS1 and RSV-NS2 are highly conserved and contain putative E3 ligase domains

Plasmids (pCI-neo vector containing either hRSV-NS1 or hRSV-NS2) were used to express RSV-NS1 and RSV-NS2 in the alveolar basal epithelial (A549) cell line. RSV has two antigenic strains, A and B, which circulate with annually altering dominance (Johnson and Collins, 1988). The RSV sequences were taken from the RSV-A2/long strain, a well-characterised laboratory strain of the virus (Pandya et al., 2019). To ascertain if the RSV-A2/long strain was homologous to RSV strains that “circulate” in the global population, we first examined the conservation between the NS1 (Fig. 3.1A) and NS2 (Fig. 3.1B) construct sequences (used in our experiments), with the most often cited full length WT “circulating” RSV-A and RSV-B sequences publicly available from Genbank. Sequences were taken from Genbank and aligned with the construct sequences using Clustal Omega.

While both NS proteins are broadly conserved between RSV-A and RSV-B, there are some minor differences. Our bioinformatic analysis found the RSV-A and RSV-B NS1 are highly conserved, with 86.33% sequence identity; the majority of substitutions between the A and B strains are of conserved amino acids which have similar properties, such as charge and hydrophobicity. There are some slight variations, with 2 non-conserved residues H36L and P99L, 3 semi-conserved residues S3C, V45A, and T121V, and 13 conserved substitutions V57I, D64E, I65V, N68D, V80I, M90L, M91I, L103M, K114R, , N124D, L129I, E131D, and F134L (Fig. 3.1A). Comparing the “construct” NS1 protein to the database sequence showed 100% sequence identity to RSV-A (Fig. 3.1A). NS2 is more variable, though still broadly conserved (Fig. 3.1B). We found there to be five conserved or semi-conserved residues between RSV-A and the NS2 construct, resulting in a 96.77% sequence identity: N8T, I26T, K38R, K50R K103E. Interestingly these deviations away from the RSV-A NS2 sequence match the RSV-B sequence, with the construct acting as a hybrid of the two. This analysis reveals that the NS1 and NS2 genes do not significantly vary between the RSV-A and RSV-B strains, and the “constructs” used in this study are representative of both NS proteins found in strains of RSV that are currently circulating in the population. As previous studies have implicated the RSV NS proteins in protein degradation we hypothesised that they contain “SOCS-box” domains that enable them to recruit E3 ligases to target proteins. The presence of putative Cul2 binding

sites and putative BC box (Fig. 3.2), suggests that both NS proteins could have E3 ligase functionality. As a functional E3 ligase, the RSV-NS1 protein contains conserved domains, collectively known as the "SOCS-box" which allows substrate-recognition of proteins for ubiquitination and proteasomal degradation. In regards to RSV NS1 these domains would drive the recognition of STAT2 for ubiquitination (Elliott et al., 2007). Previous analysis has identified the Cul2 binding site in NS1, though not in NS2, and some BC box homology, however this analysis was carried out during the early days of *in silico* technologies (Swedan et al., 2009, Elliott et al., 2007). Therefore, to thoroughly examine the SOCS-box of RSV, we aligned both RSV-NS1 and NS2 sequences from our constructs and bioinformatically searched for the E3 ligase (BC and Cul2) consensus sequences, that would determine their presence and putative functionality. It was found that both NS1 and NS2 contain putative BC and Cul2 binding sites (Fig. 3.2), supporting previous studies, which show NS1 has an E3 ligase function, and revealing that NS2 may also act as an E3 ligase.

Alongside human RSV (hRSV), the bovine form of RSV (bRSV) has been extensively studied as it causes significant respiratory disease in cattle. Interestingly, both hRSV and bRSV NS proteins have been shown to reduce IFN responsiveness of infected cells and have a high level of sequence identity; but they appear to use different mechanisms, with bRSV acting to block phosphorylation and activation of IRF3 (Bossert and Conzelmann, 2002, Schlender et al., 2000). bRSV NS1 shares 69.9% sequence identity with its hRSV counterpart, while bRSV NS2 shares 83.9% sequence identity with hRSV NS2 (Fig. 3.3). As with hRSV, bRSV infection is ubiquitous across the world and reinfections are common; bRSV has been well studied, as it has a significant impact upon beef and dairy farming outputs (Sacco et al., 2014). Understanding the bioinformatic differences between bRSV and hRSV NS proteins could provide insight into how their structure might determine their function.

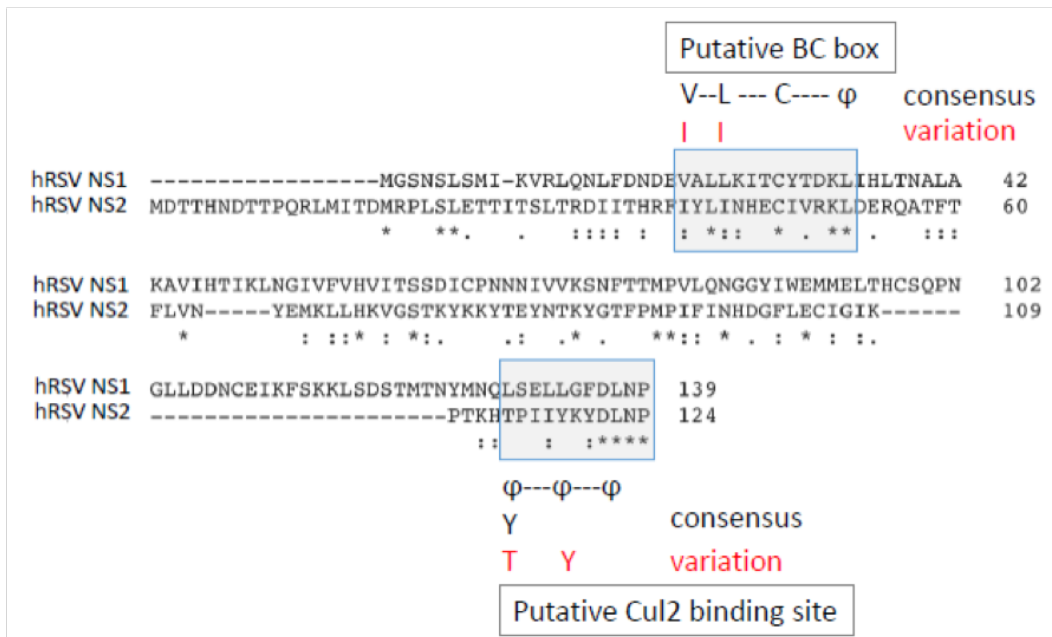


Figure 3.2: Sequence alignment of the RSV-NS1 and RSV-NS2 constructs used in our study

There is limited sequence homology apart from homology around a putative BC box and putative Cul2 binding site. The putative BC box is defined as V-L—C—φ, where φ represents hydrophobic amino acid. The putative Cul2 binding site is defined as a series of hydrophobic amino acids every 4 residues. Analysis carried out in collaboration with Dr. Fiona Roche (Trinity College Dublin)

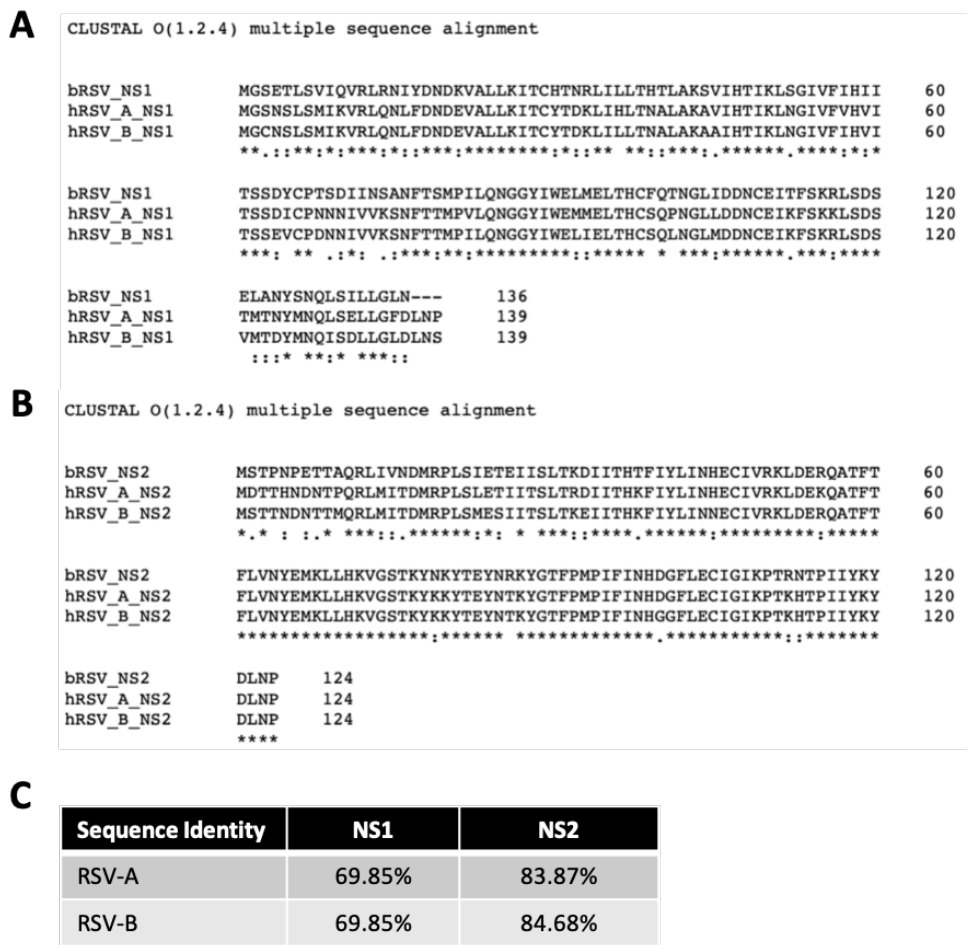


Figure 3.3: Sequence alignment of the circulating hRSV-NS1 and hRSV-NS2 protein sequences, with the bRSV-NS1 and bRSV-NS2

An alignment of A) NS1 and B) NS2 protein sequences between the bovine RSV (bRSV) circulating human RSV-A [hRSV-A-NS] and human RSV-B [hRSV-B-NS] strains was carried out using Clustal Omega sequence alignment software. An asterisk (*) represents a site of conservation. A colon (:) represents a conservative replacement (i.e. there has been a change of amino acid, but the amino acids have strong similar properties). A period (.) highlights a semi-conserved replacement. No symbol underneath a position on the sequence indicates there has been a change in amino acids that share no similar properties. C) Based on the sequence alignments the sequence identity was calculated between the bRSV and hRSV strains; both NS proteins show a high level of sequence identity between the human and bovine forms of the virus.

3.3.2 Expression of NS1 and NS2 in Epithelial Cells

Having established that the RSV-NS1 and NS2 constructs reflect circulating RSV strains, we next sought to analyse their effect upon the antiviral IFN- α JAK-STAT pathway by expressing them in human epithelial cell lines. During RSV infection the primary site of infection are the epithelial cells of the respiratory tract. To study the effect of the NS proteins in physiologically relevant cells, the alveolar basal epithelial cell line, A549, was used. A549 cells were isolated from an alveolar carcinoma of a male patient in 1973 and successfully grown in cell culture (Giard et al., 1973). These cells are well characterised and susceptible to transfection. Cells were transfected with 1 μ g plasmid DNA of either NS1, NS2 or an empty vector (EV) control; and to co-express both NS1 and NS2 a total of 2 μ g plasmid DNA was used (NS1/2) with an 2 μ g EV control (EV2). To confirm that the NS construct was successfully expressed by the cells after transfection with lipofectamine, levels of NS mRNA and protein were measured by RT-qPCR and western blotting, respectively. In the A549 epithelial cells levels of NS mRNA increased at both 24h (Fig. 3.4A) and 48h (Fig. 3.4B). The greatest increase of NS mRNA was seen after 24h transfection, with a 3000 fold increase in NS1 mRNA, and a 1000 fold increase in NS2 mRNA. Western blotting using anti-NS1 antibody (a kind gift from Prof. Mike Teng USF, USA), confirmed that the transfection resulted in translation of NS1 mRNA to protein. Levels of NS1 protein were most increased at 24h transfection, with levels falling after 48h transfection (Fig. 3.4C). Western blotting using anti-NS2 antibody (a kind gift from Prof. Mike Teng USF, USA) did not detect protein expression in A549 cells (not shown).

In addition to the A549 cells, BEAS 2b cells were also used. The BEAS 2b cell line is a non-tumorigenic immortalised epithelial cell line derived from healthy bronchial tissue in 1988 (Reddel et al., 1988), and has since been used extensively in research. BEAS 2b cells were transfected in the same way as the A549 cells (1 μ g DNA per well for single transfections and with 2 μ g DNA for co-transfections). Successful transfection was measured by RT-qPCR and western blotting, with both NS1 and NS2 mRNA peaking at 24h (Fig. 3.5A), and western blotting showing peak NS1 and NS2 protein at 24h transfection (Fig. 3.5C & D). In both cell lines, the co-transfection of NS1 and NS2 together resulted in reduced mRNA and protein expression compared to the single transfected sample, despite the same concentration of plasmid being used in each case.

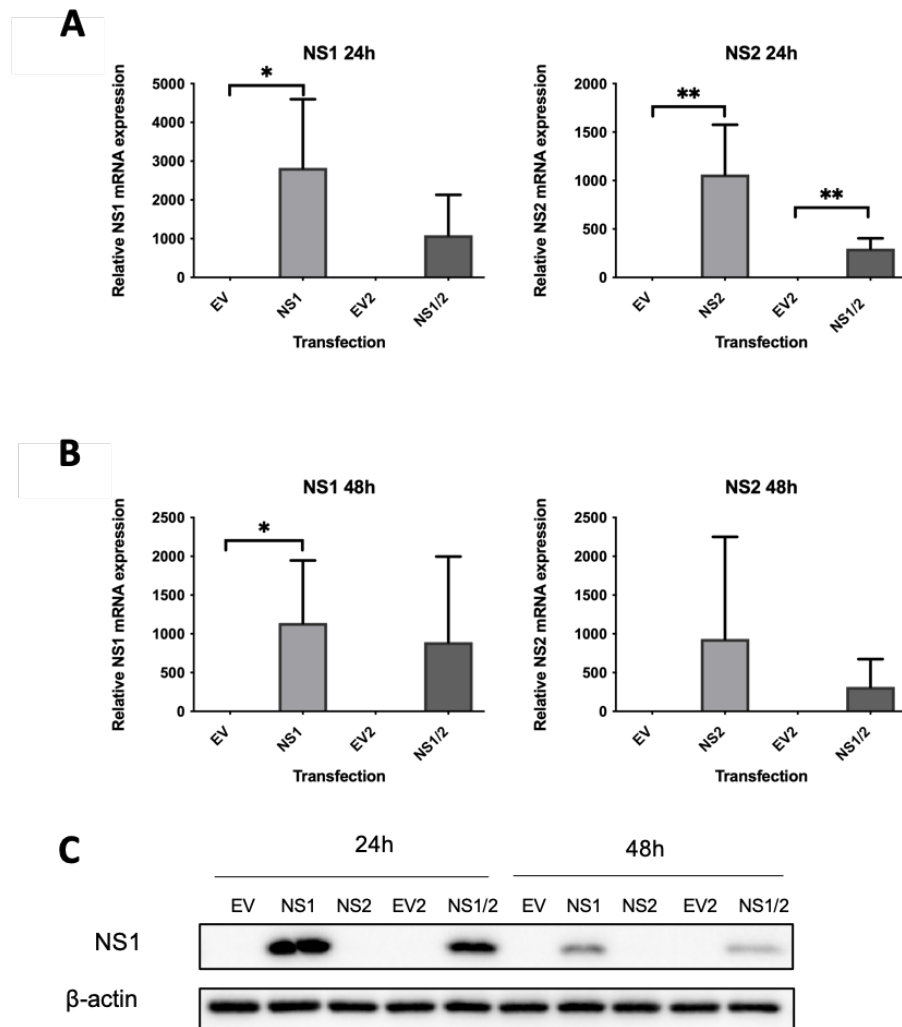


Figure 3.4: Expression levels of RSV-NS1 and NS2 after transfection of A549 cells

A549 cells were transfected with $1\mu\text{g}$ NS1, NS2, NS1 & NS2 (NS1/2) or EV controls for A) 24h and B) 48h and measured by RT-qPCR for NS1 and NS2 expression relative to the housekeeping gene, RPS15. NS1 and NS2 mRNA levels were normalised to the EV control. For the NS1/2 transfections $1\mu\text{g}$ of plasmid DNA was added of each construct, a total of $2\mu\text{g}$ per well; to account for the increased DNA used the EV2 wells had $2\mu\text{g}$ empty vector plasmid added. NS1/2 mRNA levels were normalised to the EV2 control. C) Samples of transfected cells were collected in lysis buffer and levels of NS1 protein was measured by western blotting. Graphs show mean \pm SD. Significance was determined by paired t-test for normally $* = p < 0.05$, $** = p < 0.01$ ($n=4$).

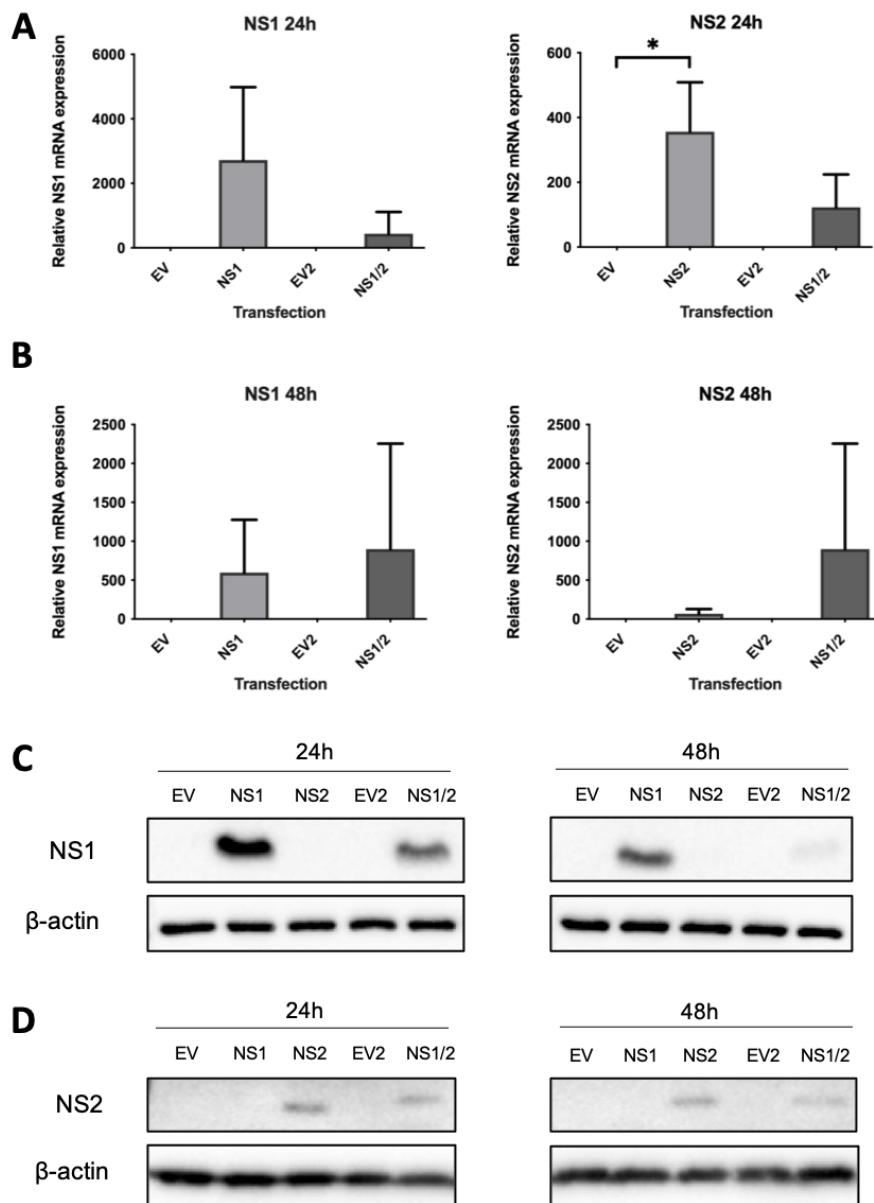


Figure 3.5: Expression levels of RSV-NS1 and NS2 after transfection of BEAS-2b cells

BEAS 2b cells transfected with $1\mu\text{g}$ NS1, NS2, NS1 & NS2 (NS1/2), or relevant EV control for A) 24h and B) 48h and measured by RT-qPCR relative to RPS15. Samples of transfected cells were collected in lysis buffer and protein levels of C) NS1 and D) NS2 were measured by western blotting at 24h and 48h. Highest levels of NS1 and NS2 were seen after 24h transfection. Graphs show mean \pm SD. Significance was determined by paired t-test, * = $p < 0.05$ ($n=3$).

3.3.3 The Effect of RSV NS1 and NS2 upon ISG Expression

Stimulation of the JAK-STAT pathway leads to the upregulation of over 500 ISGs, many of which have an antiviral function (Schneider et al., 2014). Any perturbation on the activity of expression of STAT proteins will have an impact on the ultimate output of the JAK-STAT pathway, ISGs. Our lab has previously shown that HCV and HIV can alter STAT activation to limit the ISG expression and immune response (Stevenson et al., 2013, Gargan et al., 2018). To analyse the effect of RSV NS upon ISG expression, A549 epithelial cells were transfected for 24h or 48h with 1 μ g empty vector (EV), NS1, NS2 or 2 μ g EV (EV2) or NS1/2, before measuring MxA, PKR, USP18 and ISG15 mRNA expression by RT-qPCR. We observed a significant reduction in all ISGs measured in A549 cells after 48h NS1 expression (Fig. 3.6). Expression of NS2 for 24h caused a slight increase fold change relative to the EV control in PKR (3 fold), USP18 (2.5 fold) and ISG15 (1.8 fold), although this was not statistically significant (Fig. 3.6). Transfecting A549 cells with both NS1 and NS2 caused a highly significant reduction in PKR after 24h, and a significant reduction in ISG15 after 48h transfection (Fig. 3.6B & D).

When BEAS 2b cells were transfected with the same viral genes, we observed a significant reduction in MxA, USP18 and ISG15 after only 24h NS1 expression (Fig. 3.7A, C & D). ISGs measured were significantly reduced after 48h NS1 expression (Fig. 3.7). As we observed in A549 cells, the impact of NS2 expression was less than cells expressing NS1, although, unlike in A549 cells, NS2 expression in the BEAS 2b cells significantly increased ISG15 expression after 24h transfection (Fig. 3.7D). NS1/2 expression resulted in a significant reduction in MxA and ISG15 mRNA at both 24h and 48h transfection (Fig. 3.7A & C). A summary of these results is shown in Fig. 3.8, highlighting that the expression of NS1 has the greatest impact on ISG expression and that BEAS 2b cells are more sensitive to NS1 expression.

Levels of PKR, MxA and USP18 protein expression were measured 48h after transfection with RSV NS proteins. In A549 cells the amount of MxA protein was reduced by the expression of NS1 (Fig. 3.9A & B), total PKR levels were not significantly impacted by NS expression, despite the reduced mRNA levels (Fig. 3.6B). Protein levels of USP18 were highly reduced in A549 cells (Fig. 3.9C & D), matching the result in mRNA levels of USP18 at the same time point. In BEAS 2b cells protein expression of MxA and USP18 was reduced with expression of both NS proteins, after 48h transfection (Fig.

3.10A & E) despite NS2 having only a moderate impact on mRNA levels of these genes (Fig. 3.7). Only USP18 protein levels were reduced by NS1 expression in the BEAS 2b cell line (Fig. 3.10E & F). PKR protein expression was not impacted by NS expression (Fig. 3.10C & D).

While gene expression is the first step to protein synthesis it does not guarantee that new protein will be made, expression of a protein is controlled by the transcription of mRNA, translation of mRNA to protein, and the rate of degradation of the protein. Impacting any of these steps will alter the protein concentration within the cell. There are multiple regulatory steps to control the activity of the ribosome and protein degradation; the results here show that NS1 reduces mRNA of PKR but there is no matched reduction in protein levels, with expression of PKR consistent between all transfection environments. This consistent PKR expression could be caused by PKR being a more stable protein, so although the mRNA levels drop when NS1 is expressed previously produced PKR is still present in the cytoplasm. In the BEAS 2b cells, both NS1 and NS2 expression resulted in reduced total protein of MxA and USP18, with PKR showing no change. The reduction in protein with NS2 expression, with no corresponding change in mRNA levels, could be caused by NS2 increasing the proteosomal degradation of the proteins directly or by reducing ribosomal translation of mRNA. This would suggest that NS2 uses a different mechanism to reduce ISG expression at the protein level.

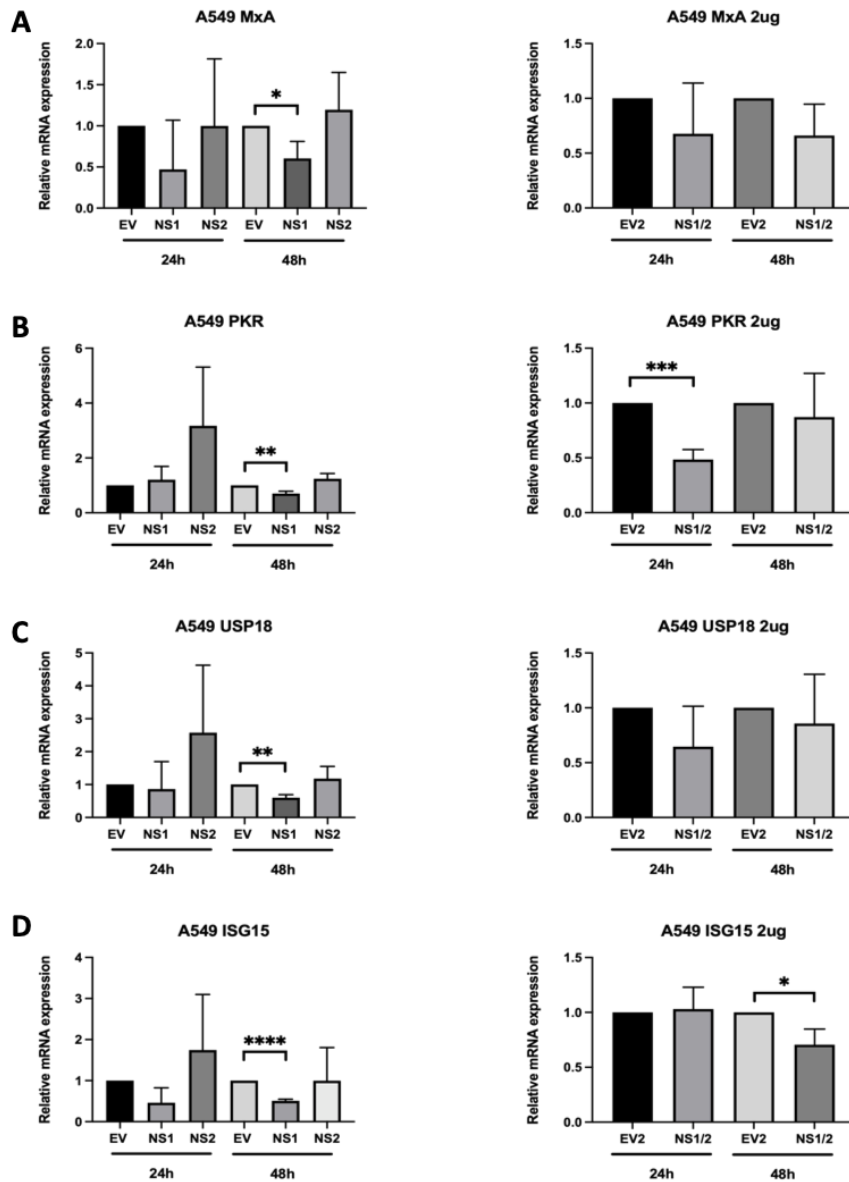


Figure 3.6: The effect of RSV NS1 and NS2 on ISG expression in A549 epithelial cells.

*A549 cells were transfected with 1µg EV, NS1, NS2 or 2µg EV (EV2) or NS1/2 for 24h or 48h as indicated. mRNA was analysed by RT-qPCR for levels of A) MxA and B) PKR C) USP18 and D) ISG15 relative to RPS15 and normalised to the EV control. All data is shown as mean \pm SD. Significance was determined by unpaired t-test * $p < 0.05$, ** $p < 0.01$, *** $p < 0.0001$ ($n = 3$)*

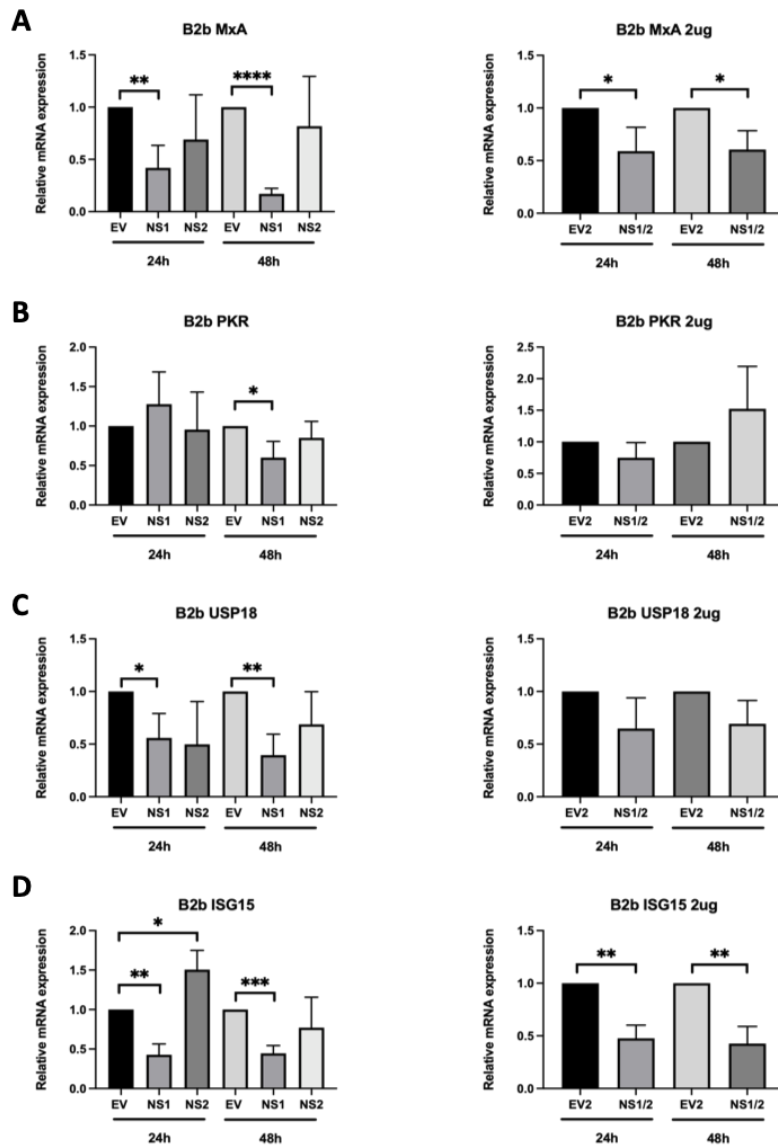
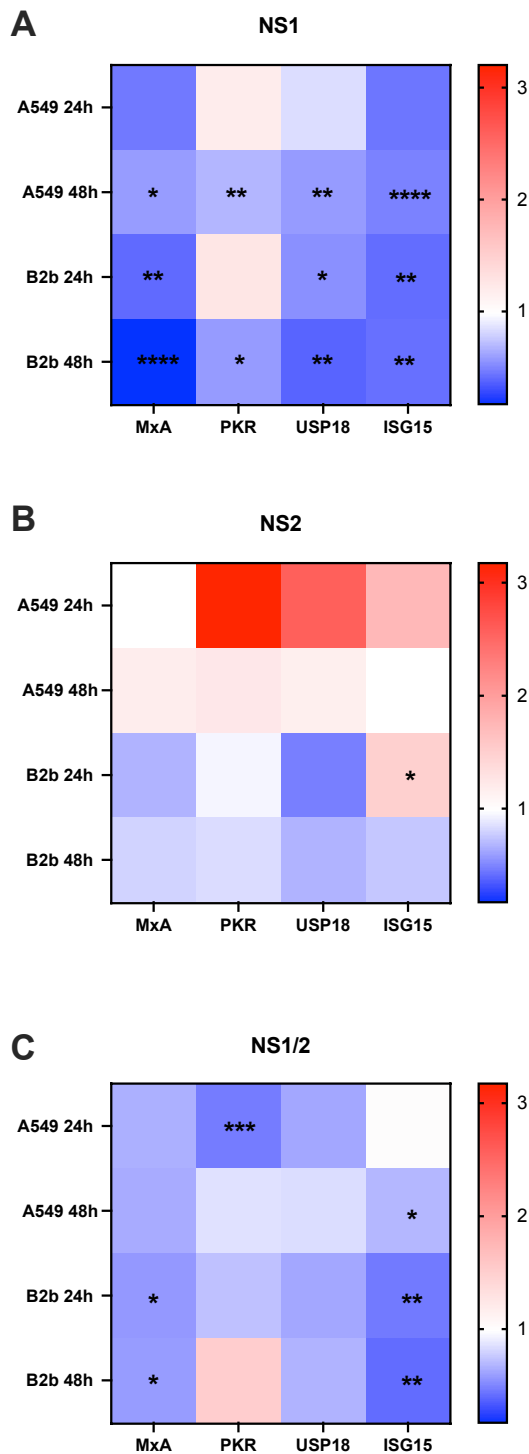


Figure 3.7: The effect of RSV NS1 and NS2 on ISG expression in BEAS-2b epithelial cells.

BEAS 2b cells were transfected with 1µg EV, NS1, NS2 or 2µg EV (EV2) or NS1/2 for 24h or 48h as indicated. mRNA was analysed by RT-qPCR for levels of A) MxA and B) PKR C) USP18 and D) ISG15 relative to RPS15 and normalised to the EV control. All data is shown as mean ±SD. Significance was determined by unpaired t-test * $p < 0.05$, ** $p < 0.01$, *** $p < 0.001$, **** $p < 0.0001$ ($n=3$)



The impact of NS expression was compared between cell type and the length of time NS were expressed. The mRNA fold change values were expressed as a heatmap. Fold change after expression of A) NS1 B) NS2 and C) NS1/2. Significance was determined by unpaired t-test * $p < 0.05$, ** $p < 0.01$, *** $p < 0.001$, **** $p < 0.0001$ ($n=3$).

Figure 3.8: Summary of the effect of RSV NS proteins on MxA, PKR, USP18 and ISG15 mRNA

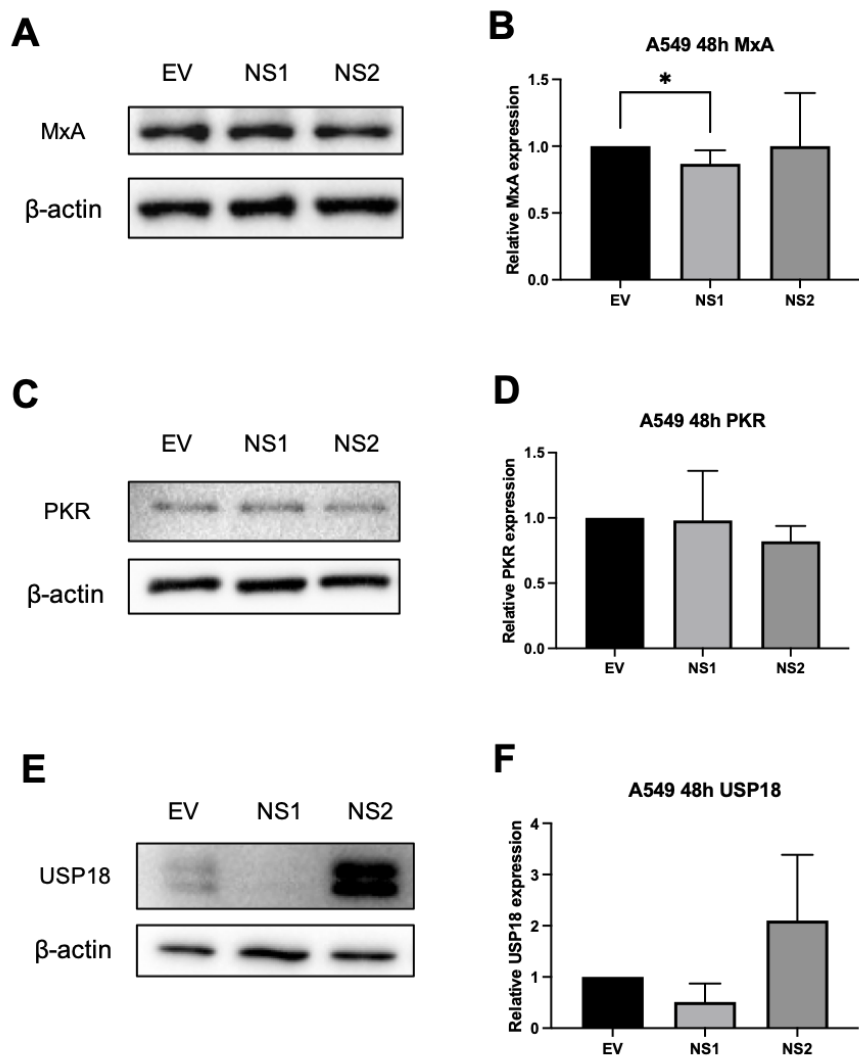


Figure 3.9: Expression of NS1 reduced MxA protein expression in A549 epithelial cells.

*A549 cells were transfected with 1 μ g EV, NS1 or NS2 for 48h, cell lysates were collected and analysed by western blotting for levels of A) MxA and B) MxA densitometry, C) PKR and D) PKR densitometry, and E) USP18 and F) USP18 densitometry. The band of interest was normalised to β -actin loading control and shown relative to the EV control. Significance was determined by unpaired t-test * $p < 0.05$ ($n=4$).*

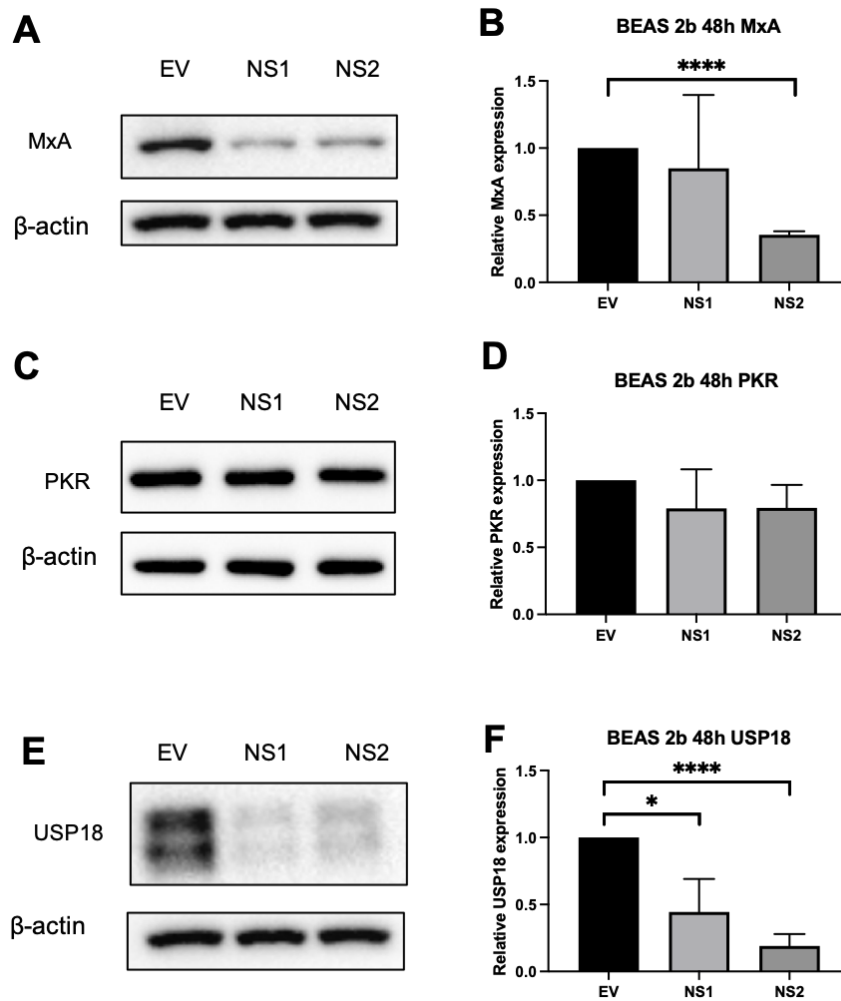


Figure 3.10: Expression of NS1 reduced USP18, while expression of NS1 and NS2 reduced MxA in BEAS 2b epithelial cells.

*BEAS 2b cells were transfected with 1 μ g EV, NS1 or NS2 for 48h, cell lysates were collected and analysed by western blotting for levels of A) MxA and B) MxA densitometry, C) PKR and D) PKR densitometry, and E) USP18 and F) USP18 densitometry. The band of interest was normalised to β -actin loading control and shown relative to the EV control. Significance was determined by unpaired t-test * $p < 0.05$, ** $p < 0.01$, *** $p < 0.001$, **** $p < 0.0001$ ($n=3$).*

3.3.4 Effect of RSV NS proteins upon SOCS expression in epithelial cell lines

During viral infections levels of the SOCS proteins will increase in order to modulate the immune response and prevent excessive JAK/STAT stimulation (Yoshimura et al., 2007, Croker et al., 2008). Several viruses have been shown to manipulate levels of these negative regulators to enhance viral replication (Collins et al., 2014, Akhtar and Benveniste, 2011). Indeed, RSV's NS proteins have been shown to increase SOCS1, SOCS3 and CIS levels (Xu et al., 2014, Zheng et al., 2015, Hashimoto et al., 2009). Therefore, we hypothesized that the RSV NS proteins could be increasing the expression of SOCS proteins, thus attenuating the JAK/STAT pathway and reducing ISG expression.

Previous studies have mainly focused on the effect of RSV on SOCS expression using Hep2 and A549 cells. To add to these reports and investigate if the cell line used had an impact on results, the A549 and BEAS 2b cell lines were transfected with 1 μ g/ml of the NS1 and NS2 plasmids, alongside an equivalent EV control. Levels of SOCS family members were measured by RT-qPCR after 24h and 48h transfection. The expression of CIS mRNA had a 4-fold increase when NS1 was expressed for 24h, though this was not significant, but after 48h CIS expression was significantly reduced with the expression of either NS protein (Fig. 3.11A). The co-expression of NS1/2 had no effect on CIS levels at 24h, but did slightly reduce CIS at 48h expression (Fig. 3.11D). Unlike previous reports, we did not see a significant increase in SOCS1 mRNA upon expression of RSV NS1 in A549 cells (Zheng et al., 2015), though NS2 did cause a significant increase at 24h expression (Fig. 3.11B). Co-expression of the NS proteins caused a 2-fold rise in SOCS1 at 24h transfection but this was not significant (Fig. 3.11E). SOCS3 mRNA expression increased with NS2 after 24h and while not reaching significance there was a mean fold increase of 1.5 with $p=0.05$ with NS1 expression (Fig. 3.11C). Interestingly, expressing both NS1 and NS2 together significantly increased SOCS3 after 24h transfection (Fig. reffig:A549 SOCS 1F). SOCS4 mRNA expression was unaffected by transfection, though there was slight increase in SOCS4 mRNA upon expression of individual NS plasmids at 24h (Fig. 3.12A). The same effect is seen in SOCS5 mRNA levels, with a greater than two-fold increase in SOCS5 mRNA with individual transfections at 24h; at 48h however, NS1 lead to a highly significant decrease in SOCS5 mRNA (Fig. 3.12B). SOCS7 mRNA levels were significantly reduced by both NS1 and NS2 at 24h, and by NS1 after 48h transfection (Fig. 3.12C). The co-expression of NS1 and NS2 (NS1/2) had no impact on SOCS4, SOCS5 or SOCS7 mRNA levels (Fig. 3.12D-F).

The BEAS 2b cell line is also of airway epithelial origin, however, it was isolated from healthy bronchial epithelium and has been shown to respond differently to RSV infection, when compared to the type II alveolar A549 cells (Hillyer et al., 2018). As before, cells were transfected with 1 μ g/ml of the NS1 and NS2 plasmids, alongside an equivalent EV control for 24h or 48h and SOCS mRNA expression was measured by RT-qPCR. In the BEAS 2b SOCS1 mRNA showed no increase with NS protein expression, instead SOCS1 showed a significant decreased after 48h transfection (Fig. 3.13B). SOCS3 mRNA levels rose slightly after expression with NS1 at both 24h (1.3 fold) and 48h (1.2 fold), however this was not a significant increase (Fig. 3.13D). SOCS4 increased with individual NS transfection after 24h, with a significant increase upon expression of NS2 (Fig. 3.14A). The remaining SOCS mRNA levels (SOCS5, SOCS7 and CIS) were unaffected by NS (Fig. 3.13A & Fig. 3.14B-F).

To see the effect of the NS expression on SOCS mRNA levels at a glance the results are shown in Fig. 3.15 as a heatmap. This uses the relative expression of each SOCS mRNA as calculated by RT-qPCR. The A549 epithelial cell line had a greater response to NS expression, with NS1 causing reductions in SOCS1 and SOCS7 at 24h, and SOCS6, SOCS7 and CIS at 48h. Expression of NS2 resulted in an increase in both SOCS1 and SOCS3, and a reduction in SOCS4 at 24h. The BEAS 2b epithelial cell line had significant reductions in SOCS1 expression at 48h with both NS1 and NS2, though this reduction was not significant when NS1/2 were co-expressed.

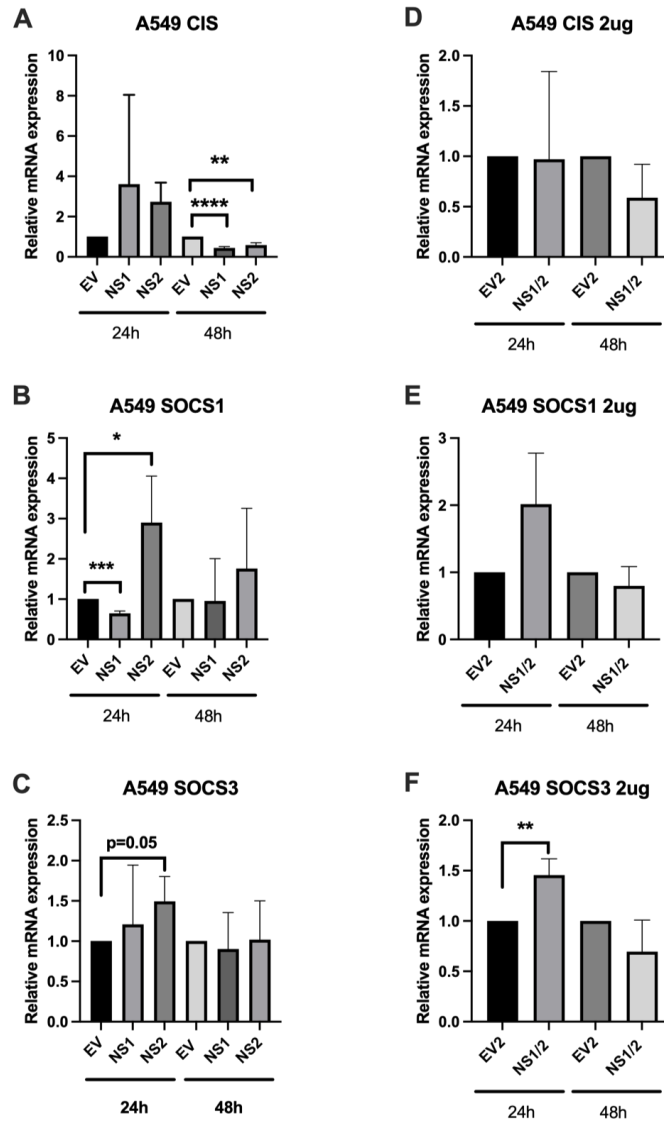


Figure 3.11: Expression of RSV NS proteins alters CIS, SOCS1 and SOCS3 in A549 cells.

A549 cells were transfected with EV, NS1, NS2 or NS1/2 for 24h or 48h as indicated. Samples were collected in Trizol and analysed by RT-qPCR for levels of A) CIS, B) SOCS1 and C) SOCS3 when expressing NS1 and NS2 individually, D) CIS, E) SOCS1 and F) SOCS3 with coexpression of NS1 and NS2. Fold change in is mRNA relative to RPS15. All data is shown as mean \pm SD. Significance was determined by unpaired t-test * $p < 0.05$, ** $p < 0.01$, *** $p < 0.001$ ($n=3$).

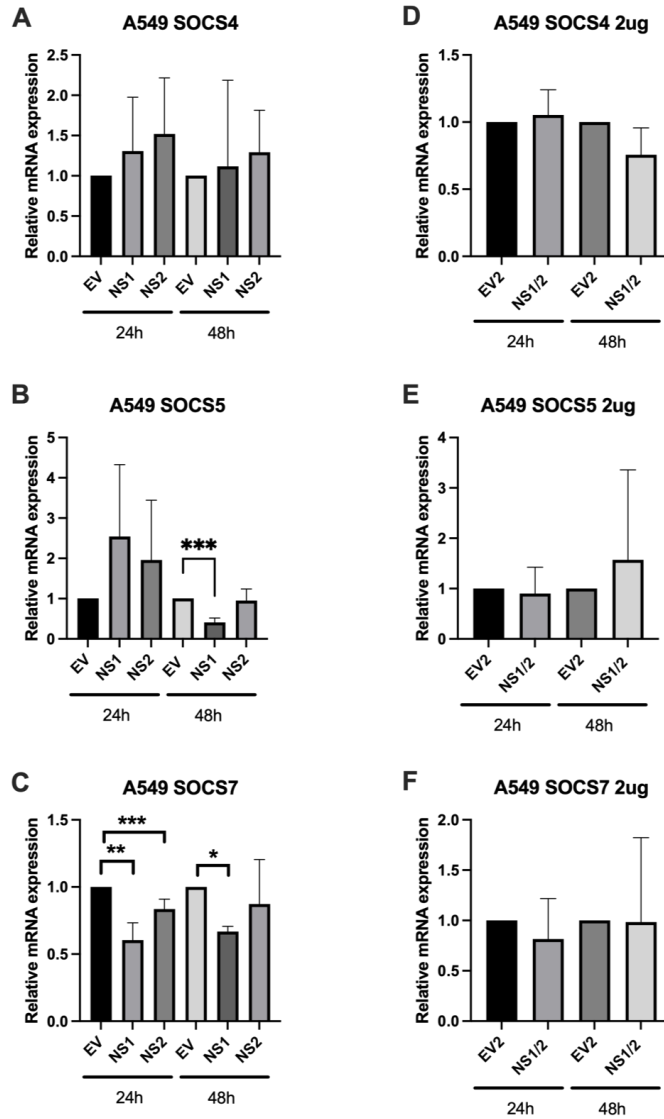


Figure 3.12: Effect of RSV NS protein expression upon SOCS5 and SOCS7 in A549 cells.

A549 cells were transfected with EV, NS1, NS2 or NS1/2 for 24h or 48h as indicated. Samples were collected in Trizol and analysed by RT-qPCR for levels of A) SOCS4, B) SOCS5 and C) SOCS7 when expressing NS1 and NS2 individually, D) SOCS4, E) SOCS5 and F) SOCS7 with coexpression of NS1 and NS2. Fold change in mRNA relative to RPS15. All data is shown as mean \pm SD. Significance was determined by unpaired t-test * $p < 0.05$, ** $p < 0.01$, *** $p < 0.001$ ($n=3$).

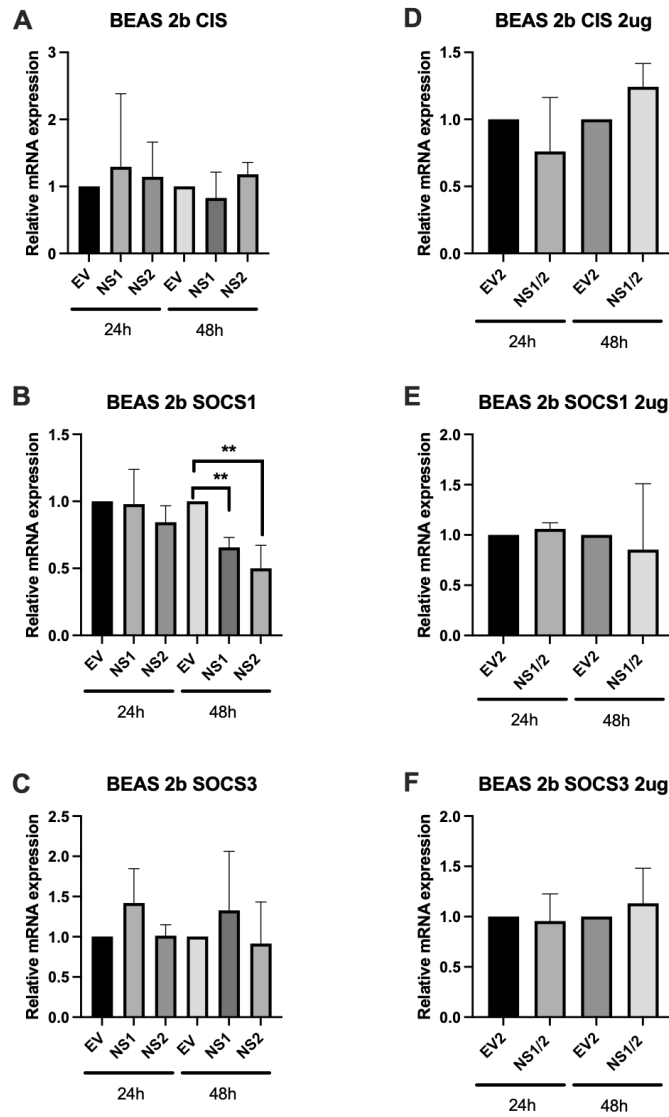


Figure 3.13: Expression of RSV NS proteins reduces SOCS1 in BEAS 2b cells.

BEAS 2b cells were transfected with EV, NS1, NS2 or NS1/2 for 24h or 48h as indicated. Samples were collected in Trizol and analysed by RT-qPCR for levels of A) CIS, B) SOCS1 and C) SOCS3 when expressing NS1 and NS2 individually, D) CIS, E) SOCS1 and F) SOCS3 with coexpression of NS1 and NS2. Fold change in is mRNA relative to RPS15. All data is shown as mean \pm SD. Significance was determined by unpaired t-test $**p < 0.01$ ($n=3$).

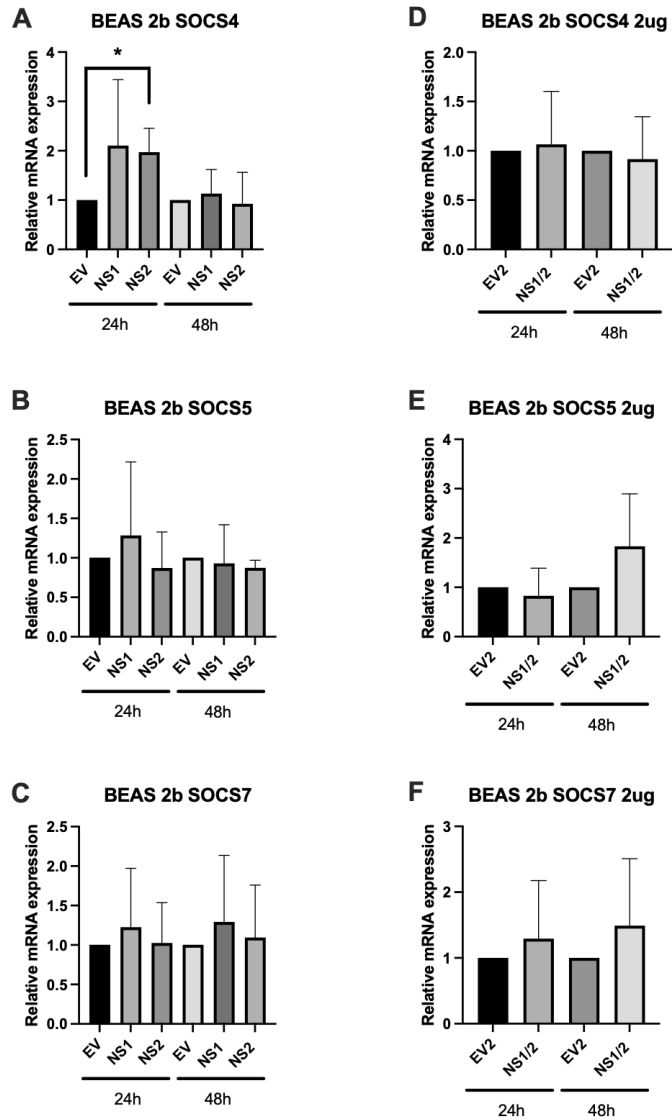


Figure 3.14: Effect of RSV NS proteins expression upon SOCS4, SOCS5 & SOCS7 in BEAS 2b epithelial cells.

BEAS 2b cells were transfected with EV, NS1, NS2 or NS1/2 for 24h or 48h as indicated. Samples were collected in Trizol and analysed by RT-qPCR for levels of A) SOCS4, B) SOCS5 and C) SOCS7 when expressing NS1 and NS2 individually, D) SOCS4, E) SOCS5 and F) SOCS7 with coexpression of NS1 and NS2. Fold change in is mRNA relative to RPS15. All data is shown as mean \pm SD. Significance was determined by unpaired t-test * $p < 0.05$ (n=3).

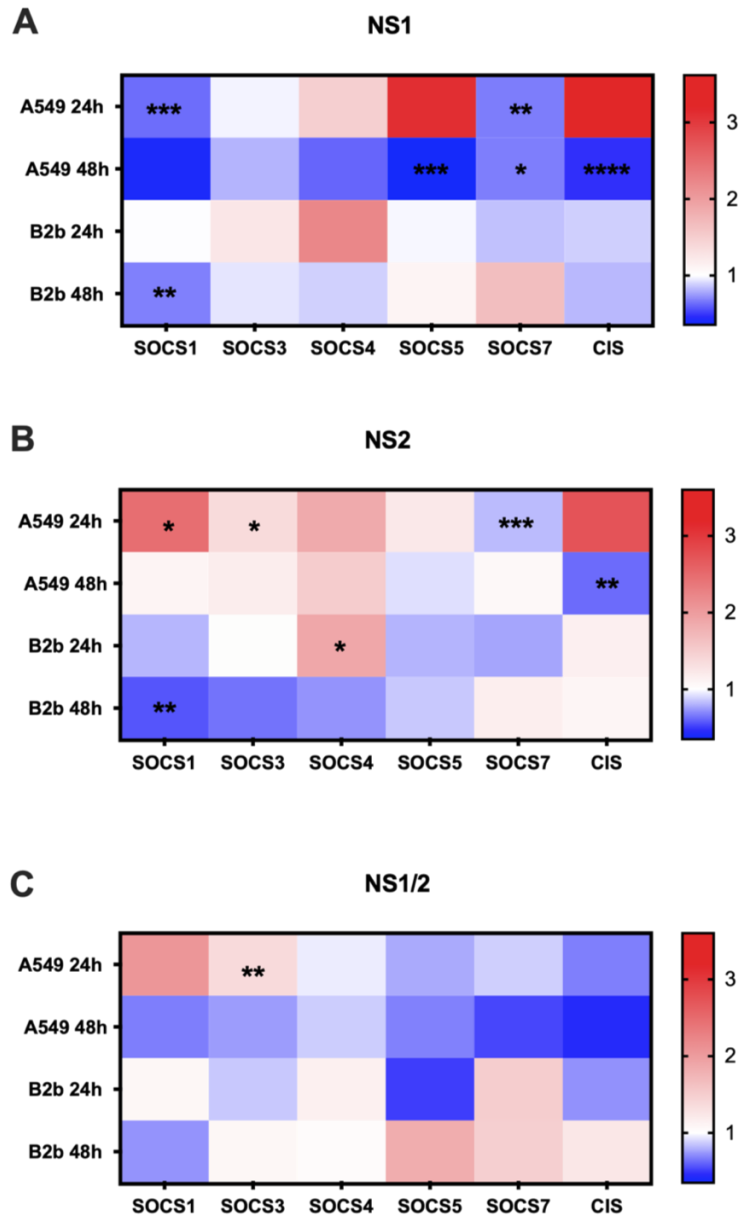


Figure 3.15: Summary of the effect of RSV NS proteins on SOCS expression.

*The impact of NS expression on SOCS mRNA varied depending on cell type and the length of time NS were expressed. The mRNA fold change values are expressed here as a heatmap. Fold change after expression of A) NS1 B) NS2 and C) NS1/2. Significance was determined by unpaired t-test * $p < 0.05$, ** $p < 0.01$, *** $p < 0.001$ ($n=3$).*

3.3.5 The Change in SOCS Levels is Not Linked to Altered Cytokine Response

SOCS proteins are induced by several stimuli in order to control signalling through specific pathways. SOCS1 can be induced by IFN- λ , while IL-6 will induce SOCS3 and SOCS5. The change in SOCS levels could be the result in cytokine expression in transfected cell. Increased cytokine production would create a corresponding increase in SOCS as the cell upregulates negative regulators to controls the signalling pathway and return to homeostasis. Levels of IFN- λ and IL-6, which are regulated by SOCS1 and SOCS3, were measured by ELISA to see if they were impacted by transfection. IL-6 production was increase with NS2 expression at both 24h and 48h in A549 cells (Fig. 3.16A & B), but in the BEAS 2b there was no change in IL-6 with NS expression, though basal levels were higher (Fig. 3.16C & D). IFN- λ was not affected by NS expression in either cell type (Fig. 3.17).

A number of cytokines will cause an increase in SOCS proteins, including IL-2, 4, 7, 10, 15, IFN-I, IFN-II and TNF. To confirm that no other soluble factor caused the change in SOCS expression conditioned media from 48h transfected A549 cells was used to treat naïve, untransfected A549 cells for 6h before harvesting for PCR. As the SOCS most affected by NS expression in A549 were SOCS1 and CIS, levels of these genes were measured. In addition, levels of NS1 and NS2 expression was also measured to confirm any difference was the result of soluble factors in the supernatant rather than low level transfections. Although low, there was significant levels of NS1 and NS2 mRNA in the samples (Fig. 3.18A & B), and there no significant change in SOCS1 or CIS (Fig. 3.18C & D). This was likely causes by transient transfection from residual lipofectamine still present in the conditioned media. From these data the change in SOCS expression with NS expression is not the result of soluble factors released by the cells, and is directly caused by the expression of NS proteins in the cell.

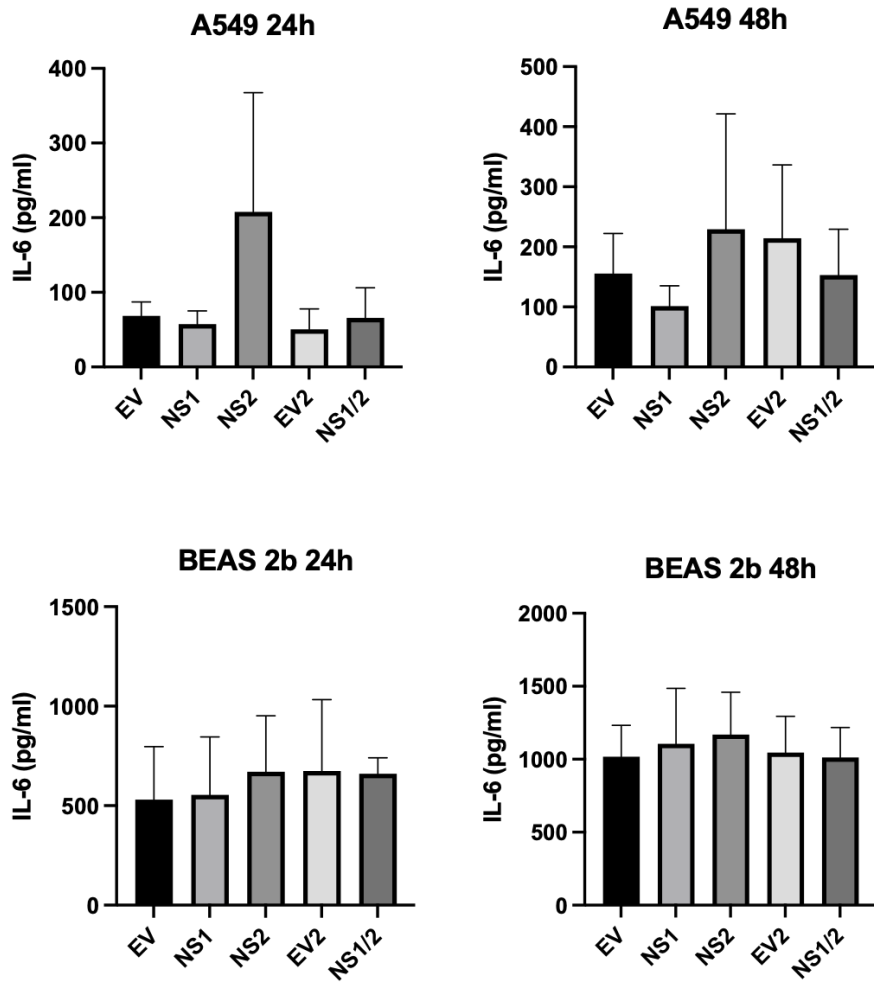


Figure 3.16: Expression of NS proteins has no impact on IL-6 expression.

A549 and BEAS 2b cells were transfected with EV, NS1, NS2 or NS1/2 for 24h or 48h as indicated. Samples were analysed by ELISA for IL-6 expression in A) A549 cells after 24h, B) A549 cells after 48h C) BEAS 2b cells after 24h and D) BEAS 2b cells after 48h. All data is shown as mean \pm SD. Significance was determined by ANOVA (n=3).

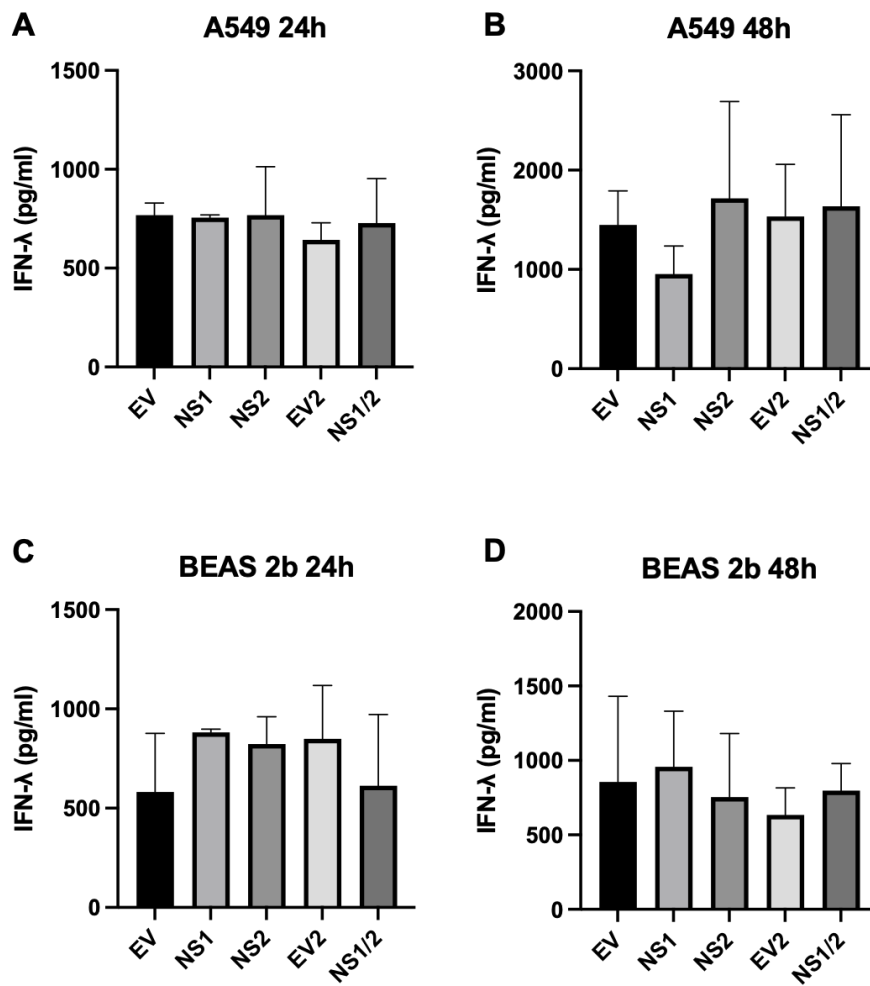


Figure 3.17: Expression of NS proteins has no impact on IFN-λ expression.

A549 and BEAS 2b cells were transfected with EV, NS1, NS2 or NS1/2 for 24h or 48h as indicated. Samples were analysed by ELISA for IFN-λ expression in A) A549 cells after 24h, B) A549 cells after 48h C) BEAS 2b cells after 24h and D) BEAS 2b cells after 48h. All data is shown as mean \pm SD. Significance was determined by ANOVA ($n=3$).

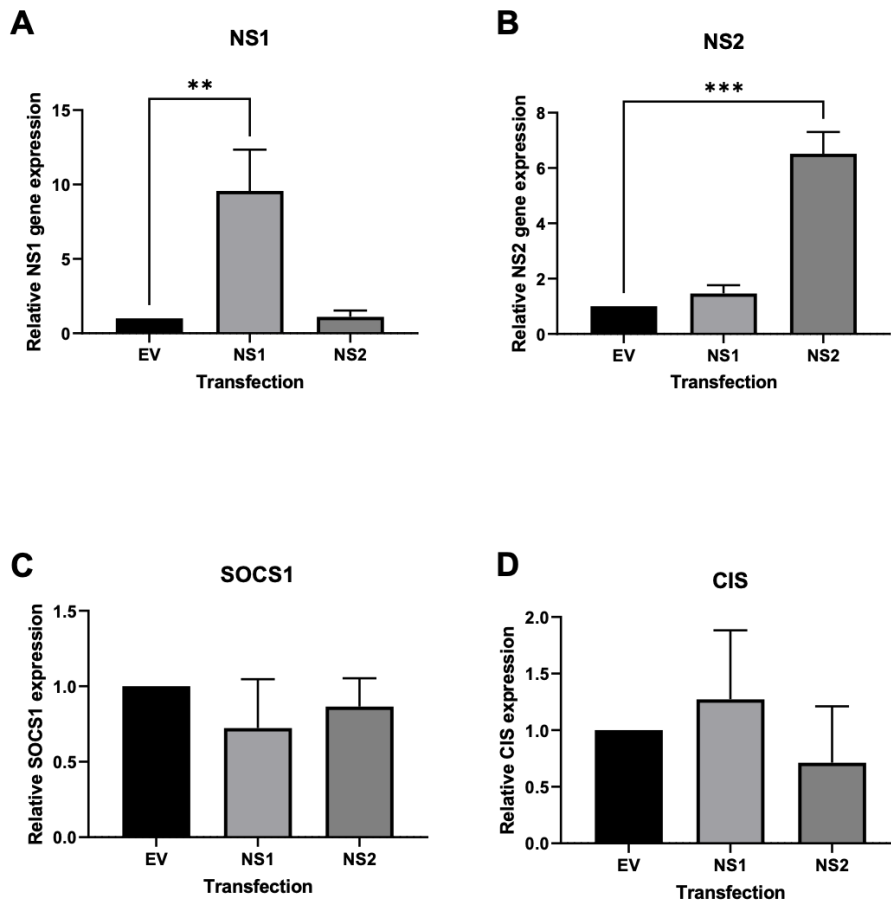


Figure 3.18: Conditioned media from NS1 and NS2 expressing A549 cells does not induce SOCS1 or CIS.

A549 cells were transfected with NS1 and NS2 for 48h, this conditioned media was added to fresh A549 cells for 6h before the cells were collected for RT-qPCR. Levels of A) NS1 and B) NS2 mRNA were measured to see if residual transfection reagents had caused NS expression in the cells. Levels of C) SOCS1 and D) CIS mRNA remained unchanged. All data is shown as mean \pm SD. Significance was determined by unpaired t-test ($n=3$).

3.3.6 RSV infection alters ISG or SOCS expression dependent on cell line

Having seen that the expression of NS proteins had different effects in the two cell lines, we next looked at how infection with full length RSV-A2 and RSV- Δ NS1/2 affected ISG levels and SOCS expression. Using the full-length RSV-A2-GFP virus, both cell lines were infected at multiplicity of infection (MOI) 1 and MOI 3 for 24h and assessed by flow cytometry. As the virus is GFP tagged all infected cells are identifiable by fluorescence. Quantification by flow cytometry showed that both A549 (Fig. 3.19) and BEAS 2b (Fig. 3.20) cell lines were competently infected with 40% of A549 cells GFP positive (GFP+) at MOI 1 and 60% GFP+ at MOI 3 (Fig. 3.21A). The BEAS 2b cell line was more permissive to infection with 55% GFP+ at MOI 1 and 75% GFP+ at MOI 3 (Fig. 3.21B). In addition to the full-length RSV infection an NS1 and NS2 knockout virus, RSV- Δ NS-GFP was used. This strain is known to infect IFN competent cells poorly, however on infection BEAS 2b cells did have a small population of GFP+ cells (Fig. 3.21D), no GFP signal was detected in the infected A549 cells (Fig. 3.21C). We had previously seen that expression of NS1 caused different levels of ISG expression in A549 compared the BEAS 2b cells. To see if this difference was maintained with infection with the full length virus both cell lines were infected with MOI 1 and MOI 3 RSV-A2-GFP for 24h and expression of MxA, ISG15 and USP18 mRNA were measured by RT-qPCR. To confirm successful infection in each case levels of RSV-F mRNA was measured, RSV-F was detected in all cells exposed to the virus, with A549 showing greatest expression of RSV-F at MOI 3 (Fig. 3.22A) and BEAS 2b showing consistent RSV-F expression at both MOI 1 and MOI 3 (Fig. 3.22E). Both MxA (Fig. 3.22B & F) and ISG15 (Fig. 3.22C & G) mRNA are induced with RSV infection, with A549 showing a greater fold change than BEAS 2b at both MOI 1 and MOI 3. USP18, an ISG and negative regulator of the pathway, is the only gene measured to have a significant induction with infection, and unlike the other ISGs measures the BEAS 2b show a greater fold induction than the A549 (Fig. 3.22D & H).

Levels of SOCS is also variable between the cells lines, SOCS1 is induced by RSV infection at MOI 1 and significantly induced at MOI 3 but no increase is seen in BEAS 2b with RSV infection (Fig. 3.23A). SOCS3 has a 10 fold rise in expression in BEAS 2b cells with MOI 3 infection but it unaffected in A549s (Fig. 3.23B). In A549 cells levels of CIS expression increase with both concentrations of RSV infection, but only limited increases are seen in BEAS 2b (Fig. 3.23C).

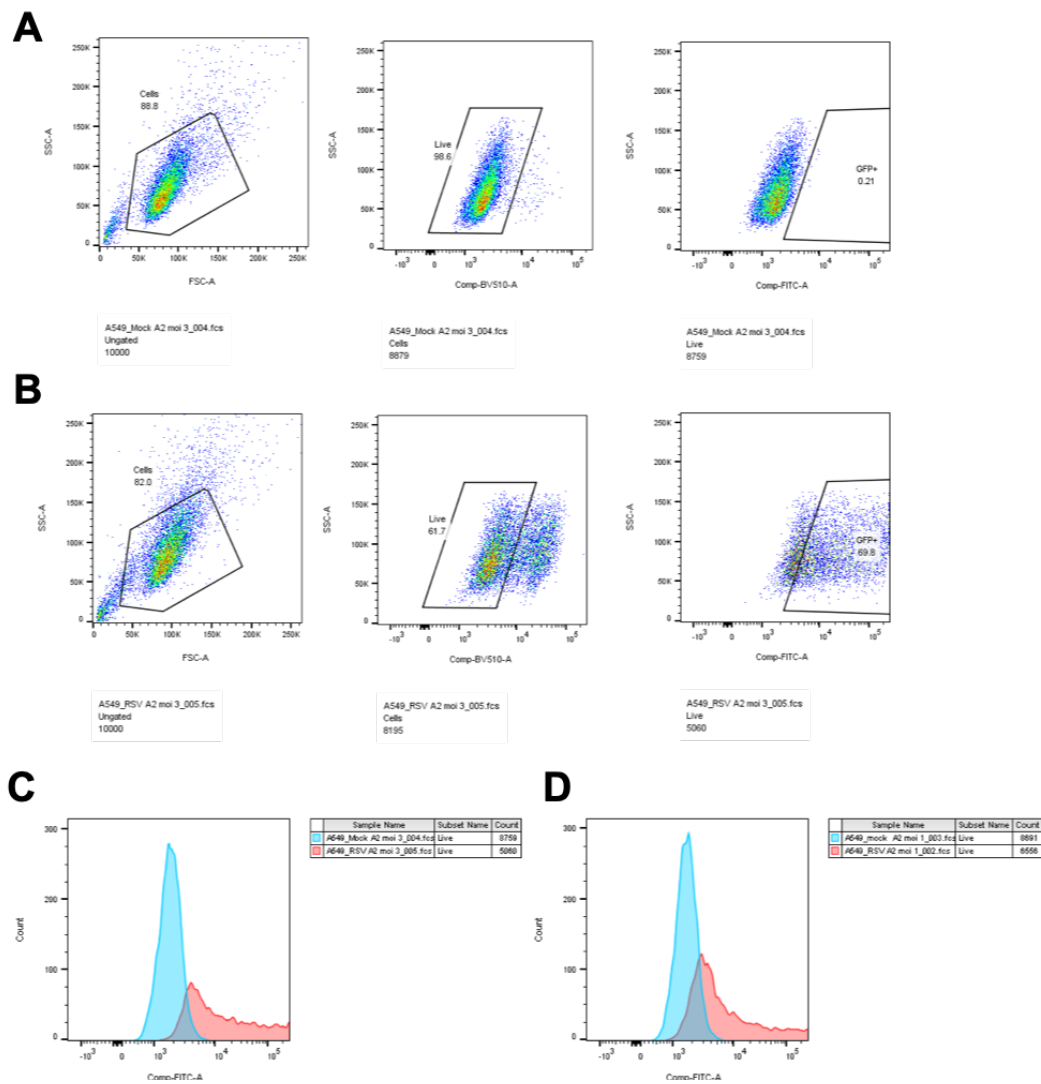


Figure 3.19: Infection of A549 cells with RSV-A2-GFP.

A549 cells were infected with RSV-A2-GFP at MOI 1 and MOI 3 for 24h. The gating strategy is shown for A) mock infected and B) RSV-A2-GFP infected at MOI 3. The cells were selected for, excluding debris, Live cells were gated using Live/Dead (L/D)-BV510, and the percentage of GFP+ cells were measured on the FITC channel. Levels of GFP staining was compared to the mock in each case for C) MOI 1 and D) MOI 3 infections.

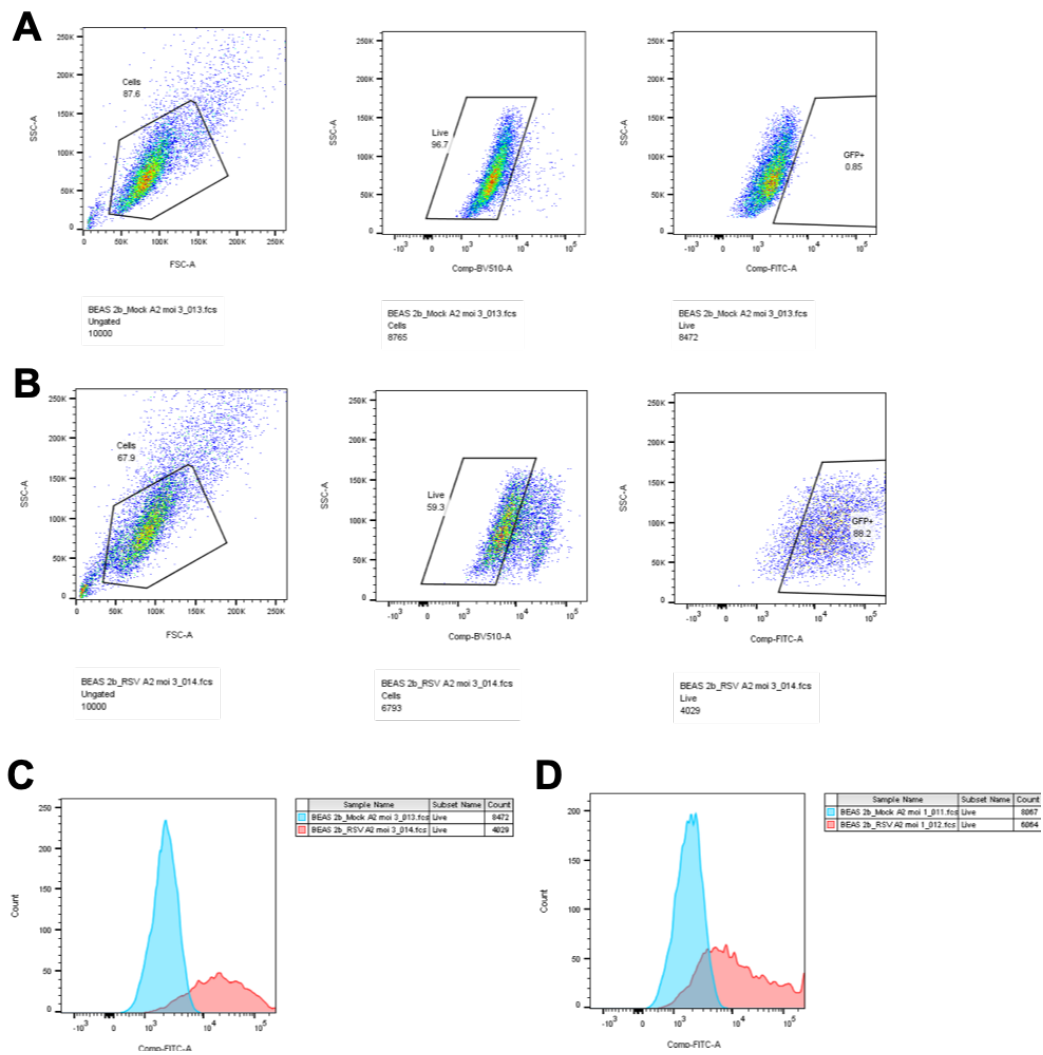


Figure 3.20: Infection of BEAS 2b cells with RSV-A2-GFP.

BEAS 2b cells were infected with RSV-A2-GFP at MOI 1 and MOI 3 for 24h. The gating strategy is shown for A) mock infected and B) RSV-A2-GFP infected at MOI 3. The cells were selected for, excluding debris, Live cells were gated using Live/Dead (L/D)-BV510, and the percentage of GFP+ cells were measured on the FITC channel. Levels of GFP staining was compared to the mock in each case for C) MOI 1 and D) MOI 3 infections.

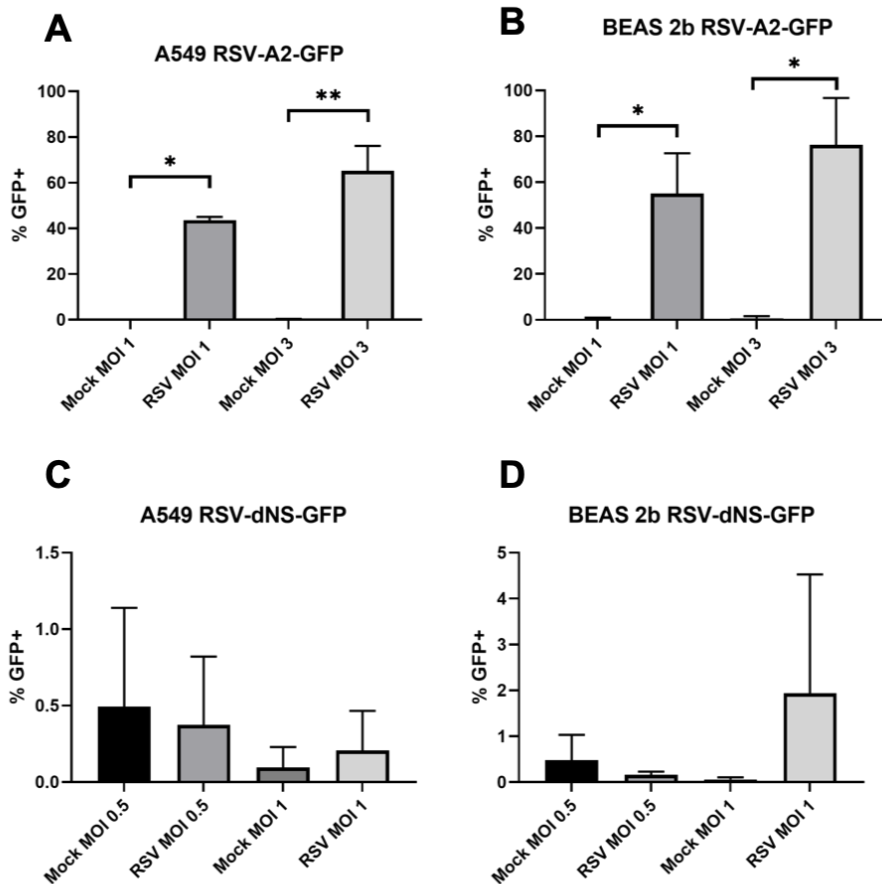


Figure 3.21: Percentage of GFP expressing cells after infection in RSV-A2-GFP or RSV- Δ NS-GFP.

*A549 and BEAS 2b were infected with the MOI shown for 24h and assessed by flow cytometry for the percentage of cells expressing GFP, indicating viral infection. A) A549 GFP+ with RSV-A2-GFP, B) BEAS 2b GFP+ with RSV-A2-GFP, C) A549 GFP+ with RSV- Δ NS-GFP, D) BEAS 2b with RSV- Δ NS-GFP. All data is shown as mean \pm SD. Significance was determined by paired t-test * p <0.05, ** p <0.01 (n =3).*

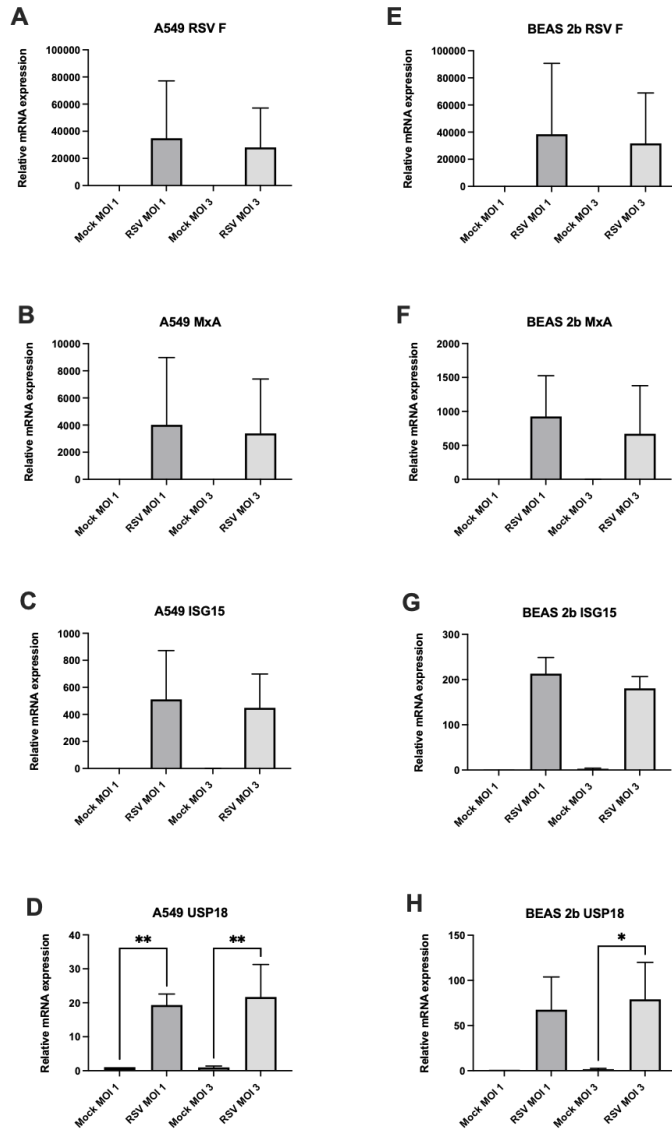


Figure 3.22: Infection with RSV-A2-GFP causes an increase in ISG mRNA expression.

*A549 and BEAS 2b cells were infected with RSV-A2-GFP, at an MOI 1 and MOI 3 for 24h before analysis by RT-qPCR. A) RSV-F gene expression was used to confirm infection, B) MxA, C) ISG15 and D) USP18 were increased at both concentrations of virus. All data is shown as mean \pm SD. Significance was determined by ANOVA * $p < 0.05$, ** $p < 0.01$ ($n=3$).*

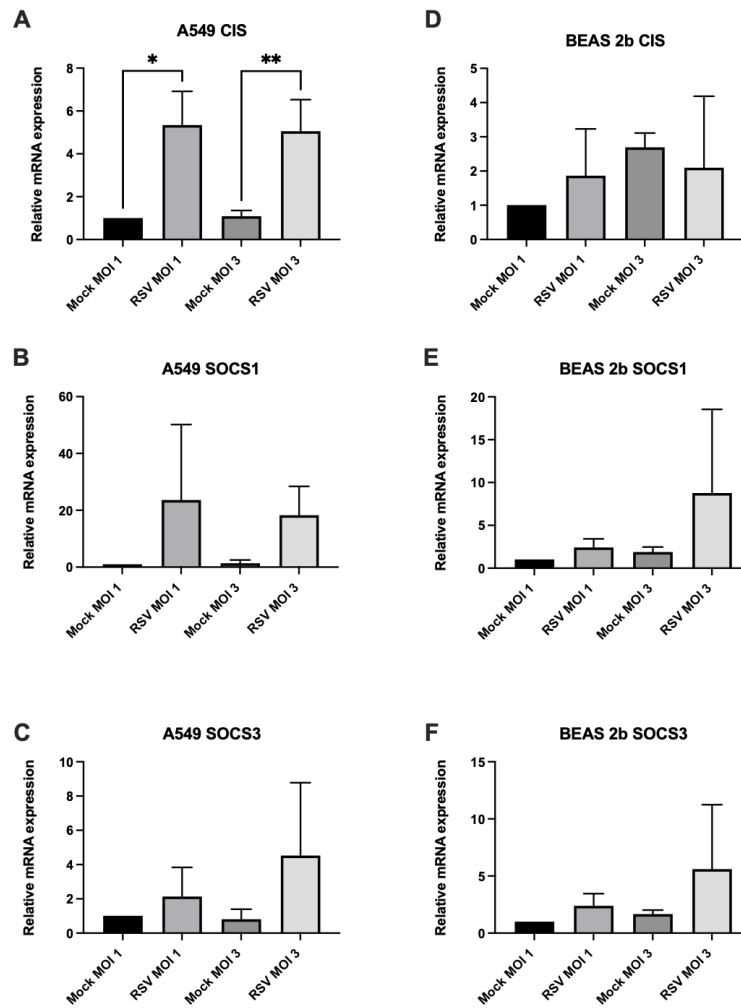


Figure 3.23: Infection with RSV-A2-GFP causes an increase in SOCS mRNA expression.

*A549 and BEAS 2b cells were infected with RSV-A2-GFP, at an MOI 1 and MOI 3 for 24h before analysis by RT-qPCR. A & D) CIS, B & C) SOCS3, and C & F) SOCS3 were increased at both concentrations of virus. All data is shown as mean \pm SD. Significance was determined by ANOVA * $p < 0.05$, ** $p < 0.01$ ($n=3$).*

3.4 Discussion

The RSV proteins are highly conserved between strains and have been shown to be integral to the effective propagation of both human RSV (hRSV) and bovine RSV (bRSV) – deletion of both NS1 and NS2 severely attenuates RSV and it is only able to replicate in IFN incompetent Vero cells. To further investigate the mechanism of NS1 and NS2 on IFN signalling, each gene was expressed in immortalised cells lines. Aligning the constructs sequence to circulating wild type (WT) RSV, the NS sequences showed a high degree of conservation, particularly with the RSV A strain; NS1 has 100% and NS2 has 96.8% similarity. This supported that these NS genes were representative of wild WT RSV A. While RSV is a human pathogen (hRSV) there is also a bovine form, bRSV, which causes a similar respiratory infection in calves. Like hRSV, the bRSV NS proteins are integral for its effective replication and deletion mutants are highly attenuated (Valarcher et al., 2003). However, bRSV NS proteins have been shown to use a different mechanism to attenuate IFN signalling, in bRSV the NS proteins cooperatively enhance resistance to IFN α treatment, with NS1/2 deletion mutants severely attenuated in IFN competent cells (Schlender et al., 2000).

Aligning the hRSV and bRSV NS proteins showed a high degree of conservation; NS1 is 69% identical between hRSV and bRSV, the divergent amino acids occur throughout the sequence rather than a single area. Conversely NS2 has 84% sequence identity between hRSV and bRSV, with the majority of the variation within the first 30 residues. This would suggest that the NS1 structures between bRSV and hRSV could be quite different due to the variability of sequence across the whole protein, while the structure of NS2 may be very similar, with the only difference at the C terminal end of the protein. Research into bRSV NS1 and NS2 has shown that the NS proteins could be host range determinants, replacing the bRSV NS proteins with the hRSV counterparts causes attenuation of bRSV in bovine cells while the chemic bRSV replicated as well in human cell lines, showing that the bRSV NS proteins specifically target the bovine IFN pathway (Bossert and Conzelmann, 2002, Schlender et al., 2000).

Further interrogation of hRSV NS sequences identified sequence homology between NS1 and NS2 in regions that could hold a putative BC box and Cul2 binding sites. The presence of these features could allow both NS1 and NS2 to act as an E3 ligase. Previously Elliott et al., (2007) identified a putative BC box within NS1, showing that this region was conserved with other proteins that interact with Elongin C, including SOCS1-3. Here we have confirmed this site is present in NS1 and also NS2, with both proteins also

containing a putative Cul2 binding site which has not been identified previously. The BC box and Cul2 binding sites are conserved regions of the SOCS proteins that allow them to form E3 ligases. Interacting with E2 proteins and cullins, directing the ubiquitination of target proteins which are then degraded by the proteasome. The identification of these motifs suggests that both NS1 and NS2 would be able to cause the proteasomal degradation of target proteins. However, the presence of these sequences alone does not guarantee they are functionally active.

Having established that the NS constructs were representative of circulating RSV, and that both may have E3 ligase function, we looked to express the proteins individually and together in cell lines. Both A549 and BEAS 2b cell lines originate from human respiratory epithelium and have been widely used to study respiratory viruses including RSV. To confirm successful transfection mRNA levels of NS1 and NS2 were measured and protein expression was confirmed by western blotting. High levels of NS1 mRNA and protein were seen in both cell lines with the greatest expression of mRNA and protein at 24h transfection. The transfection of NS2 also peaked at 24h transfection for both cell lines: however, while NS2 mRNA levels were detected in transfected cells, protein could only be detected in the BEAS 2b cells. This could mean that there was inefficient translation of the NS2 mRNA into protein in the A549 cells. Alternatively this apparent lack of protein could be an artefact of the NS2 antibody; the NS2 antibody used is a polyclonal antibody which caused a large number of non-specific bands, with more seen in the A549 samples than the BEAS 2b. As a result when developing these blots the non-specific bands developed faster than the band of interest, potentially drowning out the signal. As a result of this successful protein expression of NS2 in the A549 cell line cannot be explicitly proven. The lack of an NS2 signal in A549 cells when assessed by western blot suggests there is less NS2 expression compared to NS1 in A549 cells, even when transfected with the same amount of DNA construct. Any effects of NS2 would be less pronounced in these experiments.

To measure the functional output of the JAK-STAT pathway we measured mRNA expression of several ISGs: MxA, PKR, ISG15 and USP18. We found that NS1 expression reduced the expression of all ISGs measured at both time points, with BEAS 2b more having more significant reductions after only 24h expression, while the A549s typically only had significant reductions in ISGs after 48h NS1 expression.

The JAK-STAT pathway is highly regulated, and there have been reports of the RSV NS proteins inducing SOCS1 and SOCS3 expression to negatively regulate JAK-STAT

signalling (Xu et al., 2014, Zheng et al., 2015). We hypothesized that the mechanism for the reduction in basal ISG was a corresponding increase in relevant SOCS. However, we found that the two SOCS best understood to impact the JAK-STAT pathway, SOCS1 and SOCS3, were not increased by NS1 expression, the driver of ISG reduction. When SOCS levels were measured there was only a limited increase in SOCS3 seen in the A549 cells, and a small increase in SOCS4 in the BEAS 2b cells. This suggests that while the SOCS can be influenced by NS this is cell line specific and does not fully account for the reduction in ISGs seen. The changes in SOCS mRNA that were seen were most often reductions in SOCS expression, which was not expected. The variance between these data and previous reports could be a result of varying conditions, both Zheng (Zheng et al., 2015) and Xu (Xu et al., 2014) used at plasmid concentrations of $8\mu\text{g}/\text{ml}$ and an increased volume of lipofectamine to transfect A549 cells, we found that greater than $2\mu\text{l}$ in 1ml caused a high level of cell toxicity.

NS1 and NS2 have been reported to act cooperatively however, we have found no enhancement of function when NS were expressed together. This maybe the result of inefficient protein expression with co-transfection, as less protein was detected in co-transfected samples compared to when each plasmid was transfected singly. As a result, although the same concentration of plasmid DNA was added, and the NS mRNA increases accordingly, there is reduced protein produced with the measured protein levels failing to match the single transfections. While BEAS 2b are more sensitive to NS expression when measuring ISGs, the A549 have a greater change in SOCS after NS expression. It would have been more expected to see one of these cells lines to be overall more sensitive than the other, it seems counter intuitive that ISGs are less effected in A549 cells but these have a greater response in SOCS. Equally while BEAS 2b have a limited change in SOCS response, the ISG expression is reduced earlier than in A549s. Taken together we would suggest that while the NS do impact SOCS expression this is not the main driver or mechanism for the change in ISG expression. The difference in SOCS expression between these cell lines could relate to how they respond to RSV infection.

Infection with full length RSV (RSV-A2) caused an increase in levels of ISGs despite the presence of the NS proteins in the virus. This is likely because RSV-A2 will stimulate numerous immune pathways though PAMPs it produces, stimulating TLR8, or RIG-I, leading to an upregulation of a host of signalling pathways which will induce IFN expression, causing an upregulation of ISGs. When cells are transfected with NS DNA alone there is no additional viral proteins or RNA, and the effect on the IFN pathway

alone can be seen. Interestingly, the A549 and BEAS 2b cell lines responded differently to infection. Infection with RSV- Δ NS-GFP, which lack the NS proteins, failed to cause a significant infection in either cell line, though the BEAS 2b had 6% of cells GFP+ when infected with MOI 3.

The cell lines used are known to have different patterns of infection control when infected with RSV (Hillyer et al., 2018); A549s have lower basal levels of ISG expression and are more permissive to RSV infection with a greater IFN response, while BEAS 2b have higher levels of ISGs constitutively expression, are less permissive to RSV infection and produce less IFN on infection. This may be related to the reduction in CIS seen in A549s. CIS would normally act to reduce proinflammatory signaling and therefore reduce cytokine response. A reduction in CIS in A549 but not BEAS 2b could account for the increase cytokine output of A549 compared to BEAS 2b. Full length infection of A549 and BEAS 2b showed that BEAS 2b were more permissive to infection, with a greater number of cells GFP+ after 24h infection. Interestingly, although the BEAS 2b had the greater share of infected cells, the A549 had a more robust MxA and ISG15 mRNA increase. Levels of SOCS mRNA expression was differentially induced between the two cell lines, with SOCS1 and CIS only increased in the A549 while the BEAS 2b SOCS levels remained broadly comparable to the mock infection.

These results provide robust evidence that the RSV NS1 proteins has a significant role in reducing ISG expression, independent of its effects on the SOCS proteins.

4 RSV NS1 enhances STAT activation in BEAS 2b bronchial epithelial cells but not A549 alveolar epithelial cells

4.1 Introduction

The activation of the JAK-STAT pathway by IFN is crucial in the innate antiviral response as it results in the expression of hundreds of ISGs that limit viral replication. We have shown that the expression of NS1 in both A549 and BEAS 2b epithelial cells significantly reduces the expression of four ISGs, MxA, PKR, ISG15 and USP18, and there is no corresponding increase in SOCS1 or SOCS3, the key negative regulators of the pathway. We therefore hypothesised that NS1 inhibited JAK-STAT signal transduction to limit ISG expression.

Under normal conditions the activation of the IFN JAK-STAT pathway is initiated by the interaction of IFN with its cognate receptors - in the case of IFN α these are IFNAR1 and IFNAR2 (Schneider et al., 2014). When IFN α binds IFNAR1 and IFNAR2 the receptors are brought into close proximity with each other and the intracellular receptor tails are transphosphorylated allowing them to be bound by JAK. JAK will phosphorylate STAT proteins allowing them to form stable transcription factor complexes, including GAF (pSTAT1:pSTAT1) and ISGF3 (pSTAT1:pSTAT2:IRF9) (Schneider et al., 2014). These complexes must then be translocated to the nucleus where they bind promoter regions and drive gene expression (Meyer et al., 2004). In addition to this canonical IFN signalling, the movement of STAT into the nucleus has been seen to happen without phosphorylation, but it is much less efficient (Majoros et al., 2017). Any alteration to this process can affect the efficiency of antiviral gene expression.

The phosphorylation of STAT is regulated in several ways; firstly the receptors themselves can be down regulated or internalised to limit signalling (Zanin et al., 2020); SOCS1 and SOCS3 can interact with JAKs as a pseudo substrate to block their activity (Liau et al., 2018, Linossi et al., 2013, Babon and Nicola, 2012), and the amount of available STAT can be reduced in the cell by targeted proteasomal degradation (Gargan et al., 2018). Upregulation of any of these effects results in a reduction of ISG expression and enhanced viral replication. Once the transcription factor complexes, ISGF3 and GAF, have formed they need to be actively transported into the nucleus to bind promoter regions and initiate gene expression. This transport is mediated by a family of proteins called importins. Within the importin family there are importin α and importin β ; there are 3 subfamilies of importin- α , clade $\alpha 1$ containing importin $\alpha 5$, $\alpha 6$ and $\alpha 7$; clade $\alpha 2$ containing importin $\alpha 1$ and $\alpha 8$; and clade $\alpha 3$ containing importin $\alpha 3$ and $\alpha 4$ (Miyamoto et al., 2016). Each importin α has specific affinity for nuclear localisation signal (NLS) of specific proteins, STAT are transported by clade $\alpha 1$ and $\alpha 3$ importins (Shen et al.,

2021). This importin α :cargo complex is then bound by importin β which draw the bound proteins through the nuclear pore complex (NPC) into the nucleus. Here the importins are detached from the cargo and recycled into the cytoplasm where they traffic more proteins through. Any disruptions to this process could affect normal trafficking of STATs and related gene expression. Several viruses, including Nipah V virus, VZV, HBV and SARS-CoV-2, have been shown to impact nuclear transport, this can be a result of hijacking cellular machinery, or specifically to limiting the host antiviral response (Rodriguez et al., 2002, Nagel et al., 2014, Mitra et al., 2019, Wang et al., 2021, Shen et al., 2021).

Previous studies have shown that NS proteins attenuate JAK/STAT signalling at several different points along the pathway, however these studies were carried out in a variety of cell types yielding conflicting results. Spann et al., (2005) reported an impact of both NS1 and NS2 limit IFN α production by infected cells and limit NF- κ B signalling, (Spann et al., 2005); Lo et al., (2005) reported that NS1 and NS2 were responsible for limiting IFN response in A549 cells, and that this was associated with a reduction of STAT2 expression. Interestingly, they also showed that this effect was only seen in human cells and was not true in the mouse U6A cell line, suggesting the NS proteins could influence tropism. This reduction in STAT2 was observed in additional studies; indeed other signalling molecules, including TRAF3 and IKK ϵ were also reduced by NS1 and NS2 (Elliott et al., 2007, Swedan et al., 2009, Xu et al., 2014). NS1 was also found to reduce IRF3 (Ren et al., 2011) and NS2 was associated with the blocking of RIG-I function, thus preventing cells from mounting a IFN β response (Ling et al., 2009).

4.2 Specific Aims

- To determine if the RSV NS proteins impact STAT activation in A549 and BEAS 2b epithelial cells
- To determine if the RSV NS proteins impact total STAT levels in A549 and BEAS 2b epithelial cells
- To investigate if NS1 limits normal nuclear translocation of STATs in BEAS 2b epithelial cells

4.3 Results

4.3.1 Expression of NS1 proteins enhance STAT activation, but has no effect on total STAT protein levels in A549 cells

Having established successful transfection of RSV's NS proteins in A549 cells by RT-qPCR, we next sought to identify if NS1 and/or NS2 disrupted normal IFN I signalling in this epithelial cell line. Previously we saw that the presence of NS1 ISG mRNA levels were significantly reduced. A decrease in the level of ISG mRNA expression could be linked with decreased STAT or pSTAT availability in the cell.

The Analysis of pSTAT bands can be shown as relative to total STAT band and β -actin. Here I have chosen to show the relative level of pSTAT against β -actin, and total STAT against β -actin as the pSTAT and STAT were visualized on separate blots and STAT levels were seen to be consistent across all treatments.

To examine the effect of RSV's NS proteins on the rate of STAT phosphorylation in the A549 cell line, cells were transfected with $1\mu\text{g}$ of plasmid containing NS1, NS2, or an empty vector (EV) control. Con-transfections of NS1/NS2 were also used (with $0.5\mu\text{g}$ of each plasmid). After 24h transfection, cells were stimulated with 1000IU IFN α over a 30min time course and probed for phosphorylated STAT1 (pSTAT1), pSTAT2 and total STAT1 and STAT2. As phosphorylation of STATs is a fast modification, an increase in pSTAT1 can be seen as soon as 5min after IFN- α stimulation (Fig. 4.1). Over a time course of 30min there was little change in the protein band intensity for either pSTAT1 (Fig. 4.1) or pSTAT2 (Fig. 4.3) between the different transfections (EV, NS1, NS2 or NS1/NS2). Levels of total STAT1 nor STAT2 (Fig. 4.2 & Fig. 4.4) remain unaffected by transfection compared to the EV control, suggesting that transfection does not reduce total STAT1 or STAT2 levels after 24h transfection. These results suggest that JAK-STAT signalling in A549 cells is not impacted by RSV NS proteins, rather than driving the proteasomal degradation of STATs, as previously shown in 293T embryonic kidney cells (Elliott et al., 2007).

In order to directly compare the effects of transfection groups after treatment with IFN α , the 20min treated samples from the time course were analysed on a separate gel. This allowed any changes in the total amount of phosphorylation after 20min treatment to be measured between transfection groups. In addition to the $1\mu\text{g}$ NS1/2 transfection,

a co-transfection was included with 1 μ g of each NS1 and NS2, giving a total of 2 μ g plasmid DNA added to each well. The EV control for these used 2 μ g of EV plasmid. The 2 μ g NS1/2 was included to mirror the same plasmid concentration as the single transfections. Levels of pSTAT1 were increased upon expression of NS1 compared to the EV control (Fig. 4.5A & B), STAT1 expression is not impacted by NS expression (Fig. 4.5C & D); pSTAT2 levels were not altered by NS expression (Fig. 4.5A & B) and STAT2 levels are also broadly consistent between the transfection groups (Fig. 4.5C & D).

This suggests that the reduction in ISG transcripts seen in both cell lines is not mediated through degradation STAT signalling molecules. In the BEAS-2b cells, which saw a significant increase in pSTAT levels, the mechanism is more perplexing – an increase in pSTAT levels is usually associated with a rise in ISG expression. As the majority of STAT dephosphorylation occurs in the nucleus and there is an accumulation of pSTAT with no increase in ISG gene expression with NS1 expression, this suggests that pSTAT1 and pSTAT2 may have impaired nuclear translocation in the presence of NS1.

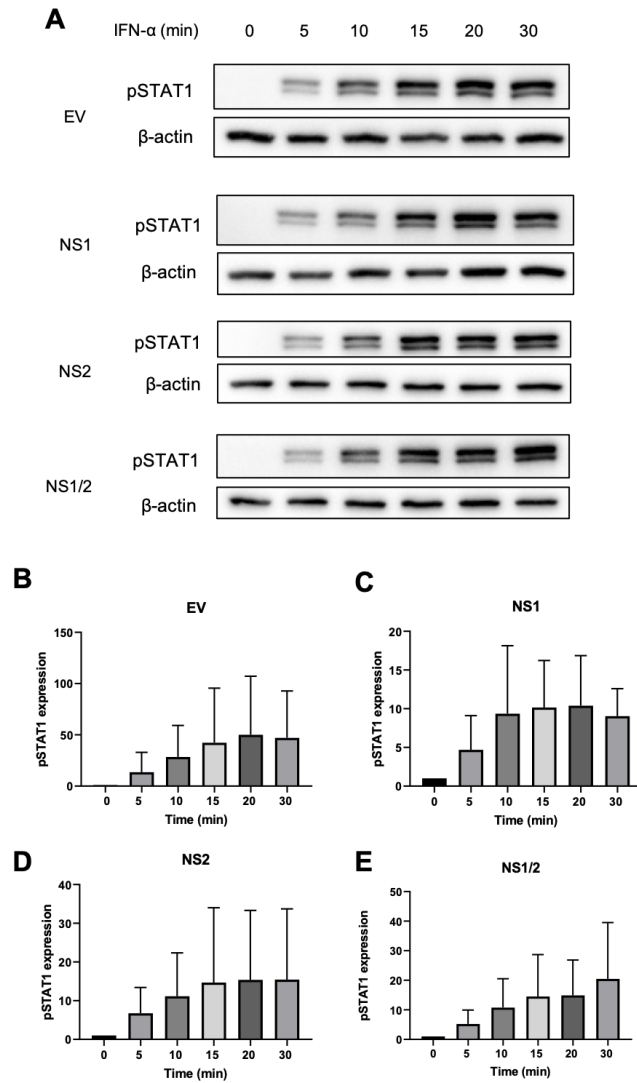


Figure 4.1: Expression of RSV NS proteins has no impact on STAT1 phosphorylation in A549 epithelial cells.

A549 cells were transfected with 1 μ g NS1, NS2, EV control or NS1 & NS2 (NS1/2) for 24h. Cells were treated with 1000IU IFN α for up to 30 min. A) pSTAT1 expression was measured by western blotting and the densitometry for pSTAT1 levels in B) EV, C) NS1, D) NS2 and E) NS1/2 transfected cells relative to β -actin control. Data shown is representative of 3 independent experiments (n=3).

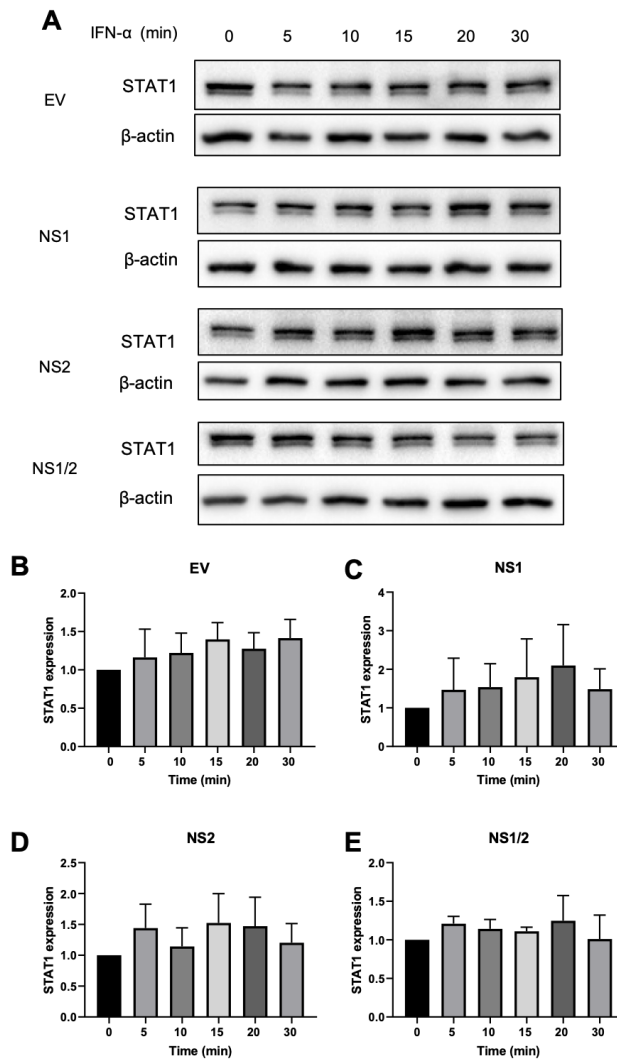


Figure 4.2: Expression of NS proteins has no impact on STAT1 levels in A549 epithelial cells.

A549 cells transfected with 1 μ g NS1, NS2, EV control or NS1 & NS2 (NS1/2) for 24h. Cells were treated with 1000IU IFN α for up to 30 min. A) STAT1 expression by western blotting and the densitometry for STAT1 levels in B) EV, C) NS1, D) NS2 and E) NS1/2 transfected cells relative to β -actin control. Data shown is representative of 3 independent experiments (n=3).

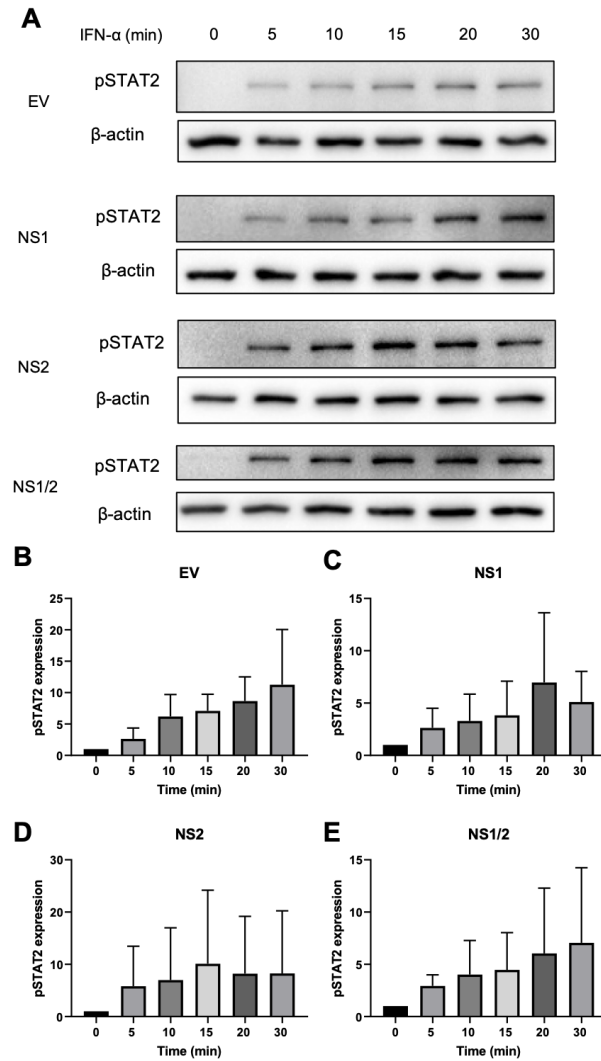


Figure 4.3: Expression of NS proteins has no significant impact on the rate of STAT2 phosphorylation in A549 epithelial cells.

A549 Cells were transfected with 1 μ g NS1, NS2, EV control or NS1 & NS2 (NS1/2) DNA for 24h and treated with 1000IU IFN α for upto 30min. Cell lysates were collected and levels of A) pSTAT2 expression by western blotting and the densitometry for pSTAT levels in B) EV, C) NS1, D) NS2 and E) NS1/2 transfected cells relative to β -actin control. Data is show is representative of 3 independent experiments (n=3).

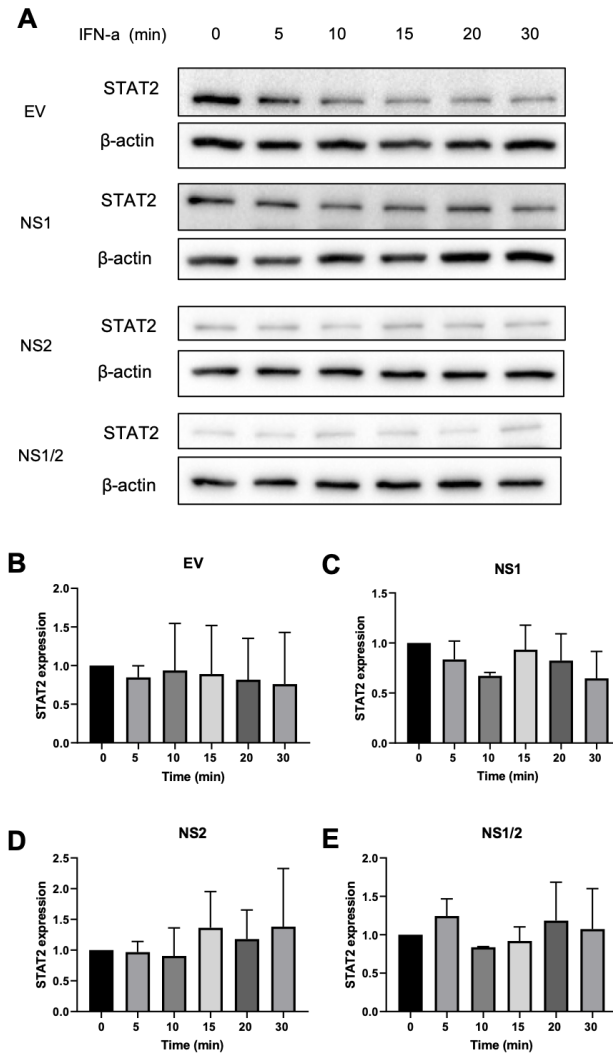


Figure 4.4: Expression of NS proteins has no impact on STAT2 levels in A549 epithelial cells

A549 cells were transfected with 1 μ g NS1, NS2, EV control or NS1 & NS2 (NS1/2) for 24h. Cells were treated with 1000IU IFN α for up to 30 min. A) STAT2 expression by western blotting and the densitometry for STAT2 levels in B) EV, C) NS1, D) NS2 and E) NS1/2 transfected cells relative to β -actin control. Data is show is representative of 3 independent experiments (n=3).

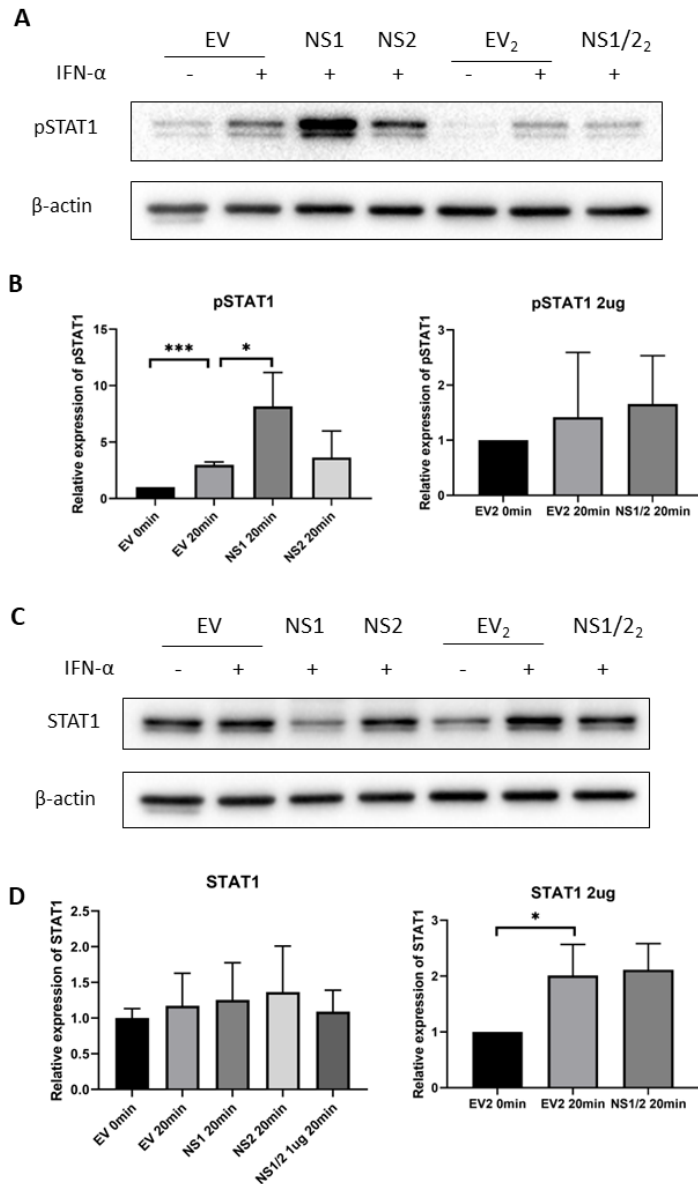


Figure 4.5: NS1 increases STAT1 phosphorylation in A549 epithelial cells

Cells were transfected with 1 μ g DNA for 24h and treated with 1000IU IFN α for 20min. Cell lysates were collected and levels of A) pSTAT1 and C) STAT1 were measured by western blotting. Densitometry of B) pSTAT1 and D) STAT1 was performed relative to β -actin control. Data is presented as mean \pm SD. Statistics calculated by unpaired t-test * = $p < 0.05$, *** = $p < 0.001$ ($n = 3$).

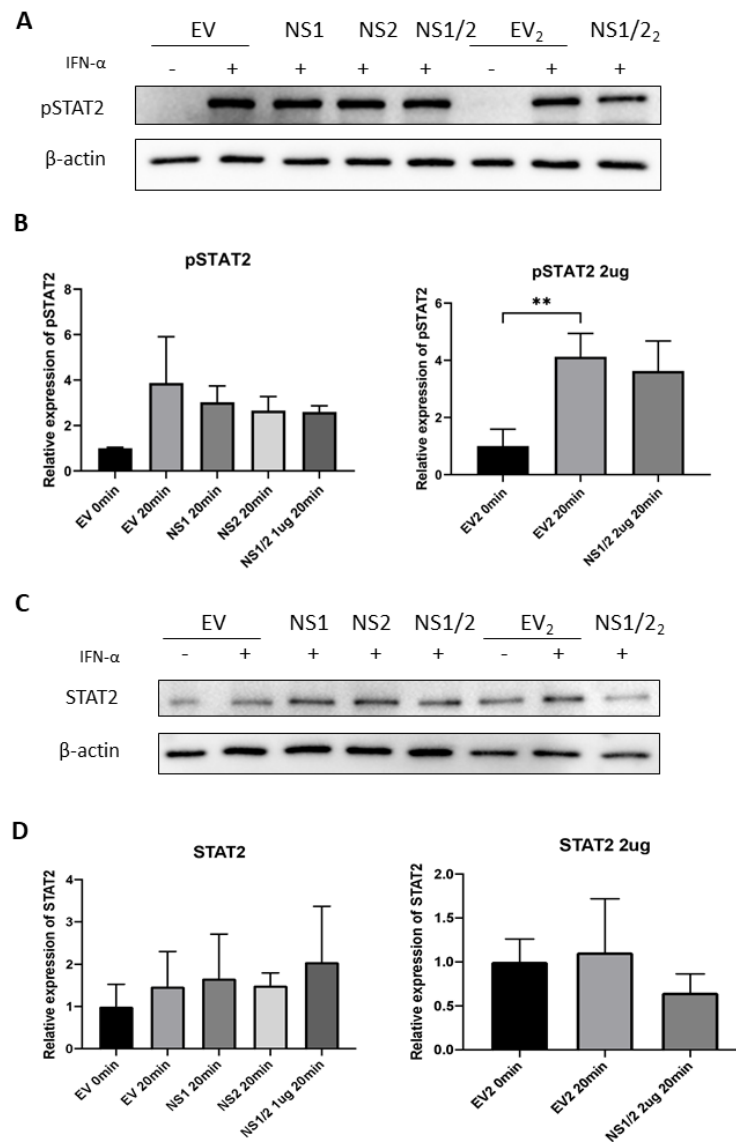


Figure 4.6: NS transfections have no effect on pSTAT2 or STAT2 levels in A549 epithelial cells.

*A549 cells were transfected with 1 μ g DNA for 24h and treated with 1000IU IFN α for 20min. Cell lysates were collected and levels of A) pSTAT2 and C) STAT2 were measured by western blotting. Densitometry of B) pSTAT2 and D) STAT2 was performed relative to β -actin control. Data is presented as mean \pm SD. Statistics calculated by unpaired *t*-test ** = $p < 0.01$ ($n = 3$).*

4.3.2 Expression of RSV NS proteins increases STAT1 and STAT2 activation and reduces total STAT2 levels in BEAS 2b cells

BEAS 2b cells were transfected with EV, NS1, NS2 or NS1/2 for 24h and treated with 1000IU IFN α -2a for 20 mins before the cell lysates were collected for western blotting. Levels of pSTAT1 and pSTAT2 were significantly increased with NS1 transfection (Fig. 4.7A & Fig. 4.8A), total STAT1 appeared to be reduced with NS1 transfection but was not significantly decreased when analysed by densitometry; transfection of both NS1 and NS2 (NS1/2) increased STAT1 (Fig. 4.7C). Levels of STAT2 were reduced by NS1 and NS2, both of these reductions were significant when measured by densitometry (Fig. 4.8C). Despite NS1 causing a significant rise in pSTAT1 when transfected alone, in the double transfection (NS1/2) there is no significant rise in pSTAT1; this was not the case with pSTAT2, where the significant increase with NS1 was reflected in the NS1/2 group.

To confirm that the decrease in STAT1 and STAT2 was due to the transfection of viral genes and not related to the IFN α treatment of cells, BEAS 2b cells were transfected with NS1, NS2 or NS1/2 alongside appropriate EV controls for 24h or 48h and levels of STAT1 and STAT2 were measured. In this case levels of total STAT1 was not affected by transfection (Fig. 4.9A), but levels of STAT2 did significantly reduce in NS1 transfected samples (Fig. 4.9B). Elliott et al., (2007) showed that the reduction of STAT2 by NS1 is through ubiquitin mediated proteasomal degradation. To determine if the same mechanism was true in the BEAS 2b cell line the transfected cells were treated with MG132 for 4h before collecting cell lysates for western blotting (Fig. 4.10). MG132 acts to prevent proteasomal degradation; therefore if the NS1 degradation of STAT2 was mediated by the proteasome the addition of MG132 should “rescue” STAT2 expression, returning it to levels seen in the EV control. The addition of MG132 to NS1 transfected cells did increase the levels of STAT2 compared to the DMSO and media controls, though levels were still below the EV control (Fig. 4.10).

Differing results are in Fig 4.9D, where NS1 caused a reduction in STAT2, and Fig 4.10B, where NS1 does not cause a significant reduction in STAT2. In the presence of media alone there is a reduction in STAT2 in the presence of NS1 which is approaching significance ($p = 0.0578$), this discrepancy is likely a result of background noise between the western blot images which would benefit from additional experimental repeats. In the presence of MG132 the significance of the difference between STAT2 levels in the

EV and NS1 expressing cells reduces to $p=0.6381$

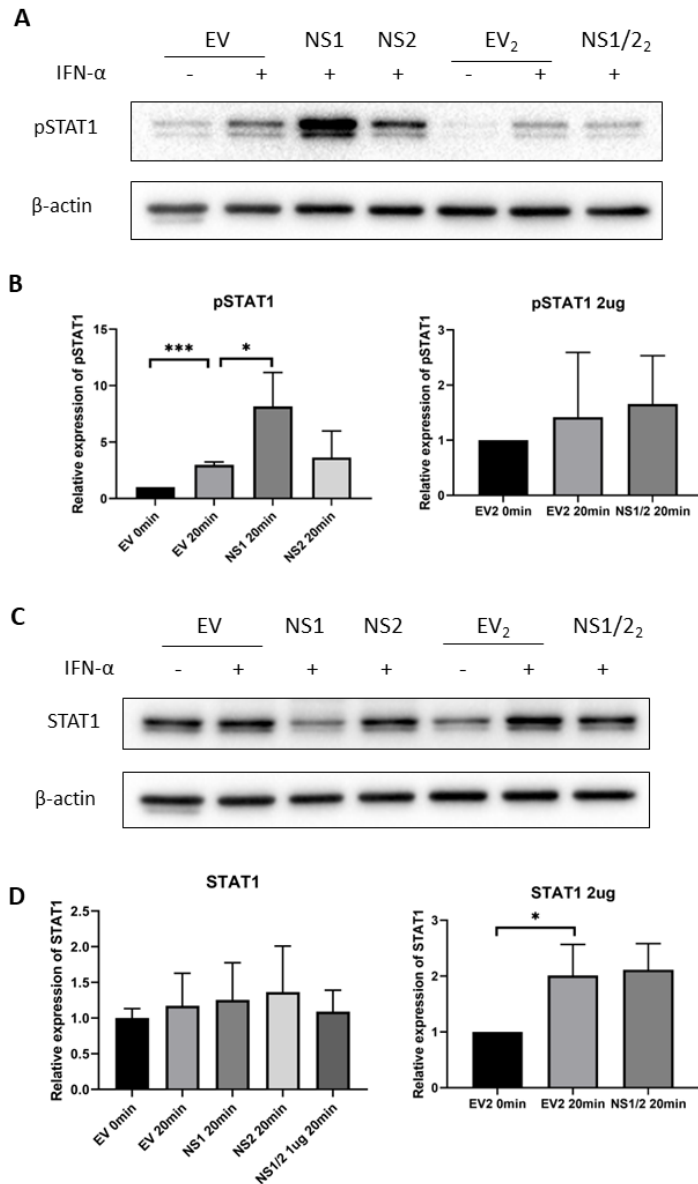


Figure 4.7: RSV NS1 increases STAT1 phosphorylation in BEAS-2b epithelial cells.

Cells were transfected with 1 μ g DNA for 24h and treated with 1000IU IFN α for 20min. Cell lysates were collected and levels of A) pSTAT1 and C) STAT1 were measured by western blotting. Densitometry of B) pSTAT1 and D) STAT1 was performed relative to β -actin control. Data is presented as mean \pm SD. Significance was determined by unpaired t-test * = $p < 0.05$, *** = $p < 0.001$ ($n=3$).

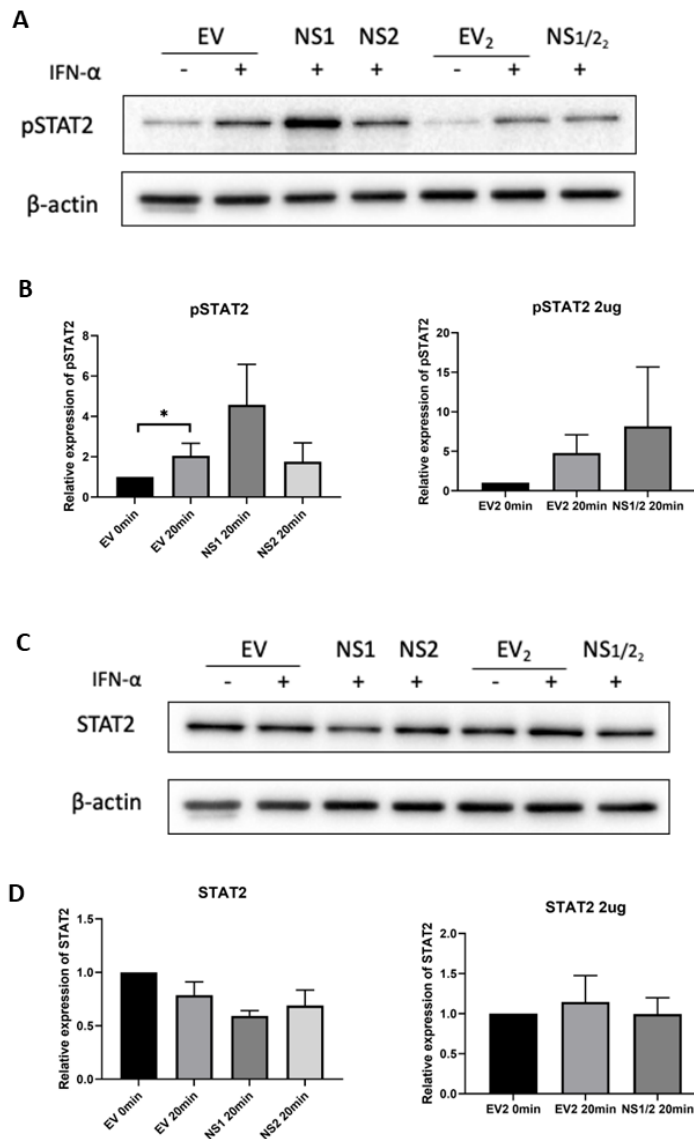


Figure 4.8: RSV NS1 increases STAT2 phosphorylation and both NS1 and NS2 decrease STAT2 in BEAS 2b epithelial cells.

Cells were transfected with 1 μ g DNA for 24h and treated with 1000IU IFN α for 20min. Cell lysates were collected and levels of A) pSTAT2 and C) STAT2 were measured by western blotting. Densitometry of B) pSTAT2 and D) STAT2 was performed relative to β -actin control. Data is presented as mean \pm SD. Significance was determined by unpaired t-test * = $p < 0.05$ ($n = 3$).

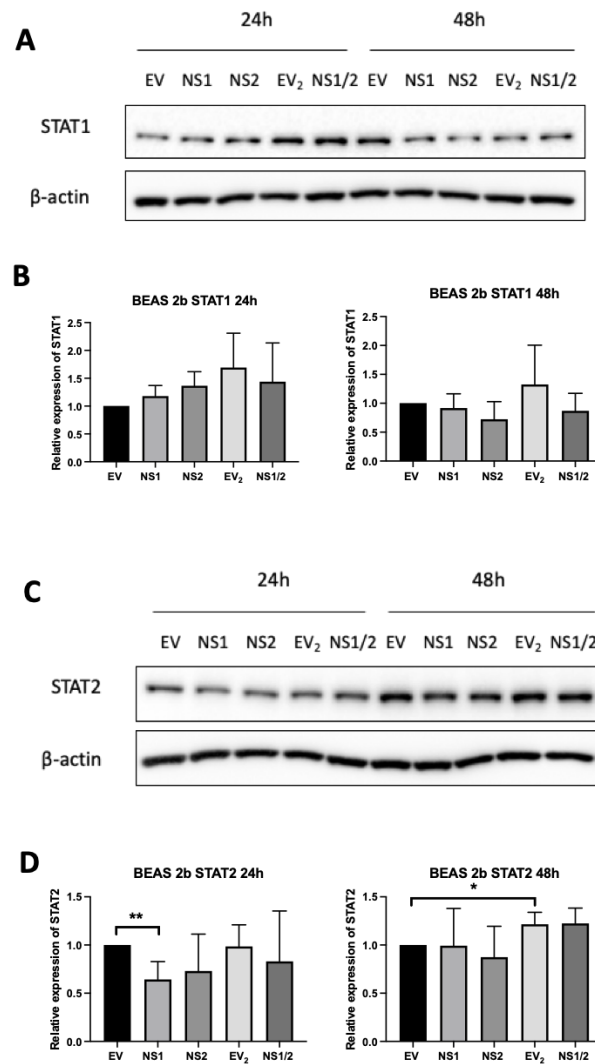


Figure 4.9: STAT2 reduced by RSV NS1 expression at 24h in BEAS 2b epithelial cell

Cells were transfected with 1 μ g DNA for 24h or 48h A) Western blotting of the cell lysates showed only slight changes in STAT1 levels with transfection B) this was confirmed by densitometry relative to β -actin control. C) Protein levels of STAT2 showed a significant reduction in cells expressing NS1 at 24h D) this was confirmed through densitometry relative to β -actin control. Data is presented as mean \pm SD. Significance was determined by unpaired t-test (n=3).

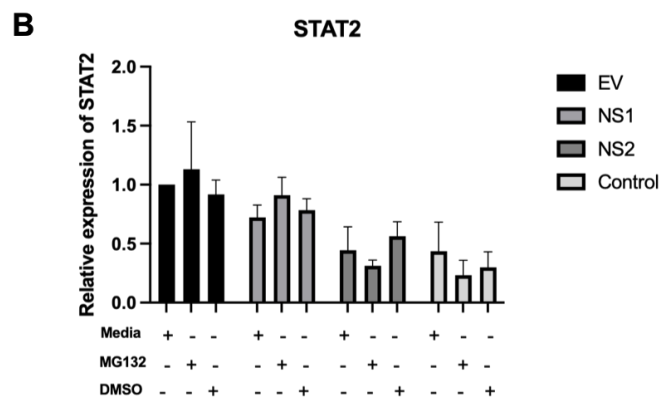
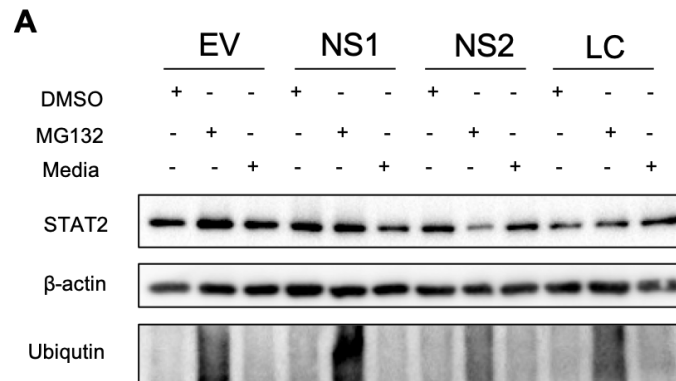


Figure 4.10: The degradation of STAT2 by RSV NS1 is not reduced by MG132.

BEAS 2b cells were transfected for 24h with NS1 or NS2 constructs before, cells were treated with 10 μ M MG132, DMSO control, or left untreated for 4h, before collection in lysis buffer. A lipofectamine control (LC) was also included, these samples were treated with the lipofectamine reagent but no plasmid was included. Protein expression levels were measured by western blotting. A) STAT2 protein expression and levels of ubiquitin were probed for to confirm the MG132 was effective B) and assessed by densitometry relative to β -actin control (n=3).

4.3.3 Transfection with pCI-neo empty vector increases basal ISG levels and renders cells insensitive to IFN α and IFN λ treatment

Having seen a significant reduction in ISG expression when cells expressed NS1, but an increase in pSTAT levels, we next investigated if ISG induction was also reduced after IFN α stimulation. A549 cells were treated with an IFN α treatment time course which showed increases in MxA, PKR and ISG15 after 4h treatment (Fig. 4.11 A-C), and IFN λ dependent expression saw significant increases from as early as 2h, which continued to increase for the duration of the time course (Fig. 4.11D-F). IFN λ plays a similar antiviral role to IFN α , but as it is a type III IFN it signals through IL-28Ra and IL10R2 receptors and has an important role in mucosal immunity (Zhou et al., 2018).

A549 cells transfected with 1 μ g DNA of EV, NS1, NS2 or NS1 & NS2 (NS1/2) were treated with 1000IU IFN α for 4h or left untreated; levels of MxA, MxB and PKR were measured by RT-qPCR (Fig. 4.12A-C); from the time course we hypothesised to see greater than 500 fold increase in MxA levels in the EV control, however no increase was seen in any of the transfection conditions. IFN λ treatment of transfected A549 also saw no significant increase in MxA or PKR expression (Fig. 4.12D-F). As this was true in all transfection conditions the effect of the pCI-neo vector (the plasmid containing the NS genes) was compared with an empty pCMV vector in both A549 and BEAS 2b cells (Fig. 4.13). This comparison showed that the addition of pCI-neo caused a greater than 200 fold increase in basal level of MxA that failed to increase with IFN α or IFN λ stimulation (Fig. 4.13A & B). Cells transfected with pCMV also saw a slight increase in basal levels in A549 cells, but, as expected MxA expression was still able to increase significantly with IFN α treatment. In the BEAS 2b cell line, pCMV had no effect on basal MxA expression and IFN α treatment caused a highly significant increase in MxA expression (Fig. 4.13C & D).

In summary, transfection with the pCIneo empty vector alone increase basal expression of MxA by over 1000 fold in A549 and 200 fold in BEAS 2b, with subsequent IFN α stimulus failing to induce further MxA expression (Fig. 4.13A & B). The pCMV empty vector also moderately increased basal MxA expression in A549 cells, with IFN α stimulation causing a significant increase in MxA expression Fig. 4.13A & B). In the BEAS 2b the pCMV caused no basal increase in MxA expression, compare to untransfected cells (Fig. 4.13).

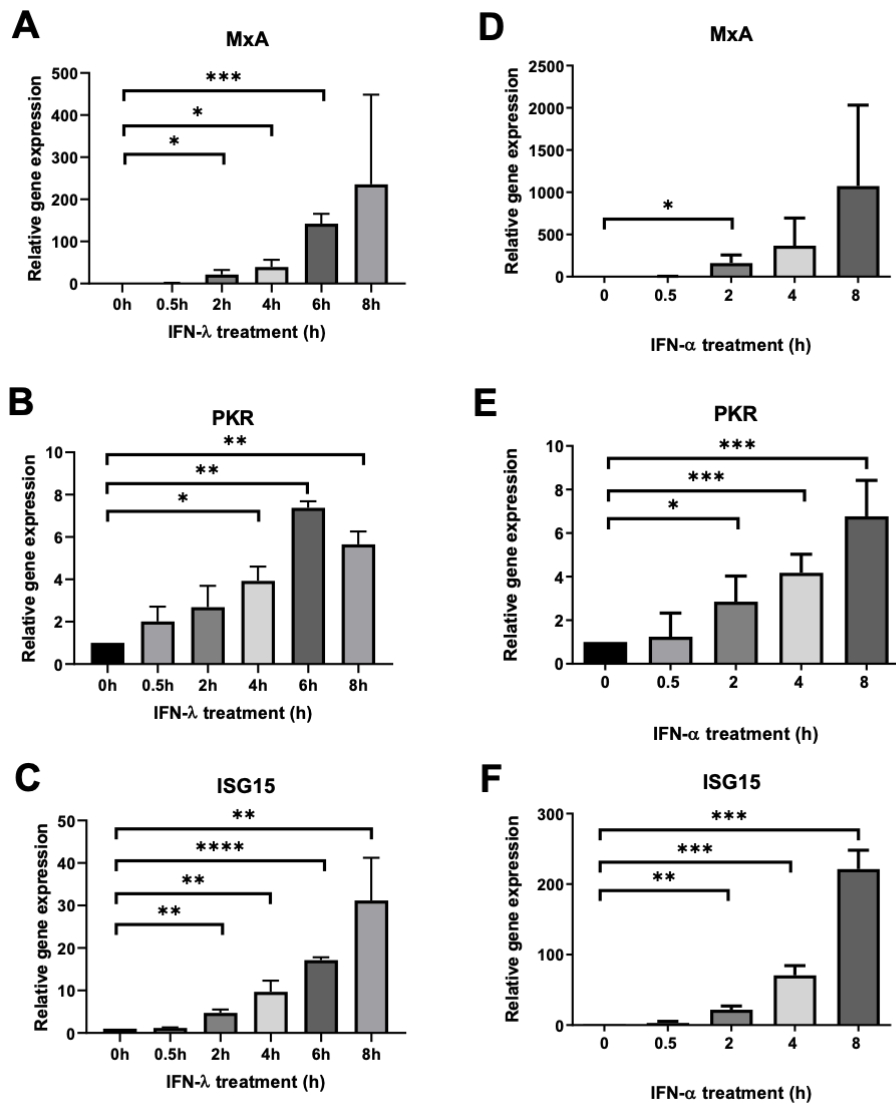


Figure 4.11: IFN α and IFN λ stimulation increases ISG expression in A549 epithelial cells.

*A549 cells treated with IFN α or IFN λ for the time indicated before collection in Trizol and analysis by RT-qPCR. Following treatment with 1000IU IFN α or 100ng/ml IFN λ , levels of A & D) MxA, B & E) PKR, and C & F) ISG15 mRNA were measured over a time course. All data is presented as mean \pm SD. Statistics calculated by unpaired t-test * p <0.05, ** p <0.01, *** p <0.001, **** p <0.0001 (n =3).*

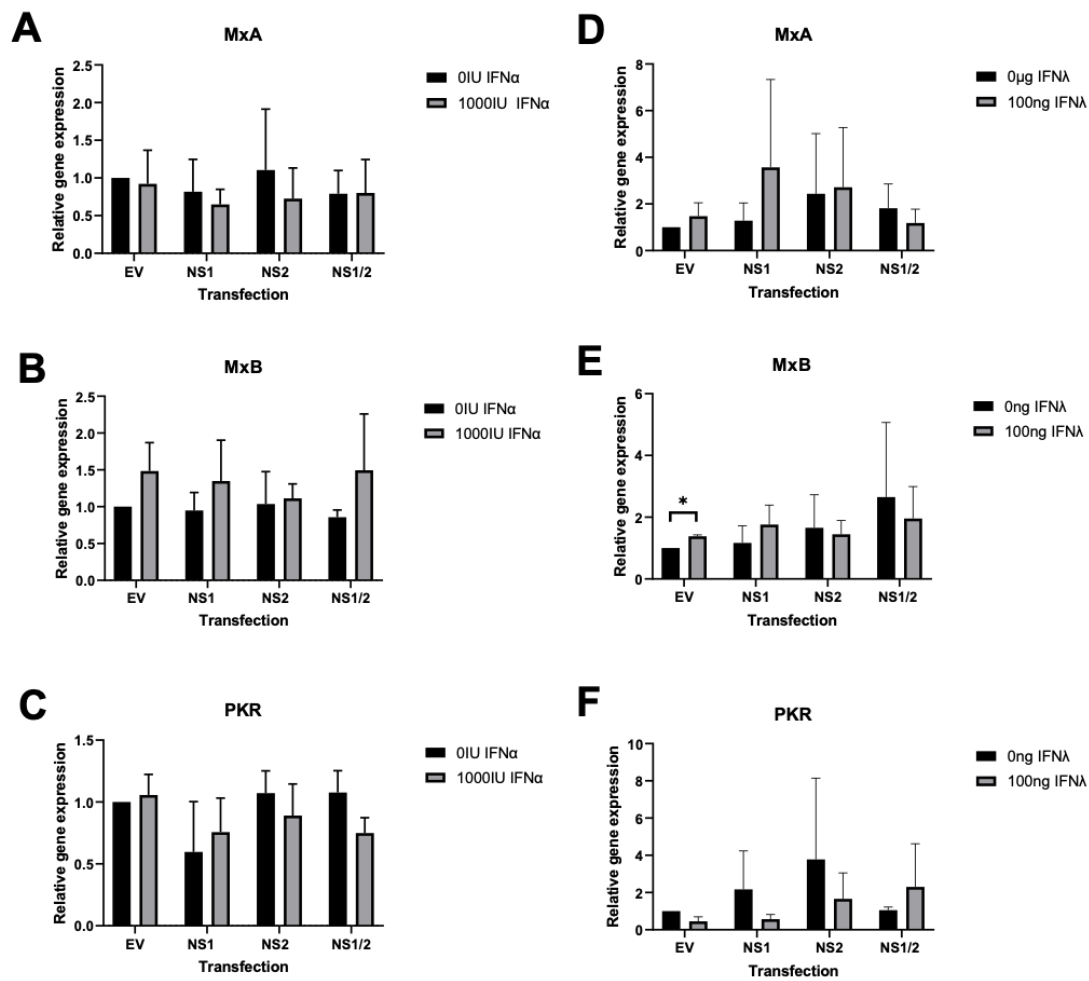


Figure 4.12: Transfection of pCI-neo vector renders A549 cells insensitive to IFN α and IFN λ stimulation

A549 cells were transfected with 1 μ g plasmid DNA, containing the NS1, NS2 or an empty vector control (EV) for 24h and treated with 1000IU IFN α for 4h. Levels of A) MxA, B) MxB and C) PKR. Treating transfected cells with 100ng IFN λ for 6h levels D) MxA, E) MxB or F) PKR were measured. All data is presented as mean \pm SD. Statistics calculated by unpaired t-test * p <0.05 (n=3).

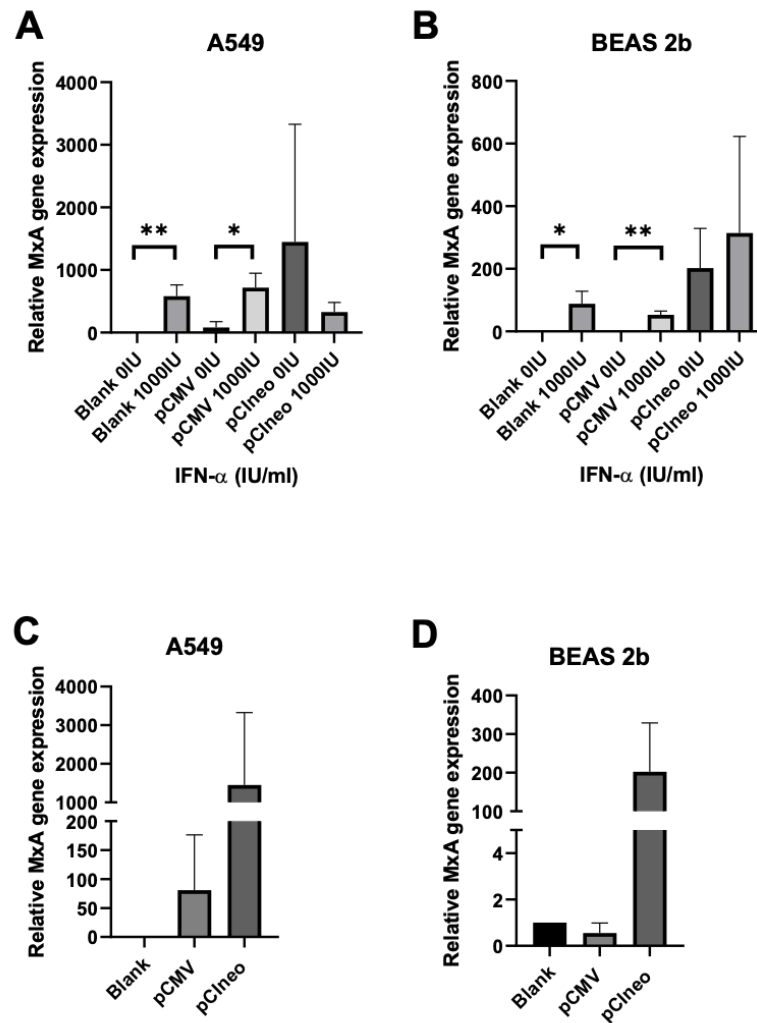


Figure 4.13: Transfection with Empty Vector pCI-neo increases basal MxA mRNA expression and reduces cells sensitivity to IFN α .

A) A549 and B) BEAS 2b cells were transfected with the pCMV or pCIneo empty vectors, or left untransfected (blank) and treated with 1000IU IFN α for 4h. The MxA mRNA levels in untreated C) A549 and D) BEAS 2b. Levels of MxA mRNA expression were measured by RT-qPCR and normalized to the blank untreated each time. All data is presented as mean \pm SD. Statistics calculated by student t-test * $p < 0.05$, ** $p < 0.01$ ($n=3$).

4.3.4 NS1 Expression Limits Nuclear Translocation of STAT1 and Alters the Cellular Localization of STAT2

As levels of pSTAT1 increased with NS1 expression in BEAS 2b cells (Fig. 4.7, but ISG expression was reduced (Fig. 3.7, we next investigated if the STAT1 was able to migrate to the nucleus as normal after activation. BEAS 2b cells were seeded onto glass slides and transfected for 24h with NS1 or EV control, before stimulating with 1000IU/ml IFN α for 30min. Slides were then fixed and stained for NS1, STAT1 and DAPI. Images were taken using a Leica confocal microscope and relative fluorescence intensity was determined using IMARIS software, as described in the methods section.

Treating BEAS 2b cells with IFN α , without any transfection, lead to a significant increase in the STAT1 signal in the nucleus, while levels in the cytoplasm remained stable (Fig. 4.14). The expression of NS1 results in reduced STAT1 present in the nucleus before treatment and this fails to increase with IFN α stimulation (Fig. 4.15). EV also has an impact on STAT1 localization, with higher levels of STAT1 in the nucleus than the untransfected control, and only a limited increase with IFN α treatment. This aligns with what was seen in the previous section, with the pCI-neo vector causing cells to have a higher basal expression of ISGs and be less sensitive to IFN α treatment. Comparing the EV to the NS1 expressing cells, there was significantly less STAT1 in the nucleus after IFN α treatment (Fig. 4.15B), and the ratio of nuclear to cytoplasmic STAT1 was significantly reduced in NS1 expressing cells with and without treatment (Fig. 4.15D). Levels of cytoplasmic STAT1 remained stable under all conditions (Fig. 4.15C).

Examining STAT2 under the same conditions there was no detectable increase of STAT2 in the nucleus after IFN α treatment in the untransfected cells (Fig. 4.16). Looking at the effect of NS1 STAT2 translocation there was no change in cytoplasmic nor nuclear levels of STAT2 (Fig. 4.17). However, the localisation of STAT2 does appear to alter with NS1 expression as highlighted in Fig. 4.18. If NS1 was expressed in the cells for 24h STAT2 accumulated the the perinuclear region. This effect is independent of IFN α treatment and suggests that NS1 sequesters STAT2 to a specific area of the cells.

As this effect was only seen with STAT2 and not STAT1 this activity could result in reduced ISGF3 forming (STAT1:STAT2:IRF9) limiting ISG expression.

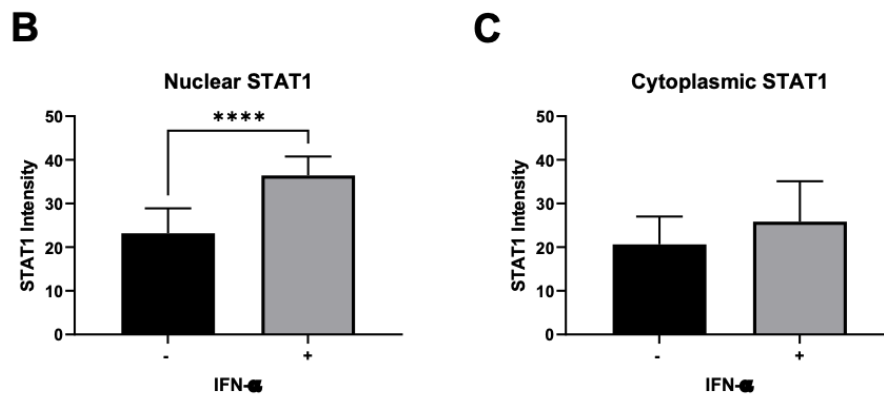
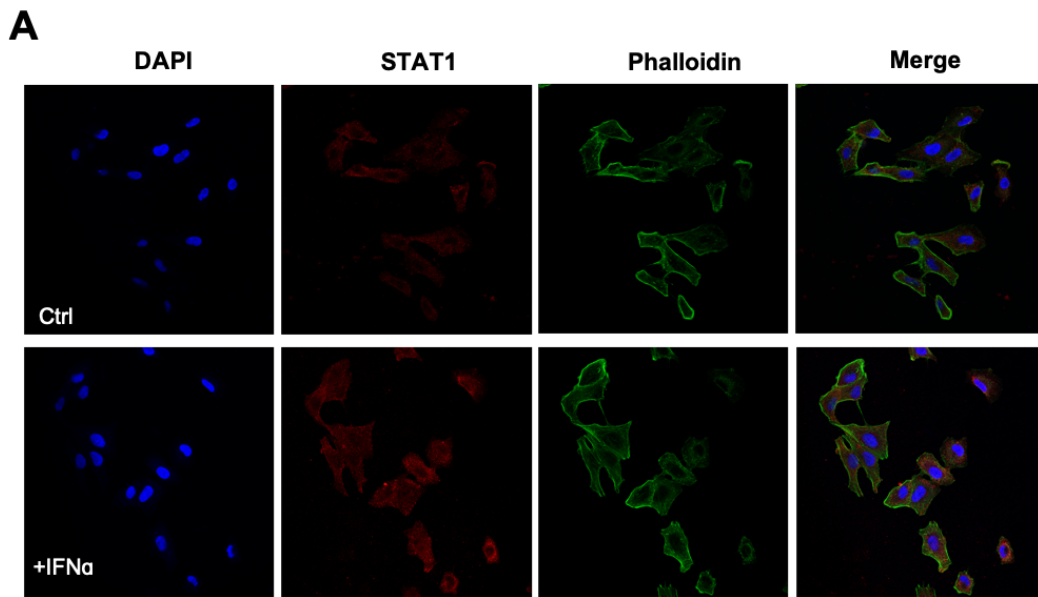


Figure 4.14: Quantification of STAT1 nuclear translocation in BEAS 2b cells by confocal microscopy.

*BEAS 2b cells were seeded onto glass cover slips and stimulated with 1000IU or 0IU IFN α for 30min. A) Cells were stained for STAT1, phalloidin-Rhodamine and DAPI, and visualised using confocal microscopy. Images are representative of 3 independent experiments. Quantification of STAT1 in the B) nucleus and C) cytoplasm was determined using Imaris software. All data is shown as mean \pm SD. Significance was determined by unpaired t-test, *** p <0.001 (n =3)*

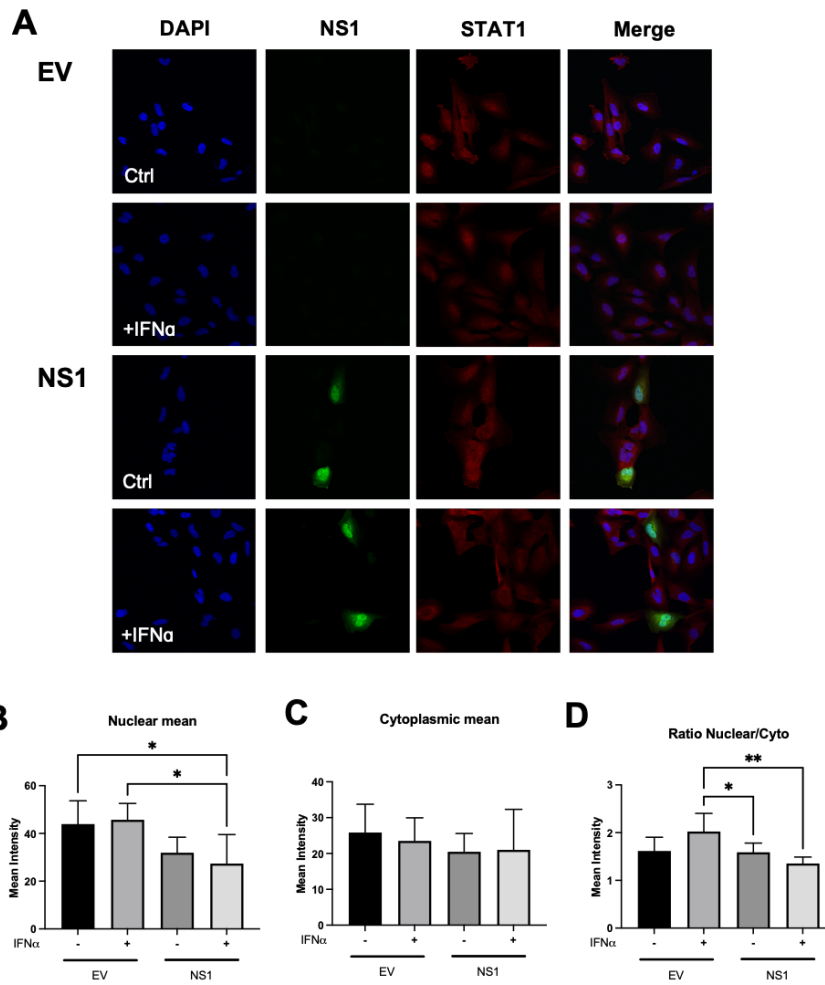


Figure 4.15: Expression of NS1 limits nuclear translocation of STAT1 in BEAS 2b cells.

BEAS 2b cells were transfected with NS1 or EV control and stimulated with 1000IU or 0IU IFN α for 30min. A) Cells were stained for STAT1, NS1 and DAPI, and visualised using confocal microscopy. Images are representative of three independent experiments. Quantification of STAT1 in the B) nucleus and C) cytoplasm was determined using Imaris software. D) the ratio of nuclear to cytoplasmic STAT1 was determined. All data is shown as mean \pm SD. Significance was determined by ANOVA and Tukey's multiple comparison test * p <0.05, ** p <0.01 (n =3)

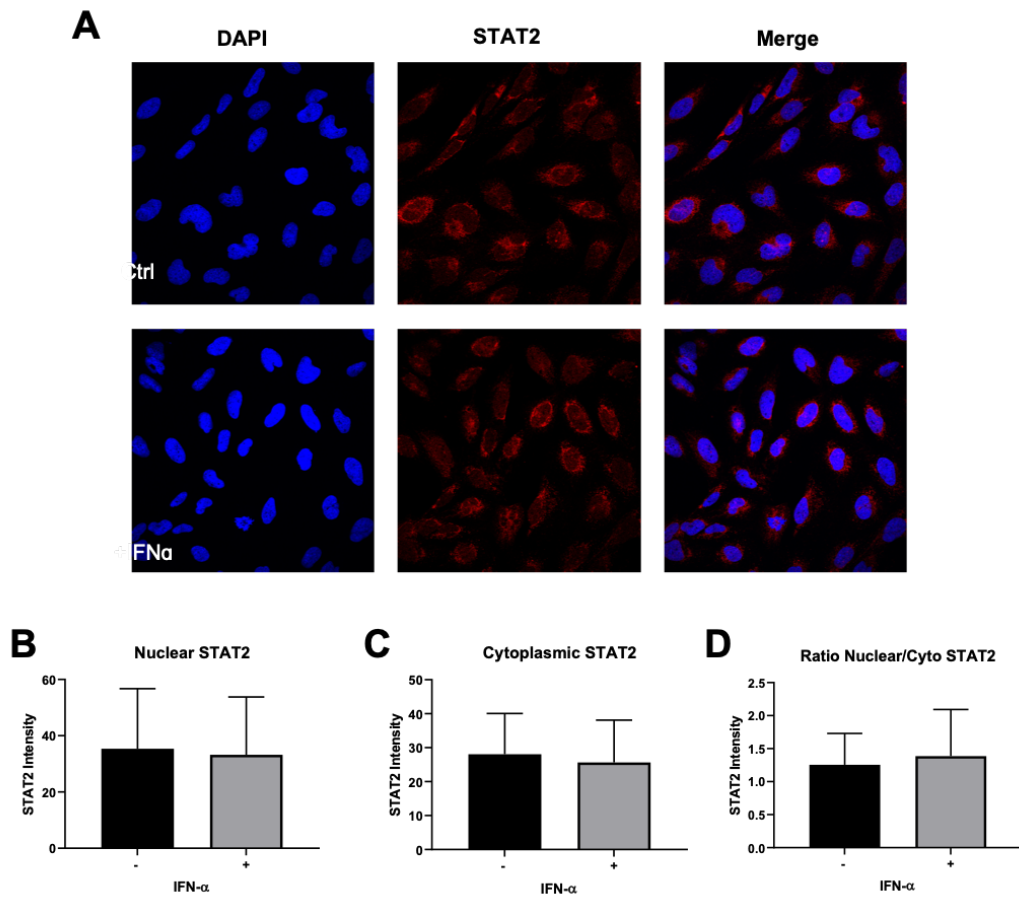


Figure 4.16: Quantification of STAT2 nuclear translocation in BEAS 2b cells by confocal microscopy.

BEAS 2b cells were seeded onto glass cover slips and stimulated with 1000IU or 0IU IFN α for 30min. A) Cells were stained for STAT2, phalloidin-Rhodamine and DAPI, and visualised using confocal microscopy. Images are representative of 3 independent experiments. Quantification of STAT2 in the B) nucleus and C) cytoplasm was determined using Imaris software. All data is shown as mean \pm SD. Significance was determined by unpaired t-test ($n=3$)

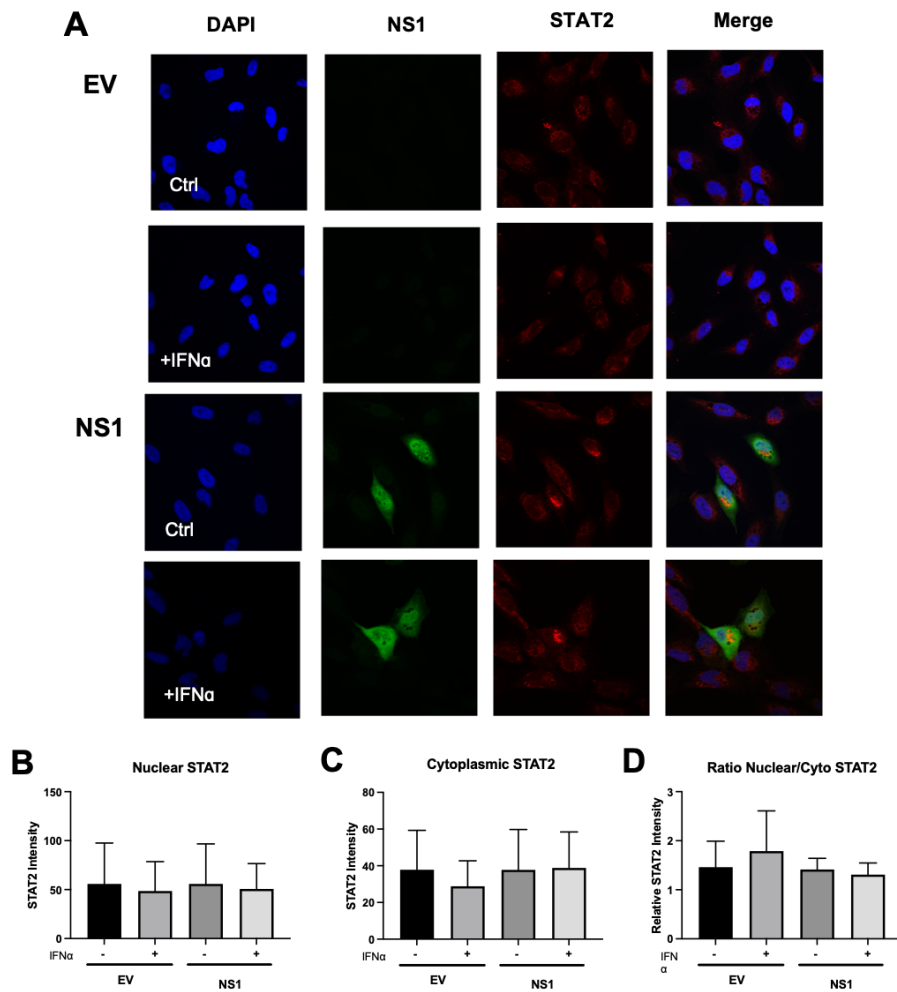


Figure 4.17: Nuclear translocation of STAT2 is not significantly impacted by IFN α treatment or NS1 expression in BEAS 2b cells.

BEAS 2b cells were transfected with NS1 or EV control and stimulated with 1000IU or 0IU IFN α for 30min. A) Cells were stained for STAT2, NS1 and DAPI, and visualised using confocal microscopy. Images are representative of three independent experiments. Quantification of STAT2 in the B) nucleus and C) cytoplasm was determined using Imaris software. D) the ratio of nuclear to cytoplasmic STAT2 was determined. All data is shown as mean \pm SD. Significance was determined by ANOVA and Tukey's multiple comparison test ($n=3$)

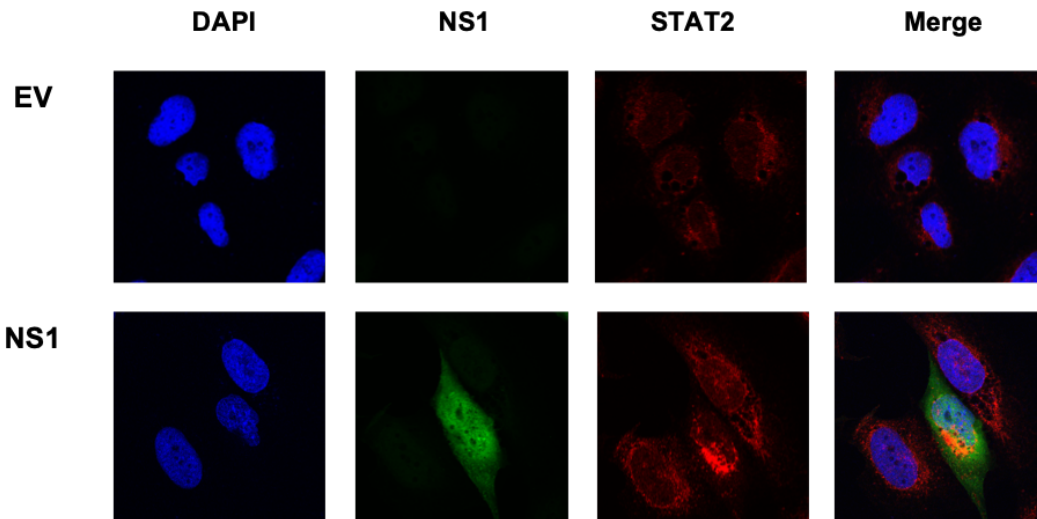


Figure 4.18: Expression of NS1 causes STAT2 to localise adjacent to the nucleus.

Sub-region of the images in Fig. 4.17 highlighting STAT2 localisation (n=3).

4.3.5 STAT1 is reduced with RSV-A2-GFP infection

To confirm that STAT1 translocation is also limited with a full length RSV infection BEAS 2b cells were seeded onto glass slides and infected with RSV-A2-GFP for 24h at MOI 1. Cells were then treated with 1000IU/ml IFN α for 30min in before fixation and stained for STAT1. Images were taken on Lecia confocal microscope. Those cells that are successfully infected with RSV produce a GFP signal which was visible by microscopy. Infection with full length RSV (RSV-A2-GFP) reduced the levels of STAT1 present throughout the infected cells (Fig. 4.19). The affect appears to be limited only to the infected cells, with total protein levels of STAT1 in whole lysates increasing with infection when measured by western blotting and flow cytometry (Fig. A1.1). STAT1 itself is upregulated in response to IFNs, with expression increasing during viral infection (Cheon and Stark, 2009). A second RSV strain was used which lacks both the NS1 and NS2 proteins, RSV- Δ NS-GFP. RSV- Δ NS-GFP is known to poorly infect IFN competent cells, however as individually infected cells can be identified by the expression of GFP it was hoped that some cells would be identified as infected. However, no GFP signal was detected in any cells (Fig. A1.2).

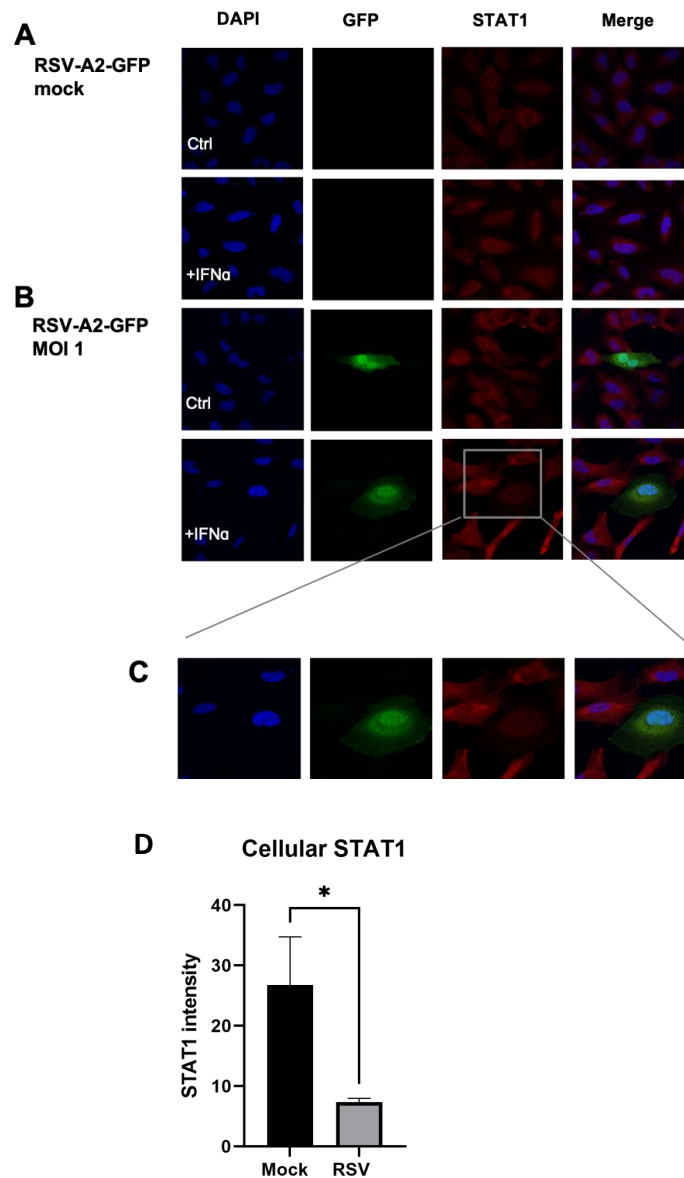


Figure 4.19: RSV-A2-GFP infection reduces STAT1.

*BEAS 2b cells infected with MOI 1 A) mock control or B) RSV-A2-GFP for 24h and stimulated with 1000IU or 0IU IFN α for 30min. C) Levels of STAT1 were reduced in the GFP expressing cells, which is more clearly seen when focusing on the sub region. Cells were stained for STAT1 and DAPI, and visualised using confocal microscopy. D) Quantification of cellular STAT1 confirms a significant reduction in STAT1 in RSV infected cells. Data is shown as mean \pm SD. Significance was determined by unpaired *t*-test. Images are representative of three independent experiments (*n*=3).*

4.4 Discussion

In the previous chapter we showed that expression of NS1 in both A549 and BEAS 2b cell lines significantly reduces the levels of ISG mRNA. To investigate if the mechanism of this was related to relative abundance of STAT1 and STAT2, level of those proteins and their activated phosphorylated forms were measured in the presence of the NS protein or a control (EV). In Fig 4.1 the impact of NS expression on STAT1 and STAT2 activation was measured with sample collected over a 30min time course. While this showed there was no alteration in the kinetics of STAT phosphorylation, it is not possible to directly compare protein levels between different western blot membrane. To see if the relative levels of pSTAT1 and pSTAT2 was affected by NS transfection the samples were rerun on the same gel to directly compare them. Expression of NS1 protein in A549 cells caused a slight increase in STAT1 phosphorylation but did not alter the kinetics of STAT phosphorylation or impact total STAT1 or total STAT2; this contradicts what might be expected given the predicted E3 ligase domains. However when NS1 is expressed in BEAS 2b cells there was a significant increase in pSTAT1 and pSTAT2 levels and a reduction in total STAT1 and STAT2. The expression of NS1 caused a greater reduction in STAT2, with NS2 also reducing STAT2 levels in BEAS 2b cells. This reduction of STAT2 with NS1 expression mirrors the result of Elliott et al., (2007) which was carried out in HEK 293 cells over expressing STAT2. As NS1 only reduced STAT2 in BEAS 2b cells and not A549 cells this suggests this mechanism is cell line dependent. NS2 did not cause the same reduction in either STAT1 or STAT2, suggesting that although the E3 ligases domains are present in NS2 they are non-functional in regards STAT degradation. We can see from the western blots that NS1 was most highly expressed at 24h post transfection and wained by 48h post transfection. This is likely why the significant reduction of STAT2 was transiently seen at 24h rather than 48h transfection.

To confirm that this reduction in STAT2 was driven by proteasomal degradation of STAT2 transfected cells were treated with the proteasomal inhibitor MG132. MG132 is a peptide-aldehyde which covalently binds the active site of the 20S proteasome preventing the degradation of ubiquitinated proteins (Guo and Peng, 2013). If the reduction in STAT2 was caused by ubiquitin mediated degradation, blocking the activity of the proteasome would return STAT2 levels to those seen in the EV control. Interestingly MG132 treatment did increase levels of STAT2 in NS1 expressing cells, but not to the level of the EV. A DMSO control was used as the MG132 was reconstituted in DMSO before use. While DMSO is often considered inert, treating NS2 expressing cells with

DMSO caused a reduction of STAT2. This may mean that the increase in STAT2 seen with MG132 treatment is a result of the DMSO rather than the active MG132. DMSO is often used as a solvent for non-polar molecules, but has been reported to have an impact on cells itself, particularly effecting cell metabolism (Verheijen et al., 2019). Therefore, we are unable to confirm if the reduction of STAT2 by NS1 is via ubiquitin mediated degradation.

Although the NS expressing cells had reduced ISG expression compared to the EV control, when transfected cells were stimulated with IFN α we did not see the expected increase in ISG expression, even in the EV control. From the time course and dose response experiments both cell lines were shown to be responsive to IFN, but this response was muted when cells were transfected. To see if this was caused by the lipofectamine reagent or the empty vector used, pCI-neo, we used a second empty vector pCMV, and a lipofectamine treated control. From these results we clearly saw that the presence of pCI-neo vector caused a higher basal level of MxA mRNA, greater than that of the pCMV or lipofectamine control, and MxA did not increase with IFN treatment. This was true in both A549 and BEAS 2b cell. A549 cells were more sensitive to EV transfection, with pCMV also causing an increase in basal MxA, though this was still able to further increase with IFN treatment. The pCMV vector did not have the same effect, with IFN α causing a significant increase in MxA levels in both cell lines. Interestingly the A549 cells did have elevated basal MxA levels with pCMV, suggesting they are overall more sensitive to plasmid transfection. The impact of pCI-neo does limit how we are able to measure IFN stimulation, particularly in the A549 cell line. As there was no increase in STAT activation in EV transfected cells, as measured by western blotting, the increase in ISG expression with transfection is likely caused by a DNA or RNA sensor in the cells that leads to up regulation of the antiviral response, including ISGs. However, it is interesting that even with this errant signalling caused by the vector, NS are still able to reduce ISG expression compared to the EV control, suggesting that the NS can overcome host signalling pathways in a stimulated cell.

The transfection of the pCI-neo vector causes an increase in basal ISG expression levels, which cannot be further increased with IFN α stimulation. This is likely cause by detection of the vector by PRR within the cell, triggering an increase in antiviral genes including MxA. This appears to be cell line specific, with A549s more sensitive to pCI-neo than the BEAS-2b cell line. As a result, the use of pCI-neo as the vector for the RSV NS proteins likely increases ISG expression levels. However, we have seen that the expression on NS1 (but not NS2) reduces ISG expression, showing that NS1 can override the stimulatory

effects of the pCI-neo vector. This highlights the role of NS1 as a disruptor of signalling, even with stimulation from the vector.

As the ISG expression is limited with NS1 expression without any increase in reduction in STAT, the mechanism may involve the translocation machinery that controls the movement of STATs to the nucleus. We investigated if STAT1 was able to translocate as normal in NS1 expressing BEAS 2b cells. Under normal conditions STAT1 is able to be transported across the nuclear membrane by importins; importin- α binds the NLS of STAT1, and with the help of importin- β shuttles it to the nucleus in an ATP dependent manner (McBride et al., 2002, Shen et al., 2021). Once in the nucleus the importins are recycled to move other cargo and the STAT complex is released, allowing it to bind promoter regions and induce gene expression (Shen et al., 2021). Imaging the cells with confocal microscopy showed that NS1 expression reduced the amount of STAT1 present in the nucleus compared to the EV control, and the amount of STAT1 in the nucleus did not increase with IFN treatment. When STAT2 translocation was examined in the same way we saw no change in the nuclear intensity of STAT2, but in cells expressing NS1 the localization of STAT2 changed; rather than being diffuse across the cell it instead was localised to an area adjacent the nucleus. A longer IFN α treatment time could show if the sequestering of STAT2 by NS1 limits its nuclear translocation, this should be investigated in future studies.

To confirm if this was also true with full length RSV infection, and not just when NS1 was expressed alone, BEAS 2b cells were infected with RSV-A2-GFP. Here we saw that levels of STAT1 were reduced in all cells expressing GFP, but neighbouring uninfected cells had no reduction in STAT1. Whole cell lysis of RSV infected cells showed now overall reduction in STAT1 (Fig. A1.1), supporting that this effect is only seen in cells with active RSV infection rates. In the cell line experiments a reduction in ISGs was seen while cells infected with RSV see an increase in ISG expression. This is likely because infection with full length virus will activate various PRR receptors which will lead to an increase in antiviral proteins, including IFNs. These are then released from the cell stimulating the neighbouring cells, increasing overall ISG expression. Transfecting cell lines with single RSV proteins prevents this additional PRR signalling, as there are no viral proteins included. Without the stimulating effect of other viral proteins, the suppressive effect of NS1 on ISG expression can be seen. Additionally, the relative increase in ISG in the RSV infected cells was seen in the global cell population (i.e. not just those actively infected), from the confocal imaging its clear that the RSV-A2-GFP infected cells have reduced STAT1 levels compared to their neighbours. Levels of ISG in RSV infected cells

may be lower than neighbouring uninfected cells.

Unfortunately, it was not possible to detect RSV- Δ NS-GFP infected cells due to poor infection (Fig. A1.2). This is likely caused by the IFN competence of BEAS 2b cells; repeating the work in Vero cells which are unable to produce endogenous IFN would most likely yield increased RSV- Δ NS-GFP infection (Teng and Collins, 1999; Jin et al., 2000). However, as Vero cells are a chimp kidney cell line they are of limited relevance when studying a human respiratory virus such as RSV (Desmyter et al., 1968).

Overall we have shown that the expression of NS1 in BEAS 2b cells increases phosphorylation of STAT1 and STAT2 while reducing the nuclear translocation of STAT1, and restricts STAT2 to the perinuclear region.

5 RSV infection of Peripheral Blood Mononuclear Cells

5.1 Introduction

During RSV infection circulating immune cells have an important role in controlling infection. The first immune cells to respond to a viral infection in the respiratory tract will likely be tissue resident dendritic cells (DCs) and macrophages. These cells will phagocytose the pathogen and migrate to the lymph nodes and present its antigens to T and B cells which undergo clonal expansion and selection. As well as phagocytosing pathogens the DCs are also a major source of type I IFNs, stimulating the surrounding epithelial cells to increase ISG production making them less permissive to viral infection, and inducing cytotoxic T cells (Farrar et al., 2002). The chemokines and cytokines produced by tissue resident immune cells are vital in immune cell recruitment to the area, with the resulting cytokine milieu responsible for shaping the immune response. Multiple studies have shown that infants with RSV infection have a skewed response, producing a Th2 cytokine profile (Becker, 2006, Lee et al., 2012). The mechanism behind the Th2 response in RSV is not fully understood, but is likely due to the altered cytokine profile at the site of infection predisposing the Th2 response.

In addition, levels of thymic stromal lymphopoietin (TSLP) which has been linked to immunopathology in RSV mouse models and the development of asthma (Malinczak et al., 2019, Lee et al., 2012). TSLP impacts the ability of DC to direct T cell differentiation, resulting in a greater number of Th2 type cytokines (Soumelis et al., 2002, Ziegler et al., 2013). RSV infection also increases expression of IL-33 which via DCs to increase the Th2 cell differentiation, increase mucus production and heighten airway sensitivity (Saravia et al., 2015, Besnard et al., 2011).

Unlike other viral respiratory infections RSV can have a lasting impact with RSV infection predisposing children to persistent wheeze after the acute infection has resolved (Zhou et al., 2021). Post-RSV wheeze is associated with increased cell infiltrates in the lung, a feature not seen with other respiratory viruses (Johnson et al., 2007). The increased immune cells infiltrates may be driven by altered signalling in local immune cells following RSV infection, resulting in changed cytokine output. For many years there has been a link between severe RSV infection in early life and the development of asthma though the mechanism for this is still unclear (Krishnamoorthy et al., 2012, Balekian et al., 2017). While studies are beginning to show the impact of RSV on the local mucosal immune response, the effect of RSV infection on circulating immune cells has not been significantly investigated. While RSV is a localised infection and does not cause systemic infection, during infection there is an increase in various immune cells to the site of

infection, making them vulnerable to infection. These cells can then travel to lymph nodes via the circulatory system. Any infection of immune cells is unlikely to be a productive infection (ie the infection will not result in effective viral replication) but the infection of the cell may alter its function which would impact the resulting immune response. The NS proteins are known to impact levels of various signalling proteins, which leads to differential gene expression, changing which cytokines are released or the expression of cell markers. Therefore, any infection of immune cells could result in the expression of NS1 and NS2 which could impact cell signalling in response to stimuli. A change in cytokine and chemokine expression will change which immune cells are recruited to the site of infection; the altered localisation of immune cells to the lung mucosa can cause dysregulation of the immune response and damage to the membranes. RSV infections are characterised by the large scale infiltration of neutrophils to the area and the predominance of a Th2 type response – ultimately causing more significant disease and could potentiate associated wheeze and asthma.

While the immune cells in the mucosa are the key for the clearance of viral infections they are hard to access, particularly from young infants. Circulating immune cells collected from the blood are a surrogate for these populations that are simple to access. There are a host of immune cells that can be separated from whole blood, the peripheral blood mononuclear cells (PBMCs) populations can be analysed by flow cytometry to identify populations of cells based on extracellular markers.

5.2 Specific Aims

- To determine the impact of RSV infection on JAK-STAT signalling in paediatric PBMC populations
- Use RSV-A2-GFP to determine if RSV can infect PBMCs
- To quantify the effect of RSV-A2-GFP infection on pSTAT1 or pSTAT3 levels in PBMCs.

5.3 Results

5.3.1 Viability of Frozen Paediatric PBMCs

RSV is a highly seasonal infection with a typical peak in cases in the winter months, between October and January each year (Broberg et al., 2018). To analyse the effect of RSV infection in infant peripheral immune response, infants admitted to the National Children's Hospital at Tallaght with bronchiolitis during this period were invited to take part in this study.

Healthy controls were recruited from the children attending the phlebotomy clinic at Tallaght with no recent history of infections. The 12 infants included with bronchiolitis all required hospital admittance and 10 underwent a viral screen which confirmed that 8 of them were positive for RSV (Table 5.1). Of the samples collected 6 RSV+ samples were included in this study Fig 5.1; two bronchiolitis patient samples were excluded due to a blood sample volume of below 1ml, the minimum volume of blood needed to PBMC isolation. Two bronchiolitis patients were not screened for viruses on admission so RSV infection cannot be confirmed. The viral screen showed that a number of other viruses were present, most commonly Rhino/Enterovirus was detected as a coinfection with 4 infants infected with both RSV and Rhino/Enterovirus. Two patient diagnosed with bronchiolitis was confirmed to be RSV negative, both of these were positive for Influenza A. The two strains of RSV, A & B, alternate in dominance in the two RSV seasons looked at, with RSV-B dominant in 2018/2019 and RSV-A dominant in 2019/2020 (Table 5.1), this changing dominance had been seen in much larger studies of RSV epidemiology (Shi et al., 2017, Price et al., 2019).

PBMCs were isolated from whole blood samples and stored in liquid nitrogen. The Dewar used developed a leak in June 2019 leading to a freeze thaw of samples, potentially compromising samples collected in the 2018/2019 season. Samples affected by this thaw are shown in blue triangles. Samples were strained with a BV510 viability dye and analysed, two adult PBMC samples which were stored separately were used as a control (Fig 5.2). The cells which had been stored in the damaged Dewar have a much lower percentage of live cells than the other paediatric cells. All paediatric PBMCs have significantly lower viability compared to the adult samples (Fig 5.2E). There was no significant difference between the percentage of T cells between adults and paediatric samples (Fig 5.3). Although there was no change seen in pSTAT levels in response to the stimulus this could be the result of the low viability of paediatric samples as only live cells

are able to respond to the stimulus therefore; a large population of dead cells will skew the results (Fig 5.4). When staining for phosphorylated STATs the fixing reagent must be added as soon as possible to capture as much of the pSTAT before it is degraded. As a result, when staining for pSTAT's it was not possible to include a live/dead stain and the lack of pSTAT response after stimulus could be caused by the large population of dead cells rather than a result of RSV infection.

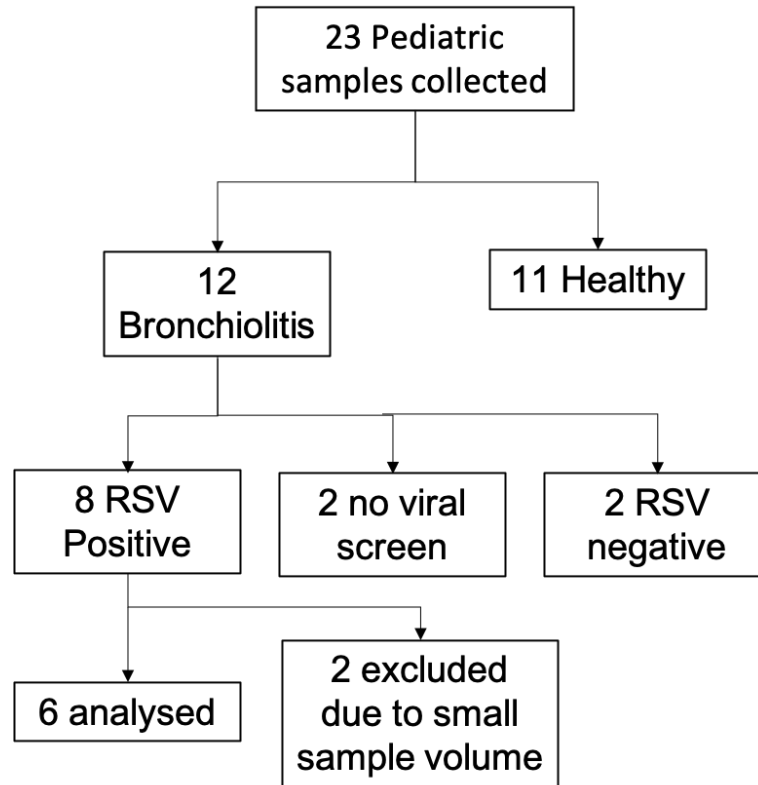


Figure 5.1: Flow chart of paediatric samples

A total of 23 samples were collected from children attending The National Children's Hospital at Tallaght. Healthy blood samples were taken from children with no recent history of infection, bronchiolitis samples were taken from children presenting with bronchiolitis, these were screened for common viral infections as shown in Table 5.1

Table 5.1: Summary of viral screens from infants in this study with RSV bronchiolitis

Sample No.	Sex	Age (months)	RSV A	RSV B	HPIV 4	Rhino/Enterovirus	CoV 229E
18110601	F	58	Y	.	.	.	Y
18121801	M	4	.	Y	.	Y	.
18121802	M	2	.	Y	.	.	.
18121901	F	9	.	Y	Y	Y	.
19122401	M	6	Y
19122601	M	5	Y
19121001	M	1	Y	.	.	Y	.
19121702	F	15	Y	.	.	Y	.

Infants admitted to The National Children's Hospital with bronchiolitis were screened for a range of viral pathogens, here we show the results from children testing positive for either RSV-A or RSV-B. Only pathogens that were detected at least once are included in this summary.

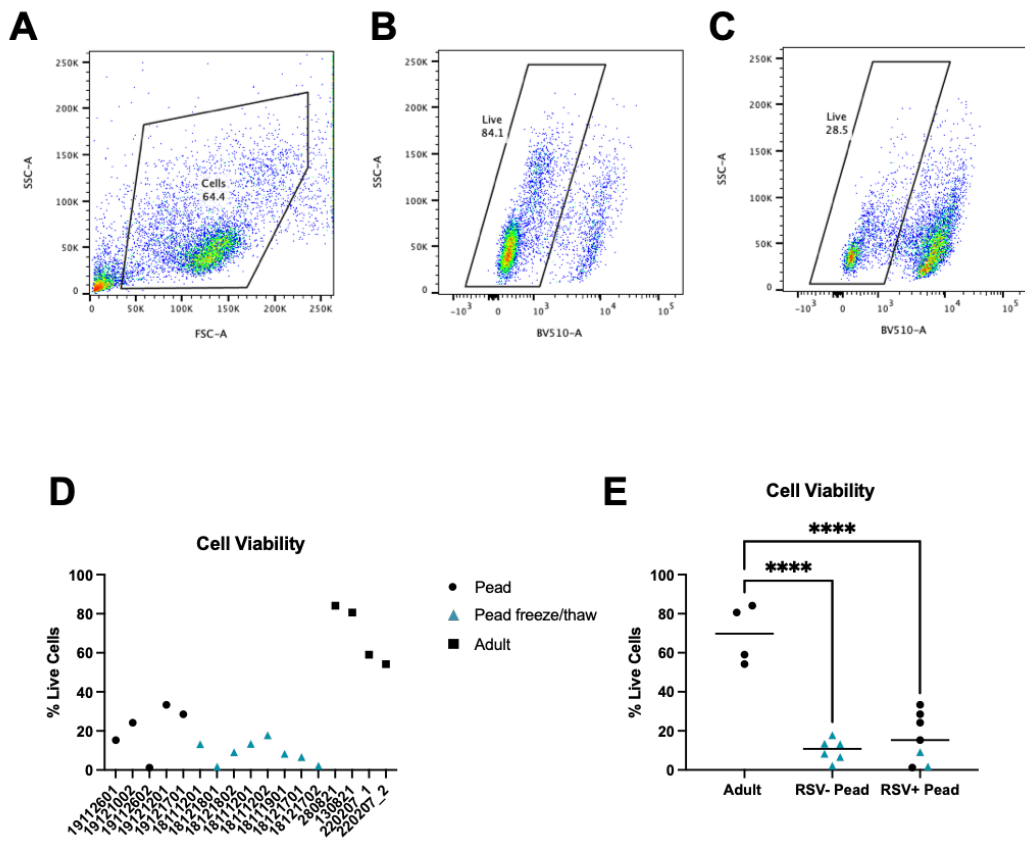


Figure 5.2: Viability of Paediatric PBMCs

The gating of samples selected A) all cells excluding debris, we stained cells using the Live/Dead stain (Zombie Live/Dead -NIR) B) the Live cells in an adult control and C) Live cells in a paediatric sample. D) the percentage of live cells in each sample E) the viability if significantly reduced in paediatric samples compared to the healthy adult controls. Statistics by unpaired t-test $n=4$ adult, $n=7$ RSV-, $n=6$ RSV+

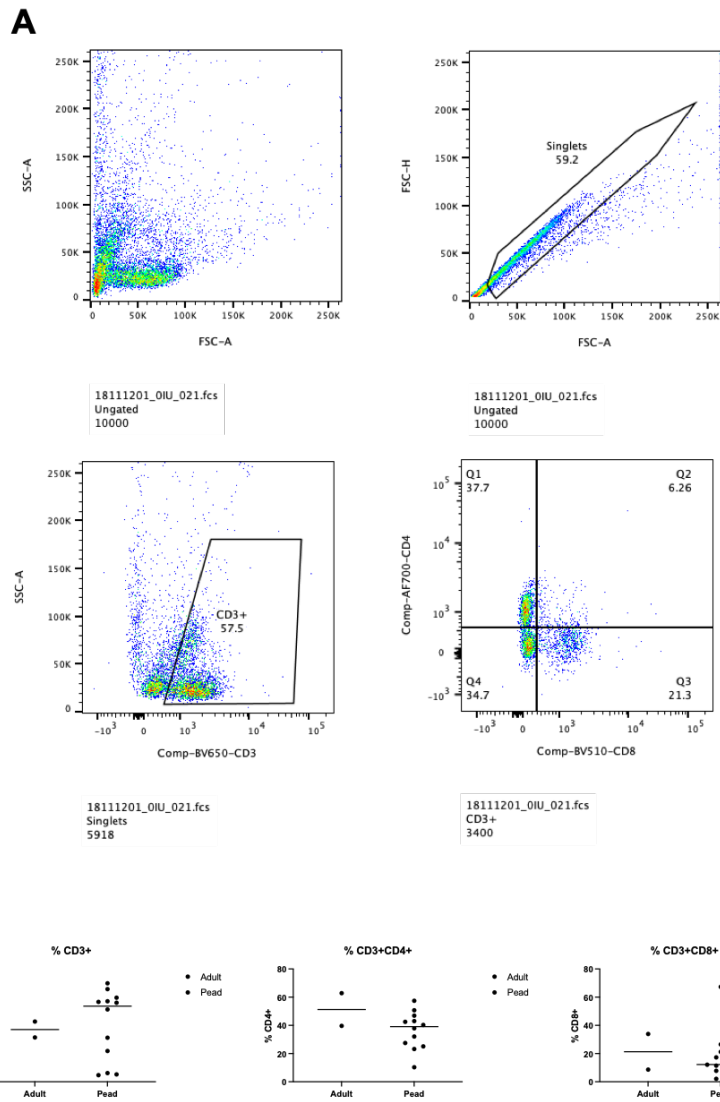


Figure 5.3: Relative abundance of T cells in adults compared to paediatric PBMCs

A) The gating strategy for analysis, single cells were selected and CD3+ cells gated on. Within the CD3+ population CD4+ (AF700) vs CD8+ (BV510) were assessed. B) the relative percentages of CD3+, CD3+CD4+ and CD3+CD8+ cells. Statistics by unpaired t-test. Adult n=2, paediatric n=12.

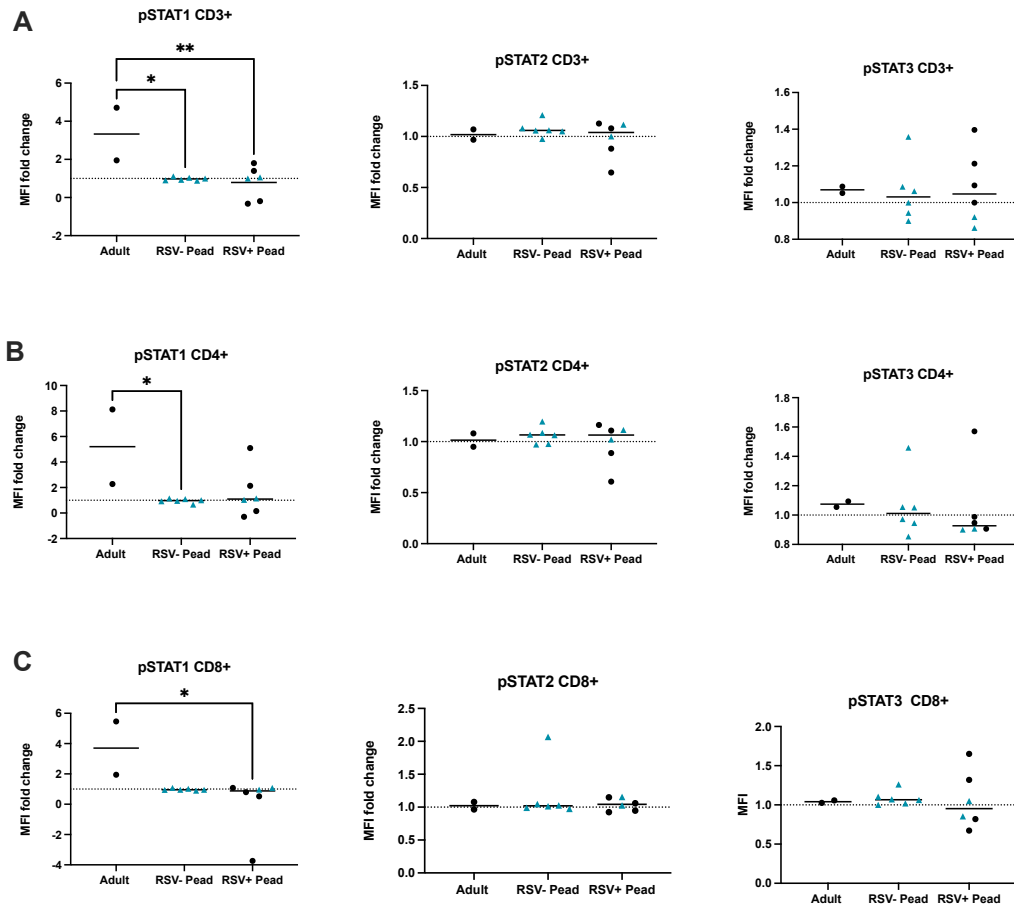


Figure 5.4: STAT activation in Paediatric PBMCs.

PMBCs from RSV positive or RSV negative paediatrics and adult controls were assessed for pSTAT1-3 levels after 15min IFN α stimulation. Results are presented as MFI fold change compared to the untreated sample, a result of 1 indicates no change, >1 = an increase in pSTAT, <1 = a decrease in pSTAT. Levels of pSTAT1, pSTAT2 and pSTAT3 were measured in A) CD3+, B) CD4+ and C) CD8+ cells. Blue triangles indicate samples stored in faulty Dewar. Adult, n=2; RSV-, n=6; RSV+, n=6

5.3.2 Infection of Adult PBMCs with RSV-A2-GFP

Adult PBMCs were isolated from whole blood samples from healthy volunteers using a ficoll density gradient and frozen until use. PBMCs were seeded in RPMI for 24h before incubation with MOI 1 RSV-A2-GFP or mock control for 10h. A 10h infection was used to ensure only the impact of the primary infection was analysed, RSV has a replication time of 30-40h (Collins and Graham, 2008). Samples were then stimulated for 15min with 1000IU or 0IU IFN α and collected for flow cytometry. Cells were either stained with a Live dead stain, Panel 1 (CD3, CD4, CD8, CD19, pSTAT1, pSTAT3 and STAT1) or Panel 2 (CD56, CD14, CD11c, pSTAT1, pSTAT3 and STAT1).

Infection at MOI 1 did not cause increased cell death compared to the mock infected sample (Fig 5.5A) and there was a small but significant population of GFP+ cells, indicating RSV-A2-GFP infection (Fig 5.5B). Within each cell population the percentage GFP+ cells was gated on (Fig 5.6 & Fig 5.8 & Fig 5.9). This indicates the number of cells actively infected by the RSV-A2-GFP strain. Compared to the mock infected control the RSV group had consistently higher % GFP+ cells in the single cells, CD3+, CD3+CD4+ and CD3+CD8+ cells (Fig 5.8). CD11c+ cells had the greatest number of GFP+ cells (7%) (Fig 5.9A). Very few CD19+ cells were present in the samples and it was therefore not possible to accurately compare the mock and RSV-A2-GFP infected groups (data not shown).

Within each cell type levels of pSTAT1, pSTAT3 and STAT1 were measured with and without an IFN α stimulus, example dotplots are shown in Fig 5.10. In the mock infected samples the median fluorescence intensity (MFI) of pSTAT1 increased following stimulus, while in the RSV infected samples the basal MFI of pSTAT1 tended to be higher and did not increase further when treated with IFN α (Fig. 5.11). The mock infected CD3+ cells show a 2 fold increase in pSTAT1 MFI with IFN α treatment, while those that had been exposed to RSV have no increase in pSTAT1 with treatment (Fig. 5.11B). The same effect is also seen in CD3+CD4+ (Fig 5.11C) and CD3+CD8+ cells (Fig 5.11E), with a 2.5 fold and 3 fold rise in pSTAT1 levels in the mock infection and no increase with RSV infection (Fig 5.11D & F). Given the low infection rate of CD3+ cells, it's surprising that even this limited infection can impact STAT phosphorylation.

When panel 2 was used (CD56, CD14, CD11c, pSTAT1, pSTAT3 and STAT1), none of the mock infected cells stimulated with IFN α show an increase in STAT1 phosphorylation (Fig. 5.12 & Fig 5.14), though RSV infection does cause an increase in the basal MFI of pSTAT1 and pSTAT3 in CD56+ cells (Fig. 5.12C & 5.14C). Incubation with RSV

caused an increase in STAT1 levels in all cell types investigated except CD11c+ cells (Fig. 5.15).

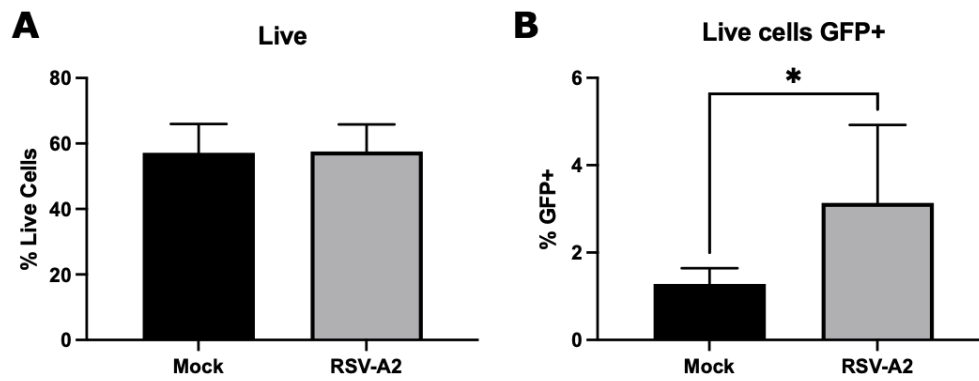


Figure 5.5: Confirmation of in vitro RSV infection of primary human immune cells

Adult PBMCs were incubated with MOI 1 RSV-A2-GFP for 10h. A) Infection did not cause significant cell death but B) did result in a GFP positive population of infected cells. Significance by paired t-test, $=p < 0.05$ (n=5)*

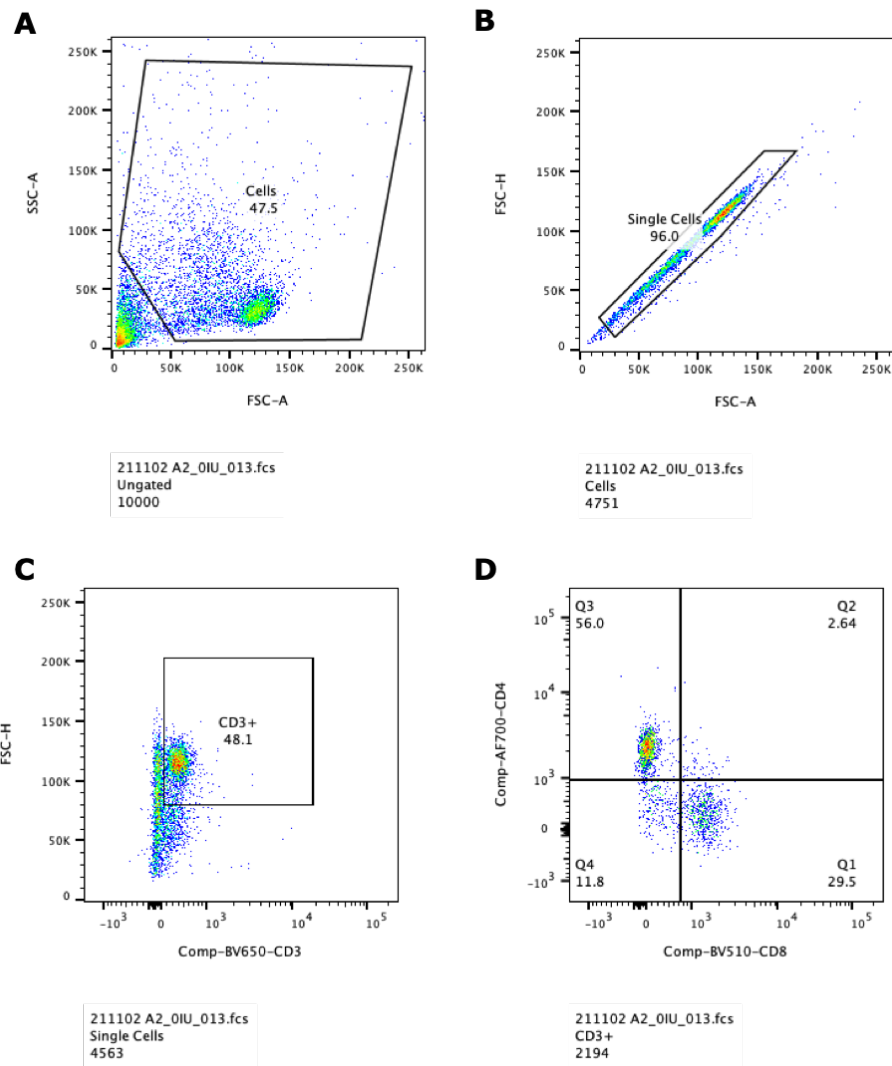


Figure 5.6: Gating strategy for adult RSV infected PBMCs

Adult PBMCs were incubated with MOI 1 RSV-A2-GFP for 10h and stained with CD3, CD4, pSTAT1, pSTAT3 and STAT1. To identify populations A) all cells, excluding debris, were gated on. Within this groups B) single cells were selected and C) the CD3+ population was identified, and with in this the C) CD4 single positive and CD8 single positive cells were identified (n=5).

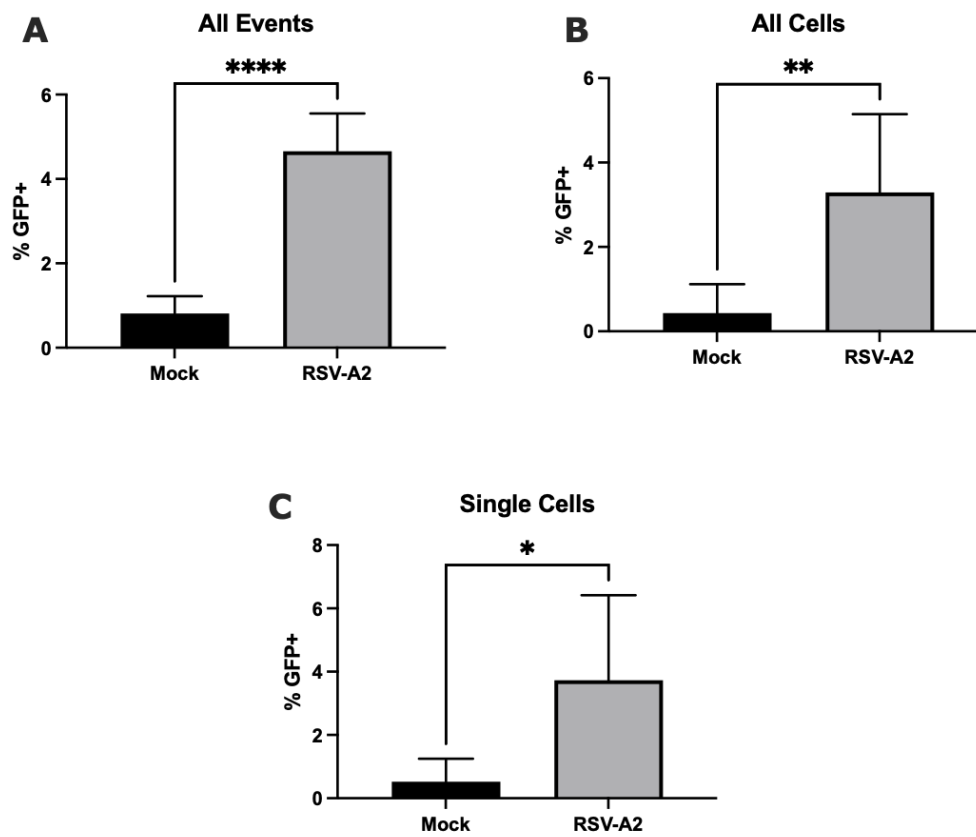


Figure 5.7: RSV infection in PBMCs

Adult PBMCs were incubated with MOI 1 RSV-A2-GFP for 10h. Comparing GFP signal in mock and RSV incubated samples shows a significantly increased GFP signal in A) all events B) all cells (excluding debris) and C) single cells. Statistics by paired t-test $*=p<0.05$, $**=p<0.01$, $***p<0.001$ ($n=5$).

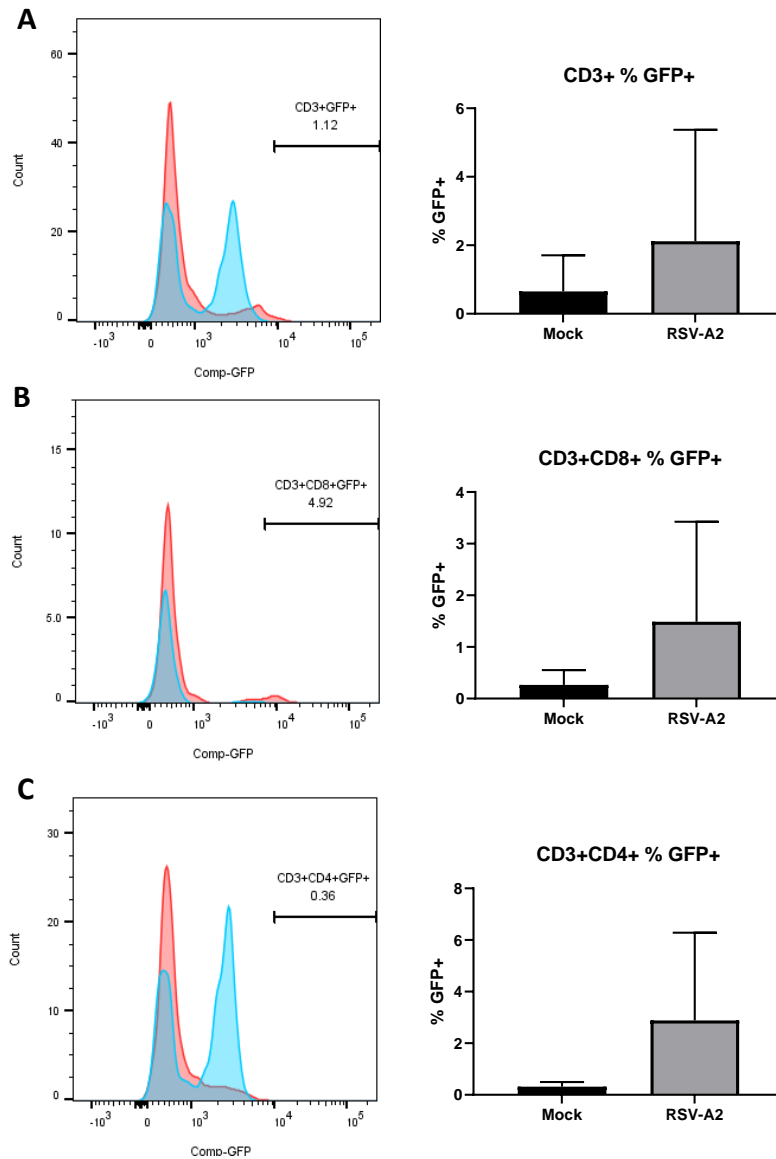


Figure 5.8: RSV infection in CD3+ T Cells

Adult PBMCs were incubated with MOI 1 RSV-A2-GFP for 10h. Comparing GFP signal in mock and RSV incubated samples shows the percentage of cell with a GFP signal increases in A) CD3+, B) CD3+CD8+, C) CD3+CD4+ cells but is not significant. Comparing histograms, GFP signal in mock (blue) and RSV incubated (red) samples shows an increased GFP signal in cells incubated with RSV. Statistics by paired t-test ($n=5$).

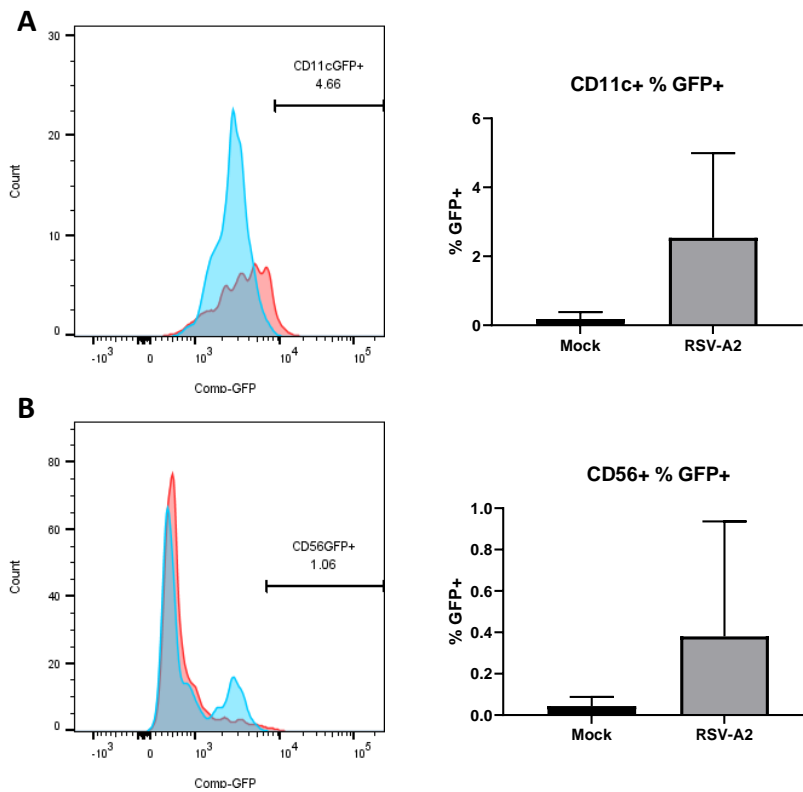


Figure 5.9: RSV infection in CD11c+ and CD56+ Cells

Adult PBMCs were incubated with MOI 1 RSV-A2-GFP for 10h. Comparing GFP signal in mock and RSV incubated samples shows the percentage of cell with a GFP signal increases in A) CD11c and B) CD56 cells but is not significant. Comparing histograms, GFP signal in mock (blue) and RSV incubated (red) samples shows an increased GFP signal in cells incubated with RSV Statistics by paired t-test (n=5).

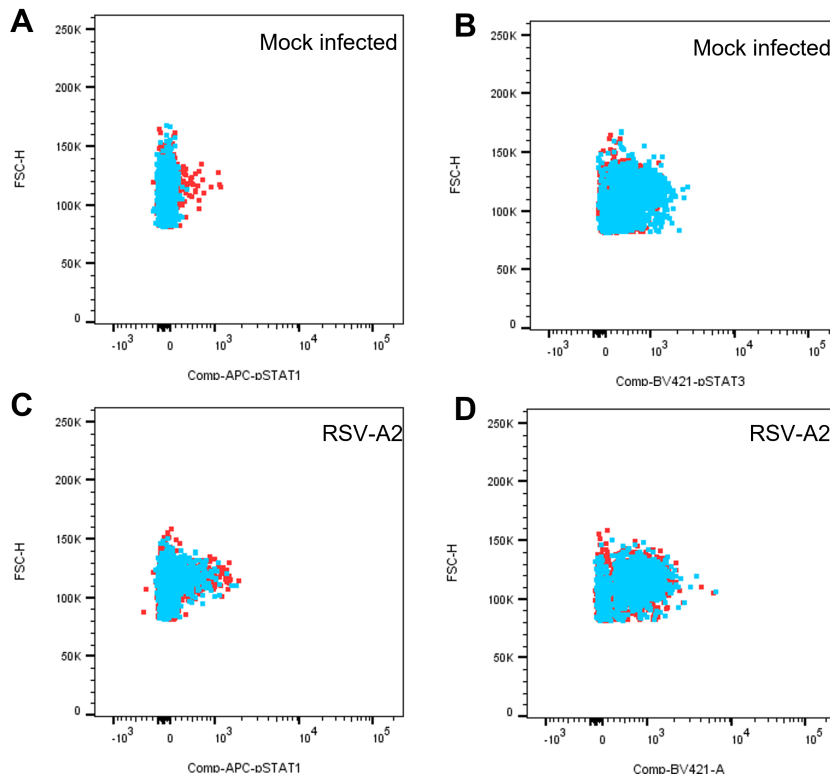


Figure 5.10: RSV infection reduces pSTAT1 and pSTAT3 response to $IFN\alpha$ stimulus

Adult PBMCs were incubated with MOI 1 RSV-A2-GFP for 10h. Cells were then stimulated with 1000IU $IFN\alpha$ for 30min, shown in red or left unstimulated shown in blue. A) pSTAT1 levels in mock infected cells increase with $IFN\alpha$ treatment. B) pSTAT3 levels in mock infected cells remain the same in $IFN\alpha$ treated and untreated cells. C) pSTAT1 levels in RSV-A2 infected cells are higher than the mock infected sample and do not increase with $IFN\alpha$ stimulation. D) pSTAT3 in RSV-A2 infected cells remained the same in $IFN\alpha$ treated and untreated cells. (n=5).

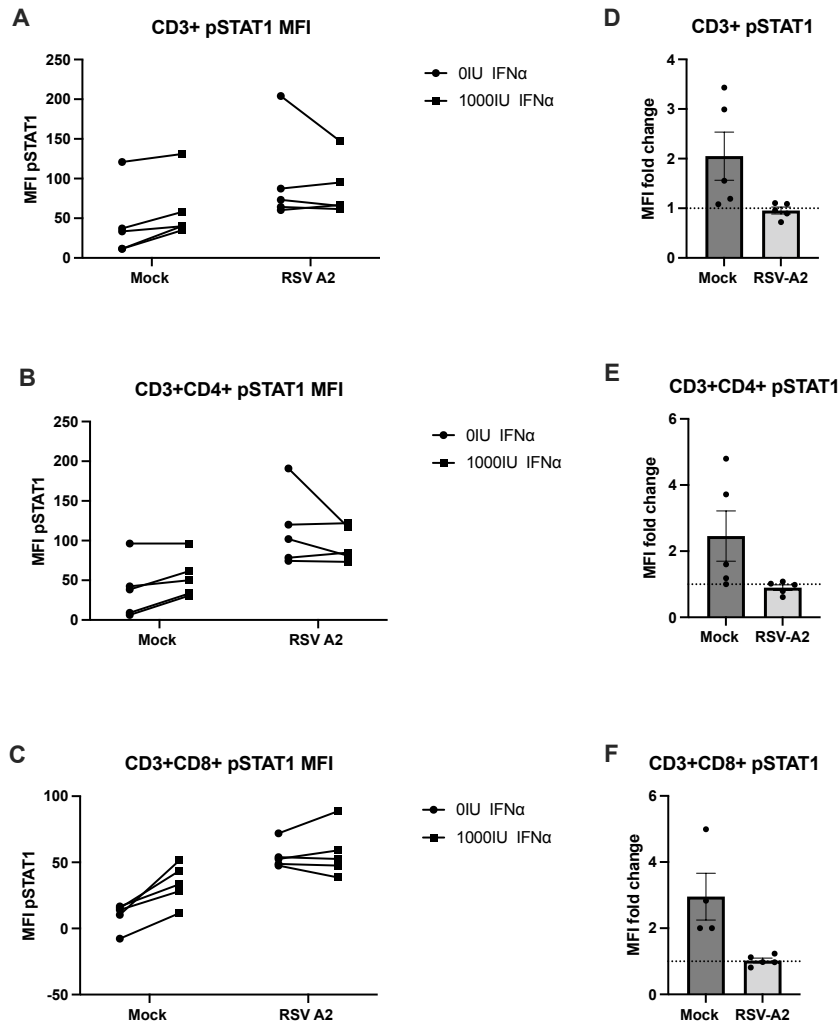


Figure 5.11: RSV infection reduces T cell pSTAT1 response to IFN α stimulus

Adult PBMCs were incubated with MOI 1 RSV-A2-GFP for 10h. Cells were then stimulated with 1000IU IFN α for 30min and stained with panel 1. Gating on single cells, CD3+, CD3+CD4+ and CD3+CD8+ cells level MFI of pSTAT1 levels were compared with and without IFN α treatment. A) MFI values of pSTAT1 in CD3+ cells and B) the fold change of pSTAT1 in CD3+ cells with IFN α treatment. C) MFI values of pSTAT1 in CD3+CD4+ cells and D) the pSTAT1 fold change in CD3+CD4+ cells with IFN α treatment. E) MFI values of pSTAT1 in CD3+CD8+ cells and D) the pSTAT1 fold change in CD3+CD8+ cells with IFN α treatment. A fold change of 1 (dotted line) indicated no increase in pSTAT1 with treatment. Statistics by paired t-test $*=p<0.05$ (n=5).

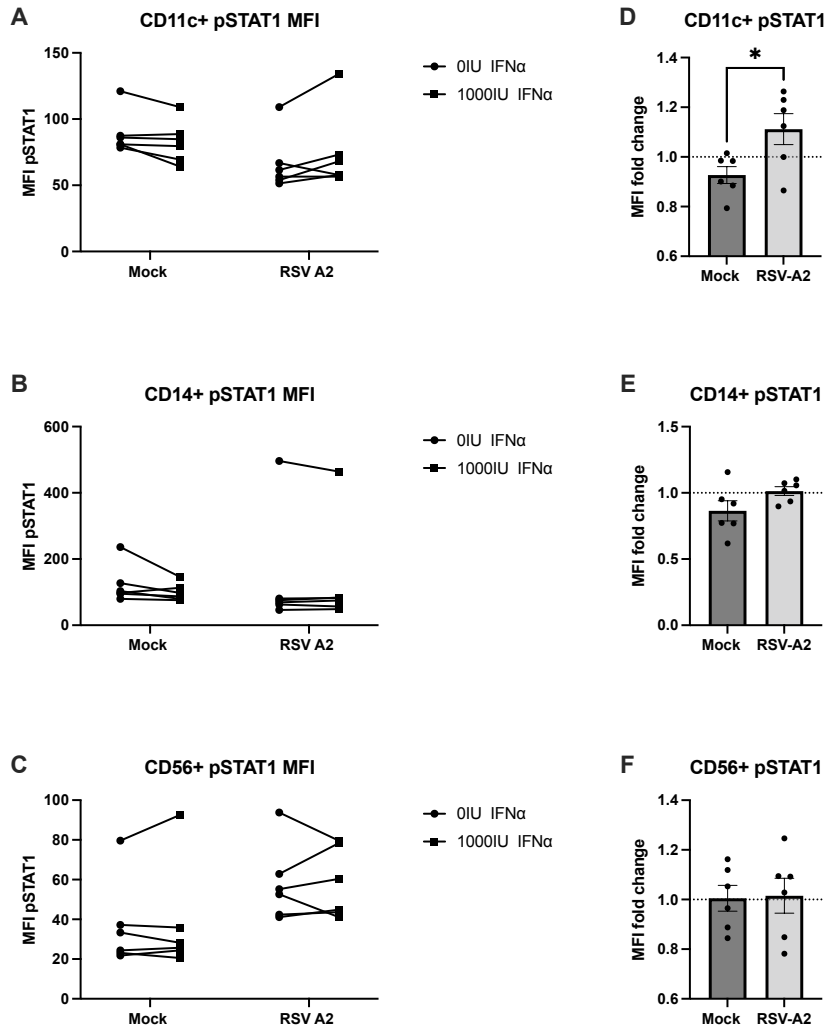


Figure 5.12: RSV infection has no impact on CD14 and CD56 cell pSTAT1 response to IFN α stimulus

Adult PBMCs were incubated with MOI 1 RSV-A2-GFP for 10h. Cells were then stimulated with 1000IU IFN α for 30min and stained with panel 2. Gating on single cells, CD11c, CD14 and CD56 cells level MFI of pSTAT1 levels were compared with and without IFN α treatment. In A) CD11c the stimulus failed to induce a measurable increase pSTAT1 MFI in both the mock infected and RSV infected groups D) there is a significant increase in RSV pSTAT1 fold change compared to the mock group. In both B) CD14+ and C) CD56+ cells the stimulus fails to cause an increase in the mock infected and RSV infected groups and this is seen when comparing the E) CD14+ pSTAT1 fold changes and F) CD56+ pSTAT1 fold changes. Statistics by paired t-test $*=p<0.05$ (n=5).

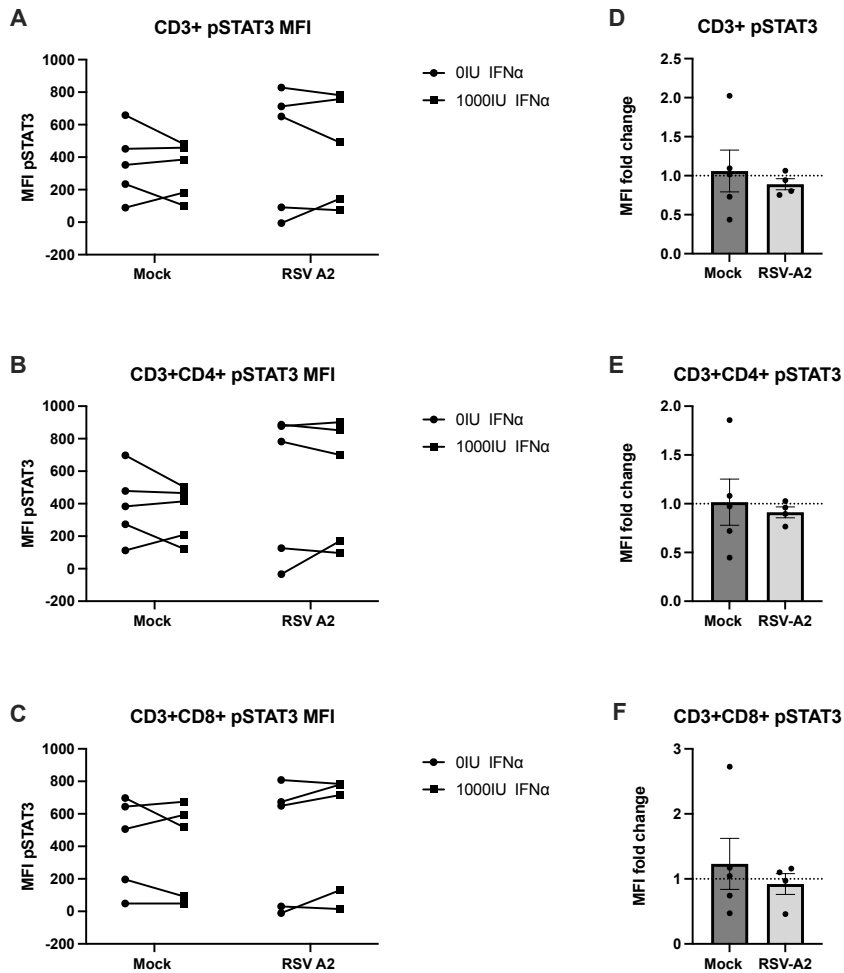


Figure 5.13: RSV infection has no significant impact on T cell pSTAT3 response to IFN α stimulus.

Adult PBMCs were incubated with MOI 1 RSV-A2-GFP for 10h. Cells were then stimulated with 1000IU IFN α for 30min and stained with panel 1. Gating on single cells, CD3+, CD3+CD4+ and CD3+CD8+ cells level MFI of pSTAT3 levels were compared with and without IFN α treatment. A) MFI values of pSTAT3 in CD3+ cells and B) the fold change of pSTAT3 in CD3+ cells with IFN α treatment. C) MFI values of pSTAT3 in CD3+CD4+ cells and D) the pSTAT3 fold change in CD3+CD4+ cells with IFN α treatment. E) MFI values of pSTAT3 in CD3+CD8+ cells and D) the pSTAT3 fold change in CD3+CD8+ cells with IFN α treatment. A fold change of 1 (dotted line) indicated no increase in pSTAT3 with treatment. Statistics by paired t-test (n=5).

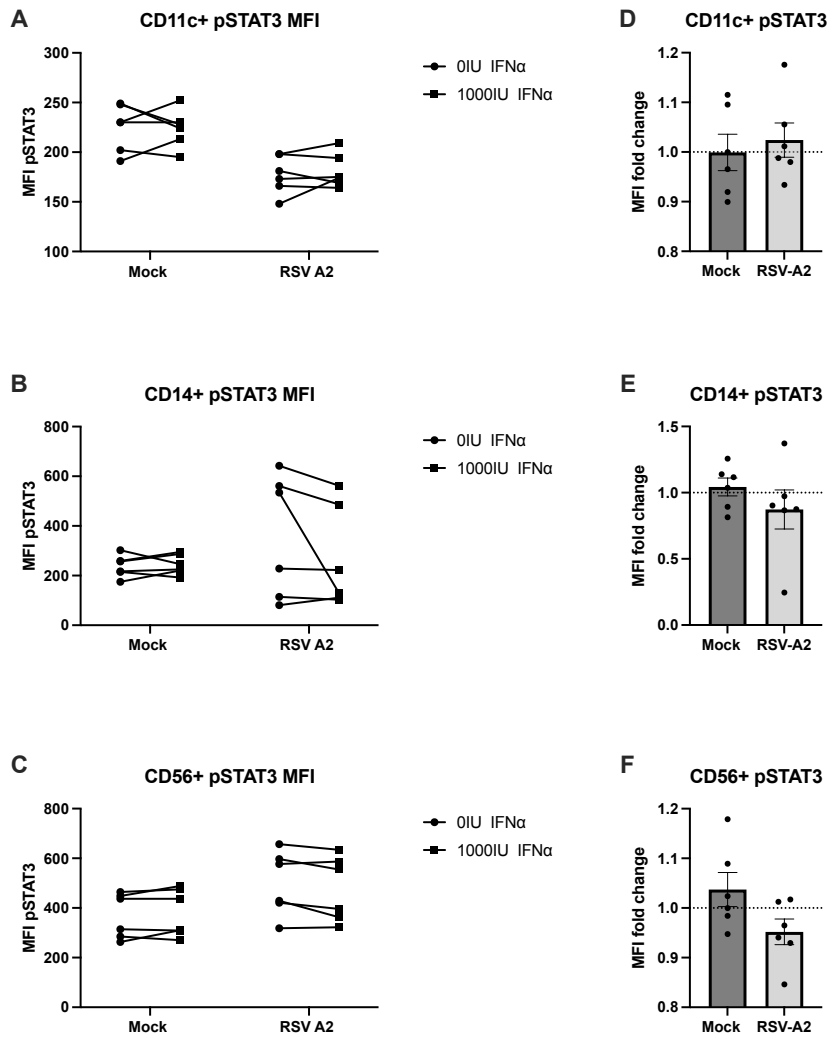


Figure 5.14: RSV infection has no significant impact on CD11c, CD14 and CD56 cell pSTAT3 response to IFN α stimulus

Adult PBMCs were incubated with MOI 1 RSV-A2-GFP for 10h. Cells were then stimulated with 1000IU IFN α for 30min and stained with panel 2. Gating on single cells, CD11c, CD14 and CD56 cells level MFI of pSTAT3 levels were compared with and without IFN α treatment. In A) CD11c the stimulus failed to induce a measurable increase pSTAT3 MFI in both the mock infected and RSV infected groups. B) CD14+ and C) CD56+ cells the stimulus fails to cause an increase in the mock infected and RSV infected groups and this is seen when comparing the D) CD11c+ pSTAT3 fold changes E) CD14+ pSTAT3 fold changes and F) CD56+ pSTAT3 fold changes. Statistics by paired t-test (n=5).

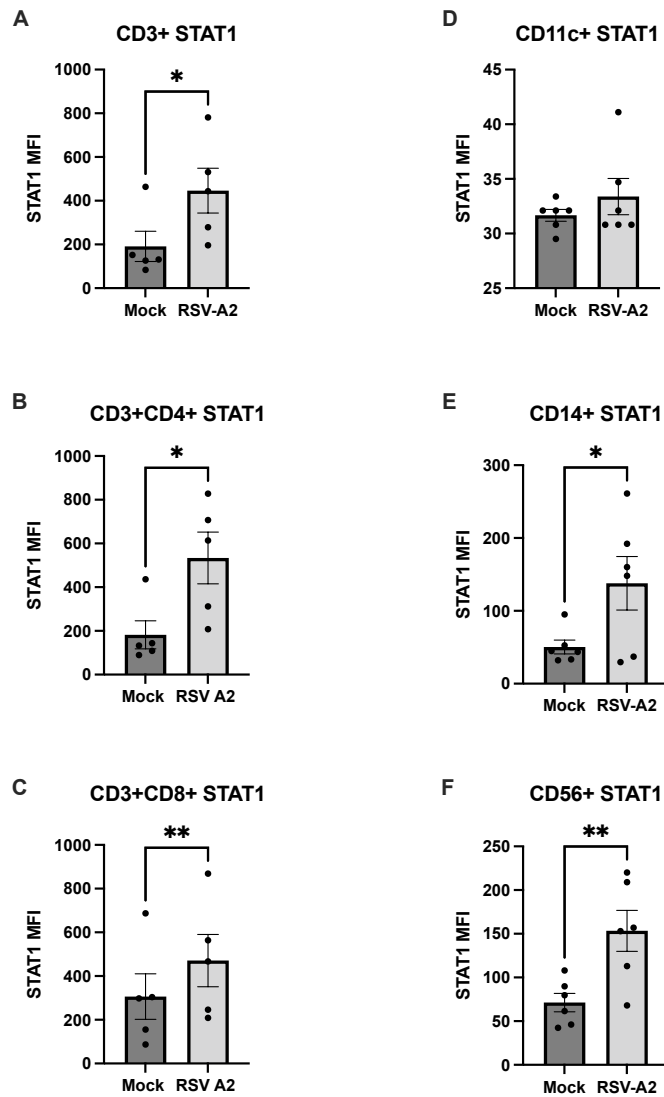


Figure 5.15: Impact of RSV infection on total STAT1 levels in PBMCs

Levels of STAT1 were measured in adult PBMCs incubated with MOI 1 RSV-A2-GFP for 10h. Levels of STAT1 in A) CD3+, B) CD3+CD4+, C) CD3+CD8+, D) CD11c+, E) CD14+ and F) CD56+ were measured in mock and RSV infected cells. Statistics by paired t-test (n=5).

5.4 Discussion

RSV infections occur regularly throughout the population, but those most at risk are infants under 6 months old and the elderly (Shi et al., 2020). To better understand the impact of RSV on paediatric immune response specifically we recruited infants admitted to the National Children's Hospital at Tallaght. From these infants we saw that the average age of admittance with bronchiolitis was 12.5 months, and that the RSV was detected in majority of bronchiolitis cases. Other larger studies have shown that RSV alters its predominance between the A and B strains annually (Pandya et al., 2019), which even in our small sample size we confirm. The viral screen also showed high levels of co-infections in our cohort; most infants were also infected with at least one other virus, most commonly Rhino/Enterovirus. The impact of the COVID-19 pandemic had a significant impact on RSV cases in Ireland, with almost no cases recorded in winter 2020/2021 (NVRL, 2022). This is likely due to the restrictions placed on household mixing the closure of schools and nurseries (Eden et al., 2022). This also prevented collection of samples beyond winter 2019.

To examine the impact of RSV infection on immune cell function, PBMCs were collected from blood samples of children in our cohort. Analysis by flow cytometry suggests that the paediatric samples collected had low viability, making functional analysis difficult, however we did see that levels of CD3+ cells were consistent between infants and adult controls. As results from the RSV infected infants had not shown clear results we sought to investigate RSV infection of immune cells using adult PBMC samples infected *in vitro* using a GFP tagged RSV (RSV-A2-GFP). This allowed for more standardised assessment with fixed infection conditions. From this we have shown that PBMC are able to be infected by RSV, with increased levels of GFP detected in the infected samples. The majority of infected cells (GFP+) are excluded during the gating strategy as these cells are fall outside the expected size and shape of the events (this will include dead cells, excluded for being too small, or cells stick together and form doublets and are excluded by the singlet gate). This suggests that many of the infected cells have altered morphology which causes them to fall outside the expected forward and side scatter. Despite most infected cells being excluded due to their morphology, around 8% of CD11c+ cells and 2% of CD3+ cells fall within the GFP+ gate after just 10h of incubation with RSV. This indicates that RSV is infecting these cells, where it may influence signalling pathways, as it does in epithelial cells.

To further this, functional analysis of infected PBMCs was performed measuring the

levels of STAT1 and STAT3 phosphorylation in infected cells compared to controls. Incubation with RSV reduced the levels of STAT1 activation in T cells, with the PBMCs incubated with a mock infection showing at least a 2 fold rise in the levels of pSTAT1 after stimulation with IFN α , while the RSV incubated samples failing to increase levels of pSTAT1 with IFN α treatment. The levels of impact of RSV on these cells marked as the T cells only had 2% of cells GFP+, suggesting that even at low levels of infection RSV could impact normal signalling. Looking at levels of total STAT1 levels are seen to significantly increase with RSV infection, after only 10h incubation. The only cell type which failed to have a significant increase in STAT1 were the CD11c+, which had the highest level of RSV infection. This mirror results in BEAS 2b cells where RSV infection caused an increase in STAT1 expression (Fig A1.1).

To determine the level of RSV infection a GFP tagged RSV was used. Any cells containing the virus, either through infection or phagocytosis of infected cells, should be identifiable by a GFP signal. A low infectious dose of virus was used, MOI = 1, to better reflect the level of virus the cells may be exposed to during infection. Only a small percentage of PBMCs identified as GFP positive, however there was a significant increase in the STAT1 levels in RSV exposed cells, and a failure to induce pSTAT1 after IFN α stimulus. The increase in STAT1 was seen in all cells incubated with RSV, not just those that were identified as GFP positive. This may stem from the infected cells releasing cytokines that act on neighbouring cells to increase STAT1 levels, STAT1 holds multiple transcription factor binding sites in its promoter region including IRF2, STAT3 and GATA2 (Fishilevich et al., 2017) which are induced by PRRs (Ivashkin & Donlin 2014). The lack of pSTAT1 expression after IFN α stimulation in all cells incubated with RSV, not just those that are GFP positive, could be the result of high basal levels of pSTAT1 in the mock infected wells, which cannot undergo further phosphorylation with IFN α stimulus. As this looks at the global population of cells, not just those that are actively infected, it is hard to determine the precise effect of RSV on these cells. Using confocal microscopy we have shown that the effect on the infected cell can vary from its uninfected neighbours. To better analyse this in the PBMCs GFP+ cells could be sorted from the total population and analysed separately, or a larger infectious dose of virus could be used to increase the GFP+ population and gate only on GFP+ cells. In these experiments around 3% of CD3+ cells were GFP+ which was too small a population to gather meaningful data.

Results from the adult cells show that RSV infection has a considerable effect on the activity of the JAK-STAT pathway of several populations of circulating immune cells,

even though only around 2% of cells are show active RSV infection. This work suggests that RSV does infect these circulating immune cells and potentially mutes their response to IFN α , though this needs to be explored further.

6 General Discussion and Future Work

6.1 General Discussion

6.1.1 Introduction

Viruses all employ techniques to evade the immune response. Understanding these techniques gives insight into both viral ingenuity and our own immune responses. RSV's NS proteins have no role in the viral replication, but are indispensable for efficient replication in IFN competent cells (Teng and Collins, 1999, Teng et al., 2000); understanding the scope of the NS proteins with the IFN pathways will offer new avenues for therapies. Multiple studies have shown that the NS proteins limit the antiviral response of cells, in particular the JAK/STAT pathway, with mutant RSV strains which lack the NS proteins unable to replicate efficiently in IFN competent cells. Designing therapies that limit the function of the RSV NS proteins could reduce RSV replication and thus limit disease severity. Additionally, the NS proteins are well conserved between the A and B RSV strains and show little antigenic drift over time, making them a stable target for therapeutic interventions. However, the full mechanism of the NS proteins is not understood with conflicting reports on how IFN signalling is limited, carried out in a range of cell lines. Mechanisms that have been linked to RSV NS proteins inhibition of IFN signalling include direct degradation of STAT2 (Elliott et al., 2007), increases in SOCS1 (Hashimoto et al., 2009) and SOCS3 expression (Xu et al., 2014b, Zheng et al., 2015) and interaction with cellular RNA sensors (Boyapalle et al., 2012, Ling et al., 2009). In this work we found that the epithelial cell line used impacts the mechanism of the RSV NS proteins and that NS1 can interrupt nuclear translocation of STAT1.

6.1.2 NS proteins as E3 ligases

Based on previous studies which showed E3 ligase activity of NS1, both NS1 and NS2 were examined for several motifs associated with SOCS activity using sequence alignment. The sequence of a protein will dictate its structure and ultimately its function; aligning the NS proteins with motifs known to govern the E3 ligase activity of the SOCS proteins showed that NS1 and NS2 both contain putative SOCS boxes and Cul binding sites. However, neither NS protein caused a proteasome mediated reduction in STAT proteins in the respiratory epithelial cell lines studied, despite previously having this effect in kidney epithelial cell line HEK293T (Elliott et al., 2007). Although this particular mechanism was not found in A549 or BEAS 2b epithelial cells, the expression of NS1 in these cells resulted in a reduction in ISG expression. This could be explained by disrup-

tion of normal JAK-STAT signalling elsewhere in the pathway, specifically a reduction of phosphorylated STATs or reducing the availability of the ISGF3 and GAF transcription factors.

6.1.3 Implications of cell line on the function of the RSV NS proteins

Upon NS expression in A549 cells there is no change in pSTAT1 or pSTAT2 levels, while in BEAS 2b there is an increase in pSTAT1 and pSTAT2 levels with NS1 expression. An increase in active STAT is typically associated with an increase in ISG expression (Schneider et al., 2014), while this thesis has shown that RSV NS1 expression increase pSTAT levels but reduces ISG mRNA production. Equally puzzling was the consistency of total STAT levels, previous studies have shown that NS1 reduces levels of STAT2 either through direct ubiquitination and proteasomal degradation (Elliott et al., 2007) or by increasing SOCS1 levels, which in turn lead to the degradation of STAT2 (Xu et al., 2014b). This increase in pSTAT alongside the reduced ISG output suggested that within the BEAS 2b epithelial cell line the NS1 protein was targeting other aspects of the pathway. The primary site of RSV infection is the epithelial cells of the upper respiratory tract. Studies using epithelial cells from disparate sites offer insight, but as we have shown, the impact of RSV NS proteins varies significantly depending on the cell line used.

RSV has been shown to have different infection patterns in A549 and BEAS 2b cells, with A549 cells producing more cytokines and being more permissive to infections, while BEAS 2b cells have a more robust ISG response and are more able to restrict viral replications (Hillyer et al., 2018). The source of these observations may be a result of the effect of the NS proteins on IFN signalling; our results found that while RSV NS reduced ISG expression in both A549 and BEAS 2b cells the levels of STAT activation were different between the cell lines, and SOCS expression was only increased in A549 on expression of NS1 while SOCS1 was unaffected in BEAS 2b cells. The ultimate result of NS1 expression was the same in both A549 and BEAS 2b with reduction of the ISGs mRNA measured, but there was no consistent mechanism observed between the two cell lines. By attenuating the JAK-STAT pathway the NS1 protein reduces the cells responsiveness to IFN, reducing the production of antiviral genes and allowing enhanced viral replication. This effect highlights the need to study RSV NS1 in physiologically relevant human cell types to identify their primary mechanism of action. Previous studies

into the NS proteins have often used HEK293T cells as these have a high transfection efficacy, but the mechanisms found in HEK293T do not appear to be consistent with cell lines derived from the respiratory epithelium.

6.1.4 RSV NS1 disrupts nuclear translocation of STAT1 and STAT2

As the STAT complexes are around 230 kDa they must be actively trafficked into the nucleus by importins in order to impact gene expression (Miyamoto et al., 2016). Other viruses are known to impact nuclear trafficking, but this effect has not been reported previously in RSV (Chiang and Liu, 2018). The VP24 protein produced by the Ebola virus blocks importin- α by binding its $\alpha 5$ and $\alpha 6$ subunits (Xu et al., 2014a); HBV has been shown to restrict pSTAT entry to the nucleus through its p22 protein (Mitra et al., 2019), and the c protein of hPIV-1 sequesters STAT1 to inhibit STAT translocation (Schomacker et al., 2012). To investigate if RSV used a similar mechanism NS1 was expressed in BEAS 2b cells and the subcellular location of STAT1 and STAT2 was quantified by confocal microscopy. On expression of the RSV NS1 protein there was significantly less STAT1 located in the nucleus after IFN α treatment. This aligns with previous observations that NS1 expression reduced ISG production in spite of an increase in pSTAT1 – in short, NS1 does not disrupt phosphorylation of STAT1 but does prevent it from entering the nucleus. This effect could be caused through NS1 directly ubiquitinating importin- α or its subunits, through its SOCS box domains, or by NS1 directly interacting with the importins to inhibit their function, similar to the Ebola VP24 mechanism (Xu et al., 2014a). Interestingly, NS1 has a different effect on STAT2; while there was no significant reduction of STAT2 in the nucleus after IFN α treatment, there was an accumulation of STAT2 directly adjacent to the nucleus, similar to the effect of hPIV-1 C protein, which sequesters STAT1 in the perinuclear region (Schomacker et al., 2012).

The accumulation of pSTAT in BEAS 2b cells led to our hypothesis that the NS1 protein was blocking normal translocation of the STAT proteins into the nucleus, thus preventing the action of the nuclear protein tyrosine kinases which dephosphorylate the STATs. The STAT proteins are able to go through multiple rounds of activation and inactivation, with phosphate groups added by JAKs on receptor activation and the phosphate groups removed in the nucleus by nuclear resident protein tyrosine kinases allowing the STAT to be returned to the cytoplasm (ten Hoeve et al., 2002).

6.1.5 Implications of RSV infection of immune cells

RSV has a significant impact on the normal signalling in epithelial cells, limiting their ability to mount an effective antiviral response. While the respiratory epithelial cells are the main cell type infected by RSV, immune cells localise to the area which puts them at risk of infection. To date there has been some evidence that RSV is able to infect immune cells including DC (Tognarelli et al., 2019), macrophages (de Souza et al., 2019) and neonatal B regulatory cells (Zhivaki et al., 2017). To investigate the potential of RSV infection of a range of PBMCs, and consider if exposure to RSV had any impact on the cell's response to IFN α , PBMCs from healthy adults were incubated with RSV and stimulated with IFN α . In the PBMC populations investigated exposure to RSV led to low levels of infection, with DCs showing the highest levels of infection. As DCs are a phagocytic cell type it's possible as infected cell die they are phagocytosed by DCs; thus, increasing the levels of GFP fluoresce in the DC population, rather than DCs being more susceptible to infection. In lymphocytes exposure to RSV was associated with a decreased sensitivity to IFN α , with lower levels of STAT1 and STAT3 phosphorylation. The impact of altered signalling in T cells by RSV may influence their ability to control infection as the STAT proteins are involved in T cell polarisation (Seif et al., 2017). Specifically, STAT1 is necessary for IFN- γ expression which drives Th1 polarisation, removing STAT1 from T cells would lead to an increase in T cells polarising to Th2 or Th17 which do not rely on STAT1 controlled cytokines (Seif et al., 2017).

In all cell types studied we found an increase in total STAT1 levels after incubation with RSV – STAT1 itself can be regarded as an ISG as it contains an ISRE region in its distal promoter (Yuasa and Hijikata, 2016). This is at odds with what was seen by confocal microscopy, where the BEAS 2b cells that were infected with RSV-A2-GFP had reduced total STAT1 levels. This suggested that while the population as a whole has increased STAT1 levels, the few cells with active RSV infection have reduced STAT1 expression. This suggests that it is possible for RSV to infect immune cells, and this can impact their function. Unlike in the BEAS 2b epithelial cells the immune cells studied had a reduction in pSTAT1, indicating that a different mechanism is used to reduce signalling in different cell types. In addition, the immune cells were infected with full-length virus, whereas, in the BEAS 2b NS1 and NS2 were expressed using transfection. Transfections allowed for the individual viral proteins to be studied however, it cannot account for the interaction of multiple viral proteins and there is not active RSV replication in these cells. As low numbers of cells appear to be infected, this work could be enhanced by sorting

the GFP+ cells from the population and investigating their function; this would require sorting live cells which we were unable to do in our facility. A larger inoculate could also be used to increase the GFP+ population. Further investigation is necessary to assess if these differences are due to the cell type or experimental design.

6.1.6 The impact of the COVID-19 pandemic on RSV infections

Prior to 2020 RSV followed a predictable seasonal pattern in Ireland, with the RSV cases beginning to rise in October, peaking in January and falling in late February (NVRL, 2022). The cause of this seasonal pattern has been associated with weather conditions (Price et al., 2019), however the restrictions and public health advice surrounding the COVID-19 pandemic has led to unusual patterns of RSV infection (Williams et al., 2021). Many countries have seen low levels of RSV during its typical season when COVID-19 restrictions were in place, followed by a rise in RSV cases as restrictions were lifted regardless of the season. This resulted in high levels of RSV even in the summer months (Agha and Avner, 2021, Eden et al., 2022). This suggests that while meteorological conditions may play a role in the spread of RSV, social interactions, particularly in schools and nurseries, are the key driver of RSV infections. The result of the COVID-19 pandemic altering RSV seasonality reduced the number of samples that could be collected from infants with RSV for this study, but has clearly shown the impact of reducing household contacts, handwashing and mask use to prevent the spread of respiratory viral infections.

6.1.7 Conclusions

RSV is a cause of significant morbidity and mortality in both paediatric, immunocompromised and elderly populations worldwide. Understanding how RSV is able to evade the immune response provides new avenues for the development of therapeutics. There are several RSV vaccine candidates currently progressing through clinical trials; though successful vaccines would limit RSV related disease there are often patients for whom vaccines are less effective, or who are unable to access vaccines. The development of treatments to limit RSV replication will still be necessary to treat severe RSV infection and improve outcomes for patients.

Using physiologically relevant cell lines and primary cells this study set out to show the impact of the RSV NS proteins on the JAK-STAT pathway. We have identified that the

RSV NS proteins have a significant impact on ISG expression in respiratory epithelial cells, independent of SOCS1 and SOCS3 expression. In BEAS 2b cells the expression of RSV NS1 reduces nuclear translocation of STAT1, and restricts the localization of STAT2. This impact on nuclear translocation has not been reported previously in NS1 expressing cells and has a highly significant role in how RSV NS1 can limit ISG expression. The reduction of nuclear translocation of signalling molecules also have the potential to affect other signalling pathways which should be investigated further.

We have also shown that RSV is able to infect circulating immune cells and reduce their response to IFN α . While the primary site of RSV infection is the epithelial cells of the respiratory tract RSV is also able to infect immune cells, altering their response to stimuli. This will likely shape how immune cells respond to the infection, resulting in increased viral replication and more severe infection.

The impact of RSV infections remains significant in the community and improving our understanding of the NS proteins could identify future therapeutic strategies. A summary of the major findings in A549 and BEAS 2b epithelial cells is presented in Figure 6.1.

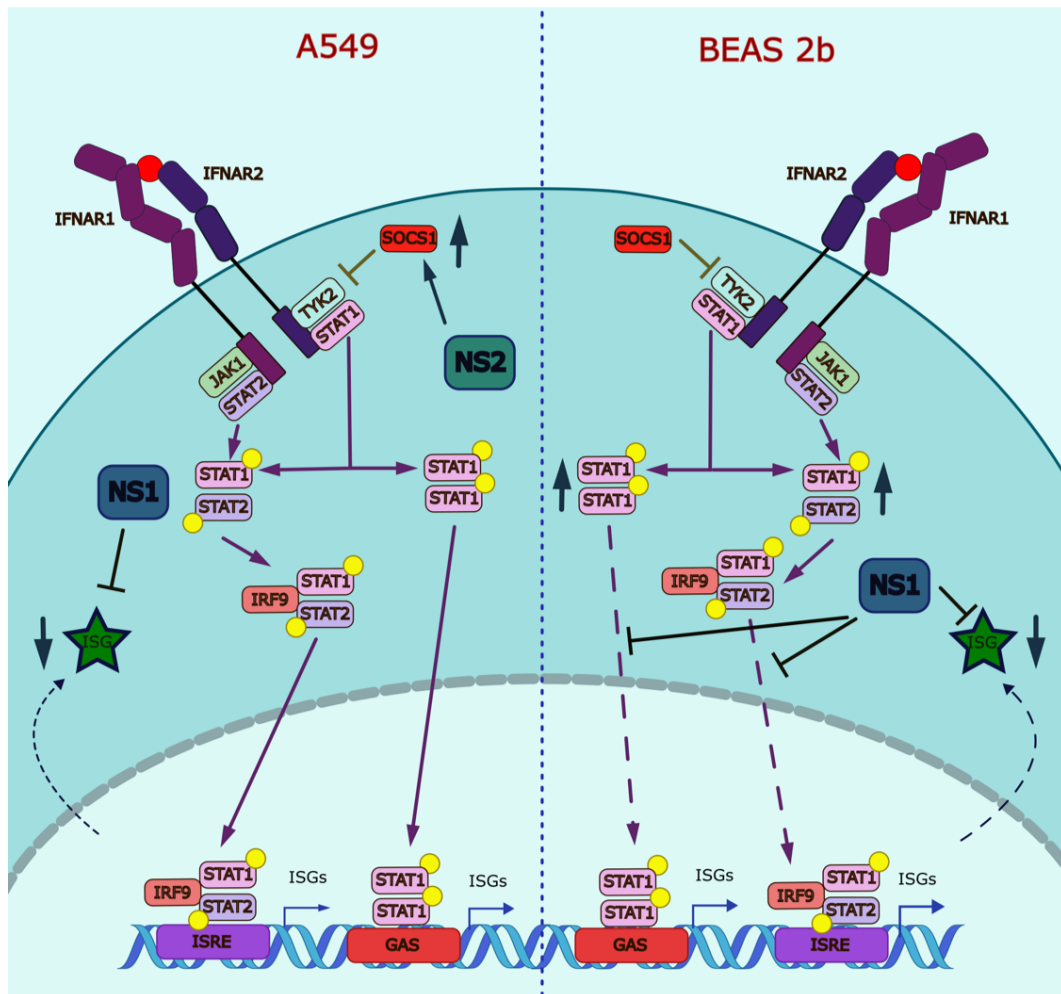


Figure 6.1: Comparison of the NS proteins on the JAK-STAT pathway in A549 and BEAS 2b epithelial cells

Schematic diagram of the effect of RSV NS proteins in A549 and BEAS 2b cells. Expression of NS1 causes the reduction of ISG mRNA expression in both A549 and BEAS 2b. In BEAS 2b there is also an increase in pSTAT levels, and a reduction in translocation of STAT1. A549 cells see an increase in SOCS1 with NS2 expression.

6.2 Future Work

This project has shown that the RSV NS1 protein limits ISG expression and reduces STAT1 nuclear translocation, that circulating immune cells can be infected with RSV and this impacts their ability to respond to IFN α treatment. Our findings have identified new areas that fell beyond the scope of this study but which should be further investigated:

SOCS box domains within NS1 and NS2

Bioinformatic analysis identified possible SOCS box domains within both NS1 and NS2 – by performing point mutations within these domains it could be confirmed if these sites are necessary for our observed NS reduction of ISG expression.

Mechanism for translocation blocking

We have shown the expression of NS1 in BEAS 2b cells reduces nuclear levels of STAT1. However, the mechanism for this has not been investigated. The process of nuclear translocation involves importin- α and importin- β , studying the levels of these and if NS1 is able to complex with them could shed light on the mechanism used to reduce STAT trafficking to the nucleus. As NS1 contains putative E3 ligase motifs it is possible that the importins are targeted for degradation. Equally, NS1 may hijack the importins to prioritise the trafficking of other proteins into the nucleus.

The role of NS1 in lymphocytes

Our study has shown a small number of lymphocytes were infected, and exposure to RSV reduces levels of pSTAT1 and pSTAT3 after IFN α stimulation. Working with a NS1 deletion mutant RSV (Δ NS1-RSV) would allow further dissection of the mechanism. From our work in epithelial cells which showed that the expression of NS1 lead to reduced ISG expression I hypothesise that a Δ NS1-RSV mutant virus would not have an effect on pSTAT1 levels in cells with active RSV infection.

The role of NS1 in primary epithelial cells

We have seen that the cell line impacts the mechanism used by NS1, but we have not assessed the impact of NS1 in primary cells. Using 3D well differentiated epithelial cells culture model at air-liquid-interface (ALI) culture, what is the impact of WT-RSV and a Δ NS1-RSV on IFN signalling in primary cells? Although there can be significant donor variation with primary cells, investigating the function of NS1 in these cells would show if the results seen here are specific to a fully submerged immortalised cell line, or if NS1 has the same effect on primary epithelial cells.

7 References

- AAP 2006. Diagnosis and management of bronchiolitis. *Pediatrics*, 118, 1774-93.
- AAP 2014. Updated guidance for palivizumab prophylaxis among infants and young children at increased risk of hospitalization for respiratory syncytial virus infection. *Pediatrics*, 134, 415-20.
- ABEL, A. M., YANG, C., THAKAR, M. S. & MALARKANNAN, S. 2018. Natural Killer Cells: Development, Maturation, and Clinical Utilization. *Front Immunol*, 9, 1869.
- ABLE, A.A., BURRELL, J.A., STEPHENS, J.M. 2017. STAT5-Interacting Proteins: A Synopsis of Proteins that Regulate STAT5 Activity. *Biology*, 11;6(1):20.
- ACOSTA, P. L., CABALLERO, M. T. & POLACK, F. P. 2015. Brief History and Characterization of Enhanced Respiratory Syncytial Virus Disease. *Clin Vaccine Immunol*, 23, 189-95.
- AGHA, R. & AVNER, J. R. 2021. Delayed Seasonal RSV Surge Observed During the COVID-19
- AIELLO, A., FARZANEH, F., CANDORE, G., CARUSO, C., DAVINELLI, S., GAMBINO, C. M., LIGOTTI, M. E., ZAREIAN, N. & ACCARDI, G. 2019. Immunosenescence and Its Hallmarks: How to Oppose Aging Strategically? A Review of Potential Options for Therapeutic Intervention. *Front Immunol*, 10, 2247.
- AKHTAR, L. N. & BENVENISTE, E. N. 2011. Viral exploitation of host SOCS protein functions. *J Virol*, 85, 1912-21.
- ALANSARI, K., TOAIMAH, F. H., ALMATAR, D. H., EL TATAWY, L. A., DAVIDSON, B. L. & QUSAD, M. I. M. 2019. Monoclonal Antibody Treatment of RSV Bronchiolitis in Young Infants: A Randomized Trial. *Pediatrics*, 143.
- ANDERSON, E. J., CAROSONE-LINK, P., YOGEV, R., YI, J. & SIMOES, E. A. F. 2017. Effectiveness of Palivizumab in High-risk Infants and Children: A Propensity Score Weighted Regression Analysis. *Pediatr Infect Dis J*, 36, 699-704.
- ANDERSON, L. J., DORMITZER, P. R., NOKES, D. J., RAPPUOLI, R., ROCA, A. & GRAHAM, B. S. 2013. Strategic priorities for respiratory syncytial virus (RSV) vaccine development. *Vaccine*, 31 Suppl 2, B209-15.
- ARIMOTO, K. I., MIYAUCHI, S., STONER, S. A., FAN, J. B. & ZHANG, D. E. 2018. Negative regulation of type I IFN signaling. *J Leukoc Biol*.
- ASTRAZENECA. 2022. Nirsevimab EMA regulatory submission accepted under accelerated assessment for RSV protection in all infants [Online]. Available: <https://www.astrazeneca.com/media->

centre/press-releases/2022/nirsevimab-ema-regulatory-submission-accepted-under-accelerated-assessment-for-rsv-protection-in-all-infants.html [Accessed 17/03/2022 2022].

- BABON, J. J., MCMANUS, E. J., YAO, S., DESOUZA, D. P., MIELKE, L. A., SPRIGG, N. S., WILLSON, T. A., HILTON, D. J., NICOLA, N. A., BACA, M., NICHOLSON, S. E. & NORTON, R. S. 2006. The structure of SOCS3 reveals the basis of the extended SH2 domain function and identifies an unstructured insertion that regulates stability. *Mol Cell*, 22, 205-16.
- BABON, J. J. & NICOLA, N. A. 2012. The biology and mechanism of action of suppressor of cytokine signaling 3. *Growth Factors*, 30, 207-19.
- BAKKER, S. E., DUQUERROY, S., GALLOUX, M., LONEY, C., CONNER, E., ELEOUET, J. F., REY, F. A. & BHELLA, D. 2013. The respiratory syncytial virus nucleoprotein-RNA complex forms a left-handed helical nucleocapsid. *J Gen Virol*, 94, 1734-8.
- BAKRE, A., WU, W., HISCOX, J., SPANN, K., TENG, M. N. & TRIPP, R. A. 2015. Human respiratory syncytial virus non-structural protein NS1 modifies miR-24 expression via transforming growth factor-beta. *J Gen Virol*, 96, 3179-91.
- BALEKIAN, D. S., LINNEMANN, R. W., HASEGAWA, K., THADHANI, R. & CAMARGO, C. A., JR. 2017. Cohort Study of Severe Bronchiolitis during Infancy and Risk of Asthma by Age 5 Years. *J Allergy Clin Immunol Pract*, 5, 92-96.
- BARNES, M. V. C., OPENSHAW, P. J. M. & THWAITES, R. S. 2022. Mucosal Immune Responses to Respiratory Syncytial Virus. *Cells*, 11.
- BASTERS, A., GEURINK, P. P., ROCKER, A., WITTING, K. F., TADAYON, R., HESS, S., SEMRAU, M. S., STORICI, P., OVAA, H., KNOBELOCH, K. P. & FRITZ, G. 2017. Structural basis of the specificity of USP18 toward ISG15. *Nat Struct Mol Biol*, 24, 270-278.
- BECKER, Y. 2006. Respiratory syncytial virus (RSV) evades the human adaptive immune system by skewing the Th1/Th2 cytokine balance toward increased levels of Th2 cytokines and IgE, markers of allergy—a review. *Virus Genes*, 33, 235-52.
- BEELER, J. A. & VAN WYKE COELINGH, K. 1989. Neutralization epitopes of the F glycoprotein of respiratory syncytial virus: effect of mutation upon fusion function. *J Virol*, 63, 2941-50.
- BEHERA, A. K., MATSUSE, H., KUMAR, M., KONG, X., LOCKEY, R. F. & MOHAPATRA,

- S. S. 2001. Blocking intercellular adhesion molecule-1 on human epithelial cells decreases respiratory syncytial virus infection. *Biochem Biophys Res Commun*, 280, 188-95.
- BERGERON, H. C. & TRIPP, R. A. 2021. Immunopathology of RSV: An Updated Review. *Viruses*, 13.
- BERNSEN, C. E. & WOLBERGER, C. 2014. New insights into ubiquitin E3 ligase mechanism. *Nature Structural & Molecular Biology*, 21, 301.
- BESNARD, A. G., TOGBE, D., GUILLOU, N., ERARD, F., QUESNIAUX, V. & RYFFEL, B. 2011. IL-33-activated dendritic cells are critical for allergic airway inflammation. *Eur J Immunol*, 41, 1675-86. BERNARD, P., DELCONTE, R., PASTOR, S. et al. 2022. Targeting CISH enhances natural cytotoxicity receptor signaling and reduces NK cell exhaustion to improve solid tumor immunity. *Journal for ImmunoTherapy of Cancer*
- BEUGELING, M., DE ZEE, J., WOERDENBAG, H. J., FRIJLINK, H. W., WILSCHUT, J. C. & HINRICHS, W. L. J. 2019. Respiratory syncytial virus subunit vaccines based on the viral envelope glycoproteins intended for pregnant women and the elderly. *Expert Rev Vaccines*, 18, 935-950.
- BITKO, V., SHULYAYEVA, O., MAZUMDER, B., MUSIYENKO, A., RAMASWAMY, M., LOOK, D. C. & BARIK, S. 2007. Nonstructural proteins of respiratory syncytial virus suppress premature apoptosis by an NF-kappaB-dependent, interferon-independent mechanism and facilitate virus growth. *J Virol*, 81, 1786-95.
- BOSSERT, B. & CONZELMANN, K. K. 2002. Respiratory syncytial virus (RSV) nonstructural (NS) proteins as host range determinants: a chimeric bovine RSV with NS genes from human RSV is attenuated in interferon-competent bovine cells. *J Virol*, 76, 4287-93.
- BOSSERT, B., MAROZIN, S. & CONZELMANN, K. K. 2003. Nonstructural proteins NS1 and NS2 of bovine respiratory syncytial virus block activation of interferon regulatory factor 3. *J Virol*, 77, 8661-8.
- BOYAPALLE, S., WONG, T., GARAY, J., TENG, M., SAN JUAN-VERGARA, H., MOHAPATRA, S. & MOHAPATRA, S. 2012. Respiratory syncytial virus NS1 protein colocalizes with mitochondrial antiviral signaling protein MAVS following infection. *PLoS One*, 7, e29386.
- BOYOGLU-BARNUM, S., CHIRKOVA, T., TODD, S. O., BARNUM, T. R., GASTON, K. A., JORQUERA, P., HAYNES, L. M., TRIPP, R. A., MOORE, M. L. & ANDERSON, L.

- J. 2014. Prophylaxis with a respiratory syncytial virus (RSV) anti-G protein monoclonal antibody shifts the adaptive immune response to RSV rA2-line19F infection from Th2 to Th1 in BALB/c mice. *J Virol*, 88, 10569-83.
- BRISSE, M. & LY, H. 2019. Comparative Structure and Function Analysis of the RIG-I-Like Receptors: RIG-I and MDA5. *Front Immunol*, 10, 1586.
- BROBERG, E. K., WARIS, M., JOHANSEN, K., SNACKEN, R., PENTTINEN, P. & EUROPEAN INFLUENZA SURVEILLANCE, N. 2018. Seasonality and geographical spread of respiratory syncytial virus epidemics in 15 European countries, 2010 to 2016. *Euro Surveill*, 23.
- BROGGI, A., GRANUCCI, F. & ZANONI, I. 2020. Type III interferons: Balancing tissue tolerance and resistance to pathogen invasion. *J Exp Med*, 217.
- BUKREYEV, A., YANG, L. & COLLINS, P. L. 2012. The secreted G protein of human respiratory syncytial virus antagonizes antibody-mediated restriction of replication involving macrophages and complement. *J Virol*, 86, 10880-4.
- BULATOV, E. & CIULLI, A. 2015. Targeting Cullin-RING E3 ubiquitin ligases for drug discovery: structure, assembly and small-molecule modulation. *Biochem J*, 467, 365-86.
- CAI, W. & YANG, H. 2016. The structure and regulation of Cullin 2 based E3 ubiquitin ligases and their biological functions. *Cell Div*, 11, 7.
- CALIFANO, D., FURUYA, Y., ROBERTS, S., AVRAM, D., MCKENZIE, A. N. J. & METZGER, D. W. 2018. IFN-gamma increases susceptibility to influenza A infection through suppression of group II innate lymphoid cells. *Mucosal Immunol*, 11, 209-219.
- CAO, D., GAO, Y. & LIANG, B. 2021. Structural Insights into the Respiratory Syncytial Virus RNA Synthesis Complexes. *Viruses*, 13.
- CESPEDES, P. F., BUENO, S. M., RAMIREZ, B. A., GOMEZ, R. S., RIQUELME, S. A., PALAVECINO, C. E., MACKERN-OBERTI, J. P., MORA, J. E., DEPOIL, D., SACRISTAN, C., CAMMER, M., CRENEGUY, A., NGUYEN, T. H., RIEDEL, C. A., DUSTIN, M. L. & KALERGIS, A. M. 2014. Surface expression of the hRSV nucleoprotein impairs immunological synapse formation with T cells. *Proc Natl Acad Sci U S A*, 111, E3214-23.
- CHANOCK, R., ROIZMAN, B. & MYERS, R. 1957. Recovery from infants with respiratory illness of a virus related to chimpanzee coryza agent (CCA). I. Isolation, properties and characterization. *Am J Hyg*, 66, 281-90.

- CHAPLIN, D. D. 2010. Overview of the immune response. *J Allergy Clin Immunol*, 125, S3-23.
- CHATTERJEE, S., LUTHRA, P., ESAULOVA, E., AGAPOV, E., YEN, B. C., BOREK, D. M., EDWARDS, M. R., MITTAL, A., JORDAN, D. S., RAMANAN, P., MOORE, M. L., PAPPU, R. V., HOLTZMAN, M. J., ARTYOMOV, M. N., BASLER, C. F., AMARASINGHE, G. K. & LEUNG, D. W. 2017. Structural basis for human respiratory syncytial virus NS1-mediated modulation of host responses. *Nat Microbiol*, 2, 17101.
- CHENG, C. Y., GILSON, T., DALLAIRE, F., KETNER, G., BRANTON, P. E. & BLANCHETTE, P. 2011. The E4orf6/E1B55K E3 ubiquitin ligase complexes of human adenoviruses exhibit heterogeneity in composition and substrate specificity. *J Virol*, 85, 765-75.
- CHENNA, R., SUGAWARA, H., KOIKE, T., LOPEZ, R., GIBSON, T. J., HIGGINS, D. G. & THOMPSON, J. D. 2003. Multiple sequence alignment with the Clustal series of programs. *Nucleic Acids Res*, 31, 3497-500.
- CHEON, H. & STARK, G. R. 2009. Unphosphorylated STAT1 prolongs the expression of interferon-induced immune regulatory genes. *Proc Natl Acad Sci U S A*, 106, 9373-8.
- CHIANG, H. S. & LIU, H. M. 2018. The Molecular Basis of Viral Inhibition of IRF- and STAT-Dependent Immune Responses. *Front Immunol*, 9, 3086.
- CHIRKOVA, T., BOYOGLU-BARNUM, S., GASTON, K. A., MALIK, F. M., TRAU, S. P., OOMENS, A. G. & ANDERSON, L. J. 2013. Respiratory syncytial virus G protein CX3C motif impairs human airway epithelial and immune cell responses. *J Virol*, 87, 13466-79.
- CHIRKOVA, T., LIN, S., OOMENS, A. G. P., GASTON, K. A., BOYOGLU-BARNUM, S., MENG, J., STOBART, C. C., COTTON, C. U., HARTERT, T. V., MOORE, M. L., ZIADY, A. G. & ANDERSON, L. J. 2015. CX3CR1 is an important surface molecule for respiratory syncytial virus infection in human airway epithelial cells. *J Gen Virol*, 96, 2543-2556.
- CHOI, E. J., LEE, C. H. & SHIN, O. S. 2015a. Suppressor of Cytokine Signaling 3 Expression Induced by Varicella-Zoster Virus Infection Results in the Modulation of Virus Replication. *Scandinavian Journal of Immunology*, 82, 337-344.
- CHOI, U. Y., KANG, J. S., HWANG, Y. S. & KIM, Y. J. 2015b. Oligoadenylate synthase-like (OASL) proteins: dual functions and associations with diseases. *Exp Mol Med*, 47,

e144.

- CHU, H. Y., TIELSCH, J., KATZ, J., MAGARET, A. S., KHATRY, S., LECLERQ, S. C., SHRESTHA, L., KUYPERS, J., STEINHOFF, M. C. & ENGLUND, J. A. 2017. Transplacental transfer of maternal respiratory syncytial virus (RSV) antibody and protection against RSV disease in infants in rural Nepal. *J Clin Virol*, 95, 90-95.
- COLLINS, A. S., AHMED, S., NAPOLETANO, S., SCHROEDER, M., JOHNSTON, J. A., HEGARTY, J. E., O'FARRELLY, C. & STEVENSON, N. J. 2014. Hepatitis C virus (HCV)-induced suppressor of cytokine signaling (SOCS) 3 regulates proinflammatory TNF-alpha responses. *J Leukoc Biol*, 96, 255-63.
- COLLINS, P. L. & GRAHAM, B. S. 2008. Viral and host factors in human respiratory syncytial virus pathogenesis. *J Virol*, 82, 2040-55.
- CONTICELLO, S. G., HARRIS, R. S. & NEUBERGER, M. S. 2003. The Vif protein of HIV triggers degradation of the human antiretroviral DNA deaminase APOBEC3G. *Curr Biol*, 13, 2009-13.
- CONVERY, O., GARGAN, S., KICKHAM, M., SCHROEDER, M., O'FARRELLY, C. & STEVENSON, N. J. 2019. The hepatitis C virus (HCV) protein, p7, suppresses inflammatory responses to tumor necrosis factor (TNF)-alpha via signal transducer and activator of transcription (STAT)3 and extracellular signal-regulated kinase (ERK)-mediated induction of suppressor of cytokine signaling (SOCS)3. *FASEB J*, 33, 8732-8744.
- CRAMERI, M., BAUER, M., CADUFF, N., WALKER, R., STEINER, F., FRANZOSO, F. D., GUJER, C., BOUCKE, K., KUCERA, T., ZBINDEN, A., MUNZ, C., FRAEFEL, C., GREBER, U. F. & PAVLOVIC, J. 2018. MxB is an interferon-induced restriction factor of human herpesviruses. *Nat Commun*, 9, 1980.
- CROKER, B. A., KIU, H. & NICHOLSON, S. E. 2008. SOCS regulation of the JAK/STAT signalling pathway. *Semin Cell Dev Biol*, 19, 414-22.
- CSUMITA, M., CSERMELY, A., HORVATH, A., NAGY, G., MONORI, F., GOCZI, L., ORBEA, H. A., REITH, W. & SZELES, L. 2020. Specific enhancer selection by IRF3, IRF5 and IRF9 is determined by ISRE half-sites, 5' and 3' flanking bases, collaborating transcription factors and the chromatin environment in a combinatorial fashion. *Nucleic Acids Res*, 48, 589-604.
- CULLEY, F.J., PENNYCOOK, A.M., TREGONING, J.S., DODD, J.S., WALZL, G., WELLS, T.N., HUSSELL, T., OPENSHAW, P.J. 2006. Role of CCL5 (RANTES) in viral lung

- disease. *J Virol*, 80(16):8151-7.
- D'CUNHA, J., RAMANUJAM, S., WAGNER, R. J., WITT, P. L., KNIGHT, E., JR. & BORDEN, E. C. 1996. In vitro and in vivo secretion of human ISG15, an IFN-induced immunomodulatory cytokine. *J Immunol*, 157, 4100-8.
- DAR, A. C., DEVER, T. E. & SICHERI, F. 2005. Higher-order substrate recognition of eIF2alpha by the RNA-dependent protein kinase PKR. *Cell*, 122, 887-900.
- DAVID, M., CHEN, H. E., GOELZ, S., LARNER, A. C. & NEEL, B. G. 1995. Differential regulation of the alpha/beta interferon-stimulated Jak/Stat pathway by the SH2 domain-containing tyrosine phosphatase SHPTP1. *Mol Cell Biol*, 15, 7050-8.
- DE SOUZA, G. F., MURARO, S. P., SANTOS, L. D., MONTEIRO, A. P. T., DA SILVA, A. G., DE SOUZA, A. P. D., STEIN, R. T., BOZZA, P. T. & PORTO, B. N. 2019. Macrophage migration inhibitory factor (MIF) controls cytokine release during respiratory syncytial virus infection in macrophages. *Inflamm Res*, 68, 481-491.
- DE WEERD, N. A. & NGUYEN, T. 2012. The interferons and their receptors—distribution and regulation. *Immunol Cell Biol*, 90, 483-91.
- DELGADO, M. F., COVIELLO, S., MONSALVO, A. C., MELENDI, G. A., HERNANDEZ, J. Z., BATALLE, J. P., DIAZ, L., TRENTO, A., CHANG, H. Y., MITZNER, W., RAVETCH, J., MELERO, J. A., IRUSTA, P. M. & POLACK, F. P. 2009. Lack of antibody affinity maturation due to poor Toll-like receptor stimulation leads to enhanced respiratory syncytial virus disease. *Nat Med*, 15, 34-41.
- DENG, Y., HERBERT, J. A., ROBINSON, E., REN, L., SMYTH, R. L. & SMITH, C. M. 2020. Neutrophil-Airway Epithelial Interactions Result in Increased Epithelial Damage and Viral Clearance during Respiratory Syncytial Virus Infection. *J Virol*, 94.
- DESHPANDE, S. A. & NORTHERN, V. 2003. The clinical and health economic burden of respiratory syncytial virus disease among children under 2 years of age in a defined geographical area. *Arch Dis Child*, 88, 1065-9.
- DESMYTER, J., MELNICK, J. L. & RAWLS, W. E. 1968. Defectiveness of interferon production and of rubella virus interference in a line of African green monkey kidney cells (Vero). *J Virol*, 2, 955-61.
- DEY, M., CAO, C., DAR, A. C., TAMURA, T., OZATO, K., SICHERI, F. & DEVER, T. E. 2005. Mechanistic link between PKR dimerization, autophosphorylation, and eIF2alpha

substrate recognition. *Cell*, 122, 901-13.

- DONALISIO, M., RUSNATI, M., CAGNO, V., CIVRA, A., BUGATTI, A., GIULIANI, A., PIRRI, G., VOLANTE, M., PAPOTTI, M., LANDOLFO, S. & LEMBO, D. 2012. Inhibition of human respiratory syncytial virus infectivity by a dendrimeric heparan sulfate-binding peptide. *Antimicrob Agents Chemother*, 56, 5278-88.
- DREOS, R., AMBROSINI, G., PERIER, R. C. & BUCHER, P. 2015. The Eukaryotic Promoter Database: expansion of EPDnew and new promoter analysis tools. *Nucleic Acids Res*, 43, D92-6.
- DUSTER, M., BECKER, M., GNIRCK, A. C., WUNDERLICH, M., PANZER, U. & TURNER, J. E. 2018. T cell-derived IFN-gamma downregulates protective group 2 innate lymphoid cells in murine lupus erythematosus. *Eur J Immunol*, 48, 1364-1375.
- EDEN, J. S., SIKAZWE, C., XIE, R., DENG, Y. M., SULLIVAN, S. G., MICHIE, A., LEVY, A., CUTMORE, E., BLYTH, C. C., BRITTON, P. N., CRAWFORD, N., DONG, X., DWYER, D. E., EDWARDS, K. M., HORSBURGH, B. A., FOLEY, D., KENNEDY, K., MINNEY-SMITH, C., SPEERS, D., TULLOCH, R. L., HOLMES, E. C., DHANASEKARAN, V., SMITH, D. W., KOK, J., BARR, I. G. & AUSTRALIAN, R. S. V. S. G. 2022. Off-season RSV epidemics in Australia after easing of COVID-19 restrictions. *Nat Commun*, 13, 2884.
- EGAN, P. J., LAWLOR, K. E., ALEXANDER, W. S. & WICKS, I. P. 2003. Suppressor of cytokine signaling-1 regulates acute inflammatory arthritis and T cell activation. *J Clin Invest*, 111, 915-24.
- EILAND, L. S. 2009. Respiratory syncytial virus: diagnosis, treatment and prevention. *J Pediatr Pharmacol Ther*, 14, 75-85.
- ELHASSAN, N. O., SORBERO, M. E. S., HALL, C. B., STEVENS, T. P. & DICK, A. W. 2006. Cost-effectiveness Analysis of Palivizumab in Premature Infants Without Chronic Lung Disease. *JAMA Pediatrics*, 160, 1070-1076.
- ELLIOTT, J., LYNCH, O. T., SUESSMUTH, Y., QIAN, P., BOYD, C. R., BURROWS, J. F., BUICK, R., STEVENSON, N. J., TOUZELET, O., GADINA, M., POWER, U. F. & JOHNSTON, J. A. 2007. Respiratory syncytial virus NS1 protein degrades STAT2 by using the Elongin-Cullin E3 ligase. *J Virol*, 81, 3428-36.
- ENGLAND, P. H. 2016. Infection control precautions to minimise transmission of acute respiratory tract infections in healthcare settings.

- EVERARD, M. L., SWARBRICK, A., WRIGHTHAM, M., MCINTYRE, J., DUNKLEY, C., JAMES, P. D., SEWELL, H. F. & MILNER, A. D. 1994. Analysis of cells obtained by bronchial lavage of infants with respiratory syncytial virus infection. *Arch Dis Child*, 71, 428-32.
- FALSEY, A. R. 2007. Respiratory syncytial virus infection in adults. *Semin Respir Crit Care Med*, 28, 171-81.
- FARRAR, J. D., ASNAGLI, H. & MURPHY, K. M. 2002. T helper subset development: roles of instruction, selection, and transcription. *J Clin Invest*, 109, 431-5.
- FAUROUX, B., SIMOES, E. A. F., CHECCHIA, P. A., PAES, B., FIGUERAS-ALOY, J., MANZONI, P., BONT, L. & CARBONELL-ESTRANY, X. 2017. The Burden and Long-term Respiratory Morbidity Associated with Respiratory Syncytial Virus Infection in Early Childhood. *Infect Dis Ther*, 6, 173-197.
- FILIPI, M. & JACK, S. 2020. Interferons in the Treatment of Multiple Sclerosis: A Clinical Efficacy, Safety, and Tolerability Update. *Int J MS Care*, 22, 165-172.
- FISHILEVICH, S., NUDEL, R., RAPPAPORT, N., HADAR, R., PLASCHKES, I., STEIN, T., ROSEN, N., Kohn, A., TWIK, M., SAFRAN, M., LANCET, D., COHEN, D. 2017. GeneHancer: genome-wide integration of enhancers and target genes in GeneCards Database.
- FRANCOIS-NEWTON, V., MAGNO DE FREITAS ALMEIDA, G., PAYELLE-BROGARD, B., MONNERON, D., PICHARD-GARCIA, L., PIEHLER, J., PELLEGRINI, S. & UZE, G. 2011. USP18-based negative feedback control is induced by type I and type III interferons and specifically inactivates interferon alpha response. *PLoS One*, 6, e22200.
- FUENTES, S., TRAN, K. C., LUTHRA, P., TENG, M. N. & HE, B. 2007. Function of the respiratory syncytial virus small hydrophobic protein. *J Virol*, 81, 8361-6.
- FULOP, T., WITKOWSKI, J. M., LE PAGE, A., FORTIN, C., PAWELEC, G. & LARBI, A. 2017. Intracellular signalling pathways: targets to reverse immunosenescence. *Clin Exp Immunol*, 187, 35-43.
- FUNCHAL, G. A., JAEGER, N., CZEPIELEWSKI, R. S., MACHADO, M. S., MURARO, S. P., STEIN, R. T., BONORINO, C. B. C. & PORTO, B. N. 2015. Respiratory syncytial virus fusion protein promotes TLR-4-dependent neutrophil extracellular trap formation by human neutrophils. *PloS one*, 10, e0124082-e0124082.

- GADOMSKI, A. M. & BROWER, M. 2010. Bronchodilators for bronchiolitis. *Cochrane Database Syst Rev*, CD001266.
- GAL-BEN-ARI, S., BARRERA, I., EHRLICH, M. & ROSENBLUM, K. 2018. PKR: A Kinase to Remember. *Front Mol Neurosci*, 11, 480.
- GAN, S. W., TAN, E., LIN, X., YU, D., WANG, J., TAN, G. M., VARARATTANAVECH, A., YEO, C. Y., SOON, C. H., SOONG, T. W., PERVUSHIN, K. & TORRES, J. 2012. The small hydrophobic protein of the human respiratory syncytial virus forms pentameric ion channels. *J Biol Chem*, 287, 24671-89.
- GAO, S., VON DER MALSBURG, A., PAESCHKE, S., BEHLKE, J., HALLER, O., KOCHS, G. & DAUMKE, O. 2010. Structural basis of oligomerization in the stalk region of dynamin-like MxA. *Nature*, 465, 502-6.
- GARGAN, S., AHMED, S., MAHONY, R., BANNAN, C., NAPOLETANO, S., O'FARRELLY, C., BORROW, P., BERGIN, C. & STEVENSON, N. J. 2018. HIV-1 Promotes the Degradation of Components of the Type 1 IFN JAK/STAT Pathway and Blocks Anti-viral ISG Induction. *EBioMedicine*, 30, 203-216.
- GERN, J. E., BROOKS, G. D., MEYER, P., CHANG, A., SHEN, K., EVANS, M. D., TISLER, C., DASILVA, D., ROBERG, K. A., MIKUS, L. D., ROSENTHAL, L. A., KIRK, C. J., SHULT, P. A., BHATTACHARYA, A., LI, Z., GANGNON, R. & LEMANSKE, R. F., JR. 2006. Bidirectional interactions between viral respiratory illnesses and cytokine responses in the first year of life. *J Allergy Clin Immunol*, 117, 72-8.
- GIANNAKOPOULOS, N. V., LUO, J. K., PAPOV, V., ZOU, W., LENSCHOW, D. J., JACOBS, B. S., BORDEN, E. C., LI, J., VIRGIN, H. W. & ZHANG, D. E. 2005. Proteomic identification of proteins conjugated to ISG15 in mouse and human cells. *Biochem Biophys Res Commun*, 336, 496-506.
- GIARD, D. J., AARONSON, S. A., TODARO, G. J., ARNSTEIN, P., KERSEY, J. H., DOSIK, H. & PARKS, W. P. 1973. In vitro cultivation of human tumors: establishment of cell lines derived from a series of solid tumors. *J Natl Cancer Inst*, 51, 1417-23.
- GIBBERT, K., SCHLAAK, J. F., YANG, D. & DITTMER, U. 2013. IFN-alpha subtypes: distinct biological activities in anti-viral therapy. *Br J Pharmacol*, 168, 1048-58.
- GINALDI, L., LORETO, M. F., CORSI, M. P., MODESTI, M. & DE MARTINIS, M. 2001. Immunosenescence and infectious diseases. *Microbes Infect*, 3, 851-7.

- GOLDSZMID, R. S., CASPAR, P., RIVOLLIER, A., WHITE, S., DZUTSEV, A., HIENY, S., KELSALL, B., TRINCHIERI, G. & SHER, A. 2012. NK cell-derived interferon-gamma orchestrates cellular dynamics and the differentiation of monocytes into dendritic cells at the site of infection. *Immunity*, 36, 1047-59.
- GONZALEZ, A. E., LAY, M. K., JARA, E. L., ESPINOZA, J. A., GOMEZ, R. S., SOTO, J., RIVERA, C. A., ABARCA, K., BUENO, S. M., RIEDEL, C. A. & KALERGIS, A. M. 2017. Aberrant T cell immunity triggered by human Respiratory Syncytial Virus and human Metapneumovirus infection. *Virulence*, 8, 685-704.
- GONZALEZ, P. A., BUENO, S. M., CARRENO, L. J., RIEDEL, C. A. & KALERGIS, A. M. 2012. Respiratory syncytial virus infection and immunity. *Rev Med Virol*, 22, 230-44.
- GONZALEZ, P. A., PRADO, C. E., LEIVA, E. D., CARRENO, L. J., BUENO, S. M., RIEDEL, C. A. & KALERGIS, A. M. 2008. Respiratory syncytial virus impairs T cell activation by preventing synapse assembly with dendritic cells. *Proc Natl Acad Sci U S A*, 105, 14999-5004.
- GRAHAM, F. L., SMILEY, J., RUSSELL, W. C. & NAIRN, R. 1977. Characteristics of a human cell line transformed by DNA from human adenovirus type 5. *J Gen Virol*, 36, 59-74.
- GREEN, D. S., YOUNG, H. A. & VALENCIA, J. C. 2017. Current prospects of type II interferon gamma signaling and autoimmunity. *J Biol Chem*, 292, 13925-13933.
- GRIFFIN, M. P., YUAN, Y., TAKAS, T., DOMACHOWSKIE, J. B., MADHI, S. A., MANZONI, P., SIMOES, E. A. F., ESSER, M. T., KHAN, A. A., DUBOVSKY, F., VILLAFANA, T., DEVINCENZO, J. P. & NIRSEVIMAB STUDY, G. 2020. Single-Dose Nirsevimab for Prevention of RSV in Preterm Infants. *N Engl J Med*, 383, 415-425.
- GRIFFITHS, C., DREWS, S. J. & MARCHANT, D. J. 2017. Respiratory Syncytial Virus: Infection, Detection, and New Options for Prevention and Treatment. *Clin Microbiol Rev*, 30, 277-319.
- GROOTHUIS, J. R., SIMOES, E. A., LEVIN, M. J., HALL, C. B., LONG, C. E., RODRIGUEZ, W. J., ARROBIO, J., MEISSNER, H. C., FULTON, D. R., WELLIVER, R. C. & ET AL. 1993. Prophylactic administration of respiratory syncytial virus immune globulin to high-risk infants and young children. The Respiratory Syncytial Virus Immune Globulin Study Group. *N Engl J Med*, 329, 1524-30.

- GUO, N. & PENG, Z. 2013. MG132, a proteasome inhibitor, induces apoptosis in tumor cells. *Asia Pac J Clin Oncol*, 9, 6-11.
- HAGBERG, N., BERGGREN, O., LEONARD, D., WEBER, G., BRYCESON, Y. T., ALM, G. V., ELORANTA, M. L. & RONNBLOM, L. 2011. IFN-alpha production by plasmacytoid dendritic cells stimulated with RNA-containing immune complexes is promoted by NK cells via MIP-1beta and LFA-1. *J Immunol*, 186, 5085-94.
- HAGLUND, K. & DIKIC, I. 2005. Ubiquitylation and cell signaling. *EMBO J*, 24, 3353-9.
- HALLER, O. & KOCHS, G. 2011. Human MxA protein: an interferon-induced dynamin-like GTPase with broad antiviral activity. *J Interferon Cytokine Res*, 31, 79-87.
- HAMMITT, L. L., DAGAN, R., YUAN, Y., BACA COTS, M., BOSHEVA, M., MADHI, S. A., MULLER, W. J., ZAR, H. J., BROOKS, D., GRENHAM, A., WAHLBY HAMREN, U., MANKAD, V. S., REN, P., TAKAS, T., ABRAM, M. E., LEACH, A., GRIFFIN, M. P., VILLAFANA, T. & GROUP, M. S. 2022. Nirsevimab for Prevention of RSV in Healthy Late-Preterm and Term Infants. *N Engl J Med*, 386, 837-846.
- HASHIMOTO, K. & HOSOYA, M. 2017. Neutralizing epitopes of RSV and palivizumab resistance in Japan. *Fukushima J Med Sci*, 63, 127-134.
- HASHIMOTO, K., ISHIBASHI, K., ISHIOKA, K., ZHAO, D., SATO, M., OHARA, S., ABE, Y., KAWASAKI, Y., SATO, Y., YOKOTA, S., FUJII, N., PEEBLES, R. S., JR., HOSOYA, M. & SUZUTANI, T. 2009. RSV replication is attenuated by counteracting expression of the suppressor of cytokine signaling (SOCS) molecules. *Virology*, 391, 162-70.
- HASTIE, M. L., HEADLAM, M. J., PATEL, N. B., BUKREYEV, A. A., BUCHHOLZ, U. J., DAVE, K. A., NORRIS, E. L., WRIGHT, C. L., SPANN, K. M., COLLINS, P. L. & GORMAN, J. J. 2012. The human respiratory syncytial virus nonstructural protein 1 regulates type I and type II interferon pathways. *Mol Cell Proteomics*, 11, 108-27.
- HENDERSON, J., HILLIARD, T. N., SHERRIFF, A., STALKER, D., AL SHAMMARI, N. & THOMAS, H. M. 2005. Hospitalization for RSV bronchiolitis before 12 months of age and subsequent asthma, atopy and wheeze: a longitudinal birth cohort study. *Pediatr Allergy Immunol*, 16, 386-92.
- HILLYER, P., MANE, V. P., CHEN, A., DOS SANTOS, M. B., SCHRAMM, L. M., SHEPARD, R. E., LUONGO, C., LE NOUEN, C., HUANG, L., YAN, L., BUCHHOLZ, U. J., JUBIN, R. G., COLLINS, P. L. & RABIN, R. L. 2017. Respiratory syncytial virus infection induces a subset of types I and III interferons in human dendritic cells. *Virology*, 504,

63-72.

- HILLYER, P., SHEPARD, R., UEHLING, M., KRENZ, M., SHEIKH, F., THAYER, K. R., HUANG, L., YAN, L., PANDA, D., LUONGO, C., BUCHHOLZ, U. J., COLLINS, P. L., DONNELLY, R. P. & RABIN, R. L. 2018. Differential Responses by Human Respiratory Epithelial Cell Lines to Respiratory Syncytial Virus Reflect Distinct Patterns of Infection Control. *J Virol*, 92.
- HO, H. H. & IVASHKIV, L. B. 2006. Role of STAT3 in type I interferon responses. Negative regulation of STAT1-dependent inflammatory gene activation. *J Biol Chem*, 281, 14111-8.
- HO, J., PELZEL, C., BEGITT, A., MEE, M., ELSHEIKHA, H.M., et al. (2016) STAT2 Is a Pervasive Cytokine Regulator due to Its Inhibition of STAT1 in Multiple Signaling Pathways. *PLOS Biology* 14(10): e2000117.
- HOGAN, A. B., CAMPBELL, P. T., BLYTH, C. C., LIM, F. J., FATHIMA, P., DAVIS, S., MOORE, H. C. & GLASS, K. 2017. Potential impact of a maternal vaccine for RSV: A mathematical modelling study. *Vaccine*, 35, 6172-6179.
- HONG, X. X. & CARMICHAEL, G. G. 2013. Innate immunity in pluripotent human cells: attenuated response to interferon-beta. *J Biol Chem*, 288, 16196-205.
- HONKE, N., SHAABANI, N., ZHANG, D. E., HARDT, C. & LANG, K. S. 2016. Multiple functions of USP18. *Cell Death Dis*, 7, e2444.
- HSPC. 2019. RSV Fact Sheet [Online]. Available: <https://www.hpsc.ie/a-z/respiratory/respiratorysyncytialvirus/factsheet/> [Accessed 08/12/2019 2019].
- IOANNIDIS, I., MCNALLY, B., WILLETTE, M., PEEPLES, M. E., CHAUSSABEL, D., DURBIN, J. E., RAMILO, O., MEJIAS, A. & FLANO, E. 2012. Plasticity and virus specificity of the airway epithelial cell immune response during respiratory virus infection. *J Virol*, 86, 5422-36.
- IVASHKIV, L. B. & DONLIN, L. T. 2014. Regulation of type I interferon responses. *Nat Rev Immunol*, 14, 36-49.
- JANEWAY, C. A., JR. & MEDZHITOV, R. 2002. Innate immune recognition. *Annu Rev Immunol*, 20, 197-216.
- JIN, H., CHENG, X., TRAINA-DORGE, V. L., PARK, H. J., ZHOU, H., SOIKE, K. & KEMBLE, G. 2003. Evaluation of recombinant respiratory syncytial virus gene deletion mu-

- tants in African green monkeys for their potential as live attenuated vaccine candidates. *Vaccine*, 21, 3647-52.
- JIN, H., ZHOU, H., CHENG, X., TANG, R., MUNOZ, M. & NGUYEN, N. 2000. Recombinant respiratory syncytial viruses with deletions in the NS1, NS2, SH, and M2-2 genes are attenuated in vitro and in vivo. *Virology*, 273, 210-8.
- JOHNSON, J. E., GONZALES, R. A., OLSON, S. J., WRIGHT, P. F. & GRAHAM, B. S. 2007. The histopathology of fatal untreated human respiratory syncytial virus infection. *Mod Pathol*, 20, 108-19.
- JOHNSON, P. R. & COLLINS, P. L. 1988. The fusion glycoproteins of human respiratory syncytial virus of subgroups A and B: sequence conservation provides a structural basis for antigenic relatedness. *J Gen Virol*, 69 (Pt 10), 2623-8.
- JOHNSON, P. R., JR., OLMSTED, R. A., PRINCE, G. A., MURPHY, B. R., ALLING, D. W., WALSH, E. E. & COLLINS, P. L. 1987a. Antigenic relatedness between glycoproteins of human respiratory syncytial virus subgroups A and B: evaluation of the contributions of F and G glycoproteins to immunity. *J Virol*, 61, 3163-6.
- JOHNSON, P. R., SPRIGGS, M. K., OLMSTED, R. A. & COLLINS, P. L. 1987b. The G glycoprotein of human respiratory syncytial viruses of subgroups A and B: extensive sequence divergence between antigenically related proteins. *Proc Natl Acad Sci U S A*, 84, 5625-9.
- JOHNSON, S. M., MCNALLY, B. A., IOANNIDIS, I., FLANO, E., TENG, M. N., OOMENS, A. G., WALSH, E. E. & PEEPLES, M. E. 2015. Respiratory Syncytial Virus Uses CX3CR1 as a Receptor on Primary Human Airway Epithelial Cultures. *PLoS Pathog*, 11, e1005318.
- KALINOWSKI, A., GALEN, B. T., UEKI, I. F., SUN, Y., MULENOS, A., OSAFO-ADDO, A., CLARK, B., JOERNS, J., LIU, W., NADEL, J. A., DELA CRUZ, C. S. & KOFF, J. L. 2018. Respiratory syncytial virus activates epidermal growth factor receptor to suppress interferon regulatory factor 1-dependent interferon-lambda and antiviral defense in airway epithelium. *Mucosal Immunol*, 11, 958-967.
- KANE, M., YADAV, S. S., BITZEGEIO, J., KUTLUAY, S. B., ZANG, T., WILSON, S. J., SCHOGGINS, J. W., RICE, C. M., YAMASHITA, M., HATZIOANNOU, T. & BIENIASZ, P. D. 2013. MX2 is an interferon-induced inhibitor of HIV-1 infection. *Nature*, 502, 563-6.

- KARRON, R. A., BUONAGURIO, D. A., GEORGIU, A. F., WHITEHEAD, S. S., ADAMUS, J. E., CLEMENTS-MANN, M. L., HARRIS, D. O., RANDOLPH, V. B., UDEM, S. A., MURPHY, B. R. & SIDHU, M. S. 1997. Respiratory syncytial virus (RSV) SH and G proteins are not essential for viral replication in vitro: clinical evaluation and molecular characterization of a cold-passaged, attenuated RSV subgroup B mutant. *Proc Natl Acad Sci U S A*, 94, 13961-6.
- KATZMANN, D. J., ODORIZZI, G. & EMR, S. D. 2002. Receptor down regulation and multivesicular-body sorting. *Nat Rev Mol Cell Biol*, 3, 893-905.
- KAWAI, T. & AKIRA, S. 2010. The role of pattern-recognition receptors in innate immunity: update on Toll-like receptors. *Nat Immunol*, 11, 373-84. KAWASAKI, T. & KAWAI, T. 2014. Toll-like receptor signaling pathways. *Front Immunol*, 5, 461.
- KE, Y., REDDEL, R. R., GERWIN, B. I., MIYASHITA, M., MCMENAMIN, M., LECHNER, J. F. & HARRIS, C. C. 1988. Human bronchial epithelial cells with integrated SV40 virus T antigen genes retain the ability to undergo squamous differentiation. *Differentiation*, 38, 60-6.
- KEDZIERSKI, L., LINOSSI, E. M., KOLESNIK, T. B., DAY, E. B., BIRD, N. L., KILE, B. T., BELZ, G. T., METCALF, D., NICOLA, N. A., KEDZIERSKA, K. & NICHOLSON, S. E. 2014. Suppressor of cytokine signaling 4 (SOCS4) protects against severe cytokine storm and enhances viral clearance during influenza infection. *PLoS Pathog*, 10, e1004134.
- KEDZIERSKI, L., TATE, M. D., HSU, A. C., KOLESNIK, T. B., LINOSSI, E. M., DAGLEY, L., DONG, Z., FREEMAN, S., INFUSINI, G., STARKEY, M. R., BIRD, N. L., CHATFIELD, S. M., BABON, J. J., HUNTINGTON, N., BELZ, G., WEBB, A., WARK, P. A., NICOLA, N. A., XU, J., KEDZIERSKA, K., HANSBRO, P. M. & NICHOLSON, S. E. 2017. Suppressor of cytokine signaling (SOCS)5 ameliorates influenza infection via inhibition of EGFR signaling. *Elife*, 6.
- KERSHAW, N. J., MURPHY, J. M., LIAU, N. P., VARGHESE, L. N., LAKTYUSHIN, A., WHITLOCK, E. L., LUCET, I. S., NICOLA, N. A. & BABON, J. J. 2013. SOCS3 binds specific receptor-JAK complexes to control cytokine signaling by direct kinase inhibition. *Nat Struct Mol Biol*, 20, 469-76.
- KIM, H. W., CANCHOLA, J. G., BRANDT, C. D., PYLES, G., CHANOCK, R. M., JENSEN, K. & PARROTT, R. H. 1969. Respiratory syncytial virus disease in infants despite prior administration of antigenic inactivated vaccine. *Am J Epidemiol*, 89, 422-34.

- KIRSEBOM, F., MICHALAKI, C., AGUEDA-OYARZABAL, M. & JOHANSSON, C. 2020. Neutrophils do not impact viral load or the peak of disease severity during RSV infection. *Scientific Reports*, 10, 1110.
- KLINKHAMMER, J., SCHNEPF, D., YE, L., SCHWADERLAPP, M., GAD, H. H., HARTMANN, R., GARCIN, D., MAHLAKOIV, T. & STAEHELI, P. 2018. IFN-lambda prevents influenza virus spread from the upper airways to the lungs and limits virus transmission. *Elife*, 7.
- KNAPP, S., YEE, L. J., FRODSHAM, A. J., HENNIG, B. J., HELLIER, S., ZHANG, L., WRIGHT, M., CHIARAMONTE, M., GRAVES, M., THOMAS, H. C., HILL, A. V. & THURSZ, M. R. 2003. Polymorphisms in interferon-induced genes and the outcome of hepatitis C virus infection: roles of MxA, OAS-1 and PKR. *Genes Immun*, 4, 411-9.
- KORANT, B. D., BLOMSTROM, D. C., JONAK, G. J. & KNIGHT, E., JR. 1984. Interferon-induced proteins. Purification and characterization of a 15,000-dalton protein from human and bovine cells induced by interferon. *J Biol Chem*, 259, 14835-9.
- KORSTEN, K., BLANKEN, M. O., BUISTEMAN, B. J. M., NIBBELKE, E. E., NAAKTGEBOREN, C. A., BONT, L. J. & WILDENBEEST, J. G. 2019. RSV hospitalization in infancy increases the risk of current wheeze at age 6 in late preterm born children without atopic predisposition. *Eur J Pediatr*, 178, 455-462.
- KOTELKIN, A., BELYAKOV, I. M., YANG, L., BERZOFSKY, J. A., COLLINS, P. L. & BUKREYEV, A. 2006. The NS2 protein of human respiratory syncytial virus suppresses the cytotoxic T-cell response as a consequence of suppressing the type I interferon response. *J Virol*, 80, 5958-67.
- KREBS, D. L., UREN, R. T., METCALF, D., RAKAR, S., ZHANG, J. G., STARR, R., DE SOUZA, D. P., HANZINIKOLAS, K., EYLES, J., CONNOLLY, L. M., SIMPSON, R. J., NICOLA, N. A., NICHOLSON, S. E., BACA, M., HILTON, D. J. & ALEXANDER, W. S. 2002. SOCS-6 binds to insulin receptor substrate 4, and mice lacking the SOCS-6 gene exhibit mild growth retardation. *Mol Cell Biol*, 22, 4567-78.
- KRISHNAMOORTHY, N., KHARE, A., ORISS, T. B., RAUNDHAL, M., MORSE, C., YARLAGADDA, M., WENZEL, S. E., MOORE, M. L., PEEBLES, R. S., JR., RAY, A. & RAY, P. 2012. Early infection with respiratory syncytial virus impairs regulatory T cell function and increases susceptibility to allergic asthma. *Nat Med*, 18, 1525-30.
- KULKARNI, H., SMITH, C. M., LEE, D. O. H., HIRST, R. A., EASTON, A. J. & O'CALLAGHAN,

- C. 2016. Evidence of Respiratory Syncytial Virus Spread by Aerosol. Time to Revisit Infection Control Strategies? *Am J Respir Crit Care Med*, 194, 308-16.
- KUMAR, H., KAWAI, T. & AKIRA, S. 2011. Pathogen recognition by the innate immune system. *Int Rev Immunol*, 30, 16-34.
- KURT-JONES, E. A., POPOVA, L., KWINN, L., HAYNES, L. M., JONES, L. P., TRIPP, R. A., WALSH, E. E., FREEMAN, M. W., GOLENBOCK, D. T., ANDERSON, L. J. & FINBERG, R. W. 2000. Pattern recognition receptors TLR4 and CD14 mediate response to respiratory syncytial virus. *Nat Immunol*, 1, 398-401.
- LAMBERT, L., SAGFORS, A. M., OPENSHAW, P. J. & CULLEY, F. J. 2014. Immunity to RSV in Early-Life. *Front Immunol*, 5, 466.
- LEE, A. J. & ASHKAR, A. A. 2018. The Dual Nature of Type I and Type II Interferons. *Front Immunol*, 9, 2061.
- LEE, H. C., HEADLEY, M. B., LOO, Y. M., BERLIN, A., GALE, M., JR., DEBLEY, J. S., LUKACS, N. W. & ZIEGLER, S. F. 2012. Thymic stromal lymphopoietin is induced by respiratory syncytial virus-infected airway epithelial cells and promotes a type 2 response to infection. *J Allergy Clin Immunol*, 130, 1187-1196 e5.
- LEE, N., LUI, G. C., WONG, K. T., LI, T. C., TSE, E. C., CHAN, J. Y., YU, J., WONG, S. S., CHOI, K. W., WONG, R. Y., NGAI, K. L., HUI, D. S. & CHAN, P. K. 2013. High morbidity and mortality in adults hospitalized for respiratory syncytial virus infections. *Clin Infect Dis*, 57, 1069-77.
- LEGG, J. P., HUSSAIN, I. R., WARNER, J. A., JOHNSTON, S. L. & WARNER, J. O. 2003. Type 1 and type 2 cytokine imbalance in acute respiratory syncytial virus bronchiolitis. *Am J Respir Crit Care Med*, 168, 633-9.
- LEMAIRE, P. A., ANDERSON, E., LARY, J. & COLE, J. L. 2008. Mechanism of PKR Activation by dsRNA. *J Mol Biol*, 381, 351-60.
- LIAU, N. P. D., LAKTYUSHIN, A., LUCET, I. S., MURPHY, J. M., YAO, S., WHITLOCK, E., CALLAGHAN, K., NICOLA, N. A., KERSHAW, N. J. & BABON, J. J. 2018. The molecular basis of JAK/STAT inhibition by SOCS1. *Nat Commun*, 9, 1558.
- LIFLAND, A. W., JUNG, J., ALONAS, E., ZURLA, C., CROWE, J. E., JR. & SANTANGELO, P. J. 2012. Human respiratory syncytial virus nucleoprotein and inclusion bodies antagonize the innate immune response mediated by MDA5 and MAVS. *Journal of virology*,

86, 8245-8258.

- LIN, H. Y., LAI, R. H., LIN, S. T., LIN, R. C., WANG, M. J., LIN, C. C., LEE, H. C., WANG, F. F. & CHEN, J. Y. 2013. Suppressor of cytokine signaling 6 (SOCS6) promotes mitochondrial fission via regulating DRP1 translocation. *Cell Death Differ*, 20, 139-53.
- LING, Z., TRAN, K. C. & TENG, M. N. 2009. Human respiratory syncytial virus nonstructural protein NS2 antagonizes the activation of beta interferon transcription by interacting with RIG-I. *J Virol*, 83, 3734-42.
- LINOSSI, E. M., BABON, J. J., HILTON, D. J. & NICHOLSON, S. E. 2013. Suppression of cytokine signaling: the SOCS perspective. *Cytokine & growth factor reviews*, 24, 241-248.
- LINSSEN, R. S. N., SRIDHAR, A., MORENI, G., VAN DER WEL, N. N., VAN WOENSEL, J. B. M., WOLTHERS, K. C. & BEM, R. A. 2022. Neutrophil Extracellular Traps Do Not Induce Injury and Inflammation in Well-Differentiated RSV-Infected Airway Epithelium. *Cells*, 11.
- LIU, Q., WU, Y., QIN, Y., HU, J., XIE, W., QIN, F. X.-F. & CUI, J. 2018. Broad and diverse mechanisms used by deubiquitinase family members in regulating the type I interferon signaling pathway during antiviral responses. *Science Advances*, 4, eaar2824.
- LLOYD, C. M. & SNELGROVE, R. J. 2018. Type 2 immunity: Expanding our view. *Sci Immunol*, 3.
- LO, M. S., BRAZAS, R. M. & HOLTZMAN, M. J. 2005. Respiratory syncytial virus non-structural proteins NS1 and NS2 mediate inhibition of Stat2 expression and alpha/beta interferon responsiveness. *J Virol*, 79, 9315-9.
- MAC, S., SUMNER, A., DUCHESNE-BELANGER, S., STIRLING, R., TUNIS, M. & SANDER, B. 2019. Cost-effectiveness of Palivizumab for Respiratory Syncytial Virus: A Systematic Review. *Pediatrics*, 143.
- MADEIRA, F., PARK, Y. M., LEE, J., BUSO, N., GUR, T., MADHUSOODANAN, N., BASUTKAR, P., TIVEY, A. R. N., POTTER, S. C., FINN, R. D. & LOPEZ, R. 2019. The EMBL-EBI search and sequence analysis tools APIs in 2019. *Nucleic Acids Res*, 47, W636-W641.
- MADHI, S. A., POLACK, F. P., PIEDRA, P. A., MUNOZ, F. M., TRENHOLME, A. A.,

- SIMÕES, E. A. F., SWAMY, G. K., AGRAWAL, S., AHMED, K., AUGUST, A., BAQUI, A. H., CALVERT, A., CHEN, J., CHO, I., COTTON, M. F., CUTLAND, C. L., ENGLUND, J. A., FIX, A., GONIK, B., HAMMITT, L., HEATH, P. T., DE JESUS, J. N., JONES, C. E., KHALIL, A., KIMBERLIN, D. W., LIBSTER, R., LLAPUR, C. J., LUCERO, M., PEREZ MARC, G., MARSHALL, H. S., MASENYA, M. S., MARTINONTORRES, F., MEECE, J. K., NOLAN, T. M., OSMAN, A., PERRETT, K. P., PLESTED, J. S., RICHMOND, P. C., SNAPE, M. D., SHAKIB, J. H., SHINDE, V., STONEY, T., THOMAS, D. N., TITA, A. T., VARNER, M. W., VATISH, M., VRBICKY, K., WEN, J., ZAMAN, K., ZAR, H. J., GLENN, G. M., FRIES, L. F. & PREPARE STUDY, G. 2020. Respiratory Syncytial Virus Vaccination during Pregnancy and Effects in Infants. *N Engl J Med*, 383, 426-439.
- MAHONY, R., GARGAN, S., ROBERTS, K. L., BOURKE, N., KEATING, S. E., BOWIE, A. G., O'FARRELLY, C. & STEVENSON, N. J. 2017. A novel anti-viral role for STAT3 in IFN- α signalling responses. *Cellular and molecular life sciences : CMLS*, 74, 1755-1764.
- MAJOR, J., CROTTA, S., LLORIAN, M., MCCABE, T. M., GAD, H. H., PRIESTNALL, S. L., HARTMANN, R. & WACK, A. 2020. Type I and III interferons disrupt lung epithelial repair during recovery from viral infection. *Science*, 369, 712-717.
- MAJOROS, A., PLATANITIS, E., KERNBAUER-HOLZL, E., ROSEBROCK, F., MULLER, M. & DECKER, T. 2017. Canonical and Non-Canonical Aspects of JAK-STAT Signaling: Lessons from Interferons for Cytokine Responses. *Front Immunol*, 8, 29.
- MALAKHOV, M. P., MALAKHOVA, O. A., KIM, K. I., RITCHIE, K. J. & ZHANG, D. E. 2002. UBP43 (USP18) specifically removes ISG15 from conjugated proteins. *J Biol Chem*, 277, 9976-81.
- MALAKHOVA, O. A., KIM, K. I., LUO, J. K., ZOU, W., KUMAR, K. G., FUCHS, S. Y., SHUAI, K. & ZHANG, D. E. 2006. UBP43 is a novel regulator of interferon signaling independent of its ISG15 isopeptidase activity. *EMBO J*, 25, 2358-67.
- MALAKHOVA, O. A., YAN, M., MALAKHOV, M. P., YUAN, Y., RITCHIE, K. J., KIM, K. I., PETERSON, L. F., SHUAI, K. & ZHANG, D. E. 2003. Protein ISGylation modulates the JAK-STAT signaling pathway. *Genes Dev*, 17, 455-60.
- MALINCZAK, C. A., FONSECA, W., RASKY, A. J., PTASCHINSKI, C., MORRIS, S., ZIEGLER, S. F. & LUKACS, N. W. 2019. Sex-associated TSLP-induced immune alterations following early-life RSV infection leads to enhanced allergic disease. *Mucosal Immunol*, 12,

969-979.

- MARCHANT, D., SINGHERA, G. K., UTOKAPARCH, S., HACKETT, T. L., BOYD, J. H., LUO, Z., SI, X., DORSCH, D. R., MCMANUS, B. M. & HEGELE, R. G. 2010. Toll-like receptor 4-mediated activation of p38 mitogen-activated protein kinase is a determinant of respiratory virus entry and tropism. *J Virol*, 84, 11359-73.
- MARTIN-FONTECHA, A., THOMSEN, L. L., BRETT, S., GERARD, C., LIPP, M., LANZAVECCHIA, A. & SALLUSTO, F. 2004. Induced recruitment of NK cells to lymph nodes provides IFN-gamma for T(H)1 priming. *Nat Immunol*, 5, 1260-5.
- MCBRIDE, K. M., BANNINGER, G., MCDONALD, C. & REICH, N. C. 2002. Regulated nuclear import of the STAT1 transcription factor by direct binding of importin-alpha. *EMBO J*, 21, 1754-63.
- MCFARLAND, E. J., KARRON, R. A., MURESAN, P., CUNNINGHAM, C. K., VALENTINE, M. E., PERLOWSKI, C., THUMAR, B., GNANASHANMUGAM, D., SIBERRY, G. K., SCHAPPELL, E., BARR, E., REXROAD, V., YOGEV, R., SPECTOR, S. A., AZIZ, M., PATEL, N., CIELO, M., LUONGO, C., COLLINS, P. L., BUCHHOLZ, U. J. & INTERNATIONAL MATERNAL PEDIATRIC ADOLESCENT, A. C. T. S. T. 2018. Live-Attenuated Respiratory Syncytial Virus Vaccine Candidate With Deletion of RNA Synthesis Regulatory Protein M2-2 is Highly Immunogenic in Children. *J Infect Dis*, 217, 1347-1355.
- MCKENZIE, A. N. 2014. Type-2 innate lymphoid cells in asthma and allergy. *Ann Am Thorac Soc*, 11 Suppl 5, S263-70.
- MCMANUS, P. S., RITSON, P., SELBY, A., HART, C. A. & SMYTH, R. L. 2003. Bronchoalveolar lavage cellularity in infants with severe respiratory syncytial virus bronchiolitis. *Arch Dis Child*, 88, 922-6.
- MEDIMMUNE 1999. SYNAGIS® (PALIVIZUMAB).
- MELERO, J. A. & MOORE, M. L. 2013. Influence of respiratory syncytial virus strain differences on pathogenesis and immunity. *Curr Top Microbiol Immunol*, 372, 59-82.
- METCALF, D., GREENHALGH, C. J., VINEY, E., WILLSON, T. A., STARR, R., NICOLA, N. A., HILTON, D. J. & ALEXANDER, W. S. 2000. Gigantism in mice lacking suppressor of cytokine signalling-2. *Nature*, 405, 1069-73.
- MIAH, M.A., YOON, C.H., KIM, J., Jang, J., SEONG, Y.R., & BAE Y.S. CISH is induced

- during DC development and regulates DC-mediated CTL activation. *Eur J Immunol*. 2012 Jan;42(1):58-68.
- MICHALSKA, A., BLASZCZYK, K., WESOLY, J. & BLUYSSSEN, H. A. R. 2018. A Positive Feedback Amplifier Circuit That Regulates Interferon (IFN)-Stimulated Gene Expression and Controls Type I and Type II IFN Responses. *Front Immunol*, 9, 1135.
- MILLS, C. D., KINCAID, K., ALT, J. M., HEILMAN, M. J. & HILL, A. M. 2000. M-1/M-2 macrophages and the Th1/Th2 paradigm. *J Immunol*, 164, 6166-73.
- MITRA, B., WANG, J., KIM, E. S., MAO, R., DONG, M., LIU, Y., ZHANG, J. & GUO, H. 2019. Hepatitis B Virus Precore Protein p22 Inhibits Alpha Interferon Signaling by Blocking STAT Nuclear Translocation. *J Virol*, 93.
- MIYAMOTO, Y., YAMADA, K. & YONEDA, Y. 2016. Importin alpha: a key molecule in nuclear transport and non-transport functions. *J Biochem*, 160, 69-75.
- MOORE, M., HORIKOSHI, N. & SHENK, T. 1996. Oncogenic potential of the adenovirus E4orf6 protein. *Proc Natl Acad Sci U S A*, 93, 11295-301.
- MORDSTEIN, M., KOCHS, G., DUMOUTIER, L., RENAULD, J.-C., PALUDAN, S. R., KLUCHER, K. & STAEHELI, P. 2008. Interferon- λ Contributes to Innate Immunity of Mice against Influenza A Virus but Not against Hepatotropic Viruses. *PLOS Pathogens*, 4, e1000151.
- MORRIS, R., KERSHAW, N. J. & BABON, J. J. 2018. The molecular details of cytokine signaling via the JAK/STAT pathway. *Protein Sci*, 27, 1984-2009.
- MORRIS, S. K., DZOLGANOVSKI, B., BEYENE, J. & SUNG, L. 2009. A meta-analysis of the effect of antibody therapy for the prevention of severe respiratory syncytial virus infection. *BMC Infect Dis*, 9, 106.
- MUFSON, M. A., ORVELL, C., RAFNAR, B. & NORRBY, E. 1985. Two distinct subtypes of human respiratory syncytial virus. *J Gen Virol*, 66 (Pt 10), 2111-24.
- MUNIR, S., HILLYER, P., LE NOUEN, C., BUCHHOLZ, U. J., RABIN, R. L., COLLINS, P. L. & BUKREYEV, A. 2011. Respiratory syncytial virus interferon antagonist NS1 protein suppresses and skews the human T lymphocyte response. *PLoS Pathog*, 7, e1001336.
- MURARO, E., MERLO, A., MARTORELLI, D., CANGEMI, M., DALLA SANTA, S., DOLCETTI, R. & ROSATO, A. 2017. Fighting Viral Infections and Virus-Driven Tumors

- with Cytotoxic CD4(+) T Cells. *Front Immunol*, 8, 197.
- MURRAY, P. J. & WYNN, T. A. 2011. Protective and pathogenic functions of macrophage subsets. *Nat Rev Immunol*, 11, 723-37.
- MUSUMECI, A., LUTZ, K., WINHEIM, E. & KRUG, A. B. 2019. What Makes a pDC: Recent Advances in Understanding Plasmacytoid DC Development and Heterogeneity. *Front Immunol*, 10, 1222.
- NAGEL, M. A., JAMES, S. F., TRAKTINSKIY, I., WYBORNYY, A., CHOE, A., REMPEL, A., BAIRD, N. L. & GILDEN, D. 2014. Inhibition of phosphorylated-STAT1 nuclear translocation and antiviral protein expression in human brain vascular adventitial fibroblasts infected with varicella-zoster virus. *J Virol*, 88, 11634-7.
- NAIR, H., NOKES, D. J., GESSNER, B. D., DHERANI, M., MADHI, S. A., SINGLETON, R. J., O'BRIEN, K. L., ROCA, A., WRIGHT, P. F., BRUCE, N., CHANDRAN, A., THEODORATOU, E., SUTANTO, A., SEDYANINGSIH, E. R., NGAMA, M., MUNYWOKI, P. K., KARTASASMITA, C., SIMOES, E. A., RUDAN, I., WEBER, M. W. & CAMPBELL, H. 2010. Global burden of acute lower respiratory infections due to respiratory syncytial virus in young children: a systematic review and meta-analysis. *Lancet*, 375, 1545-55.
- NAN, Y., WU, C. & ZHANG, Y. J. 2018. Interferon Independent Non-Canonical STAT Activation and Virus Induced Inflammation. *Viruses*, 10.
- NGUYEN, K.B., WATFORD, W.T., SALOMON, R., HOFMANN, S.R., PIEN, G.C., MORINOBU, A., GADINA, M., O'SHEA, J.J., & BIRON, C.A. (2002). Critical role for STAT4 activation by type 1 interferons in the interferon-gamma response to viral infection. *Science* 297, 2063–2066.
- NIKONOVA, A., SHILOVSKIY, I., GALITSKAYA, M., SOKOLOVA, A., SUNDUKOVA, M., DMITRIEVA-POSOCCO, O., MITIN, A., KOMOGOROVA, V., LITVINA, M., SHAROVA, N., ZHERNOV, Y., KUDLAY, D., DVORNIKOV, A., KURBACHEVA, O., KHAITOV, R. & KHAITOV, M. 2021. Respiratory syncytial virus upregulates IL-33 expression in mouse model of virus-induced inflammation exacerbation in OVA-sensitized mice and in asthmatic subjects. *Cytokine*, 138, 155349.
- NOGUCHI, S., YAMADA, N., KUMAZAKI, M., YASUI, Y., IWASAKI, J., NAITO, S. & AKAO, Y. 2013. *socs7*, a target gene of microRNA-145, regulates interferon- induction through STAT3 nuclear translocation in bladder cancer cells. *Cell Death & Disease*, 4,

e482-e482.

NOVAVAX 2018. A Study to Determine the Safety and Efficacy of the RSV F Vaccine to Protect Infants Via Maternal Immunization. *Clinical Trials*. 29/03/2018 ed.

NUIJTEN, M., LEBMEIER, M. & WITTENBERG, W. 2009. Cost effectiveness of palivizumab for RSV prevention in high-risk children in the Netherlands. *J Med Econ*, 12, 291-300.

NVRL 2022. Influenza Week 20 2022. Influenza Surveillance in Ireland – Weekly Report: Influenza Week 20 2022.

O'BRIEN, K. L., BAGGETT, H. C., BROOKS, W. A., FEIKIN, D. R., HAMMITT, L. L., HIGDON, M. M., HOWIE, S. R. C., DELORIA KNOLL, M., KOTLOFF, K. L., LEVINE, O. S., MADHI, S. A., MURDOCH, D. R., PROSPERI, C., SCOTT, J. A. G., SHI, Q., THEA, D. M., WU, Z., ZEGER, S. L., ADRIAN, P. V., AKARASEWI, P., ANDERSON, T. P., ANTONIO, M., AWORI, J. O., BAILLIE, V. L., BUNTHI, C., CHIPETA, J., CHISTI, M. J., CRAWLEY, J., DELUCA, A. N., DRISCOLL, A. J., EBRUKE, B. E., ENDTZ, H. P., FANCOURT, N., FU, W., GOSWAMI, D., GROOME, M. J., HADDIX, M., HOSAIN, L., JAHAN, Y., KAGUCIA, E. W., KAMAU, A., KARRON, R. A., KAZUNGU, S., KOUROUMA, N., KUWANDA, L., KWENDA, G., LI, M., MACHUKA, E. M., MACKENZIE, G., MAHOMED, N., MALONEY, S. A., MCLELLAN, J. L., MITCHELL, J. L., MOORE, D. P., MORPETH, S. C., MUDAU, A., MWANANYANDA, L., MWANSA, J., SILABA OMINDE, M., ONWUCHEKWA, U., PARK, D. E., RHODES, J., SAWATWONG, P., SEIDENBERG, P., SHAMSUL, A., SIMÕES, E. A. F., SISSOKO, S., WASOMWE, S., SOW, S. O., SYLLA, M., TAMBOURA, B., TAPIA, M. D., THAMTHITIWAT, S., TOURE, A., WATSON, N. L., ZAMAN, K. & ZAMAN, S. M. A. 2019. Causes of severe pneumonia requiring hospital admission in children without HIV infection from Africa and Asia: the PERCH multi-country case-control study. *The Lancet*.

OKABAYASHI, T., KOJIMA, T., MASAKI, T., YOKOTA, S., IMAIZUMI, T., TSUTSUMI, H., HIMI, T., FUJII, N. & SAWADA, N. 2011. Type-III interferon, not type-I, is the predominant interferon induced by respiratory viruses in nasal epithelial cells. *Virus Res*, 160, 360-6.

OKUMURA, A., LU, G., PITHA-ROWE, I. & PITHA, P. M. 2006. Innate antiviral response targets HIV-1 release by the induction of ubiquitin-like protein ISG15. *Proc Natl Acad Sci U S A*, 103, 1440-5.

OKUMURA, A., PITHA, P. M. & HARTY, R. N. 2008. ISG15 inhibits Ebola VP40 VLP

- budding in an L-domain-dependent manner by blocking Nedd4 ligase activity. *Proc Natl Acad Sci U S A*, 105, 3974-9.
- OKUMURA, F., OKUMURA, A. J., UEMATSU, K., HATAKEYAMA, S., ZHANG, D. E. & KAMURA, T. 2013. Activation of double-stranded RNA-activated protein kinase (PKR) by interferon-stimulated gene 15 (ISG15) modification down-regulates protein translation. *J Biol Chem*, 288, 2839-47.
- OPENSHAW, P. J., CULLEY, F. J. & OLSZEWSKA, W. 2001. Immunopathogenesis of vaccine-enhanced RSV disease. *Vaccine*, 20 Suppl 1, S27-31.
- OWHASHI, M., TAOKA, Y., ISHII, K., NAKAZAWA, S., UEMURA, H. & KAMBARA, H. 2003. Identification of a ubiquitin family protein as a novel neutrophil chemotactic factor. *Biochem Biophys Res Commun*, 309, 533-9.
- PALMER, D.C., GUITTARD, G.C., FRANCO, Z., CROMPTON, J.G., EIL, R.L., PATEL, S.J., JI, Y., VAN PANHUYS, N., KLEBANOFF, C.A., SUKUMAR, M., CLEVER, D., CHICHURA, A., ROYCHOUDHURI, R., VARMA, R., WANG, E., GATTINONI, L., MARINCOLA, F.M., BALAGOPALAN, L., SAMELSON, L.E. & RESTIFO, N.P. Cish actively silences TCR signaling in CD8+ T cells to maintain tumor tolerance. *J Exp Med*. 2015 Nov 16;212(12):2095-113.
- PANDA, S.K. & COLONNA, M. Innate Lymphoid Cells in Mucosal Immunity. *Front Immunol*. 2019 May 7;10:861.
- PANDYA, C. M., CALLAHAN, M. S., SAVCHENKO, G. K. & STOBART, C. C. 2019. A Contemporary View of Respiratory Syncytial Virus (RSV) Biology and Strain-Specific Differences. *Pathogens*, 8.
- PAULI, E. K., SCHMOLKE, M., WOLFF, T., VIEMANN, D., ROTH, J., BODE, J. G. & LUDWIG, S. 2008. Influenza A virus inhibits type I IFN signaling via NF-kappaB-dependent induction of SOCS-3 expression. *PLoS Pathog*, 4, e1000196.
- PEI, J., BERI, N. R., ZOU, A. J., HUBEL, P., DORANDO, H. K., BERGANT, V., ANDREWS, R. D., PAN, J., ANDREWS, J. M., SHEEHAN, K. C. F., PICHLMAIR, A., AMARASINGHE, G. K., BRODY, S. L., PAYTON, J. E. & LEUNG, D. W. 2021. Nuclear-localized human respiratory syncytial virus NS1 protein modulates host gene transcription. *Cell Rep*, 37, 109803.
- PERNG, Y. C. & LENSCHOW, D. J. 2018. ISG15 in antiviral immunity and beyond. *Nat Rev Microbiol*, 16, 423-439.

- PHILIPS, R.L., WANG, Y., CHEON, H., KANNO, Y., GADINA, M., SARTORELLI, V., HORVATH, C.M., DARNELL, J.E. JR, STARK, G.R. & O'SHEA, J.J. The JAK-STAT pathway at 30: Much learned, much more to do. *Cell*. 2022 Oct 13;185(21):3857-3876.
- PICKART, C. M. 2001. Mechanisms underlying ubiquitination. *Annu Rev Biochem*, 70, 503-33.
- PLATANITIS, E., DEMIROZ, D., SCHNELLER, A. et al. A molecular switch from STAT2-IRF9 to ISGF3 underlies interferon-induced gene transcription. *Nat Commun* 10, 2921 (2019).
- PRICE, R. H. M., GRAHAM, C. & RAMALINGAM, S. 2019. Association between viral seasonality and meteorological factors. *Sci Rep*, 9, 929.
- RALLABHANDI, P., PHILLIPS, R. L., BOUKHVALOVA, M. S., PLETNEVA, L. M., SHIREY, K. A., GIOANNINI, T. L., WEISS, J. P., CHOW, J. C., HAWKINS, L. D., VOGEL, S. N. & BLANCO, J. C. 2012. Respiratory syncytial virus fusion protein-induced toll-like receptor 4 (TLR4) signaling is inhibited by the TLR4 antagonists *Rhodobacter sphaeroides* lipopolysaccharide and eritoran (E5564) and requires direct interaction with MD-2. *mBio*, 3.
- RALSTON, S. L., LIEBERTHAL, A. S., MEISSNER, H. C., ALVERSON, B. K., BAILEY, J. E., GADOMSKI, A. M., JOHNSON, D. W., LIGHT, M. J., MARAQA, N. F., MENDONCA, E. A., PHELAN, K. J., ZORC, J. J., STANKO-LOPP, D., BROWN, M. A., NATHANSON, I., ROSENBLUM, E., SAYLES, S., 3RD, HERNANDEZ-CANCIO, S. & AMERICAN ACADEMY OF, P. 2014. Clinical practice guideline: the diagnosis, management, and prevention of bronchiolitis. *Pediatrics*, 134, e1474-502.
- RAMASWAMY, M., SHI, L., VARGA, S. M., BARIK, S., BEHLKE, M. A. & LOOK, D. C. 2006. Respiratory syncytial virus nonstructural protein 2 specifically inhibits type I interferon signal transduction. *Virology*, 344, 328-39.
- REDDEL, R. R., KE, Y., GERWIN, B. I., MCMENAMIN, M. G., LECHNER, J. F., SU, R. T., BRASH, D. E., PARK, J. B., RHIM, J. S. & HARRIS, C. C. 1988. Transformation of human bronchial epithelial cells by infection with SV40 or adenovirus-12 SV40 hybrid virus, or transfection via strontium phosphate coprecipitation with a plasmid containing SV40 early region genes. *Cancer Res*, 48, 1904-9.
- REN, J., LIU, T., PANG, L., LI, K., GAROFALO, R. P., CASOLA, A. & BAO, X. 2011. A novel mechanism for the inhibition of interferon regulatory factor-3-dependent gene expression

- by human respiratory syncytial virus NS1 protein. *J Gen Virol*, 92, 2153-9.
- REN, S., CHEN, X., HUANG, R., ZHOU, G. G. & YUAN, Z. 2019. SOCS4 expressed by recombinant HSV protects against cytokine storm in a mouse model. *Oncol Rep*, 41, 1509-1520.
- RODRIGUEZ, J. J., PARISIEN, J. P. & HORVATH, C. M. 2002. Nipah virus V protein evades alpha and gamma interferons by preventing STAT1 and STAT2 activation and nuclear accumulation. *J Virol*, 76, 11476-83.
- RODRIGUEZ, W. J., GRUBER, W. C., GROOTHUIS, J. R., SIMOES, E. A., ROSAS, A. J., LEPOW, M., KRAMER, A. & HEMMING, V. 1997. Respiratory syncytial virus immune globulin treatment of RSV lower respiratory tract infection in previously healthy children. *Pediatrics*, 100, 937-42.
- RODRIGUEZ-FERNANDEZ, R., TAPIA, L. I., YANG, C. F., TORRES, J. P., CHAVEZ-BUENO, S., GARCIA, C., JARAMILLO, L. M., MOORE-CLINGENPEEL, M., JAFRI, H. S., PEEPLES, M. E., PIEDRA, P. A., RAMILO, O. & MEJIAS, A. 2017. Respiratory Syncytial Virus Genotypes, Host Immune Profiles, and Disease Severity in Young Children Hospitalized With Bronchiolitis. *J Infect Dis*, 217, 24-34.
- RONG, L. & PERELSON, A. S. 2010. Treatment of hepatitis C virus infection with interferon and small molecule direct antivirals: viral kinetics and modeling. *Crit Rev Immunol*, 30, 131-48.
- RUDD, P. M., ELLIOTT, T., CRESSWELL, P., WILSON, I. A. & DWEK, R. A. 2001. Glycosylation and the immune system. *Science*, 291, 2370-6.
- RUSSELL, R. F., MCDONALD, J. U., IVANOVA, M., ZHONG, Z., BUKREYEV, A. & TREGONING, J. S. 2015. Partial Attenuation of Respiratory Syncytial Virus with a Deletion of a Small Hydrophobic Gene Is Associated with Elevated Interleukin-1beta Responses. *J Virol*, 89, 8974-81.
- SACCO, R. E., MCGILL, J. L., PILLATZKI, A. E., PALMER, M. V. & ACKERMANN, M. R. 2014. Respiratory syncytial virus infection in cattle. *Vet Pathol*, 51, 427-36.
- SARAVIA, J., YOU, D., SHRESTHA, B., JALIGAMA, S., SIEFKER, D., LEE, G. I., HARDING, J. N., JONES, T. L., ROVNAGHI, C., BAGGA, B., DEVINCENZO, J. P. & CORMIER, S. A. 2015. Respiratory Syncytial Virus Disease Is Mediated by Age-Variable IL-33. *PLoS Pathog*, 11, e1005217.

- SCHELTEMA, N. M., NIBBELKE, E. E., POUW, J., BLANKEN, M. O., ROVERS, M. M., NAAKTGEBOREN, C. A., MAZUR, N. I., WILDENBEEST, J. G., VAN DER ENT, C. K. & BONT, L. J. 2018. Respiratory syncytial virus prevention and asthma in healthy preterm infants: a randomised controlled trial. *Lancet Respir Med*, 6, 257-264.
- SCHLENDER, J., BOSSERT, B., BUCHHOLZ, U. & CONZELMANN, K. K. 2000. Bovine respiratory syncytial virus nonstructural proteins NS1 and NS2 cooperatively antagonize alpha/beta interferon-induced antiviral response. *J Virol*, 74, 8234-42.
- SCHMIDT, M. E. & VARGA, S. M. 2017. Modulation of the host immune response by respiratory syncytial virus proteins. *J Microbiol*, 55, 161-171.
- SCHNEIDER, W. M., CHEVILLOTTE, M. D. & RICE, C. M. 2014. Interferon-stimulated genes: a complex web of host defenses. *Annu Rev Immunol*, 32, 513-45.
- SCHOMACKER, H., HEBNER, R. M., BOONYARATANAKORNKIT, J., SURMAN, S., AMARO-CARAMBOT, E., COLLINS, P. L. & SCHMIDT, A. C. 2012. The C proteins of human parainfluenza virus type 1 block IFN signaling by binding and retaining Stat1 in perinuclear aggregates at the late endosome. *PLoS One*, 7, e28382.
- SCHULZ, O., PICHLMAIR, A., REHWINKEL, J., ROGERS, N. C., SCHEUNER, D., KATO, H., TAKEUCHI, O., AKIRA, S., KAUFMAN, R. J. & REIS E SOUSA, C. 2010. Protein kinase R contributes to immunity against specific viruses by regulating interferon mRNA integrity. *Cell Host Microbe*, 7, 354-61.
- SEIF, F., KHOSHMIRSAFA, M., AAZAMI, H., MOHSENZADEGAN, M., SEDIGHI, G. & BAHAR, M. 2017. The role of JAK-STAT signaling pathway and its regulators in the fate of T helper cells. *Cell Commun Signal*, 15, 23.
- SEONG, R. K., LEE, J. K. & SHIN, O. S. 2020. Zika Virus-Induction of the Suppressor of Cytokine Signaling 1/3 Contributes to the Modulation of Viral Replication. *Pathogens*, 9.
- SHAHABI, A., PENEVA, D., INCERTI, D., MCLAURIN, K. & STEVENS, W. 2018. Assessing Variation in the Cost of Palivizumab for Respiratory Syncytial Virus Prevention in Preterm Infants. *PharmacoEconomics - Open*, 2, 53-61.
- SHAW, G., MORSE, S., ARARAT, M. & GRAHAM, F. L. 2002. Preferential transformation of human neuronal cells by human adenoviruses and the origin of HEK 293 cells. *FASEB J*, 16, 869-71.

- SHEN, Q., WANG, Y. E. & PALAZZO, A. F. 2021. Crosstalk between nucleocytoplasmic trafficking and the innate immune response to viral infection. *J Biol Chem*, 297, 100856.
- SHI, H. X., YANG, K., LIU, X., LIU, X. Y., WEI, B., SHAN, Y. F., ZHU, L. H. & WANG, C. 2010. Positive regulation of interferon regulatory factor 3 activation by Herc5 via ISG15 modification. *Mol Cell Biol*, 30, 2424-36.
- SHI, T., DENOUEL, A., TIETJEN, A. K., CAMPBELL, I., MORAN, E., LI, X., CAMPBELL, H., DEMONT, C., NYAWANDA, B. O., CHU, H. Y., STOSZEK, S. K., KRISHNAN, A., OPENSHAW, P., FALSEY, A. R., NAIR, H. & INVESTIGATORS, R. 2020. Global Disease Burden Estimates of Respiratory Syncytial Virus-Associated Acute Respiratory Infection in Older Adults in 2015: A Systematic Review and Meta-Analysis. *J Infect Dis*, 222, S577-S583.
- SHI, T., MCALLISTER, D. A., O'BRIEN, K. L., SIMOES, E. A. F., MADHI, S. A., GESSNER, B. D., POLACK, F. P., BALSELLS, E., ACACIO, S., AGUAYO, C., ALASSANI, I., ALI, A., ANTONIO, M., AWASTHI, S., AWORI, J. O., AZZIZ-BAUMGARTNER, E., BAGGETT, H. C., BAILLIE, V. L., BALMASEDA, A., BARAHONA, A., BASNET, S., BASSAT, Q., BASUALDO, W., BIGOGO, G., BONT, L., BREIMAN, R. F., BROOKS, W. A., BROOR, S., BRUCE, N., BRUDEN, D., BUCHY, P., CAMPBELL, S., CAROSONE-LINK, P., CHADHA, M., CHIPETA, J., CHOU, M., CLARA, W., COHEN, C., DE CUELLAR, E., DANG, D. A., DASH-YANDAG, B., DELORIA-KNOLL, M., DHERANI, M., EAP, T., EBRUKE, B. E., ECHAVARRIA, M., DE FREITAS LÁZARO EMEDIATO, C. C., FASCE, R. A., FEIKIN, D. R., FENG, L., GENTILE, A., GORDON, A., GOSWAMI, D., GOYET, S., GROOME, M., HALASA, N., HIRVE, S., HOMAIRA, N., HOWIE, S. R. C., JARA, J., JROUNDI, I., KARTASASMITA, C. B., KHURI-BULOS, N., KOTLOFF, K. L., KRISHNAN, A., LIBSTER, R., LOPEZ, O., LUCERO, M. G., LUCION, F., LUPISAN, S. P., MARCONE, D. N., MCCRACKEN, J. P., MEJIA, M., MOISI, J. C., MONTGOMERY, J. M., MOORE, D. P., MORALEDA, C., MOYES, J., MUNYWOKI, P., MUTYARA, K., NICOL, M. P., NOKES, D. J., NYMADAWA, P., DA COSTA OLIVEIRA, M. T., OSHITANI, H., PANDEY, N., PARANHOS-BACCALÀ, G., PHILLIPS, L. N., PICOT, V. S., RAHMAN, M., RAKOTO-ANDRIANARIVELO, M., RASMUSSEN, Z. A., RATH, B. A., ROBINSON, A., ROMERO, C., RUSSOMANDO, G., SALIMI, V., SAWATWONG, P., SCHELTEMA, N., SCHWEIGER, B., et al. 2017. Global, regional, and national disease burden estimates of acute lower respiratory infections due to respiratory syncytial virus in young children in 2015: a systematic review

- and modelling study. *Lancet*, 390, 946-958.
- SIGURS, N., ALJASSIM, F., KJELLMAN, B., ROBINSON, P. D., SIGURBERGSSON, F., BJARNASON, R. & GUSTAFSSON, P. M. 2010. Asthma and allergy patterns over 18 years after severe RSV bronchiolitis in the first year of life. *Thorax*, 65, 1045-52.
- SMITH, L. J., MCKAY, K. O., VAN ASPEREN, P. P., SELVADURAI, H. & FITZGERALD, D. A. 2010. Normal development of the lung and premature birth. *Paediatr Respir Rev*, 11, 135-42.
- SMITH-GARVIN, J. E., KORETZKY, G. A. & JORDAN, M. S. 2009. T cell activation. *Annu Rev Immunol*, 27, 591-619.
- SMYTH, M. J., CRETNEY, E., KELLY, J. M., WESTWOOD, J. A., STREET, S. E., YAGITA, H., TAKEDA, K., VAN DOMMELEN, S. L., DEGLI-ESPOSTI, M. A. & HAYAKAWA, Y. 2005. Activation of NK cell cytotoxicity. *Mol Immunol*, 42, 501-10.
- SOBAH, M.L., LIONGUE, C. & WARD, A.C. SOCS Proteins in Immunity, Inflammatory Diseases, and Immune-Related Cancer. *Front Med (Lausanne)*. 2021 Sep 16;8:727987.
- SOMMEREYNS, C., PAUL, S., STAEHELI, P. & MICHIELS, T. 2008. IFN-lambda (IFN-lambda) is expressed in a tissue-dependent fashion and primarily acts on epithelial cells in vivo. *PLoS Pathog*, 4, e1000017.
- SOUMELIS, V., RECHE, P. A., KANZLER, H., YUAN, W., EDWARD, G., HOMEY, B., GILLIET, M., HO, S., ANTONENKO, S., LAUERMA, A., SMITH, K., GORMAN, D., ZURAWSKI, S., ABRAMS, J., MENON, S., MCCLANAHAN, T., DE WAAL-MALEFYT RD, R., BAZAN, F., KASTELEIN, R. A. & LIU, Y. J. 2002. Human epithelial cells trigger dendritic cell mediated allergic inflammation by producing TSLP. *Nat Immunol*, 3, 673-80.
- SPANN, K. M., TRAN, K. C., CHI, B., RABIN, R. L. & COLLINS, P. L. 2004. Suppression of the induction of alpha, beta, and lambda interferons by the NS1 and NS2 proteins of human respiratory syncytial virus in human epithelial cells and macrophages [corrected]. *J Virol*, 78, 4363-9.
- SPANN, K. M., TRAN, K. C. & COLLINS, P. L. 2005. Effects of nonstructural proteins NS1 and NS2 of human respiratory syncytial virus on interferon regulatory factor 3, NF-kappaB, and proinflammatory cytokines. *J Virol*, 79, 5353-62.
- SPEER, S. D., LI, Z., BUTA, S., PAYELLE-BROGARD, B., QIAN, L., VIGANT, F., RUBINO,

- E., GARDNER, T. J., WEDEKING, T., HERMANN, M., DUEHR, J., SANAL, O., TEZCAN, I., MANSOURI, N., TABARSI, P., MANSOURI, D., FRANCOIS-NEWTON, V., DAUSSY, C. F., RODRIGUEZ, M. R., LENSCHOW, D. J., FREIBERG, A. N., TORTORELLA, D., PIEHLER, J., LEE, B., GARCIA-SASTRE, A., PELLEGRINI, S. & BOGUNOVIC, D. 2016. ISG15 deficiency and increased viral resistance in humans but not mice. *Nat Commun*, 7, 11496.
- SPELLBERG, B. & EDWARDS, J. E., JR. 2001. Type 1/Type 2 immunity in infectious diseases. *Clin Infect Dis*, 32, 76-102.
- STEVENSON, N. J., BOURKE, N. M., RYAN, E. J., BINDER, M., FANNING, L., JOHNSTON, J. A., HEGARTY, J. E., LONG, A. & O'FARRELLY, C. 2013. Hepatitis C virus targets the interferon- α JAK/STAT pathway by promoting proteasomal degradation in immune cells and hepatocytes. *FEBS Lett*, 587, 1571-8.
- STIER, M. T., GOLENIEWSKA, K., CEPHUS, J. Y., NEWCOMB, D. C., SHERRILL, T. P., BOYD, K. L., BLOODWORTH, M. H., MOORE, M. L., CHEN, K., KOLLS, J. K. & PEEBLES, R. S., JR. 2017. STAT1 Represses Cytokine-Producing Group 2 and Group 3 Innate Lymphoid Cells during Viral Infection. *J Immunol*, 199, 510-519.
- STOKES, K. L., CURRIER, M. G., SAKAMOTO, K., LEE, S., COLLINS, P. L., PLEMPER, R. K. & MOORE, M. L. 2013. The respiratory syncytial virus fusion protein and neutrophils mediate the airway mucin response to pathogenic respiratory syncytial virus infection. *J Virol*, 87, 10070-82.
- STRUNK, T., CURRIE, A., RICHMOND, P., SIMMER, K. & BURGNER, D. 2011. Innate immunity in human newborn infants: prematurity means more than immaturity. *J Matern Fetal Neonatal Med*, 24, 25-31.
- SWEDAN, S., MUSIYENKO, A. & BARIK, S. 2009. Respiratory syncytial virus nonstructural proteins decrease levels of multiple members of the cellular interferon pathways. *J Virol*, 83, 9682-93.
- TABATABAI, J., PRIFERT, C., PFEIL, J., GRULICH-HENN, J. & SCHNITZLER, P. 2014. Novel respiratory syncytial virus (RSV) genotype ON1 predominates in Germany during winter season 2012-13. *PLoS One*, 9, e109191.
- TAHAMTAN, A., BESTEMAN, S., SAMADIZADEH, S., RASTEGAR, M., BONT, L. & SALIMI, V. 2021. Neutrophils in respiratory syncytial virus infection: From harmful effects to therapeutic opportunities. *Br J Pharmacol*, 178, 515-530.

- TAN, L., COENJAERTS, F. E., HOUSPIE, L., VIVEEN, M. C., VAN BLEEK, G. M., WIERTZ, E. J., MARTIN, D. P. & LEMEY, P. 2013. The comparative genomics of human respiratory syncytial virus subgroups A and B: genetic variability and molecular evolutionary dynamics. *J Virol*, 87, 8213-26.
- TAYYARI, F., MARCHANT, D., MORAES, T. J., DUAN, W., MASTRANGELO, P. & HEGELE, R. G. 2011. Identification of nucleolin as a cellular receptor for human respiratory syncytial virus. *Nat Med*, 17, 1132-5.
- TE, H. S., RANDALL, G. & JENSEN, D. M. 2007. Mechanism of action of ribavirin in the treatment of chronic hepatitis C. *Gastroenterol Hepatol (N Y)*, 3, 218-25.
- TELCIAN, A. G., LAZA-STANCA, V., EDWARDS, M. R., HARKER, J. A., WANG, H., BARTLETT, N. W., MALLIA, P., ZDRENGHEA, M. T., KEBADZE, T., COYLE, A. J., OPENSHAW, P. J., STANCIU, L. A. & JOHNSTON, S. L. 2011. RSV-induced bronchial epithelial cell PD-L1 expression inhibits CD8+ T cell nonspecific antiviral activity. *J Infect Dis*, 203, 85-94.
- TEN HOEVE, J., DE JESUS IBARRA-SANCHEZ, M., FU, Y., ZHU, W., TREMBLAY, M., DAVID, M. & SHUAI, K. 2002. Identification of a nuclear Stat1 protein tyrosine phosphatase. *Mol Cell Biol*, 22, 5662-8.
- TENG, M. N. & COLLINS, P. L. 1999. Altered Growth Characteristics of Recombinant Respiratory Syncytial Viruses Which Do Not Produce NS2 Protein. *Journal of Virology*, 73, 466-473.
- TENG, M. N., WHITEHEAD, S. S., BERMINGHAM, A., ST CLAIRE, M., ELKINS, W. R., MURPHY, B. R. & COLLINS, P. L. 2000. Recombinant respiratory syncytial virus that does not express the NS1 or M2-2 protein is highly attenuated and immunogenic in chimpanzees. *J Virol*, 74, 9317-21.
- THOMAS, E., GHANY, M. G. & LIANG, T. J. 2012. The application and mechanism of action of ribavirin in therapy of hepatitis C. *Antivir Chem Chemother*, 23, 1-12.
- THWAITES, R.S., COATES, M., ITO, K., GHAZALY, M., FEATHER, C., ABDULLA, F., TUNSTALL, T., JAIN, P., CASS, L., RAPEPORT, G., HANSEL, T.T., NADEL, S. & OPENSHAW, P. Reduced Nasal Viral Load and IFN Responses in Infants with Respiratory Syncytial Virus Bronchiolitis and Respiratory Failure. *Am J Respir Crit Care Med*. 2018 Oct 15;198(8):1074-1084.
- TOGNARELLI, E. I., BUENO, S. M. & GONZALEZ, P. A. 2019. Immune-Modulation by

- the Human Respiratory Syncytial Virus: Focus on Dendritic Cells. *Front Immunol*, 10, 810.
- TRIPP, R. A., JONES, L. P., HAYNES, L. M., ZHENG, H., MURPHY, P. M. & ANDERSON, L. J. 2001. CX3C chemokine mimicry by respiratory syncytial virus G glycoprotein. *Nat Immunol*, 2, 732-8.
- TRIPP, R. A., MOORE, D., JONES, L., SULLENDER, W., WINTER, J. & ANDERSON, L. J. 1999. Respiratory syncytial virus G and/or SH protein alters Th1 cytokines, natural killer cells, and neutrophils responding to pulmonary infection in BALB/c mice. *Journal of virology*, 73, 7099-7107.
- TSAI, M. H. & LEE, C. K. 2018. STAT3 Cooperates With Phospholipid Scramblase 2 to Suppress Type I Interferon Response. *Front Immunol*, 9, 1886.
- TSAI, M. H., PAI, L. M. & LEE, C. K. 2019. Fine-Tuning of Type I Interferon Response by STAT3. *Front Immunol*, 10, 1448.
- ULANE, C. M., RODRIGUEZ, J. J., PARISIEN, J. P. & HORVATH, C. M. 2003. STAT3 ubiquitylation and degradation by mumps virus suppress cytokine and oncogene signaling. *J Virol*, 77, 6385-93.
- VALARCHER, J. F., FURZE, J., WYLD, S., COOK, R., CONZELMANN, K. K. & TAYLOR, G. 2003. Role of alpha/beta interferons in the attenuation and immunogenicity of recombinant bovine respiratory syncytial viruses lacking NS proteins. *J Virol*, 77, 8426-39.
- VAN ERP, E. A., LAKERVELD, A. J., DE GRAAF, E., LARSEN, M. D., SCHEPP, R. M., HIPGRAVE EDERVEEN, A. L., AHOUT, I. M., DE HAAN, C. A., WUHRER, M., LUYTJES, W., FERWERDA, G., VIDARSSON, G. & VAN KASTEREN, P. B. 2020. Natural killer cell activation by respiratory syncytial virus-specific antibodies is decreased in infants with severe respiratory infections and correlates with Fc-glycosylation. *Clin Transl Immunology*, 9, e1112.
- VAN HAL, S. J., JENSEN, S. O., VASKA, V. L., ESPEDIDO, B. A., PATERSON, D. L. & GOSBELL, I. B. 2012. Predictors of Mortality in Staphylococcus aureus Bacteremia. *Clinical Microbiology Reviews*, 25, 362-386.
- VERHEIJEN, M., LIENHARD, M., SCHROODERS, Y., CLAYTON, O., NUDISCHER, R., BOERNO, S., TIMMERMANN, B., SELEVSEK, N., SCHLAPBACH, R., GMUENDER,

- H., GOTTA, S., GERAEDTS, J., HERWIG, R., KLEINJANS, J. & CAIMENT, F. 2019. DMSO induces drastic changes in human cellular processes and epigenetic landscape in vitro. *Sci Rep*, 9, 4641.
- VERHELST, J., HULPIAU, P. & SAELENS, X. 2013. Mx proteins: antiviral gatekeepers that restrain the uninvited. *Microbiol Mol Biol Rev*, 77, 551-66.
- VERHELST, J., PARTHOENS, E., SCHEPENS, B., FIERS, W. & SAELENS, X. 2012. Interferon-inducible protein Mx1 inhibits influenza virus by interfering with functional viral ribonucleoprotein complex assembly. *J Virol*, 86, 13445-55.
- VU, L.D., SIEFKER, D., JONES, T.L., YOU, D., TAYLOR, R., DEVINCENZO, J. & CORMIER, S.A. Elevated Levels of Type 2 Respiratory Innate Lymphoid Cells in Human Infants with Severe Respiratory Syncytial Virus Bronchiolitis. *Am J Respir Crit Care Med*. 2019 Dec 1;200(11):1414-1423.
- VILLENAVE, R., THAVAGNANAM, S., SARLANG, S., PARKER, J., DOUGLAS, I., SKIBINSKI, G., HEANEY, L. G., MCKAIGUE, J. P., COYLE, P. V., SHIELDS, M. D. & POWER, U. F. 2012. In vitro modeling of respiratory syncytial virus infection of pediatric bronchial epithelium, the primary target of infection in vivo. *Proceedings of the National Academy of Sciences of the United States of America*, 109, 5040-5045.
- WACK, A., TERCZYNSKA-DYLA, E. & HARTMANN, R. 2015. Guarding the frontiers: the biology of type III interferons. *Nat Immunol*, 16, 802-9.
- WALSH, E. E., FALSEY, A. R., SCOTT, D. A., GURTMAN, A., ZAREBA, A. M., JANSEN, K. U., GRUBER, W. C., DORMITZER, P. R., SWANSON, K. A., RADLEY, D., GOMME, E., COOPER, D. & SCHMOELE-THOMA, B. 2022. A Randomized Phase 1/2 Study of a Respiratory Syncytial Virus Prefusion F Vaccine. *J Infect Dis*, 225, 1357-1366.
- WANG, F., ZHANG, S., JEON, R., VUCKOVIC, I., JIANG, X., LERMAN, A., FOLMES, C. D., DZEJA, P. D. & HERRMANN, J. 2018. Interferon Gamma Induces Reversible Metabolic Reprogramming of M1 Macrophages to Sustain Cell Viability and Pro-Inflammatory Activity. *EBioMedicine*, 30, 303-316.
- WANG, W., YIN, Y., XU, L., SU, J., HUANG, F., WANG, Y., BOOR, P. P. C., CHEN, K., WANG, W., CAO, W., ZHOU, X., LIU, P., VAN DER LAAN, L. J. W., KWEKKEBOOM, J., PEPPELENBOSCH, M. P. & PAN, Q. 2017. Unphosphorylated ISGF3 drives constitutive expression of interferon-stimulated genes to protect against viral infections. *Sci Signal*, 10.

- WANG, W., ZHOU, Z., XIAO, X., TIAN, Z., DONG, X., WANG, C., LI, L., REN, L., LEI, X., XIANG, Z. & WANG, J. 2021. SARS-CoV-2 nsp12 attenuates type I interferon production by inhibiting IRF3 nuclear translocation. *Cell Mol Immunol*, 18, 945-953.
- WANG, W. B., LEVY, D. E. & LEE, C. K. 2011. STAT3 negatively regulates type I IFN-mediated antiviral response. *J Immunol*, 187, 2578-85.
- WEGZYN, C., TOH, L. K., NOTARIO, G., BIGUENET, S., UNNEBRINK, K., PARK, C., MAKARI, D. & NORTON, M. 2014. Safety and Effectiveness of Palivizumab in Children at High Risk of Serious Disease Due to Respiratory Syncytial Virus Infection: A Systematic Review. *Infect Dis Ther*, 3, 133-58.
- WELLIVER, R. C., CHECCHIA, P. A., BAUMAN, J. H., FERNANDES, A. W., MAHADEVIA, P. J. & HALL, C. B. 2010. Fatality rates in published reports of RSV hospitalizations among high-risk and otherwise healthy children. *Curr Med Res Opin*, 26, 2175-81.
- WERNEKE, S. W., SCHILTE, C., ROHATGI, A., MONTE, K. J., MICHAULT, A., ARENZANA-SEISDEDOS, F., VANLANDINGHAM, D. L., HIGGS, S., FONTANET, A., ALBERT, M. L. & LENSCHOW, D. J. 2011. ISG15 is critical in the control of Chikungunya virus infection independent of Ube1L mediated conjugation. *PLoS Pathog*, 7, e1002322.
- WHELAN, B., MUSTERS, E., MURRAY, A., MOORE, E., LIEVAART, L., VISSER, S., TOXOPEUS, E., VAN VEEN, A., NOTARIO, G. & CAMPBELL, F. J. 2016a. Review of the home care programmes for respiratory syncytial virus (RSV) prophylaxis in Ireland and The Netherlands. *Drugs Ther Perspect*, 32, 119-130.
- WHELAN, J. N., TRAN, K. C., VAN ROSSUM, D. B. & TENG, M. N. 2016b. Identification of Respiratory Syncytial Virus Nonstructural Protein 2 Residues Essential for Exploitation of the Host Ubiquitin System and Inhibition of Innate Immune Responses. *J Virol*, 90, 6453-6463.
- WHITEHEAD, S. S., BUKREYEV, A., TENG, M. N., FIRESTONE, C. Y., ST CLAIRE, M., ELKINS, W. R., COLLINS, P. L. & MURPHY, B. R. 1999. Recombinant respiratory syncytial virus bearing a deletion of either the NS2 or SH gene is attenuated in chimpanzees. *J Virol*, 73, 3438-42.
- WILLIAMS, T. C., SINHA, I., BARR, I. G. & ZAMBON, M. 2021. Transmission of paediatric respiratory syncytial virus and influenza in the wake of the COVID-19 pandemic. *Euro Surveill*, 26.
- WONG, P. K., EGAN, P. J., CROKER, B. A., O'DONNELL, K., SIMS, N. A., DRAKE, S.,

- KIU, H., MCMANUS, E. J., ALEXANDER, W. S., ROBERTS, A. W. & WICKS, I. P. 2006. SOCS-3 negatively regulates innate and adaptive immune mechanisms in acute IL-1-dependent inflammatory arthritis. *J Clin Invest*, 116, 1571-81.
- WU, C., XUE, Y., WANG, P., LIN, L., LIU, Q., LI, N., XU, J. & CAO, X. 2014. IFN-gamma primes macrophage activation by increasing phosphatase and tensin homolog via downregulation of miR-3473b. *J Immunol*, 193, 3036-44.
- WU, P. & HARTERT, T. V. 2011. Evidence for a causal relationship between respiratory syncytial virus infection and asthma. *Expert review of anti-infective therapy*, 9, 731-745.
- WU, Y. H., LAI, A. C., CHI, P. Y., THIO, C. L., CHEN, W. Y., TSAI, C. H., LEE, Y. L., LUKACS, N. W. & CHANG, Y. J. 2020. Pulmonary IL-33 orchestrates innate immune cells to mediate respiratory syncytial virus-evoked airway hyperreactivity and eosinophilia. *Allergy*, 75, 818-830.
- XU, W., EDWARDS, M. R., BOREK, D. M., FEAGINS, A. R., MITTAL, A., ALINGER, J. B., BERRY, K. N., YEN, B., HAMILTON, J., BRETT, T. J., PAPPU, R. V., LEUNG, D. W., BASLER, C. F. & AMARASINGHE, G. K. 2014a. Ebola virus VP24 targets a unique NLS binding site on karyopherin alpha 5 to selectively compete with nuclear import of phosphorylated STAT1. *Cell Host Microbe*, 16, 187-200.
- XU, X., ZHENG, J., ZHENG, K., HOU, Y., ZHAO, F. & ZHAO, D. 2014b. Respiratory Syncytial Virus NS1 Protein Degrades STAT2 by Inducing SOCS1 Expression. *Intervirology*, 57, 65-73.
- YAMAJI, Y., YASUI, Y. & NAKAYAMA, T. 2016. Development of Acquired Immunity following Repeated Respiratory Syncytial Virus Infections in Cotton Rats. *PLoS One*, 11, e0155777.
- YAN, S. J., LIM, S. J., SHI, S., DUTTA, P. & LI, W. X. 2011. Unphosphorylated STAT and heterochromatin protect genome stability. *FASEB J*, 25, 232-41.
- YANG, X.O., ZHANG, H., KIM, B.S., NIU, X., PENG, J., CHEN, Y., KERKETTA, R., LEE, Y.H., CHANG, S.H., CORRY, D.B., WANG, D., WATOWICH, S.S. & DONG, C. The signaling suppressor CIS controls proallergic T cell development and allergic airway inflammation. *Nat Immunol*. 2013 Jul;14(7):732-40
- YOSHIMURA, A., NAKA, T. & KUBO, M. 2007. SOCS proteins, cytokine signalling and immune regulation. *Nature Reviews Immunology*, 7, 454.

- YOU, M., YU, D. H. & FENG, G. S. 1999. Shp-2 tyrosine phosphatase functions as a negative regulator of the interferon-stimulated Jak/STAT pathway. *Mol Cell Biol*, 19, 2416-24.
- YUASA, K. & HIJIKATA, T. 2016. Distal regulatory element of the STAT1 gene potentially mediates positive feedback control of STAT1 expression. *Genes Cells*, 21, 25-40.
- ZANIN, N., VIARIS DE LESEGNO, C., LAMAZE, C. & BLOUIN, C. M. 2020. Interferon Receptor Trafficking and Signaling: Journey to the Cross Roads. *Front Immunol*, 11, 615603.
- ZHANG, D., YANG, J., ZHAO, Y., SHAN, J., WANG, L., YANG, G., HE, S. & LI, E. 2022a. RSV Infection in Neonatal Mice Induces Pulmonary Eosinophilia Responsible for Asthmatic Reaction. *Front Immunol*, 13, 817113.
- ZHANG, J., WU, J., WANG, W., WU, H., YU, B., WANG, J., LV, M., WANG, X., ZHANG, H., KONG, W. & YU, X. 2014. Role of cullin-elonginB-elonginC E3 complex in bovine immunodeficiency virus and maedi-visna virus Vif-mediated degradation of host A3Z2-Z3 proteins. *Retrovirology*, 11, 77.
- ZHANG, W., YANG, H., KONG, X., MOHAPATRA, S., SAN JUAN-VERGARA, H., HELLERMANN, G., BEHERA, S., SINGAM, R., LOCKEY, R. F. & MOHAPATRA, S. S. 2005. Inhibition of respiratory syncytial virus infection with intranasal siRNA nanoparticles targeting the viral NS1 gene. *Nat Med*, 11, 56-62.
- ZHANG, X., BOGUNOVIC, D., PAYELLE-BROGARD, B., FRANCOIS-NEWTON, V., SPEER, S. D., YUAN, C., VOLPI, S., LI, Z., SANAL, O., MANSOURI, D., TEZCAN, I., RICE, G. I., CHEN, C., MANSOURI, N., MAHDAVIANI, S. A., ITAN, Y., BOISSON, B., OKADA, S., ZENG, L., WANG, X., JIANG, H., LIU, W., HAN, T., LIU, D., MA, T., WANG, B., LIU, M., LIU, J. Y., WANG, Q. K., YALNIZOGLU, D., RADOSHEVICH, L., UZE, G., GROS, P., ROZENBERG, F., ZHANG, S. Y., JOUANGUY, E., BUSTAMANTE, J., GARCIA-SASTRE, A., ABEL, L., LEBON, P., NOTARANGELO, L. D., CROW, Y. J., BOISSON-DUPOUIS, S., CASANOVA, J. L. & PELLEGRINI, S. 2015. Human intracellular ISG15 prevents interferon-alpha/beta over-amplification and auto-inflammation. *Nature*, 517, 89-93.
- ZHANG, Y., GARGAN, S., ROCHE, F. M., FRIEMAN, M. & STEVENSON, N. J. 2022b. Inhibition of the IFN-alpha JAK/STAT Pathway by MERS-CoV and SARS-CoV-1 Proteins in Human Epithelial Cells. *Viruses*, 14.

- ZHAO, C., DENISON, C., HUIBREGTSE, J. M., GYGI, S. & KRUG, R. M. 2005. Human ISG15 conjugation targets both IFN-induced and constitutively expressed proteins functioning in diverse cellular pathways. *Proc Natl Acad Sci U S A*, 102, 10200-5.
- ZHENG, J., YANG, P., TANG, Y., PAN, Z. & ZHAO, D. 2015. Respiratory Syncytial Virus Nonstructural Proteins Upregulate SOCS1 and SOCS3 in the Different Manner from Endogenous IFN Signaling. *J Immunol Res*, 2015, 738547.
- ZHIVAKI, D., LEMOINE, S., LIM, A., MORVA, A., VIDALAIN, P. O., SCHANDENE, L., CASARTELLI, N., RAMEIX-WELTI, M. A., HERVE, P. L., DERIAUD, E., BEITZ, B., RIPAUX-LEFEVRE, M., MIATELLO, J., LEMERCIER, B., LORIN, V., DESCAMPS, D., FIX, J., ELEOUET, J. F., RIFFAULT, S., SCHWARTZ, O., PORCHERAY, F., MASCART, F., MOUQUET, H., ZHANG, X., TISSIERES, P. & LO-MAN, R. 2017. Respiratory Syncytial Virus Infects Regulatory B Cells in Human Neonates via Chemokine Receptor CX3CR1 and Promotes Lung Disease Severity. *Immunity*, 46, 301-314.
- ZHOU, J. H., WANG, Y. N., CHANG, Q. Y., MA, P., HU, Y. & CAO, X. 2018. Type III Interferons in Viral Infection and Antiviral Immunity. *Cell Physiol Biochem*, 51, 173-185.
- ZHOU, Y., TONG, L., LI, M., WANG, Y., LI, L., YANG, D., ZHANG, Y. & CHEN, Z. 2021. Recurrent Wheezing and Asthma After Respiratory Syncytial Virus Bronchiolitis. *Front Pediatr*, 9, 649003.
- ZHU, J., YAMANE, H. & PAUL, W. E. 2010. Differentiation of effector CD4 T cell populations (*). *Annu Rev Immunol*, 28, 445-89.
- ZIEGLER, S. F., ROAN, F., BELL, B. D., STOKLASEK, T. A., KITAJIMA, M. & HAN, H. 2013. The biology of thymic stromal lymphopoietin (TSLP). *Adv Pharmacol*, 66, 129-55.

A1 Supplementary Figures

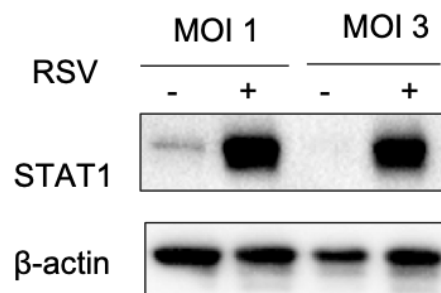


Figure A1.1: RSV infection increases total STAT1 in BEAS 2b cells

BEAS 2b cells were infected at an MOI of 1 and 2 for 24h before collection in lysis buffer and prepared for western blotting. The membrane was probed for STAT1 and β -actin (n=1)

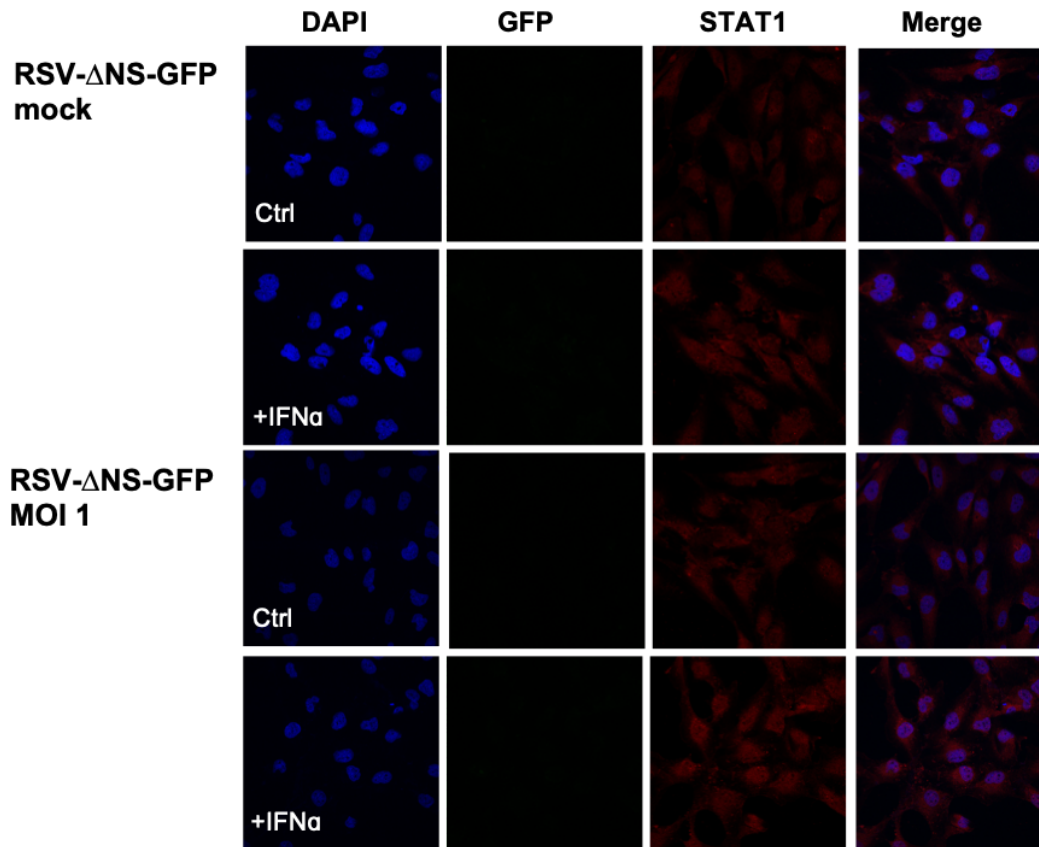


Figure A1.2: Incubation of BEAS 2b cells with RSV- Δ NS-GFP does not result in substantial infection

BEAS 2b cells infected with MOI 1 A) mock control or B) RSV- Δ NS-GFP for 24h and stimulated with 1000IU or 0IU IFN α for 30min. Cells were stained for STAT1 and DAPI, and visualised using confocal microscopy n=2.